# JC and BK Polyomavirus-Like Particles as Targets of Innate and Adaptive Humoral Immunity

**Inauguraldissertation**

zur

Erlangung der Würde eines Doktors der Philosophie

vorgelegt der

Philosophisch Naturwissenschaftlichen Fakultät

der Universität Basel

von

Piotr Kardas

aus Piotrków Trybunalski, Polen

Basel, 2015

Genehmigt von der Philosophisch-Naturwissenschaftlichen Fakultät

auf Antrag von

Prof. Dr. Antonius G. Rolink

Prof. Dr. Hans H. Hirsch

Prof. Dr. Roberto Speck

Basel, den 23.06.2015

Prof. Dr. Jörg Schibler

*Dekan*

# Contents


**1 Abbreviations ..... 1**

**2 Summary ..... 4**

**3 Introduction ..... 7**

**3.1 Human Polyomaviruses (HPyVs) ..... 7**

3.1.1 JC and BK Polyomaviruses ..... 9

3.1.1.1 Viral Background ..... 9

3.1.1.1.1 Virion and Genome Organization ..... 9

3.1.1.1.2 Genotypes ..... 11

3.1.1.1.2.1 JCPyV Genotypes and Subtypes ..... 11

3.1.1.1.2.2 BKPyV Genotypes and Subtypes ..... 12

3.1.1.1.3 Viral Life Cycle ..... 13

3.1.2 Clinical Implications ..... 16

3.1.2.1 Epidemiology of JCPyV Infection ..... 16

3.1.2.2 JCPyV-Associated Diseases ..... 16

3.1.2.2.1 Progressive Multifocal Leukoencephalopathy (PML) ..... 17

3.1.2.2.1.1 Risk of Developing PML Among People with Different Cause of Immunodeficiency ..... 17

3.1.2.2.1.2 Various Hypotheses Concerning PML Pathogenesis ..... 19

3.1.2.2.1.3 Unique JCPyV Non-Coding Control Region (NCCR) Rearrangements ..... 19

3.1.2.2.1.4 Major Capsid Protein (VP1) Mutations Characteristic for PML Patients 20

3.1.2.2.1.5 Diagnosis and Clinical Presentation of PML ..... 21

3.1.2.2.1.6 PML Treatment Strategies ..... 23

3.1.2.2.2 Other JCPyV-Associated Diseases ..... 23

3.1.2.3 Epidemiology of BKPyV Infection ..... 25

3.1.2.4 BKPyV-Associated Diseases ..... 25

3.1.2.4.1 Polyomavirus-Associated Nephropathy (PyVAN) ..... 26

3.1.2.4.1.1 PyVAN Pathogenesis ..... 26

3.1.2.4.1.2 Diagnosis and Clinical Presentation of PyVAN ..... 27

3.1.2.4.1.3 PyVAN Treatment Strategies ..... 27

3.1.2.4.2 Polyomavirus-Associated Haemorrhagic Cystitis (PyVHC) ..... 28

3.1.2.4.2.1 PyVHC Pathogenesis ..... 28

3.1.2.4.2.2 Diagnosis and Clinical Presentation of PyVHC ..... 29

3.1.2.4.2.3 PyVHC Treatment Strategies ..... 29

3.1.2.4.3 Other BKPyV-Related Diseases ..... 29

**3.2 Immune Response to Viral Infection ..... 30**

3.2.1 Innate Immune Response to Viruses ..... 30

3.2.1.1 Specific Viral DNA sensors ..... 36

3.2.2 Adaptive Immune Response to Viral Infection ..... 39

3.2.2.1 Adaptive Immune Response to HPyVs ..... 44

**3.3 Antibody Assays for Studying Adaptive Humoral Immunity to JC and BK Polyomaviruses ..... 47**

3.3.1 Technical Aspects of JCPyV and BKPyV Antibody Assays ..... 47

3.3.2 Virus-Like Particles as the Antigen in Antibody Assays .....49

**4 Aims of the Thesis .....53**

**5 Results .....54**

**5.1 Efficient Uptake of Blood-Borne BK and JC Polyomavirus-Like Particles in Endothelial Cells of Liver Sinusoids and Renal Vasa Recta .....54**

**5.2 Inter- and Intralaboratory Comparison of JC Polyomavirus Antibody Testing Using Two Different Virus-Like Particle-Based Assays.....72**

**5.3 Optimizing JC and BK Polyomavirus IgG Testing for Seroepidemiology and Patient Counseling .....82**

**5.4 Progressive Multifocal Leukoencephalopathy in Common Variable Immunodeficiency: Mitigated Course Under Mirtazapine and Mefloquine .....90**

**5.5 A Case of Primary JC Polyomavirus Infection–Associated Nephropathy..99**

**5.6 BK Polyomavirus-Specific Cellular Immune Responses Are Age-Dependent and Strongly Correlate With Phases of Virus Replication.....106**

**5.7 Diffuse Gastrointestinal Bleeding and BK Polyomavirus Replication in a Pediatric Allogeneic Haematopoietic Stem Cell Transplant Patient.....119**

**5.8 Antibody Response to BK Polyomavirus as a Prognostic Biomarker and Potential Therapeutic Target in Prostate Cancer .....125**

**6 Discussion .....138**

**7 References .....144**

**8 Acknowledgements .....179**

# 1 Abbreviations

| | |
|---|---|
| $5HT_{2A}R$ | 5-hydroxy-tryptamine-2A serotonin receptor |
| AIDS | acquired immune deficiency syndrome |
| APCs | antigen-presenting cells |
| ASC | apoptosis-associated speck-like protein containing a CARD |
| at-NCCR | archetype non-codin control region |
| BKPyV | BK polyomavirus |
| BMDCs | bone marrow-derived dendritic cells |
| bp | base pairs |
| c-di-GMP | cyclic diguanylate monophosphate |
| cART | combination antiretroviral therapy |
| CMV | cytomegalovirus |
| CNS | central nervous system |
| CSF | cerebrospinal fluid |
| DAI | DNA-dependent activator of IRFs |
| DC | dendritic cells |
| DNA | deoxyribonucleic acid |
| EBV | Epstein- Barr virus |
| ER | endoplasmic reticulum |
| EVGR | early viral gene region |
| HA | hemagglutination assay |
| HAI | hemagglutination inhibition assay |
| HBV | hepatitis B virus |
| HC | hemorrhagic cystitis |
| HIV | human immunodeficiency virus |
| HMGB | high-mobility group box (proteins) |
| HPyV10 | human polyomavirus 10 |
| HPyV12 | human polyomavirus 12 |
| HPyV6 | human polyomavirus 6 |
| HPyV7 | human polyomavirus 7 |
| HPyV9 | human polyomavirus 9 |

| | |
|---|---|
| HPyVs | human polyomaviruses |
| HSCT | hematopoietic stem cell transplantation |
| HSV-1 | herpes simplex virus-1 |
| IFN | interferon |
| IRIS | immune reconstitution inflammatory syndrome |
| JCPyV | JC polyomavirus |
| KIR(s) | killer-cell immunoglobulin-like receptor(s) |
| KTR | kidney transplant recipient |
| LRO | lysosome-related organelles |
| LTag | large T-antigen |
| LVGR | late viral gene region |
| MCMV | murine cytomegalovirus |
| MCPyV | Merkel cell polyomavirus |
| mDCs | myeloid dendritic cells |
| MEFs | mouse embryonic fibroblasts |
| MHC | major histocompatibility complex |
| MITA | mediator of IRF3 activation |
| MRI | magnetic resonance imaging |
| mRNA | messenger ribonucleic acid |
| MS | multiple sclerosis |
| NCCR | non-coding control region |
| NK cells | natural killer cells |
| NLR(s) | (NOD)-like receptor(s) |
| NLS | nuclear localization signal |
| NOD | nucleotide-binding oligomerization domain |
| ORF | open reading frame |
| PAMPs | pathogen- associated molecular patterns |
| PBMCs | peripheral blood mononuclear cells |
| PCNA | proliferating cell nuclear antigen |
| pDCs | plasmacytoid dendritic cells |
| PML | progressive multifocal leukoencephalopathy |
| pRb | retinoblastoma protein |
| PRR | pattern recognition receptors |
| PYD | pyrin domain |

| | |
|---|---|
| PyVAN | polyomavirus associated nephropathy |
| PyVHC | polyomavirus associated hemorrhagic cystitis |
| PyVs | polyomaviruses |
| RBC | red blood cells |
| RFC | replication factor C |
| RIG-I | retinoic acid-inducible gene I |
| RLR(s) | (RIG-I)-like receptor(s) |
| RNA | ribonucleic acid |
| RPA | replication protein A |
| rr-NCCR | rearranged non-coding control region |
| SOT | solid organ transplantation |
| sTag | small T antigen |
| STLPyV | Saint Louis polyomavirus |
| SV40 | simian vacuolating virus 40 |
| TAP1/2 | transporters associated with antigen processing-1/2 |
| TCR | T cell receptor |
| TLR(s) | Toll-like receptor(s) |
| TsPyV | *Trichodysplasia spinulosa* polyomavirus |
| VLP(s) | virus-like particle(s) |
| VP1 | major capsid protein 1 |
| VP2 | minor capsid protein 2 |
| VP3 | minor capsid protein 3 |
| VSV | vesicular stomatitis virus |
| wt | wild type |

# 2 Summary

JC polyomavirus (JCPyV) and BK polyomavirus (BKPyV) were identified as the first of now more than 12 human polyomaviruses (HPyVs). The average JCPyV and BKPyV seroprevalence rates in adults are 70% and 90%, respectively. After asymptomatic infection both viruses persist in the renourinary tract. In fact, asymptomatic viruria is detectable in one-third of general population. However, in immunocompromised patients, JCPyV and BKPyV replication may progress to significant diseases. Hence, JCPyV can cause progressive multifocal leukoencephalopathy (PML) in patients with HIV-AIDS, malignancies or autoimmune diseases under immunosuppressive treatment. BKPyV can be a cause of polyomavirus-associated nephropathy (PyVAN) in kidney transplant recipients or hemorrhagic cystitis (PyVHC) after allogeneic hematopoietic stem cell transplantation. Due to more frequent application of immunosuppression, the risk of developing these diseases has increased in the last few decades. The risk of PML development is estimated to be 100-fold higher for JCPyV-seropositive patients in comparison to JCPyV-seronegatives. Most cases of PyVAN and PyVHC have been tested positive for BKPyV at the moment of disease diagnosis. Unfortunately, there is no specific antiviral therapy against any of these HPyV diseases. Thus, current strategies to avert PyVAN or PyVHC aim at identifying patients with BKPyV viremia and reducing immunosuppression. Similar strategies for PML have not been effective, since JCPyV viremia is usually not detected prior to or at the diagnosis of disease.

The fate of BKPyV and JCPyV virus-like particles (VLPs) was examined in an animal model corresponding to primary viremia in non-immune host. Radioactively labeled VLPs were used to assess blood decay, organ, and hepatocellular distribution of ligand, and non-labeled VLPs to examine cellular uptake by immunohisto- and cytochemistry. Rapid distribution of both BKPyV and JCPyV VLPs to the liver was observed, with lesser uptake in kidney and spleen. Liver uptake was predominantly observed in LSECs. Blood half-life and tissue distribution of both wild-type JCPyV VLPs and two mutant JCPyV VLPs (L55F and S269F), lacking sialic acid binding affinity, were similar, indicating involvement of non-sialic acid receptors in cellular uptake. We concluded that LSECs very effectively cleared a large fraction of blood-borne BKPyV and JCPyV VLPs, indicating a central role of these cells in early removal of polyomavirus from the circulation. Moreover, we observed that a subpopulation of endothelial cells in kidney, the main organ of polyomavirus persistence, showed selective and rapid uptake of VLPs, suggesting a role in viremic organ tropism (Simon-Santamaria et al., p. 54).

Giving the increasing clinical need to reliably determine JCPyV and BKPyV IgG levels in patients at risk, we first reviewed and optimized serological tools for JCPyV and BKPyV IgG detection including virus-like particle (VLP)-based ELISA. We demonstrated that although no statistically significant differences in intraassay and interassay variability were revealed for JCPyV serology of 400-fold diluted sera from healthy donors, qualitative differences were seen in the identification of the individual JCPyV serostatus. The cause of discordance for approximately 10% of sera resulted from a low IgG activity close to the cutoff of the assay. Therefore we standardized the ELISA using reference serum for normalization. Moreover, we developed a preadsorption assay with cutoff of 35% reduction of the JCPyV IgG activity after preincubation with JCPyV VLPs. Importantly, we excluded BKPyV antibody cross-reactivity by testing JCPyV IgG positive sera in preadsorption assay using BKPyV VLPs. In conclusion, we showed that VLP-based ELISA with normalization can serve as a reliable tool for JCPyV IgG serology. Additionally, the preadsorption assay can help with unequivocal determination of JCPyV serostatus for samples with low IgG levels. (Kardas et al., p. 72).

We also normalized this VLP-based ELISA for BKPyV IgG detection and showed that for seroepidemiology studies, normalized JCPyV and BKPyV IgG ELISA at 1:200 serum dilution provides optimal sensitivity and specificity with the lowest false-positive and false-negative rate. However, for individual risk assessment, 100-, 200-, and 400-fold dilutions combined with preadsorption for low-reactive sera might be the most appropriate (Kardas et al., p. 82).

This improved ELISA was used to investigate JCPyV and BKPyV specific antibody levels in several clinical studies: (1) one case of PML patient where positive JCPyV IgG status was compatible with other PML-indicating symptoms (Kurmann et al., p. 90); (2) one case of PyVAN caused by JCPyV rather than BKPyV, as confirmed by JCPyV IgG/IgM positive and BKPyV IgG/IgM negative results (Lautenschlager et al., 99); (3) one case of PyVHC patient after allogeneic hematopoietic stem cell transplantation where increasing BKPyV IgG activities were in line with progression of BKPyV viremia (Koskenvuo et al., p. 106). Further, by serological testing of 122 immunocompetent and 63 immunocompromised patients we demonstrated that the BKPyV IgG level is age-dependent, with the highest values between 20 and 30 years (Schmidt et al., p. 119).

In another study we compared serological outcomes of ELISA utilizing two different antigens in terms of prognostic value in prostate cancer development. To accomplish this we utilized improved ELISA for BKPyV IgG activity to both BKPyV VLPs and BKPyV LTag. Testing of 226 patients undergoing radical prostatectomy for primary prostate cancer revealed that BKPyV

VP1 serostatus, in contrast to BKPyV LTag, has no prognostic value in prostate cancer progression (Keller et al., p. 125).

In conclusion, we provided a new input into knowledge about tropism and clearance of polyomaviruses from blood. Moreover, we established a reliable and sensitive VLP-based assay for specific detection of JCPyV and BKPyV IgG and IgM. Serostatus based on ELISA results was compatible with other symptoms of BKPyV- and JCPyV-related diseases.

# 3 Introduction

## 3.1 Human Polyomaviruses (HPyVs)

The family *Polyomaviridae* comprises of three genera: two mammalian genera designated *Orthopolyomavirus* and *Wukipolyomavirus*, and the avian genus *Avipolyomavirus* (**Fig. 1**) (1, 2). JC and BK polyomaviruses (JCPyV and BKPyV), closely related to most intensely studied animal virus simian virus 40 (SV40), were the first PyVs to be discovered in humans (3-5). More recently, increased interest in innovative screening methods have led to discovery of ten previously unknown human polyomaviruses (HPyVs), including Merkel cell polyomavirus (MCPyV). This virus can be found in tumor cells of Merkel cell carcinoma, a skin cancer affecting mostly immunocompromised individuals (6). Another HPyV *Trichodysplasia spinulosa* polyomavirus (TsPyV) was identified in a rare skin disease with a typical striking development of keratin spicules originating from unusual hair follicles in immunocompromised patients (7). Further, human polyomavirus 6 (HPyV6) and 7 (HPyV7) were first detected on the skin of healthy individuals. Human polyomavirus 9 (HPyV9) was found in a serum sample from kidney transplant recipient and human polyomavirus 10 (HPyV10) was identified in papillomavirus-induced anal condylomata (8-10). Saint Louis polyomavirus (STLPyV), which is closely related to HPyV10, was identified in stool samples from both healthy and diarrhea-inflicted children, whereas human polyomavirus 12 (HPyV12) was detected in liver tissue (11). New Jersey polyomavirus (NJPyV) is a novel polyomavirus that may have been discovered recently in a pancreatic transplant recipient with retinal blindness and vascuolitic myopathy showing tropism for vascular endothelial cells (12). According to the International Committee on Taxonomy of Viruses JCPyV, BKPyV, MCPyV, TsPyV, HPyV9/10/12, STLPyV, NJPyV belong to *Orthopolyomavirus* genus, whereas HPyV6/7 and another two HPyV, Karolinska Institute polyomavirus (KIPyV) and Washington University polyomavirus (WUPyV) identified in airway samples from patients with respiratory disease, are part of *Wukipolyomavirus* genus (**Fig. 1**) (2, 13).

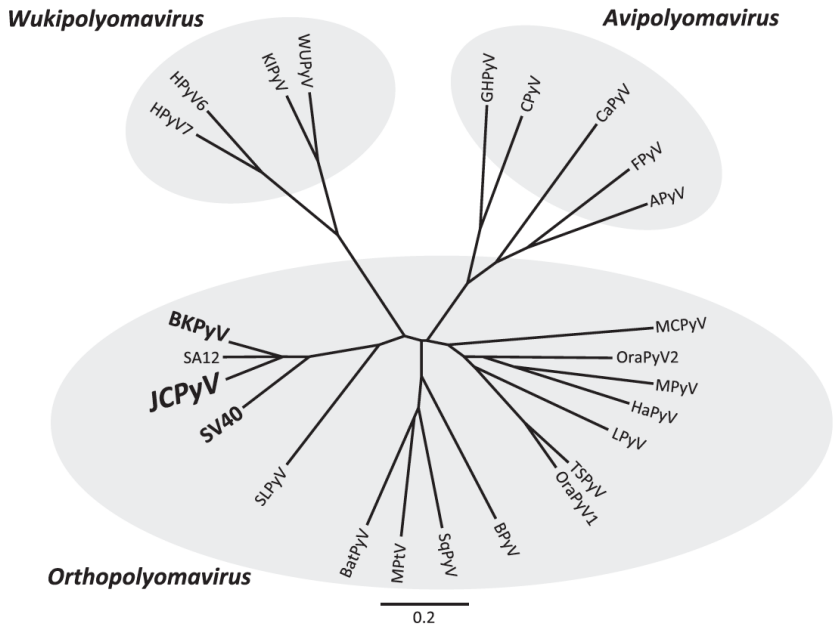


**Figure 1.** Phylogenetic tree of *Polyomaviridae* family [from (2)]

HPyVs infect a large part of the general population with different age-dependent patterns (14-16). MCPyV seroprevalence increases drastically in childhood and remains constant through life (17). For JCPyV, seroprevalence increases slowly during childhood and continues increasing during life (15). On the other hand the seroprevalence of BKPyV increases during childhood but starts declining at the age of 40 (15). Those seroprevalence differences indicate that HPyVs are transmitted independently of one another and carry various risks of exposure and reexposure throughout the entire life (18).

### 3.1.1 JC and BK Polyomaviruses

#### 3.1.1.1 Viral Background

##### 3.1.1.1.1 Virion and Genome Organization

The outer surface of every polyomavirus is a naked protein capsid composed entirely of a single virus-encoded protein called major capsid protein 1 (VP1). The virion contains a total of 72 pentameric VP1 capsomers arranged in T=7 icosahedral structure of approximately 40-45 nm in diameter. Inside the capsid, one molecule of either minor capsid protein 2 (VP2) or minor capsid protein 3 (VP3) is attached to each VP1 pentamer (**Fig. 2**). The N-terminus of VP1 is responsible for the interaction with other VP1 proteins in the same pentamer, while the C-terminus reaches out into the neighboring pentamer to interact with VP1, thereby stabilizing the capsid. VP2 and VP3 interact with the VP1 molecule through hydrophobic interactions (19). It is believed that both VP2 and VP3 are important for packing JC polyomavirus (JCPyV) and BK polyomavirus (BKPyV) genomes into virions as well as for uncoating and delivery of viral genome to the host cell nucleus (20, 21).

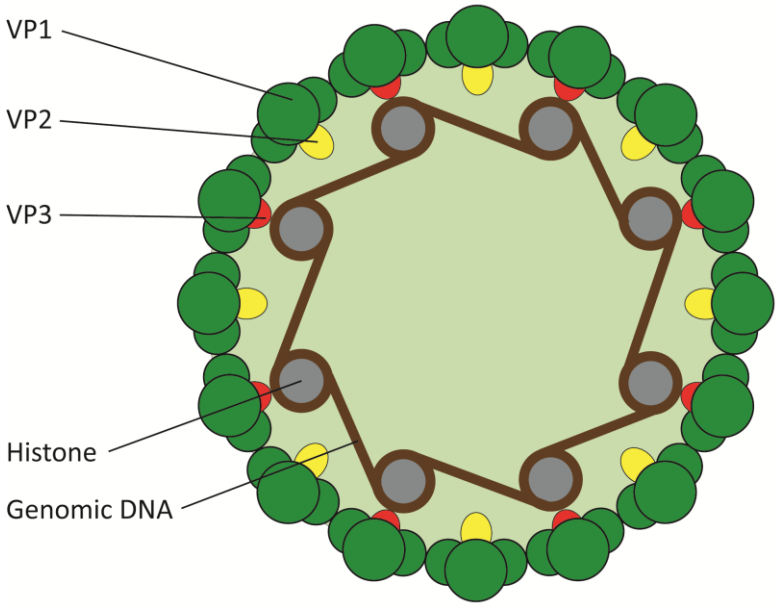


**Figure 2.** JCPyV and BKPyV structure

The HPyV virion encapsidates a circular double-stranded DNA of about 5100-5300 base pairs (bp), organized around histones in a core-like structure. The BKPyV genome shares 75% of overall homology with JCPyV (22). Similar to other PyVs, the genome of both viruses can be divided into three parts: the non-coding control region (NCCR), the early viral gene region (EVGR) and the late viral gene region (LVGR) (**Fig. 3**).

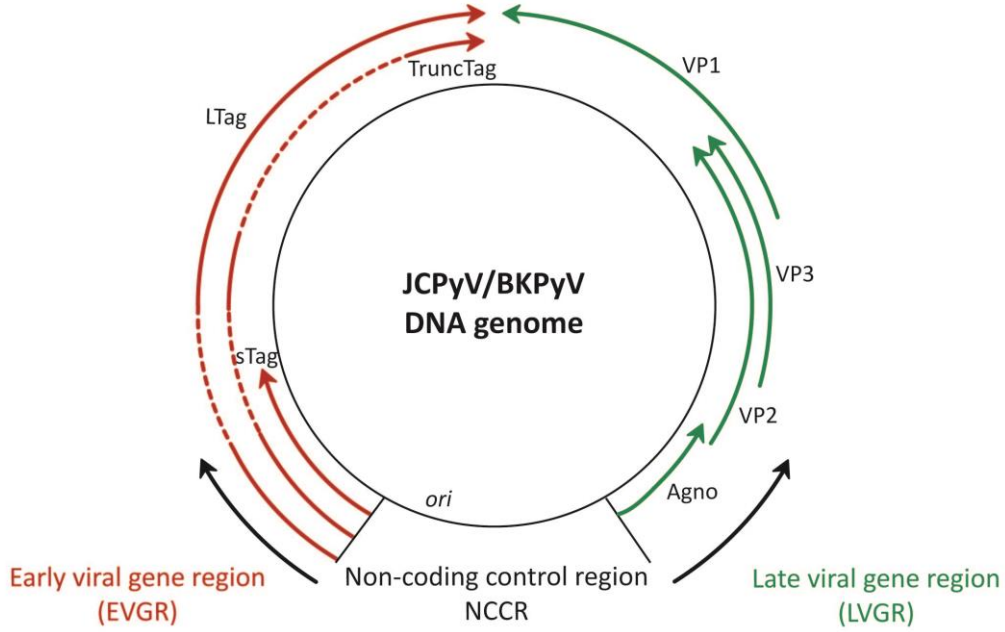


**Figure 3.** JCPyV and BKPyV genome organization [adapted from (2)]

The NCCR covers about 400 bp and corresponds to the nucleosome-free area between early and late region (19). It contains origin of viral replication *ori*, TATA- and TATA-like sequences for both early and late viral gene transcription, many DNA- and transcription factor- binding sites, promoter and enhancer elements as well as binding sites for large T-antigen (LTag).

The EVGR is about 2400 bp in size close to the left side of the origin of replication *ori* and encodes small T-antigen (sTag), LTag, and the truncated LTag (TruncTag). TruncTags have a common N-terminal part but differ in C-terminal part, due to alternative splicing of one pre-mRNA. Polyomaviruses do not encode viral DNA polymerases, therefore the genome replication relies on host-cell enzymes. However, LTag contains DNA unwinding/helicase activity and therefore regulates DNA replication as well as LVGR expression. All the transcription processes of the virus are completely dependent on host-cell transcription factors (23). Thus, cell activation by growth factors and other signals may initiate and facilitate these events.

The LVGR covers about 2300 bp more distant to the origin of replication *ori* and contains the open reading frames (ORFs) of the structural proteins VP1, VP2 and VP3. Additionally, the JCPyV LVGR encodes a small protein called Agno, found only in BKPyV and simian vacuolating virus 40 (SV40). Although, there are many speculations about its properties, the function of Agno remains unknown (24, 25).

#### 3.1.1.1.2 Genotypes

##### 3.1.1.1.2.1 JCPyV Genotypes and Subtypes

Sequencing of the JCPyV genome revealed at least seven major genotypes and numerous subtypes (26). All genotypes were detected in different geographic areas of the world (**Fig. 4**). Types 1 and 4 are the most common genotypes in Europeans, Types 2 and 7 are more frequent among Asians, and Types 3 and 6 in Africans. For each of the genotype one to five subtypes have been identified.

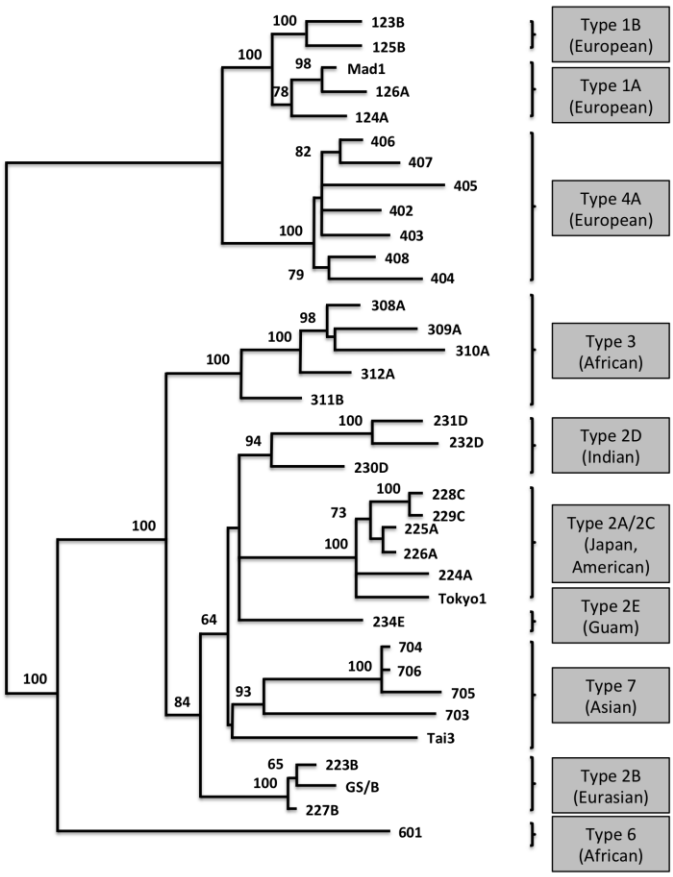


**Figure 4.** Phylogenetic reconstruction of JCPyV genome development

[modified from (27) and (28)]

#### 3.1.1.1.2.2 BKPyV Genotypes and Subtypes

Based on nucleotide sequence analysis of all known genome-full-length isolates, BKPyV can be categorized into four major genotypes, namely I, II, III, and IV (29). Neutralization experiments show that all BKPyV genotypes are fully distinct serotypes (30, 31). Due to expansion of BKPyV diversity and arising difficulties in assigning viral strains to existing subtypes, additional subgroups within the four major subtypes have been appointed (32-34). Thus, subtype I is the most frequent and has a worldwide distribution, subtype IV is the second most frequent and might be more frequently detected in Eastern Asia. Although subtypes II and III are found worldwide, their frequencies are low (35, 36). Additionally, according to the phylogenic investigations subtype I can be divided into 4 subgroups including subgroups Ia, Ib1, Ib2 and Ic, with broad geographical distribution. Subtype IV is divided into six subgroups in phylogenic studies including IVa1, IVa2, IVb1, IVb2, IVc1 and

IVc2 (6, 7) (**Fig. 5**). It might be that different BKPyV genotypes have different cellular tropisms and pathogenic potentials *in vivo* (30).

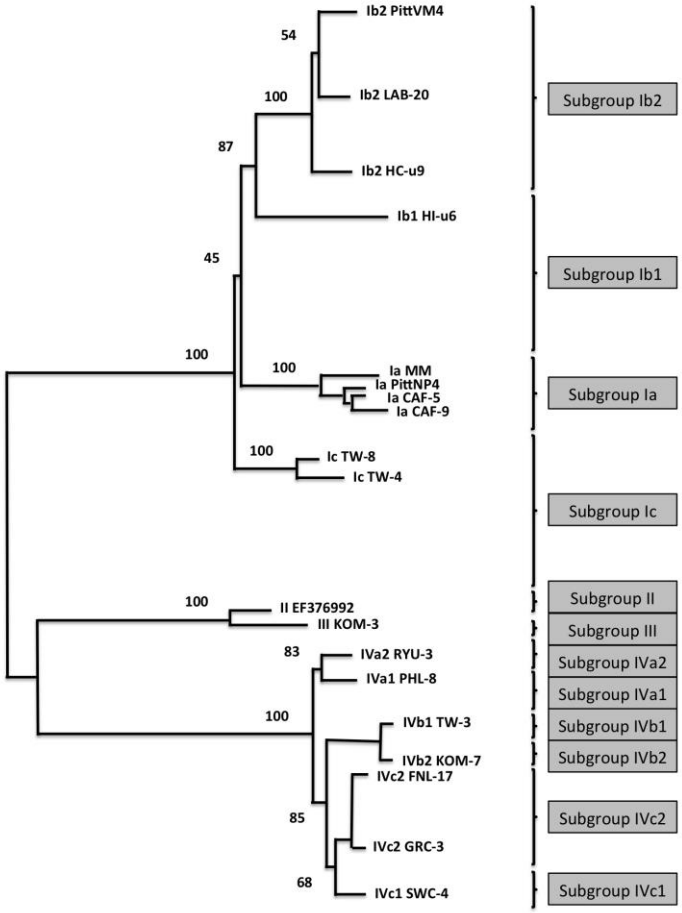


**Figure 5.** Phylogenetic reconstruction of BKPyV genomes development [modified from (34)]

#### 3.1.1.1.3 Viral Life Cycle

JCPyV attaches to the terminal α2,6-linked sialic acid-bearing structures (mostly glycoproteins and glycolipids) on the host cell surface (**Fig. 6**). Additional or alternative receptor might also be involved, such as the 5-hydroxy-tryptamine-2A serotonin receptor ($5HT_{2A}R$) (37). Terminal α2,6-linked sialic acids which could bind virions have been identified on oligodendrocytes and astrocytes, on B-lymphocytes in tonsils and spleen, and in kidney and lung tissue, which stays in line with results from studies on the tissue distribution of JCPyV DNA (38-41). It is suggested that after attachment of JCPyV to $5HT_{2A}R$ and terminal α2,6-linked sialic acid, internalization of the virus mediated via clathrin-coated pits takes place. Further steps include caveolin-1 and pH-dependent transport along the cellular

cytoskeleton to the endoplasmic reticulum (ER) (42-44). The caveolae are then transported to the caveosome, a vacuolar structure with a neutral pH, functioning as a sorting compartment.

BKPyV infection is mediated by binding of major capsid protein VP1 to the α2,3-linked sialic acid structures including GD1b and GT1b gangliosides, responsible for mediating cellular recognition and cell-to-cell interaction (19, 42, 45, 46). Both GD1b and GT1b are present on kidney and urinary tract cells making them the main sites of the viral infection and replication (47). After binding to the receptor on the cell surface, the virus is internalized via caveolae-mediated endocytosis (48, 49) (**Fig. 6**). Caveolin-1 and cholesterol-enriched lipid rafts mediate plasma membrane invagination and vesicle generation (50-52).

The following steps of life cycle are similar for both JCPyV and BKPyV (49, 53). After transport to the ER, partial uncoating of the virion takes place. Disulfide isomerases available in ER induce conformational changes in the VP1 structure of both viruses, facilitating capsid disassembly prior to its entry into the nucleus. For BKPyV, it has been shown that Derlin-1, a member of the ER-associated degradation (ERAD) pathway, works as a retro-translocation channel to transport the virus to the cytosol through the interaction with VP1, prior to entry into nucleus (49, 54). It has been proposed, that BKPyV might use the proteasome to enable a more efficient disassembly of the capsid in the cytosol (49, 55, 56).

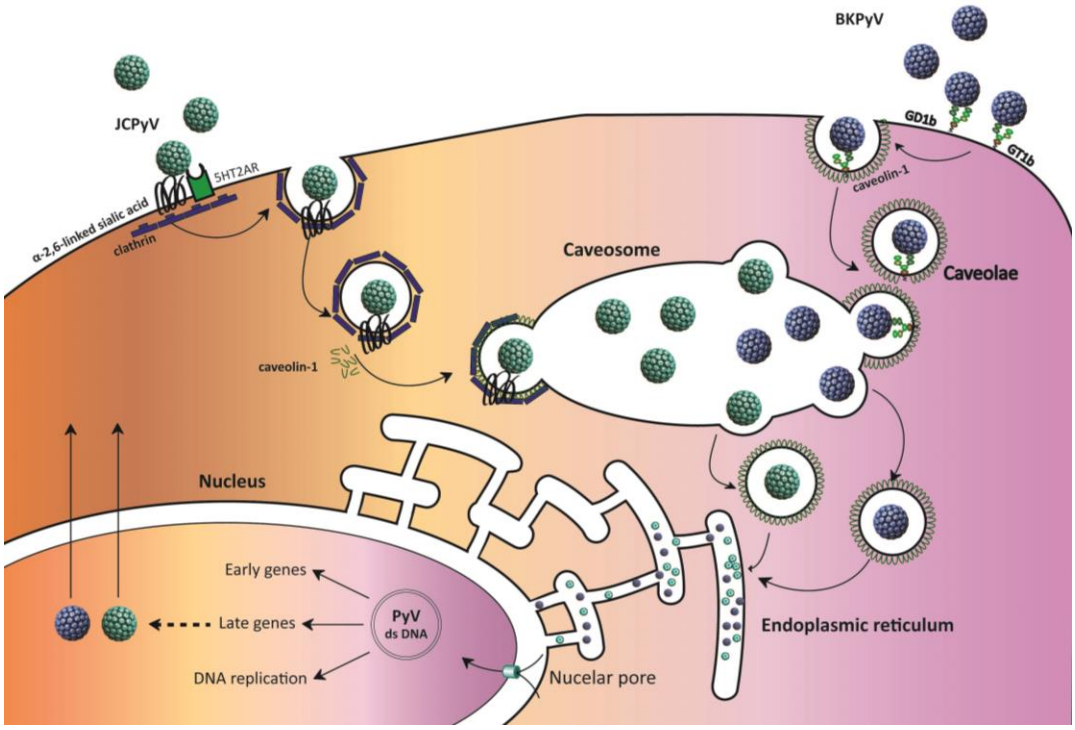


**Figure 6.** JCPyV and BKPyV life cycle

The detailed steps of the viral entry into the nucleus are not well defined. Nevertheless, due to size of the virion (40-45 nm), its transport might be limited, as the nuclear pore complex allows to pass only particles up to 39 nm (57). Moreover, a nuclear localization signal (NLS) located at the N-terminus of VP2 and VP3 has to be exposed to enable efficient transport into the nucleus. Therefore, the virion has to be partially disassembled in the ER for the NLS recognition and the passage through the nuclear pore.

After the entry of a viral DNA into the nucleus, decision on replication or latency must occur. This decision is well defined and the latency depends on host cell fitness, its differentiation potential and the immune status of the host.

In case of the EVGR, expression begins from the left TATA box promoter and progresses in one direction half around the circular genome. Although mRNA of LTag and sTag are translated in the cytosol (58), LTag is immediately transported to the nucleus, whereas sTag stays in the cytoplasm. sTag interacts with retinoblastoma proteins (pRb) enabling the release of members of the E2F family of transcription factors from their Rb partners to promote cell cycle progression (59). sTag also inhibits phosphatase 2A (PP2A). However, a direct role of sTag in promoting viral replication has not been defined. LTag on the other hand is necessary for replication of the viral genome as a result of its DNA binding and helicase activities (60). LTag is thought to promote viral replication directly by binding to viral DNA and viral proteins, as well as indirectly by interaction with key regulatory proteins of the host cell. Taking SV40, six copies of LTag assemble into two hexameric structures at the NCCR and initiate bidirectional melting of viral genome (61). Hexameric LTag also recruits host cell polymerase and DNA-binding proteins to the replication fork in order to facilitate viral DNA replication. LTag also conveys a negative expression feedback of its own transcription by interaction with binding sites in NCCR, thereby initiating expression of LVGR proteins (2). Similarly to sTag, LTag ensures activity of the cell through binding to the pRb and inhibition of its function. In an active state, pRbs cause a cell cycle arrest through formation of a complex with histone deacetylases (HDACs) and the transcription factor E2F (19, 62). After binding of pRb by LTag, E2F is released, thereby inducing the transcription of E2F-dependent genes encoding cyclins, checkpoint regulators. The expression of proteins promoting DNA repair and replication leads to a cell cycle progression accompanied by viral replication (19, 62). LTag also prevents the host cell from p53-mediated apoptosis which would be caused by accumulating amplified DNA fragments and metabolic exhaustion (60, 63).

The LVGR expression is initiated by interaction of LTag with cellular transcription factors, including DNA polymerase α, topoisomerases and replication protein A (RPA), and their binding to the NCCR (64, 65). After transcription of LCGR, its common mRNA is alternatively spliced and translated into proteins. Thereafter, capsid proteins undergo posttranslational modifications including myristoylation of the N-terminus of VP2 and VP3 as well as formation of disulfide bridges between VP1 proteins, which prevents the single pentamers from dissociation (19). After translation of capsid proteins, they are transported from cytosol into the nucleus, whose mechanism is still not revealed. The assembly of the virions with viral encapsidated viral DNA then takes place, leading to nuclear inclusions and enlargement and eventual lysis of the cell (19, 66).

### 3.1.2 Clinical Implications

#### 3.1.2.1 Epidemiology of JCPyV Infection

Numerous reports on JCPyV seroprevalence indicate presence of anti-JCPyV antibodies in 30 to 70% of healthy individuals (2, 14-16). Diverse rates among different age groups indicate that JCPyV exposure occurs at least in two life periods: in childhood with seroprevalence reaching around 25% in early adolescence, followed by the second phase in adulthood with up to 70% JCPyV seroprevalence among old people (14-16, 67). There is also a regional variation of JCPyV seropositivity ranging from 47% in Norway to 68% in Turkey (68). JCPyV persists in the renourinary tract and viral replication is detected as asymptomatic viruria in approximately 30% of immunocompetent JCPyV seropositive individuals (15). Since seroprevalence of around 80% has been reported for BKPyV, it can be assumed that both viruses are transmitted independently and probably through various routes. Exposure and re-exposure to JCPyV is associated with a seroconversion of 1 to 2% per year, which has been not observed for BKPyV (15, 69).

#### 3.1.2.2 JCPyV-Associated Diseases

In immunocompetent individuals JCPyV infection is not definite and may be subclinical or unspecific. The major JCPyV-associated diseases occur in the context of immunological impairment of an efficient control of viral replication in the central nervous system (CNS)

and kidney and possibly in other sites, e.g. colon (2). The interest in progressive multifocal leukoencephalopathy (PML) has increased due to a widespread use of different immunosuppressive drugs. Moreover, cases of JCPyV-associated nephropathy in kidney transplant recipients have appeared as well as other pathologies including some forms of cancer (**Table 1**) (70).

#### 3.1.2.2.1 Progressive Multifocal Leukoencephalopathy (PML)

JCPyV is the causative agent of PML, a rare and frequently fatal brain disease preferentially affecting the white brain matter and is caused by cytopathic replication of the virus in myelin-producing oligodendrocytes (2, 71-74). The pathology of the affected brain tissues demonstrates oligodendroglia-like cells with viral inclusions in their enlarged nuclei, one of the diagnostic hallmarks of this disease (68, 71, 73, 74). The lack of an animal model and the need to investigate PML only in humans made the understanding of the disease very difficult. However, it has changed in the last 50 years. Due to an increased rate of PML in HIV-AIDS patients and more common use of new biologic therapies of multiple sclerosis (MS) and autoimmune conditions (e.g. rheumatoid arthritis), there are more opportunities to study this disease (75). Moreover, highly sensitive molecular techniques allow nowadays detecting even very low level of virus. Additionally, estimation of PML risk for patients undergoing newer therapies for cancer, solid-organ and hematologic transplantation, multiple sclerosis, and other autoimmune diseases has increased the general knowledge in this field (76-81).

##### 3.1.2.2.1.1 Risk of Developing PML Among People with Different Cause of Immunodeficiency

PML affects a small fraction of immunocompromised patients, including those with HIV-AIDS and transplant recipients on immunosuppressive drug therapies. Nowadays, HIV infection is still the most frequent setting for PML, 80% of the cases, followed by hematologic malignancies (approximately 8%), solid cancers (around 3%), organ transplantation, and autoimmune diseases treated with immunomodulators (82). Due to various immunosuppressants being used, the risk of PML development varies between different groups of patients. The incidence of PML in the general population was estimated as 0.3 per 100 000 persons years compared to 1.0 for patients with rheumatoid arthritis (83, 84). The

incidence in HIV-AIDS individuals is estimated as 2.4 cases per 1 000 patients years (reported for Switzerland and Denmark) (85, 86). Among patients after solid organ transplantation (heart or lung) the PML incidence have been observed for 1.24 patients out of 1 000 (76). In patients with rheumatoid arthritis treated with rituximab, a depleting monoclonal antibody targeting CD20+ B cells, the prevalence of PML was estimated as 1 in 25 000 patients (87).

For multiple sclerosis patients approximate risk of PML development depends on several factors including JCPyV serostatus, prior therapy of multiple sclerosis with immunosuppressive drugs and duration of natalizumab treatment (**Fig. 7**).

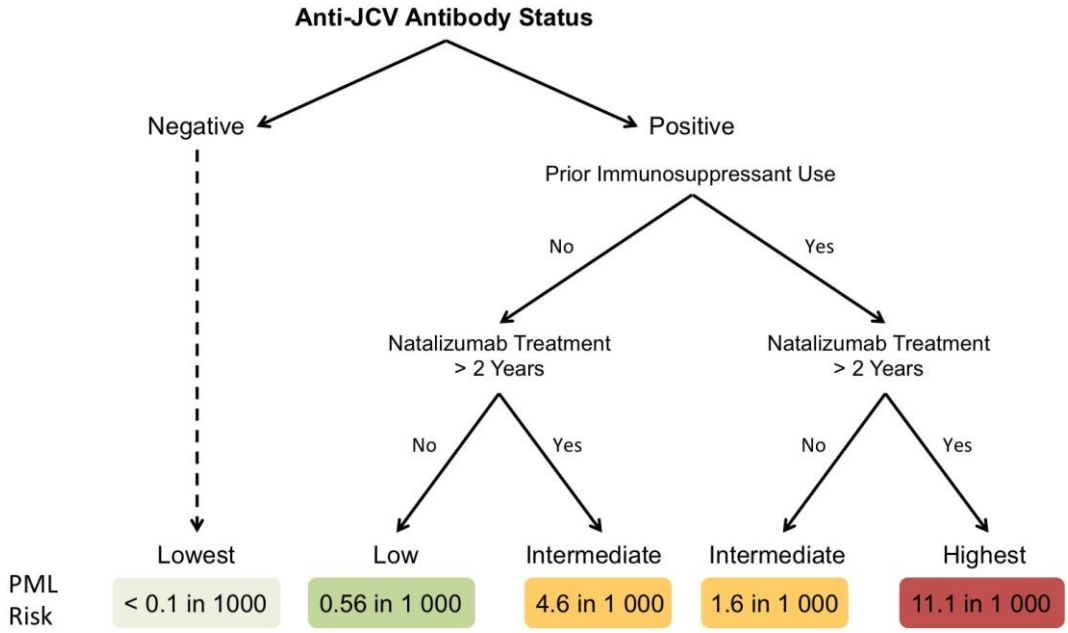


**Figure 7.** Approximate incidence of PML among multiple sclerosis patients stratified according to different risk factors

For patients receiving natalizumab for at least 2 months, 2.13 PML cases per 1 000 patients were reported (2, 88). Taking the risk of PML stratified according to three risk factors, the incidence of PML is the lowest among the patients who are negative for anti–JCPyV antibodies, with the estimation of less than 0.09 cases per 1 000 patients. Patients who are positive for anti–JCPyV antibodies, had taken immunosuppressants before the initiation of natalizumab therapy, and have received 25 to 48 months of natalizumab treatment have the highest estimated risk of 11.1 cases per 1 000 patients (68).

#### 3.1.2.2.1.2 Various Hypotheses Concerning PML Pathogenesis

The detailed steps of PML development remain unknown due to the lack of definitive human data (73). The time between onset of JCPyV replication in the brain and accumulation of cytopathic damages leading to clinical and radiological abnormalities is still unclear. Moreover, the relevant sites of JCPyV latency, including compartments where the virus acquires the most pathogenomic NCCR rearrangements (rr-NCCR) and VP1 capsid protein mutations, are not defined (2). However, it is postulated that JCPyV reaches CNS during primary viremia where its reactivation is locally censored by specific T-cell effectors. The decrease of T-cells function in the CNS permits local replication of JCPyV and cytopathic damage progressing to PML. Another theory presents lymphocytes, hematopoietic progenitor cells and other cells of the body as a site of JCPyV persistence, where in case of decreased activity of JCPyV-specific T-cells the virus can reactivate and occult secondary viremia resulting in colonization of susceptible cells in CNS and their eventual cytopathic damage. It has been hypothesized that the virus could persist in other cells of besides the kidney (lymphocytes or bone marrow progenitor cells) and reach CNS via infected lymphocytes migrating to the CNS. The entry of the virus into nervous system would result in colonization, local replication and eventual cytopathic damage of CNS cells. The virus reactivation hypothesis is supported by the fact that practically all PML patients are JCPyV seropositive at the time of PML diagnosis, although the serology testing was performed exclusively on HIV-AIDS or MS patients (69, 71, 88-90).

#### 3.1.2.2.1.3 Unique JCPyV Non-Coding Control Region (NCCR) Rearrangements

The archetype JCPyV NCCR has been arbitrary divided into 6 blocks, designated from A to F (**Fig. 8**). Block A covers 36, B - 23, C - 55, D - 66, E - 18 and F - 69 base pairs. The highly variable rearrangements in JCPyV NCCR (rr-NCCR) can affect any of the blocks and can comprise of duplications (partial, multiple or tandem repeats) or deletions of archetype NCCR (at-NCCR) sequence or combination of both (91-93). Some of the NCCR rearrangements are unique for PML cases, suggesting their role in the disease pathogenesis. PCR amplification and direct sequencing of rr-NCCR sequences allowed the identification of some typical rearrangement patterns. The rearrangements in rr-NCCR sequences found in PML cases were observed in an *ori*-distal part of the NCCR close to LVGR and D-block of

NCCR, affecting a part or the entire D-block, whereas duplications occurred in *ori*-proximal part of the NCCR close to EVGR TATA-box as well as in C-block alone or in combination with mutations in blocks A and B. Less frequent partial deletions have been observed in blocks E and F (92, 94, 95). Sequence analysis of NCCRs from single-sampling site from the same PML patient indicates the presence of many different rr-NCCR sequences with a common signature but with one dominant rr-NCCR sequence (96). The major JCPyV quasispecies can change within 2 days in CSF, retaining nevertheless a rearrangement signature. The NCCR rearrangements might appear due to uncontrolled dynamic replication of JCPyV in the brain. Errors occurring during viral DNA replication result in generation of quasispecies of JCPyV with rr-NCCR with varied replication fitness (92).

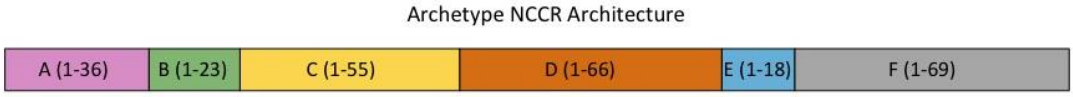


**Figure 8**. JCPyV archetype NCCR architecture

However, it cannot be excluded that independent replication generates in parallel new NCCR rearrangements. Despite the high variety of NCCR rearrangements, the majority of JCPyV quasispecies with rr-NCCR invariably show increased EVGR expression in comparison to JCPyV with at-NCCR (92).

#### 3.1.2.2.1.4 Major Capsid Protein (VP1) Mutations Characteristic for PML Patients

Analysis of JCPyV VP1 sequences reveals that a small number of mutations can be found exclusively in cerebrospinal fluid (CSF) or brain of PML patients. In fact, between 80 and 90% of viral isolates from PML patients exhibit mutations in one or more of the VP1 and these mutations have never been found in JCPyV isolates from individuals without PML (97). These substitutions affect amino acids located at or close to binding sites for sialic acid structures, which enables viral interactions with cellular receptors and hence viral infectivity (98). The most frequent changes occur in amino acids 269 and 55 (L55F and S269F) (**Fig. 9**) (99, 100).

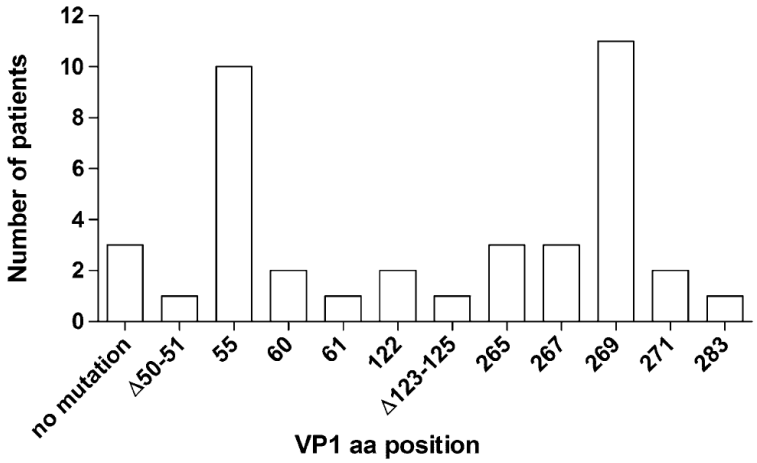


**Figure 9**. Frequency of JCPyV VP1 mutations among 37 PML patients [from (99)]

While wild-type JCPyV causes agglutination of red blood cells (RBC) (due to JCPyV binding activity to sialic acid structures present on RBC), the virus with 55F, 267F, 269F or 269Y mutation is no longer able to achieve this (99). For some of the mutants, e.g. 60E, 265D and 271H, hemagglutination is still possible but at much lower level. Those changes in hemagglutination ability suggest that these mutations may influence the cell tropism of JCPyV in human by abrogating the ability to bind to sialylated molecules on a variety of peripheral cell types, but retain the ability to bind CNS glial cells (99). It is not well defined where the mutagenesis of JCPyV VP1 takes place. Nevertheless, approximately 10% of PML patients carrying the virus without VP1 mutations is still consistent with the hypothesis that the mutations occur prior to viral entry into the CNS (99).

#### 3.1.2.2.1.5 Diagnosis and Clinical Presentation of PML

The diagnosis of PML can be viewed as a loss of myelin-producing oligodendrocytes which leads to asymmetric and focal lesions in the initial stages of the disease, followed by a dramatic subcortical expansion, confluence and even contralateral spread along the corpus callosum (73). Magnetic resonance imaging (MRI) is the key non-invasive diagnostic method for PML diagnosis (accompanied by clinical symptoms). Typically the lesions are located in the subcortical white matter with a sharp border towards the gray matter and diffuse border towards the white matter (**Fig. 10**).

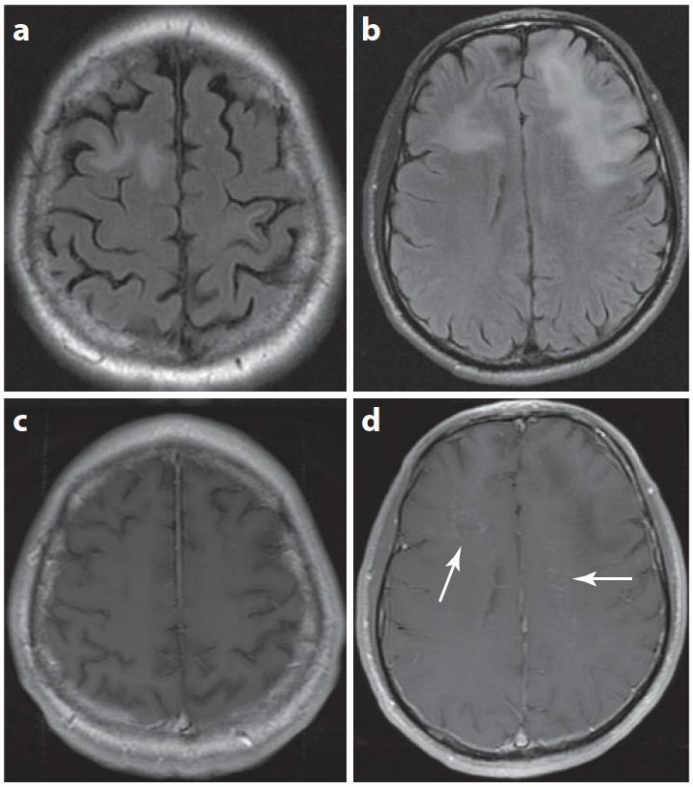


**Figure 10**. Cerebral PML lesions (a, c) of an HIV-negative patient without IRIS and (b, d) an HIV-positive patient with IRIS [from (73)]

The diagnosis of histologically confirmed PML requires demyelination in the white matter of the brain, compatible cytopathic alterations and specific JCPyV involvement, proven with immunohistochemistry for virus proteins (LTag or VP1) or DNA detection by *in situ* hybridization. Detection of JCPyV DNA in CSF is usually accepted as probable PML, called as well virologically- or laboratory-confirmed PML (2, 101, 102).

Based on observations of case series from different PML eras (pre-AIDS era, AIDS-associated PML and natalizumab-related PML), the clinical presentation of PML is variable and reflects severity and location of the lesions. The general symptoms might include cognitive and behavioral abnormalities, visual deficits, motor weakness, gait abnormalities, incoordination, sensory loss and headaches (68). Epilepsy, although rare in the initial clinical presentation of PML in HIV-AIDS, can be frequently observed among patients with PML lesions in more cortical location (103) as well as in patients with radiological signs of inflammation due to local immune responses (2).

#### 3.1.2.2.1.6 PML Treatment Strategies

There is currently no specific antiviral therapy to PML and the treatment aims at regaining control of immune system over JCPyV replication. In transplant recipients, this approach requires reduction of immunosuppression, which is limited by increased risk of organ dysfunction or even graft rejection. For kidney transplant recipients, a return of hemodialysis or discontinuation of immunosuppressive treatment may be indicated for a successful outcome (104). For other SOT patients, the reduction of immunosuppression might be not feasible to allow for timely recovery of immune control over JCPyV replication. Reduction or discontinuation of immunosuppression in HSCT case could lead to a worsening of the graft-versus-host disease. For HIV-AIDS patients with PML, the combination antiretroviral therapy (cART) might improve the overall outcome. Unfortunately, still approximately half of the HIV-patients develop the disease or suffer from significant neurological impairment. In case of MS patients undergoing natalizumab treatment, immune reconstitution can be successful but sometimes can also lead to significant side effects, e.g. immune reconstitution inflammatory syndrome (IRIS). In high-risk patients with PML-IRIS, the use of intravenous immunoglobulins may be beneficial due to their immunomodulatory activity dempening IRIS (105). Also, adoptive transfer of JCPyV-specific T-cells has been reported for a child after allogeneic HSCT (106). This immunologic treatment was well tolerated and no recurrence of PML was noted. More attention has been also paid to the antivirals cytarabine and cidofovir and uptake blockers mirtazapine, chlorpromazine, and mefloquine alone or in combination, with varying success, typically in uncontrolled case studies (107-113).

### 3.1.2.2.2 Other JCPyV-Associated Diseases

JCPyV can also cause other diseases including JCPyV-mediated granule cell neuronopathy caused by replication of the virus in granule cell neurons of the cerebellum (114, 115). The disease is associated with VP1 C-terminal JCPyV mutations, approximately 10 bp deletions resulting in frame shift and a total change of the C-terminal amino acid sequence of the protein (116, 117). Clinical symptoms include a cerebellar syndrome with ataxia and progressive cerebellar atrophy without involvement of the white matter (114). The JCPyV can be detected in CSF. The lesions frequently coexist with PML in the white matter of the

cerebellum and cerebrum. The proposed treatment is based on regaining immune control over JCPyV replication.

JCPyV-associated encephalopathy is another disease caused by cytopathic JCPyV replication in the gray matter, this time targeting the cortical pyramidal neurons (118). It is characterized by lesions expanding from the gray matter to subcortical areas and by presence of the virus in the CSF of the patient.

JCPyV-associated meningitis and encephalitis have been discovered in patients with typical symptoms of meningeal inflammation, including neck stiffness, headache, fever and JCPyV present in CSF (119, 120). However, no clinical sign of neurologic deficits characteristic for PML has been found. The diagnosis is based on clinical symptoms of meningitis and presence of JCPyV in the CSF.

| | **Classic PML** | **PML-IRIS** | **JCPyV granule cell neuronopathy** | **JCPyV encephalopathy** | **JCPyV meningitis** |
|---|---|---|---|---|---|
| **Onset** | Subacute | Immune recovery | Chronic | Subacute | Acute |
| **Radiological findings (MRI)** | Asymmetric, well demarcated, non-enhancing subcortical white matter lesions, hyperintense in T2 and FLAIR, hyperintense in T1 | Contrast enhancement and mass effect | Cerebellar atrophy | Cortical lesions | No defined lesions, ventricular dilatation |
| **Neurological symptoms** | Based on location | Based on location and inflammation | Cerebellar syndrome | Encephalopathy | Headache, stiff neck, fever |
| **Diagnosis** | JCPyV detection in the CSF, brain biopsy, radiographical findings and symptoms | JCPyV in the CSF, brain biopsy, radiographical findings and symptoms | Cerebellar biopsy, JCPyV in the CSF, radiographical findings and symptoms | Brain biopsy, JCPyV PCR in the CSF, radiographical findings and symptoms | JCPyV in the CSF and exclusion of other viruses |
| **Histology** | Demyelinating lesions often at grey/white junction, JCPyV detected in enlarged oligodendrocytes, bizarre astrocytes | Demyelination similar to classic PML, with addition of inflammatory infiltrates | Lytic infection of granule cell neurons in the cerebellum by JCPyV | Lytic infection of cortical pyramidal neurons and cortical astrocytes by JCPyV | |
| **Treatment** | cART for HIV-positive patients, discontinue or decrease immunosuppression for HIV-negative patients, plasma exchange for natalizumab-treated patients | Similar to PML, consider steroids in cases with notable neurological worsening or signs of impending brain herniation | Similar to classic PML | Similar to classic PML | Similar to classic PML |

**Table 1.** Clinical presentations of JCPyV-related neurological diseases [from (121)]

Nephropathy due to JCPyV (JCPyVAN) is a rare complication affecting approximately 1% of kidney transplant recipients causing severe graft dysfunction and its eventual loss (122, 123). This complication leads to the decline of the renal allograft function, very high JCPyV load and decoy cells shedding in urine. Morphologically, JCPyVAN and BKPyVAN are indistinguishable. Blood or plasma test could be unreliable due to frequently very low or even undetectable amount of JCPyV DNA (124). JCPyVAN is usually confirmed with immunohistochemical detection of LTag in renal tubular epithelial cells by cross-reactive SV40 antibodies. The pathology of JCPyVAN occurs without NCCR rearrangements (125). JCPyVAN can be treated by reducing immunosuppression leading to stabilization of allograft function during follow-up and to clearance of the virus (122).

The transforming potential of JCPyV makes it interesting in terms of human malignancies. Numerous human malignancies have been associated with JCPyV including oligodendroglioma, astrocytoma, medulloblastoma, ependymona and glioblastoma (103, 126-129).

#### 3.1.2.3 Epidemiology of BKPyV Infection

Epidemiological studies revealed that BKPyV infection occurs during early childhood at a median age of 4–5 years through the respiratory or oral route (14, 130). After primary infection BKPyV persists in the renourinary tract as the principal site (131). It is unknown if this is a truly latent infection, with no replication and limited or no viral gene expression, or if it is a persistent infection, with low-level viral replication. However, it has been shown that spontaneous reactivation of BKPyV and its asymptomatic urinary shedding occurs in up to 62% of healthy BKPyV-seropositive individuals (130, 132, 133). The overall seroprevalence for BKPyV among human population reaches up to 90% (14-16). The number of seropositive individuals increases until the age of 40 years and then slightly decreases (14, 16). Interestingly, this is in contrast to JCPyV which seroprevalence increases throughout life (14-16, 29).

#### 3.1.2.4 BKPyV-Associated Diseases

Primary BKPyV infection is not associated with any well-defined clinical symptoms in immunocompetent individuals. Reactivation of latent virus could however occur in old age, diabetes mellitus, pregnancy, congenital immunodeficiency, HIV-AIDS and most importantly,

kidney transplantation. The first sign of reactivation is BKPyV viruria, which has been reported in 15-60% of kidney transplant patients (134, 135). This is followed by BKPyV viremia and BKPyV-associated nephropathy (BKPyVAN) seen respectively in 5-30% and 1-10% of kidney transplant patients (134-138). In bone marrow transplant recipients, hemorrhagic cystitis is an important clinical syndrome attributed to BKPyV infection, particularly after radiation and chemotherapy (139-142). Other diseases caused by BKPyV infection include ureteric stenosis and bladder cancer. Diseases affecting regions outside of the urogenital tract associated with BKPyV have only rarely been seen in the form of myopathy in kidney transplant recipient or disseminated infection in AIDS patients as well as single cases of encephalitis and meningoencephalitis (143, 144).

#### 3.1.2.4.1 Polyomavirus-Associated Nephropathy (PyVAN)

It has been reported, that PyVAN affects between 1 and 10% of kidney transplant patients during the first two years post-transplantation (135, 145-147). PyVAN rarely affects patients other than kidney transplant recipients and so far only few cases of the disease in native kidneys of other immunocompromised patients have been reported (148).

##### 3.1.2.4.1.1 PyVAN Pathogenesis

The impairment of immune response allows BKPyV to be reactivated, leading to its replication and host cell death. The nephropathy is manifested as damage of tubular epithelial cells due to extensive viral replication causing their eventual lysis (136, 149). The damage to the tubules can be observed along the whole nephron. However, the proximal tubules, the collective duct and the distal tubules are usually the most affected by extensive viral replication (150, 151). As a consequence, virus leaks into the bloodstream and inflammatory cells infiltrate the interstitium leading to tubular atrophy and interstitial fibrosis (152, 153). This impairs the graft function and increases the risk of graft rejection. Importantly, the urothelial cells may also play a role in PyVAN. Modeling of BKPyV replication in kidney transplant patients with PyVAN suggests that although viral replication starts in the renal tubular epithelial cells, BKPyV is later carried to the urothelial cell compartment where more than 90% of urine BKPyV loads are generated (154). Histopathological data revealing extensively infected urothelial cells in the bladder of

patients with PyVAN confirm the suggested model (150).

#### 3.1.2.4.1.2 Diagnosis and Clinical Presentation of PyVAN

The clinical presentation of PyVAN is insidious and allograft function decreases with persistent disease indicating progressive involvement of BKPyV replication. Typical signs of viral replication can be observed in tubular epithelial cells including enlargement of nuclei with smudgy chromatin changes, intranuclear inclusions, rounding, and eventual detachment of the cell from tubular walls (146, 151, 155, 156). In further phase of PyVAN development, extensive renal involvement is observed with multifocal cytopathic alterations, necrosis, accompanied by inflammatory response, and first signs of fibrosis. The inflammatory infiltrate contains polymorphonuclear cells, monocytes, and plasmacytoid cells in varying distributions (146, 150, 157). Further on, interstitial fibrosis, scarring, and even calcifications could occur. The tubuli become flattened and atrophic and sometimes few polyomavirus-infected cells are detectable.

It is strongly recommended to screen kidney transplant patients regularly for early diagnosis (158). Screening for PyVAN can be achieved by detection of BKPyV replication in the urine to identify patients at risk. Various techniques and urine cytology have been used to identify decoy cells or quantitative PCR of urine and/or plasma for detection of high-level BKPyV viruria (159). Importantly, plasma PCR has a higher positive predictive value in comparison to urine PCR as episodic viruria is quite frequent in this patient group, while viremia is less common and usually precedes PyVAN (135). Alternatively, cytological examination of urine in search of decoy cells or electron microscopy can be performed (160). Most of the time the complete diagnosis of PyVAN requires a histological demonstration of BKPyV replication. However, a negative biopsy result cannot exclude PyVAN, due to its focal nature (149, 161).

#### 3.1.2.4.1.3 PyVAN Treatment Strategies

The management of PyVAN is difficult due to the lack of standard protocol and effective antiviral drugs. BKPyV infection remains latent with its predisposition to reactivation and regaining of patient immune function is needed to eventually control BKPyV replication. The most widely used interventions include reduction, change or discontinuation of immunosuppression. These approaches are nevertheless connected with a risk of acute graft rejection. After decrease of immunosuppression, the serum creatinine value has to be

monitored in 1-2 week intervals and the BKPyV viremia in 2-4 week intervals (158). When the disease is detected at an early stage, a reduction in the immunosuppression is often sufficient to clear BKPyV viremia and stop the progression of disease (162-164). Clearance of BKPyV occurs in >85% of BKPyVAN cases, although more advanced stage of PyVAN may require more comprehensive intervention (138, 163, 165). In comparison to strategy based on reduction in immunosuppression alone, there is no evidence to support the use of any other drugs combined with reduction in immunosuppression (166). Nevertheless, cidofovir (intravenously administered nucleoside analogue of deoxycytidine monophosphate), leflunomide (orally administered drug which indirectly leads to decrease of T- and B-lymphocytes proliferation), fluroquinolones (synthetic broad spectrum antimicrobial agents suggested to interfere with the helicase activity of BKPyV LTag) and intravenous immunoglobulins are sometimes used as adjunctive therapies (167-170).

#### 3.1.2.4.2 Polyomavirus-Associated Haemorrhagic Cystitis (PyVHC)

Haemorrhagic cystitis has an incidence of 5 to 15% in allogeneic haematopoietic stem-cell transplantation (171-173). Causative factors include urotoxic conditioning procedures and total body irradiation as well as viral infections including BKPyV and adenovirus. In terms of further therapy, it is important to distinguish BKPyV-associated hemorrhagic cystitis from cyclophosphamide-associated HC (174). Although PyVHC usually affects allogeneic HSCT patients, single cases have been reported in other immunocompromised patients (130).

##### 3.1.2.4.2.1 PyVHC Pathogenesis

Although the pathogenesis of PyVHC is not well understood, sequence of events has been suggested as cause of the disease (150, 175). Those include subclinical damage of bladder mucosa by acroleine - a toxic metabolite of cyclophosphamide (used as conditioning protocol prior HSCT), immunologically uncontrolled high-level replication of BKPyV resulting in uncovering of the damaged bladder mucosa, and inflammation occurring during engraftment of the stem cell graft.

#### 3.1.2.4.2.2 Diagnosis and Clinical Presentation of PyVHC

In contrast to PyVAN cases, BKPyV viremia is not consistently seen in patients with haemorrhagic cystitis (176). To discriminate PyVHC from haemorrhagic cystitis occurring prior to the engraftment due to urotoxic conditioning or total body irradiation, the triad of cystitis, hematuria (grade II or more) and high-level BKPyV replication need to be reported. Additionally, plasma BKPyV load should be also measured (135, 177, 178). As viral determinants of haemorrhagic cystitis, altered nuclear factor 1 (SP1) transcription sites in the BKPyV NCCR have been reported (179). Organ determinants may reside in tissue injury elicited by conditioning, which may provide an increased number of regenerating cells for BKPyV replication. Conditioning for HSCT impairs the BKPyV-specific cellular immune surveillance and provides the grounds for extensive BKPyV replication. On engraftment, recovering immune cells including polymorphonuclear and NK cells engage with BKPyV targets and elicit a pronounced inflammatory response typical for late onset of HC.

#### 3.1.2.4.2.3 PyVHC Treatment Strategies

Therapy for PyVHC is challenging and purely supportive, consisting mainly of pain relief, bladder irrigation to prevent clot formation, hyperhydration to increase diuresis and urosurgical intervention (153). Additionally, lost platelets and red blood cells are substituted. There have been reports of effective interventions with vidarabine or cidofovir (180, 181). However, renal drug toxicity is a critical issue in stem-cell transplant patients, which calls for a cautious use of cidofovir. Interestingly, hyperbaric oxygen is frequently used for radiation induced haemorrhagic cystitis and has also been reported to be beneficial for patients with PyVHC (182) causing stimulation of mucosal repair in the urinary bladder.

#### 3.1.2.4.3 Other BKPyV-Related Diseases

BKPyV can also cause other diseases, such as ureteric stenosis found in kidney transplant recipients and in allogeneic HSCT patients (4, 183-185). Few reports describe some cases of BKPyV influence on CNS diseases among immunocompromised patients (186, 187). There are also reports on detection of BKPyV proteins and/or DNA in some tumors (188). However, a definitive causal role for BKPyV in human malignancy is still missing (189, 190).

## 3.2 Immune Response to Viral Infection

All living organisms have developed several kinds of mechanisms to protect themselves from invasion by microorganisms, including viruses (191). The main function of immune system is the recognition and distinction of self and non-self antigens (192-194). The mammalian immune system can be generally divided into two parts: (1) the innate or non-specific immunity, which is a first line of defense causing immediate not antigen-specific response against invading organisms, and does not demonstrate immunological memory; (2) the adaptive or specific immunity, which is a second line of defense causing delayed antigen-specific response against invading organisms, and demonstrates immunological memory (195).

### 3.2.1 Innate Immune Response to Viruses

Body surfaces like skin, mucosa or surfaces within the body, including endothelial cells and basement membranes, are typical anatomic barriers, which are partly effective in preventing virus entry and its spread within the host organism (196). Under normal conditions, these barriers have a low permeability for viruses provided that the body surfaces stay intact. However, viruses can sometimes penetrate endothelial border by replicating in the capillary endothelial cells or in circulating leukocytes (197-202). Additionally, most of body fluids and tissues contain soluble viral inhibitors, including chemically diverse lipids, polysaccharides, proteins, lipoproteins and glycoproteins, which prevent viral attachment, inactivate virus or inhibit virus replication (203, 204). In the gastrointestinal tract, some viruses can be also inactivated by acid, bile salts and enzymes (204, 205).

The complement system is one of the major effector mechanisms of the innate immune response. It is complex network of more than 30 plasma and membrane-associated serum proteins, constituting more than 15% of the globular fraction of plasma which can elicit cytolitic immune responses against the virus (206, 207). All complement proteins are organized into a hierarchy of proteolytic cascades that start when pathogenic surfaces are identified. The recognition of an antigen leads to generation of potent proinflammatory mediators (anaphylatoxins), opsonization of the pathogenic surface through various complement opsonins (e.g., C3b), targeted lysis of the pathogenic surface through the

assembly of membrane-penetrating pores known as the membrane attack complex (MAC), as well as production of classical proinflammatory response molecules, e.g. interferons (206). Type I interferons (IFNs) are the principal cytokines involved in the antiviral response and can be produced by all nucleated cells (208). Some members of type II and III IFNs have also been shown to play a role in blocking viral DNA synthesis (209-211). Despite different receptors for each of these IFNs, they share downstream signaling molecules and initiate a signaling cascade through the Janus kinase (JNK) signal transducer and activator of transcription (JAK-STAT) pathway. The activation of this pathway leads to the transcriptional regulation of hundreds of IFN-regulated genes (IRGs) including the signal transducer and activator of transcription (STAT) and IFN regulatory factor (IRF) families of transcription factors, which are involved in the regulation of both ISG and IFN gene expression (212, 213). This leads to a remarkable antiviral state, effective against positive-, negative-, and double-stranded RNA viruses, DNA viruses, and intracellular bacteria and parasites. Therefore, IFNs have multiple functions: (1) they increase expression of proteins responsible for the apoptosis of virus-infected cells, including TNF-alpha related apoptosis inducing ligand (TRAIL/Apo2L), Fas/FasL, XIAP associated factor-1 (XAF-1), caspase-4, caspase-8, dsRNA activated protein kinase (PKR), 2'5'A oligoadenylate synthetase (OAS), death activating protein kinases (DAP kinase), phospholipid scramblase, galectin 9, IFN regulatory factors (IRFs), promyelocytic leukemia gene (PML) and regulators of IFN induced death (RIDs) (214, 215); (2) they activate NK cells and DCs and trigger the adaptive immune response (216).

The cells involved in the innate immune response include natural killers (NKs), dendritic cells (DCs), macrophages, γ/δ-T lymphocytes, neutrophils, basophils, and eosinophils (191). These cells express a set of germline encoded pattern recognition receptors (PRRs) that are able to recognize conserved molecular patterns associated with viruses (191, 196, 217-219). These receptors trigger a rapid inflammatory response by production of proinflammatory cytokines and chemokines, thereby inducing the killing of infected/transformed cells or stimulating phagocytosis or apoptosis. They can also upregulate expression of co-stimulatory molecules responsible for activation of the adaptive arm of the immune responses. Another essential function of PRRs is discrimination between self and non-self nucleic acids. According to recent reports on innate immunity this discrimination relies mostly on Toll-like receptors (TLRs), retinoic acid-inducible gene I (RIG-I)-like receptors (RLRs), and nucleotide-binding oligomerization domain (NOD)-like receptors (NLRs).

TLRs are single, membrane-spanning receptors on sentinel cells such as macrophages and dendritic cells, that recognize structurally conserved molecules derived from pathogens. TLR

mediate the antiviral immune responses by recognizing virus infection, activating signaling pathways and inducing the production of antiviral cytokines and chemokines. TLRs 1, 2, 4, 5, and 6 are located primarily in the plasma membrane and therefore interact with components of microbial pathogens that come into contact with the cell. In contrast, TLRs 3, 7, 8, and 9 are situated in the membranes of endosomes and lysosomes. The extracellular domain with ligand-binding site is exposed inside these organelles. Genomic material derived from endocytosed pathogens can be bound by TLRs and trigger immune response. After binding their respective ligands, TLRs 3, 4, 5, 7 and 9 send the signal through their homodimers. However, TLR2 may heterodimerize with TLR1 or TLR6 depending on the ligand. TLR4 requires in addition MD2 for signal transduction (Fig. 11).

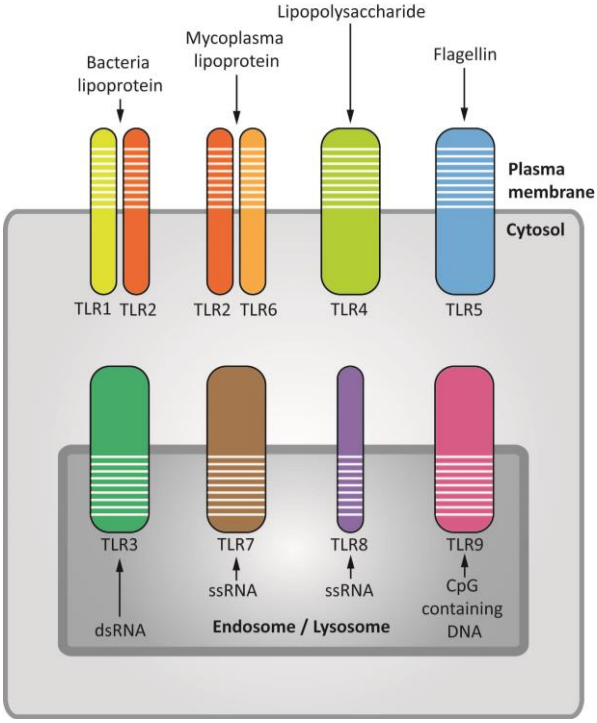


**Figure 11.** Cellular distribution of TLRs and their recognized molecules.

Although TLR2 has been best studied in the context of antibacterial and anti-fungal responses, it has been also shown in a limited number of cases to be involved in the recognition of DNA viruses, e.g. by recognition of envelope glycoproteins B and H of human cytomegalovirus (HCMV) or glycoproteins gH/gL and gB of herpes simplex virus (HSV) (220-224). Therefore it is believed that it might be also involved in recognition of other DNA viruses. However, the most important member of the TLR family able to detect viral DNA is TLR9. This receptor is primarily expressed in B cells and plasmacytoid dendritic cells (pDCs). The main function of TLR9 is to recognize viruses containing genomes rich in CpG DNA

motifs, which is commonly found in prokaryotes and viruses but not in vertebrates. Studies have shown that TLR9 is involved in recognition of hepatitis B virus (HBV), murine cytomegalovirus (MCMV) and Epstein-Barr virus (EBV) (225, 226). After recognition of cytoplasmic viral DNA, TLR9 recruits its adaptor protein MyD88 to initiate two signaling pathways in pDCs. MyD88 interacts with IRF7 resulting in IRF7 phosphorylation by the serine/threonine kinases IRAK-1 and IKKα. Phosphorylated IRF7 is translocated into the nucleus in order to induce the transcription of type I IFN genes (227, 228). MyD88 is also associated with TRAF6 which interacts with IKK kinase complex resulting in IKK activation by phosphorylation (229). The activated IKK initiates α inhibitor of κB (IκBα) phosphorylation at specific NH2-terminal serine residues. Phosphorylated IκBα is then ubiquitinated, thereby releasing NF-κB dimers from the cytoplasmic NF-κB-IκBα complex allowing them to translocate to the nucleus, binding to κB enhancer elements and inducing transcription of proinflammatory genes (230-232). Upon stimulation by viral nucleic acids, TLR9 is transported to the early endosomes to activate the NF-κB. Once activated, it is able to induce cytokine genes in dendritic cells (DCs) and subsequently traffics to lysosome-related organelles (LRO) to induce type I IFNs (230, 233). Also RLRs can trigger signal that induces type I IFNs and other inflammatory cytokines through the IPS-1 adaptor molecule (234, 235).

Dendritic cells (DCs) are antigen-presenting cells, whose main function is to process an antigen and present it on the cell surface to the T cells of the immune system. They act as messengers between the innate and the adaptive immune system.

Macrophages are another type of innate immune cells, which can act as messenger for the adaptive immune system. Along with dendritic cells, they are foremost among the cells that present antigens, playing a crucial role in initiation of an immune response. As secretory cells, monocytes and macrophages are vital to the regulation of immune responses and the development of inflammation. They produce a wide array of chemical substances including enzymes, complement proteins, and regulatory factors such as interleukin-1 (IL-1).

Natural Killer (NK) cells are another key component of innate immunity. They display an antigen-independent lytic activity (236). NK effector functions are controlled by a balance of activating and inhibitory signals provided by killer-cell immunoglobulin-like receptors (KIRs) through the interaction with specific Human Leukocyte Antigen (HLA)-class I ligands. In HSCT recipients, the role of NK cells in mediating graft-versus-leukemia effect and in controlling infections has been well described, but little is still known about NK cells in solid organ transplantation (237). It has been observed that NK cells are able to suppress graft-versus-host disease (GVHD). It has been also shown that donor T cells exhibited less proliferation

and decreased IFN-γ production in the presence of NK cells (238, 239). *In vivo* studies revealed perforin- and Fas ligand (FasL)-mediated reduction of donor T cell proliferation and increased T cell apoptosis in the presence of NK cells (238). *In vitro*, activated NK cells mediate direct lysis of reisolated GVHD-inducing T cells (238). The correlation between KIRs genotype and viral infection following kidney transplantation has been described for CMV (240). HLA-C/KIR interactions were associated with the control of primary CMV infection as measured by the time to CMV viremia in CMV D+/R- solid organ transplant recipients. The presence of the activating receptor (KIR2DS2) in combination with a weaker inhibitory receptor (KIR2DL3 on at least one allele) was associated with protection against CMV viremia. However, this protective effect was only present if neither the donor nor the recipient expressed any HLA-C2 molecules (240). Another study showed significantly reduced rate of CMV viremia in kidney transplant recipients carrying KIR B haplotypes in the subpopulation of kidney transplant recipients (241). In contrast, a lack of such association has been observed for BKPyV reactivation (237). A recent study reported a genetic predisposition to BKPyV infection and PyVAN development by demonstrating a protective effect of the activating receptor KIR3DS1 as it has been shown for other viruses such as human papillomavirus (HPV), hepatitis C virus (HCV), human immunodeficiency virus (HIV) and CMV (242).

Although it is well known that the spleen plays a key role in detection and clearance of pathogens from blood, these processes are redundant with immune surveillance by other tissues. With the exception of clearance of encapsulated bacteria by the spleen, the host's ability to detect and clear pathogens is not affected by splenectomy (243). Such functional redundancy is not seen for immune surveillance mediated by the liver, suggesting this organ is a primary surveillance mechanism for intravascular infections (244). By receiving both portal vein blood and arterial blood, the liver is an important and critical component in the defense against blood-borne infection due to innate and adaptive immune cells specialized in detection and capture of pathogens from the blood. Additionally, these immune cells participate in coordinated immune responses leading to pathogen clearance, leukocyte recruitment and antigen presentation to lymphocytes within the vasculature. The role of liver in host defense has to be tightly regulated to ensure that inappropriate immune responses are not raised against non-pathogenic exogenous blood-borne molecules, e.g. food. Therefore, this characteristic for the liver balance between activation and tolerance makes the liver a frontline immunological organ (244). The liver contains the largest population of macrophages (resident liver macrophages, namely Kuffler cells (KCs)) and NK

cells. The role of the liver in detection and response to infectious organisms is a function of not only the population of cells residing in this organ, but also specific anatomy. Liver sinusoidal endothelial cells (LSECs) play a major role in pathogen detection, capture and most probably antigen presentation. LSECs comprise approximately 50% of the non-parenchymal cells in the liver, meaning more than twice more abundant than either macrophages or lymphocytes in the liver (245). LSECs separate the underlying hepatocytes from the blood in the sinusoidal lumen. Due to lack of organized basement membrane there is a gap between the endothelial lining and hepatocytes, called the space of Disse. This physical separation serves to limit direct contact between the liver parenchyma and the sinusoidal lumen (246). The LSECs can selectively regulate the passage of molecules from the sinusoid lumen to the space of Disse and the underlying hepatocytes, and facilitate direct contact between hepatocytes and intraluminal lymphocytes (246). LSECs are also important immune APCs due to expression of wide variety of PRRs, including Toll-like receptors TLR3, TLR4, TLR7 and TLR9 (247, 248). Furthermore, LSECs constitutively express major histocompatibility complex (MHC) I and MHC II, costimulatory molecules (CD80 and CD86) and adhesion molecules (such as ICAM) needed for interaction with lymphocytes (248). Surface scavenger receptors, mannose receptors and receptors for immunoglobulins and immune complexes, enable LSECs to directly internalize antigens, cellular debris and immune complexes of the size up to 1 μm in diameter (248, 249). Innate immune responses in the liver are summarized in **Figure 12**.

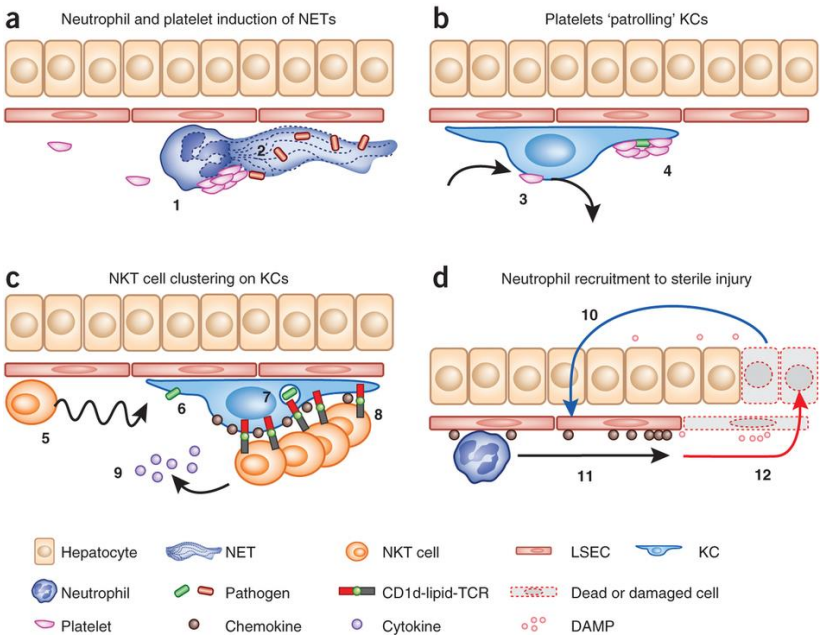


**Figure 12**. Innate immune responses in the liver [from (244)]

#### 3.2.1.1 Specific Viral DNA sensors

So far, several candidates of viral DNA sensors together with their signaling pathways have been reported (250, 251).

The first protein suggested being a cytoplasmic DNA sensor is DNA-dependent activator of interferon-regulatory factors (DAI). Overexpression of DAI enhances the induction of type I IFN by cytosolic DNA from different sources including bacterial and mammalian DNA. Moreover, DAI knockdown experiments point out that HSV infection also induces type I IFN. Recently, it has been also reported that DAI is an important partner of receptor-interacting protein kinase (RIP) 3 and is essential for murine cytomegalovirus (MCMV)-induced cell death (252). DAI partners with RIP3 and induces RIP3 binding to RIP homotypic interaction motif (RHIM) and RHIM-dependent necrosis. Expression of DAI sensitizes cells to virus-induced necrosis and DAI knockdown or knockout cells are resistant to this death pathway (252).

Although RIG-I is well known as an RNA-binding protein, some study reported that RLRs, including RIG-I and MDA5, might also act as DNA-binding proteins. Two groups identified RNA polymerase III as a cytosolic DNA sensor, which subsequently activates the induction of type I IFNs through the RIG-I pathway (253). Both studies demonstrated that AT-rich dsDNA serves as a template, which is consequently converted into dsRNA by RNA polymerase III. The transcript acts as a preferred ligand of RIG-I and as a result induces IFN-β through the RIG-I pathway (253). Moreover, it has been shown that HSV-1 and EBV all trigger the RNA polymerase III-mediated induction of type I IFNs (253). Recognition of dsRNA intermediates produced by RNA polymerase III-mediated transcription of dsDNA by RIG-I could be therefore the possible mechanisms of innate immune detection of DNA viruses. It has been shown that PyVAN innate immune mechanisms through TLR3 and RIG-I are responsible for both anti-BKPyV responses and inflammatory events. These mechanisms might therefore contribute to PyVAN development due to enhanced expression of cytokines and chemokines (254).

MITA (Mediator of IRF3 Activation, or STING [Stimulator of Interferon Genes]) was identified as an important adapter protein for virus-triggered type I IFN induction. MITA occurs on the outer membranes of mitochondria and ER. In certain cell types, MITA is recruited to VISA and RIG-I upon RNA virus infection. MITA can also recruit serine/threonine-protein kinase TBK1 and IRF3 to the complex, in which TBK1 phosphorylates IRF3 (255). It has been shown that IFN-β production in response to the infection of HSV-1 or transfection of purified DNA from *Escherichia coli* is abolished in mouse embryonic fibroblasts (MEFs) with MITA

deficiency, suggesting that MITA is crucial in mediating DNA-induced innate immune responses (256). Mice with MITA knockout failed to produce type I IFNs upon infection with *Listeria monocytogenes*, or treatment with c-di-GMP *in vivo*.

Another protein called IFI16, containing a C-terminal HIN-200 domain for DNA binding and an N-terminal pyrin domain (PYD) for protein-protein interaction, binds to both ss and ds DNAs. The subcellular localization of IFI16 differ in different cell types and can be detected in nucleus, cytoplasm or both (257). The cytoplasmic activated IFI16 recruits MITA, which phosphorylates IRF3. Phosphorylated IRF3 activates NF-κB and induces IFN-β production, resulting in inhibition of HCMV replication. Furthermore, knockdown of IFI16 inhibits DNA- and HSV-1-mediated activation of IRF3 and NF-κB (258, 259). When localized in the nucleus, IFI16 functions as a nuclear sensor to recruit ASC (apoptosis-associated speck-like protein containing a CARD) via their respective PYD domain and therefore induce the formation of inflammasomes. However, further studies are required in order to understand the significance of the nuclear IFI16-inflammasomes (250, 251).

DDX41, a member of DEXDc family of helicases, has also been suggested as a cytosolic sensor for DNA virus (260). It has been shown that DDX41 is responsible for cytosolic DNA sensing in human mDCs (myeloid dendritic cells), BMDCs (bone marrow derived dendritic cells) and monocytes. DDX41 can also bind to poly-AT or HSV-1 DNA, resulting in its interaction with MITA and activation of TBK1 (260).

LTTFIP1 can possibly also take part in non-self DNA recognition. It is able to detect the infection of vesicular stomatitis virus (VSV) in macrophages. Moreover, its knockdown inhibits VSV-induced production of IFN-β (261). After recognition of dsRNA, B-DNA or Z-DNA in the cytoplasm, LRRFIP1 promotes the activation of β-catenin, which binds to the C-terminal domain of IRF3 and recruits the acetyltransferase p300 to induce the expression of IFN-β (261). However, more studies are needed to establish a specific role of LRRFIP1 in innate immune recognition of DNA viruses *in vivo*.

Recently, high-mobility group box (HMGB) proteins have been also reported to sense non-self nucleic acids. The family includes highly conserved HMGB1, 2 and 3. Each protein contains two DNA binding domains. Whereas HMGB1 is ubiquitously and abundantly expressed, the expression of HMGB2 and HMGB3 are limited to lymphoid organs and hematopoietic stem cells. While HMGB1 and HMGB3 have been suggested to recognize both cytosolic DNAs and RNAs, HMGB2 recognizes only cytosolic DNAs. HMGB1 deficiency results in reduction of type I IFNs as response to both DNA and RNA, whereas HMGB2 deficiency only affects DNA-triggered induction of type I IFNs in MEFs.

LSm14A, has been also demonstrated as a sensor of viral nucleic acids in the early phase of viral infection (262). LSm14A is translocated to peroxisomes upon infection by both RNA and DNA viruses. In the peroxisomes, LSm14A binds MITA to induce IFN-β as a response to DNA viruses, leading to the recruitment of RIG-I and VISA thereby inducing IFN-γ in response to RNA viruses (262). The constitutively expressed LSm14A may act as the earliest sensor of viral nucleic acids. Therefore, it has been assumed that P-bodies are important cellular structures involved in viral life cycles (263). Interestingly, a recent study shows that nonstructural protein (NS1) of influenza A virus inhibits cellular antiviral response by targeting the P-body-localized LSm14A/RAP55 (264). These findings indicate an important role of LSm14A as well as the P-bodies in cellular antiviral response.

Besides the activation of TBK1 and IRF3, which results in the induction of type I IFNs, innate recognition of viral DNA also activates pathways leading to the assembly of inflammasomes, which, via caspase-1, result in the cleavage and maturation of certain proinflammatory cytokines such as IL-1β and IL-18 (265). So far, four types of inflammasomes have been identified, including the NLRP1, NLRP3, IPAF, and AIM2. Whereas NLRP1- and IPAF-inflammasomes mainly function against bacterial infection, AIM2 was reported to be a regulator of DNA-mediated inflammatory responses (266). AIM2 contains a conserved DNA binding domain and a PYD domain. It has been reported that AIM2 directly senses dsDNA from both bacteria and virus in the cytoplasm and recruits the adaptor protein ASC that interacts with pro-caspase-1. Procaspase-1 is activated in this complex, leading to the processing and maturation of inflammatory cytokines, like IL-1β and IL-18 . Such AIM2-ASC-Caspase-1 complex is called AIM2-inflammasome. Since the expression of AIM2 is induced by IFNs, it is likely that after DNA virus infection the host cells utilize both the TBK1-IRF3 and AIM2-inflammasome pathways to ensure a fulfilled innate response against viral infection.

Defensins are small cationic peptides that intrinsically possess antimicrobial properties and are key mediators of the innate immune system (267). It had been proposed that defensins primarily target enveloped viruses by disrupting the envelope membrane in a manner similar to their antibacterial activities. However, the recent studies demonstrates that defensins exhibit complex functions by positively or negatively modulating infection of both enveloped and non-enveloped viruses (267). Human defensins are classified into two subfamilies, $\alpha$ and $\beta$, which differ in their three disulfide bond paring. Neutrophil $\alpha$-defensins (HNPs 1-4) are synthesized in promyelocytes and the mature peptide is stored in primary granules of neutrophils (267). However, HNPs 1–3 can also be found in other immune cells, including natural killer cells, B cells, T cells, monocytes, macrophages and immature dendritic cells.

Two additional human α-defensins, human defensins 5 and 6 (HD5 and HD6), are constitutively expressed in intestinal Paneth cells but also found in the genital mucosa.

HNP release can be induced by chemokines, FCγ receptor cross linking, phorbol myristate acetate and bacterial components that activate Toll-like receptors (TLR) 2 and 5. Human β-defensins (HBDs) 1–3 are expressed by epithelial cells, monocytes, macrophages and monocyte-derived dendritic cells. HBDs expression can be induced by viruses, bacteria, microbial products, Toll-like receptor (TLR) ligands, EGF and pro-inflammatory cytokines. It has been shown that defensins are frequently induced in response to viral infection (268-270). Recent studies revealed that HD5 neutralizes JCPyV infection at early post entry step in the viral cycle by stabilizing the viral capsid and disturbance of JCPyV trafficking (271). The same effect of HD5 has been observed for BKPyV. However, due to different receptors in comparison to JCPyV, disturbance of virus trafficking occurs at the entry level thereby preventing virus entry to the host cell (272).

In conclusion, only few studies have been performed to investigate innate immune responses to JCPyV and BKPyV (237, 242, 254, 271, 272). Since both viruses, similarly to other polyomaviruses, have dsDNA as a genome, all above described DNA sensoring mechanism should be taken under consideration whilst speculation about the innate immunity to HPyV.

The innate immune response makes a crucial contribution to the activation of adaptive immunity. The inflammatory response increases the flow of lymph containing antigen and APCs into lymphoid tissues, while complement fragments on virus surface together with cells which have taken up the virus provide signals to activate lymphocytes, which receptors bind to presented antigens.

### 3.2.2 Adaptive Immune Response to Viral Infection

The induction of the adaptive immune response is activated once the virus is ingested by immature dendritic cells (DCs). These specialized phagocytic cells are localized in most tissues. The immature DCs carry receptors on its surface that recognize common features of many pathogens which enable DCs to engulf pathogen and degrade it intracellulary. When a DC takes up a pathogen in infected tissue, it becomes activated, and travels to a nearby lymph node. Viruses do not carry invariant molecules similar to those of bacteria and are rarely directly recognized by macrophages. However, viruses can still be taken up by

dendritic cells through nonreceptor-depending process. Antigens can then be presented to the lymphocytes (**Fig. 13**). Each naive lymphocyte entering the bloodstream bears antigen receptor of a single specificity. This specificity is determined by unique genetic mechanism that operates during lymphocyte development in the bone marrow and thymus to generate numerous different variants of the genes encoding the receptor molecules. Lymphocytes undergo a process akin to natural selection and only those lymphocytes that encounter an antigen to which their receptor binds will be activated to proliferate and differentiate into effector cells. Clonal selection of lymphocytes is the most important principle of adaptive immunity. The lymphocyte population comprises of the thymus-derived lymphocytes (T lymphocytes), bone-marrow-derived (B lymphocytes), and the natural killer cells (NK cells). T-lymphocytes mediate the cellular immunity and require thymus to mature before being deployed to the peripheral lymphoid organs for further antigen-mediated differentiation. A small subset of the $CD4^+$ cells, including natural regulatory cells and NK cells are already distinct differentiated cells on release from the thymus. $CD4^+$ T cells, along with $CD8^+$ T cells, comprise the majority of T-lymphocytes. CD4 T cells recognize approximately 17 amino acid peptides presented by APCs on MHC class II. After being activated and differentiated into distinct effector subtypes $CD4^+$ T cells play a major role in mediating immune response through the secretion of specific cytokines. The $CD4^+$ T cells carry out multiple functions, ranging from activation of the cells of the innate immune system, B-lymphocytes, cytotoxic T cells, as well as nonimmune cells, and also play critical role in the suppression of immune reaction. The subset of $CD4^+$ helper T cells remaining in the lymphoid organ helps B lymphocytes to respond to the microbial antigens. $CD8^+$ T cells are stimulated by 10 amino acid peptides on MHC class I molecule of APCs. As a result of clonal expansion, activated $CD8^+$ T cells rapidly increase from virtually undetectable in the naive host to levels that are readily detectable. $CD8^+$ T cells are typically cytotoxic and express enzymes such as perforin, granzyme and granulysin. After clearance of the virus $CD8^+$ T cells decline in number to a memory level. Memory $CD8^+$ T cells may be present lifelong and are able to mount rapid, heightened responses to reinfection with the certain virus.

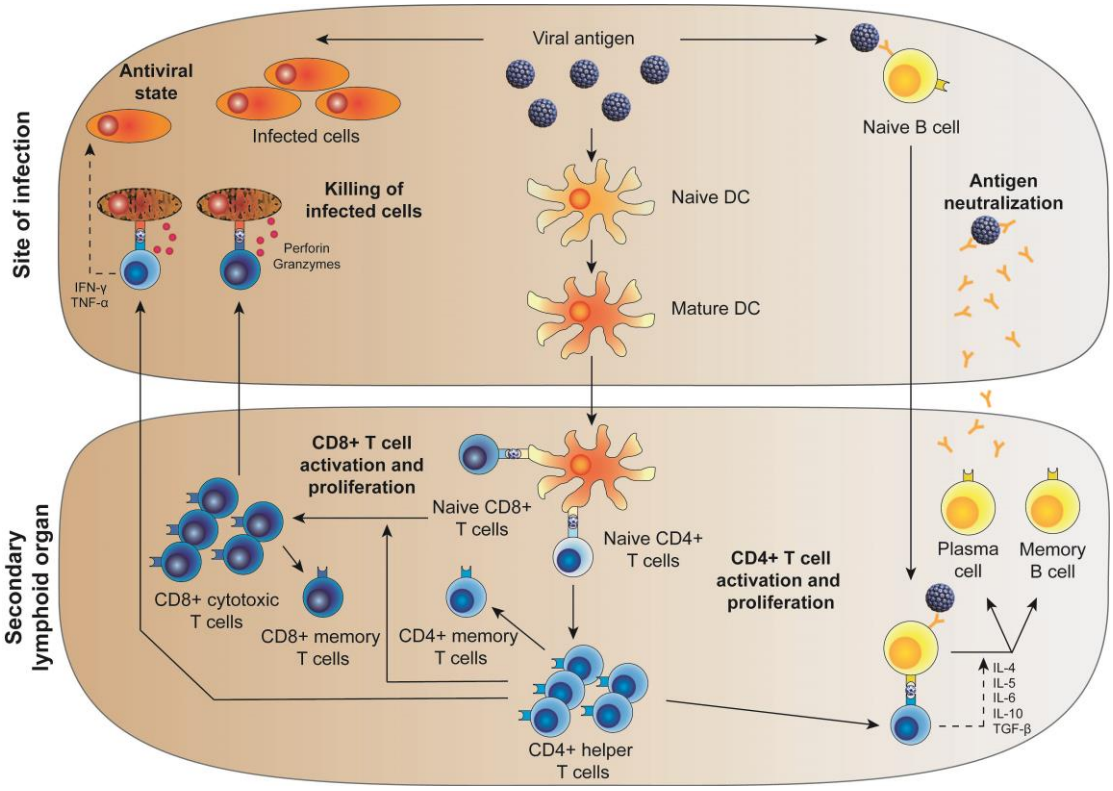


**Figure 13.** Adaptive immune responses to viral infection.

The critical event in antigen recognition by T cells is the manner the antigenic peptides are presented and thus recognized by the T cell receptor (TCR). The main molecules presenting antigen peptide are major histocompatibility complex (MHC) molecules, divided into two classes: MHC class I and II. They deliver peptides from two diverse intracellular compartments reflecting the origin of the antigen which is processed: either intracellular or taken up from the outside of the cell. MHC molecules are glycoproteins localized on the cell surface. These two classes of MHC molecules differ both in function, structure and cell distribution. While MHC class I is present on all nucleated cells, MHC class II are present mostly on specialized antigen-presenting cells.

The MHC class I molecules bind peptides derived from virus-encoded proteins in a size of up to 10 amino acids in size. Such peptides are mainly formed through degradation of cytosolic proteins by the proteasome and translocated to the ER by proteins called transporters associated with antigen processing-1 and -2 (TAP1 and TAP2) where they associate with MHC class I complex (273). At this stage, the fully folded MHC class I-peptide complex is released from the TAP complex in the ER and is transported to the plasma membrane, where the peptides are presented to appropriate $CD8^+$ T cells (**Fig. 14a**).

The MHC class II molecules bind extracellular antigens comprised of up to 17 amino acids. This occurs usually in specialized APC. Extracellular proteins are endocytosed and due to low

pH, endosomal and lysosomal proteases are activated and degrade the proteins into peptides, followed by their binding by MHC class II molecules. During their synthesis in the endoplasmic reticulum, MHC class II molecules are covalently bound to a polypeptide called the invariant chain (274). The invariant chain protects MHC class II molecule from binding unwanted peptide and targets the MHC class II-invariant chain complex to the endosomal compartment, where the invariant chain is replaced with the antigen peptide. The peptides are presented to $CD4^+$ cells on the membrane surface of APC (**Fig. 14b**).

Thus, MHC class I-peptide complexes activate $CD8^+$ T cells committed to kill, while MHC class II-peptide complexes activate $CD4^+$ T cells aimed at activating macrophages (Th1 cells) or B cells (Th2 cells).

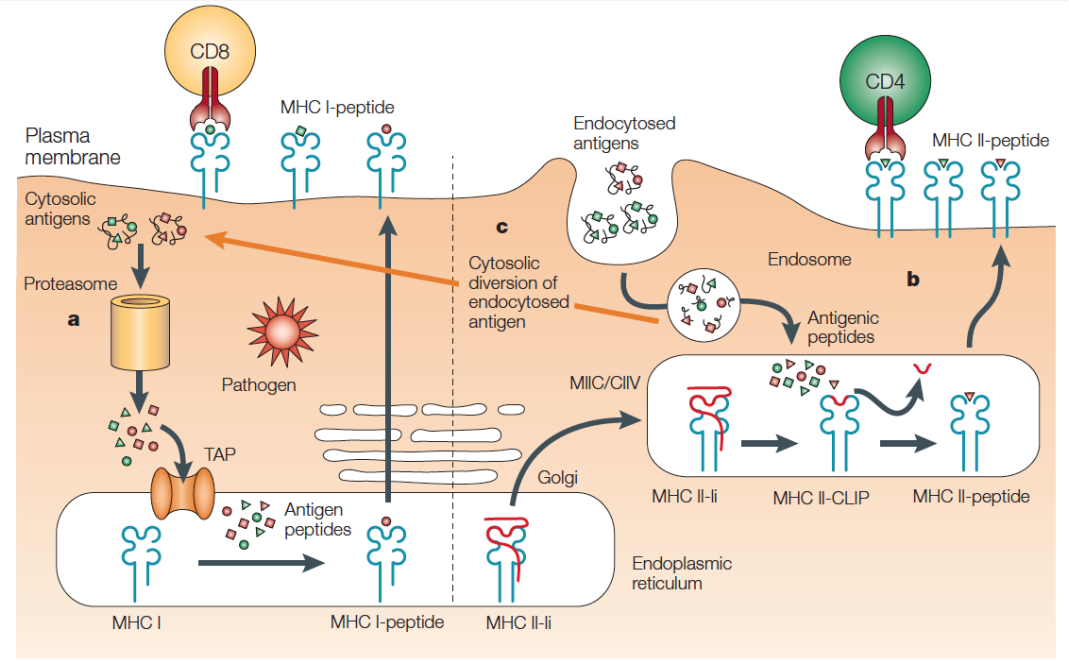


**Figure 14.** Different antigen-processing pathways for the MHC class I and class II molecules [from (275)]

However, dendritic cells can endocytose antigens from other cells and cross-present them to $CD8^+$ cytotoxic T lymphocytes. Cross-presentation is of particular importance, because it permits the presentation of exogenous antigens, which are normally presented by MHC class II on the surface of infected dendritic cells to be also presented by MHC class I without infecting the dendritic cell. Cross-presentation allows the dendritic cell to avoid using the endogenous proteasomal processing pathway, which otherwise would divert cellular resources away from MHC class II presentation processes that present endogenous antigens after infection. Such a diversion could functionally impair the dendritic cell (Fig. 14c).

Another important lymphocytes are B cells, or bone marrow-derived lymphocytes. They comprise up to 20% of all circulating peripheral lymphocytes, but can be also found in bone marrow or other lymphoid tissues, including spleen, lymph nodes, and tonsils. Produced in the bone marrow B cells can migrate to the spleen and lymph nodes in order to mature and differentiate into immunocompetent B cells. B cells are responsible for generating antibodies to specific antigens, which they bind via B cell receptors (BCR). Activation of B cells occurs through antigen recognition by BCRs and a required co-stimulatory, secondary activation signal from either helper T cells or the antigen itself. This results in in B cell proliferation and formation of germinal centers where B cells differentiate into plasma cells or memory B cells. Importantly, all B cells derived from a specific progenitor B cell are clones that recognize the same antigen epitope. Plasma cells are found in the spleen and lymph nodes and are responsible for secreting different classes of clonally unique antibodies. Following the primary response, a small number of B cells develop into memory B cells, which express high-affinity surface immunoglobulins (mainly IgG), survive for a longer period of time, and enable a rapid secondary response.

B cells are the only cells producing antibodies in order to mediate humoral response. Upon stimulation with viral antigen, B cells differentiate into plasma cells and secrete large amounts of antibodies. The antibodies circulate in the bloodstream and permeate the other body fluids, where they specifically bind to the antigen of a pathogen and mark it for elimination by phagocytosis. After the response, some of the B cells differentiate into memory B cells, which are ready to rapid response in case of re-exposure to the viral antigen. The antibody response is most of the time directed to the structural proteins of the virus (276). However, usually not all of the elicited antibodies have neutralizing activity, which inhibit the viral infection (277, 278). Neutralization is often considered as the most efficient mode of antibody-mediated defense against viral infections. During neutralization antibodies interfere with virion in many different ways including blocking viral receptors, inhibiting uptake into cells, preventing uncoating of the genomes in endosomes, or causing aggregation of virus particles. All of these mechanisms lead to virus neutralization (**Fig. 15a**). However, effector functions mediated by virus-specific non-neutralizing antibodies can also have a substantial impact on virus clearance (279, 280). Non-neutralizing antibodies can still bind to the virus/infected cell and are able to lyse the virus/infected cell through activation of complement (complement-dependent lysis). Polymerization of specific activated complement components on a foreign cell or enveloped virus leads to the formation of pores. The lipid bilayer of the cell or (enveloped) virus is disrupted (281) (**Fig. 15b**).

Antibodies can also cause opsonization, by which the marked virus is ingested and destroyed by a phagocyte (282) (**Fig. 15c**). Antibody-coated virus can be killed by a cytotoxic effector cell through a non-phagocytic process, characterized by the release of the content of cytotoxic granules or by the expression of cell death-inducing molecules (**Fig. 15d**). Effector cells that mediate ADCC include natural killer (NK) cells, monocytes, macrophages, neutrophils, eosinophils and dendritic cells (283).

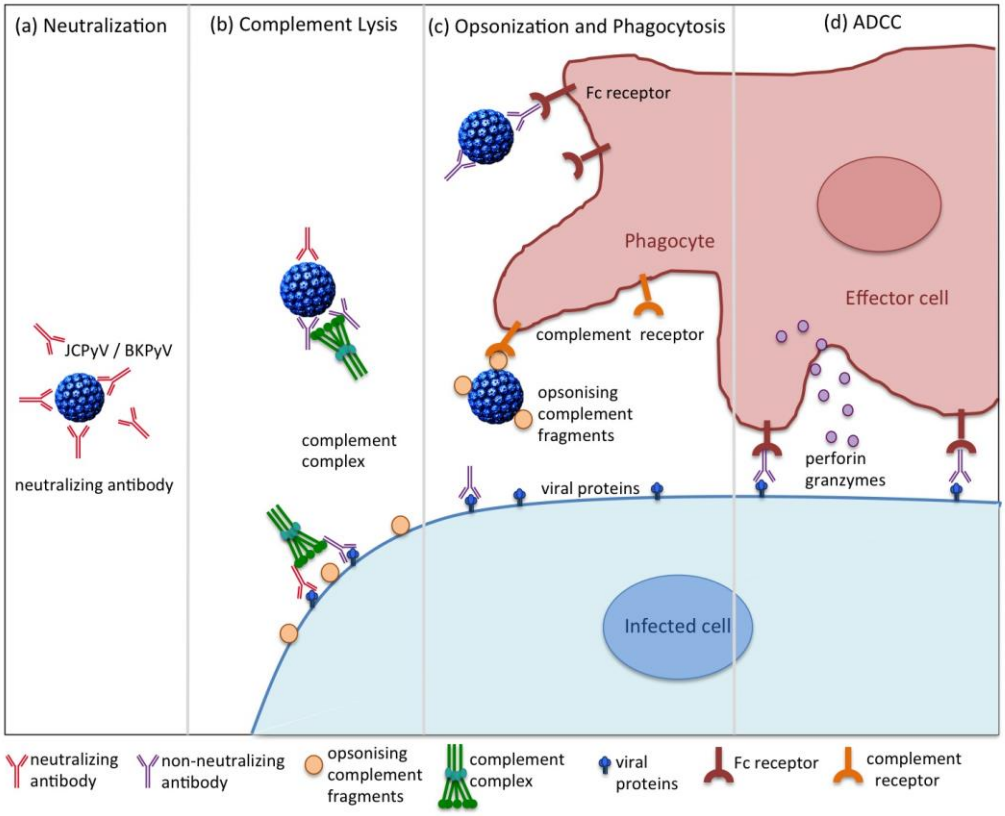


**Figure 15.** Different antibody strategies to combat a virus [modified from (276)]

### 3.2.2.1 Adaptive Immune Response to HPyVs

Polyomaviruses belong to the group of infectious non-self agents delivering PAMPs that are recognized by cell surface pattern recognition receptors PRRs on APC (192-194, 196, 284).
T cell immunity to polyomaviruses has been studied mostly for LTag and capsid protein VP1 (285-297). LTag is very suitable to examine due to its immunogenicity and capability to stimulate both T and B cell responses (298). T cell responses to LTag have been studied in selected healthy humans by stimulating isolated peripheral blood mononuclear cells (PBMCs) with purified SV40 LTag. Eventually all responded by T cell proliferation and T cell lines could have been established by LTag and nucleosome-LTag complexes (298, 299).

Because LTag from BKPyV, JCPyV and SV40 demonstrate approximately 75% amino acid homology, it might be that the data obtained for SV40 LTag do not reflect a high incidence of SV40 infected individuals, but more likely that most individuals have cross-reactive LTag-specific memory T cells (298-301). The T cell responses were caused by $CD4^+$ T cells, as demonstrated by a substantial decrease in proliferation upon adding human anti-CD4 antibodies to the cultures prior to antigenic stimulation and weak proliferation reduction after anti-CD8 treatment (300). Similar results have been observed in mice after immunization with SV40 LTag (298). The established $CD4^+$ T cell lines had the potential to induce low level anti-LTag antibody production *in vitro* when cocultured with highly purified autologous B cells (302). It has been reported that all of healthy BKPyV seropositive individuals had T cells proliferating *in vitro* as a response to antigens prepared from BKPyV-infected fibroblasts, whereas this was not the case for seronegative individuals (303). It has been also reported that BKPyV replication in healthy individuals and in immunosuppressed patients is controlled by $CD8^+$ and $CD4^+$ T lymphocytes (285, 297, 304).

A recent study investigated circulating BKPyV-specific T cells in healthy donors (HDs) by using VP1 antigen to identify BKPyV-specific $CD8^+$ T cells (296). BKPyV VP1-specific T cells circulate in the peripheral blood at low levels. Moreover, they display a resting memory phenotype and are polyfunctional upon stimulation in terms of cytokines production (296). These results consorts with lack of the virus in the blood but virus presence in distal sites, urinary tract and kidneys, implying that circulating T cells are lacking BKPyV specific-stimulation for large periods of time. Additional *in vitro* studies showed that pulsing of monocyte-derived dendritic cells with inactivated BKPyV or peptide pools covering either structural or regulatory BKPyV proteins results in generation of BKPyV-specific T cells (305, 306). Those BKPyV-specific T cells displayed both production of cytokines and cytotoxic activity. It has been reported that both VP1 and LTag responses are significantly higher in KTRs in comparison to healthy individuals (285, 307). Overall $CD8^+$ T cell responses were identified as LTag-specific rather than VP1-specific (285). In the same study, JCPyV VP1 and LTag immune responses were investigated in JCPyV-seropositive KTRs and showed that *in vitro* stimulation with BKPyV VP1 peptides induce limited JCPyV VP1 responses. However, similar responses to BKPyV LTag and JCPyV LTag were observed after *in vitro* stimulation with BKPyV LTag peptides, suggesting that BKPyV- and JCPyV- specific immune responses mediated by LTag are more conserved among HPyVs than those mediated by VP1 (285). Furthermore, LTag-specific immune responses have been shown to be correlated with the recovery from viremia in KTRs (291). This comes along with results from more recent study

where BKPyV-specific immunity to structural and non-structural BKPyV proteins at different phases of BKPyV reactivation was studied in KTRs (308). T cells specific for non-structural proteins such as LTag were detected earlier than T cells specific for structural proteins, and appearance of T cells specific for non-structural proteins correlates with recovery from BKPyV reactivation. Therefore, immunity to non-structural proteins, and not to structural proteins, are thought to be a reliable marker of recovery from BKPyV viremia (308).

The presence of JCPyV-specific $CD8^+$ cytotoxic lymphocytes among healthy and immunocompetent individuals seems to protect from PML development (309-312). It has been also shown that $CD8^+$ T cell response was significantly lower in PML progressors in comparison to survivors (313). Additionally, an early detection of JCPyV-specific $CD8^+$ T cells in PML patients seems to be associated with a better outcome and eventual higher survival (314, 315). Among multiple sclerosis patients, it has been shown that natalizumab treatment preventing T cell homing to the brain does not impair peripheral JCPyV-specific T cells responses and even increase JCPyV-specific memory or effector responses in some patients after 12 months of therapy (316). The presence of $CD4^+$ T cells seems to be necessary for an efficient immune control of PML (313). Individuals with low $CD4^+$ T cell numbers, including HIV-AIDS patients or individuals with idiopathic $CD4^+$ lymphocytopenia, have a higher risk of developing PML and a lower survival rate (310, 315, 317). Estimated 1-year survival was 48% in HIV+ patients with PML with CD4 count less than 200/µl at PML diagnosis compared to 67% in those with CD4 more than 200/µl (315). Nevertheless, PML does not affect all HIV patients with very low $CD4^+$ T cells counts (90). Surprisingly, individuals with a low $CD4^+$ T cell activity showed very strong humoral response against JCPyV. This phenomenon might be explained either by a T cell-independent virus-specific antibody production or by the establishment of B cell memory directly after primary infection (310, 318).

Cellular immune responses directed against the VP2 and VP3 capsid proteins and regulatory (sTag, Agno) proteins have also been investigated (296, 307, 308, 319-321). It has been demonstrated that VP2, VP3 and sTag proteins are targets of JCPyV and BKPyV-specific immune responses in healthy donors, KTRs and PyVAN patients. Moreover, memory T cells directed against VP1, VP2, VP3, LTag and sTag have been detected in BKPyV-seropositive KTRs (307). In the same study, memory T cells specific for VP3 were found to be more prevalent than memory T cells specific for the other BKPyV proteins in patients with a PyVAN history (307). Despite the high expression of Agno, it seems to be ignored by the immune system, since only 15% of HDs and 7.5% of KTRs are Agno seropositive (320).

## 3.3 Antibody Assays for Studying Adaptive Humoral Immunity to JC and BK Polyomaviruses

### 3.3.1 Technical Aspects of JCPyV and BKPyV Antibody Assays

The detection of JCPyV- or BKPyV-specific antibodies can be accomplished by different techniques.

Hemagglutination assay (HA) utilizes ability of JCPyV and BKPyV to bind to sialic acid structures; virus binds to sialic acid residues on RBCs and forms a lattice (hemagglutination) and can be used for rapid determination of level of virus in a sample. RBCs which are not bound by virus precipitate to the bottom of the well. However, the RBCs bound by the virus form a lattice. The titer of the virus is calculated as the highest dilution at which virus causes hemagglutination. The HA can be modified in order to investigate level of antibodies to JCPyV or BKPyV in a serum sample. The basis of hemagglutination inhibition assay (HAI) is that antibodies against the virus will prevent attachment of the virus to RBCs resulting in hemagglutination inhibition. The highest dilution of serum preventing hemagglutination is called hemagglutination inhibition titer. However, HAI fails to detect JCPyV with VP1 mutations characteristic for PML. Virus with 55F, 267F, 269F and 269Y mutations cannot agglutinate RBCs (99). Whereas for some of the mutants, e.g. 60E, 265D and 271H, hemagglutination is still possible but at much lower level. Moreover, another disadvantage is a need of removal of unspecific inhibitors from sera prior testing.

For neutralization test a serum sample is mixed with a viral suspension and incubated to allow the antibodies to react with the virus, followed by plating the mixture on virus-susceptible cells. Depending on the virus, the results of the neutralizing test can be examined in different ways, including direct microscopic examination for evidence of viral cytopathic effect, immunofluorescent staining or reduction of plaque numbers. A modified virus neutralization assay, called the log serum neutralization index (LNI), can also be used to evaluate the potential of a serum specimen to neutralize virus infectivity. In this test concentration of serum stays constant while the challenge dose of the virus is increased. The advantage of this method is that it measures the capacity of a serum to protect from virus infection because serum is usually being tested undiluted. However, because the used serum is undiluted, routinely securing volumes of serum sufficient to perform this test is difficult and mitigates against general implementation of this assay. Moreover there is a

need to remove non-specific inhibitors which naturally occurring in sera, to standardize antigen each time a test is performed, and the need for specialized expertise in proper reading the test results (322).

The current enzyme-linked immunosorbent assays (ELISAs) for JCPyV and BKPyV are usually based on either LTag or VP1 (31, 285, 302, 323-326). VP1 can be used as antigen in in a form of monomers, pentamers, or virus-like particles (VLPs) (2, 99, 327-329). Alike for BKPyV, there are currently no data comparing JCPyV HAI, anti-VP1, anti-VLP, and anti-LTag responses, except from experimental tumor exposure models (320, 325, 328, 330). However, it can be presumed that the high-level JCPyV antibody responses are directed against the viral capsid proteins due to their abundance and repetitive structure (325, 331). Moreover, based on the reports for BKPyV, some responses to sTag can be expected (90, 325). In healthy individuals, these anti-N-terminal Tag responses are hidden in the background signals, but might become detectable after high-level PyV replication or from PyV-associated tumor formation (325, 330, 332, 333).

Some studies have compared HAI and VLP-based ELISA for structural protein antibodies, but it becomes clear that the assays are not equivalent with respect to their immunological and clinical implications (334). A low percentage of tested samples showed low HAI antibody titers and high ELISA antibody titers to JCPyV or BKPyV (335). The reasons for these discordant results are unknown. However, it could be that antibody responses to epitopes other than those involved with HAI or to strain differences between the virus initiating an infection and that used in antibody assays. The major points of each antibody testing include: (1) choice, preparation, and the purity of antigens; (2) background reactivity; (3) definition of analytically significant and clinically relevant results; (4) detection and interpretation of different antibody classes and subclasses; (5) selection of most appropriate testing method; (6) appropriate cutoff to define positive and negative test results; and (7) sensitivity and specificity influenced by conformation of the epitopes (2, 71).

The choice of antigen and background reactivity has an impact on assay specificity and sensitivity. Therefore, the source of PyV virions or the recombinant viral antigens may impact the serological background activity as a result of preparative impurities from an expression system of choice.

Discrimination of seropositive and seronegative samples is highly dependent on sensitivity and specificity of the assay and the appropriate cutoff. Sensitivity is the probability that the test result will be positive when the disease is present (true-positive rate). Whereas specificity is the probability that the test result will be negative when the disease is not

present (true-negative rate). A false-positive result occurs when the assay indicates the disease, although the disease is not present. Whereas a false-negative result occurs when the assay indicates the absence of disease, although the disease is present. ELISA with low sensitivity or too low cutoff may result in false-positive readouts, whereas low specificity and too high cutoff - in false-negative readouts. This might be detrimental by underestimating disease risk (in case of false-negative serology result) or unnecessary withhold of the immunosuppressive therapy (in false-positive serology result). The antigen conformation is another important aspect of proper antibody testing. In recent years serology based on virus-like particles in enzyme immunoassays (ELISA) has become widely used in many viral systems, including polyomavirus infections (2, 14, 337).

### 3.3.2 Virus-Like Particles as the Antigen in Antibody Assays

Virus-like particles (VLPs) are multisubunit self-assembling protein structures with identical or highly related overall structure to their corresponding native viruses (338). After the first demonstration of the polyomavirus VP1 self-assembling into VLPs in the absence of viral genetic material, VLPs have been produced from a broad spectrum of enveloped and non-enveloped viruses. Until now more than 110 VLPs have been constructed from viruses belonging to 35 different families (339).

The interest in VLPs has significantly increased due to the successful development and introduction of HBV surface antigen and HPV capsid protein L1 as commercial vaccines against HBV and HPV-induced cervical cancer, respectively (340, 341). The recent reports describe high immunogenicity of VLPs via B cell activation and production of antibodies against the viral motifs presented on VLP surface (342, 343). In addition, due to a small size VLPs can be taken up by antigen-presenting cells and degraded, which ultimately leads to T cell activation (344). Moreover, due to their symmetric and highly repetitive structure, VLPs are capable of inducing strong humoral and cellular immune responses even in the absence of frequently used adjuvants (344). Furthermore, particular attention has recently been given to the development of new nanomaterials. This new area, called bionanotechnology, employs ideas and methodologies from biology, chemistry, physics, and engineering (345).

VLPs can be produced by several expression systems (339). More than half of these systems employ bacterial or insect cells, other systems use yeasts (20%), mammalian (15%) or plant cells (9%) (339).

Bacterial systems are mostly based on *Escherichia coli* strains. *E. coli* systems, based on

vector transformation, are generally accepted and widely used technology for VLP production (346). However, such a system has several disadvantages including inability to perform post-translational modifications of recombinant protein, their inability to generate the proper disulfide bonds, protein solubility problems, and the presence of endotoxins in the preparations of recombinant proteins (339, 341).

In contrast to bacteria, yeasts are able to introduce post-translational modifications of proteins, including glycosylation, phosphorylation, acetylation, ubiquitination, sumoylation (347, 348). Different yeast systems have been used for the construction of numerous VLPs. Unfortunately, they are more complex than *E. coli* systems because yeast shuttle-vectors have to be prepared first in bacteria and only then introduced to the yeast cells as plasmid vectors. Moreover, yeast-based systems provide only 30% of the properly folded protein yield obtained in *E. coli* (347, 348).

Plant systems could be a cost-effective and scalable alternative for the production of different VLPs in comparison to above mentioned bacteria- and yeast-based systems. One of the most effective plant expression systems is based on the *Agrobacterium* (339). It has been shown that tobacco and potato plants can be successfully used in production of HPV VLPs (349). Also transgenic tobacco has been successfully utilized for HBs antigen and HBc antigen VLPs (350, 351).

More than half of all of the recombinant proteins in the pharmaceutical industry are produced in different mammalian cell lines (339). Alternatively, much simpler in setup insect cell-based system has become common for VLPs expression on laboratory or industrial scale. The latter is characterized by the capacity for large-scale VLP production, fast growth rates in serum-free media, and possible post-translational modifications similar to mammalian cells.

Baculovirus expression systems enable generation of recombinant baculoviruses in order to express the protein of interest in insect cell culture (**Fig. 16**). The method is based on site-specific transposition of an expression cassette into a baculovirus shuttle vector (bacmid) propagated in *E. coli*. The system comprises of: (1) pFastBac donor plasmid allowing generation of expression construct containing the gene of interest under control of a baculovirus-specific promoter; (2) *E. coli* host strain containing baculovirus shuttle vector (bacmid) and helper plasmid, and allowing generation of recombinant bacmid by transposition of the pFastBac expression construct; (3) Sf9 *Spodoptera frugiperda* insect cells in a liquid culture. After successful transposition, the high molecular weight recombinant bacmid DNA is isolated and used for transfection into insect cells. After generation of a recombinant baculovirus stock, it can be used to infect insect Sf9 cells for large-scale

expression of the recombinant protein of interest.

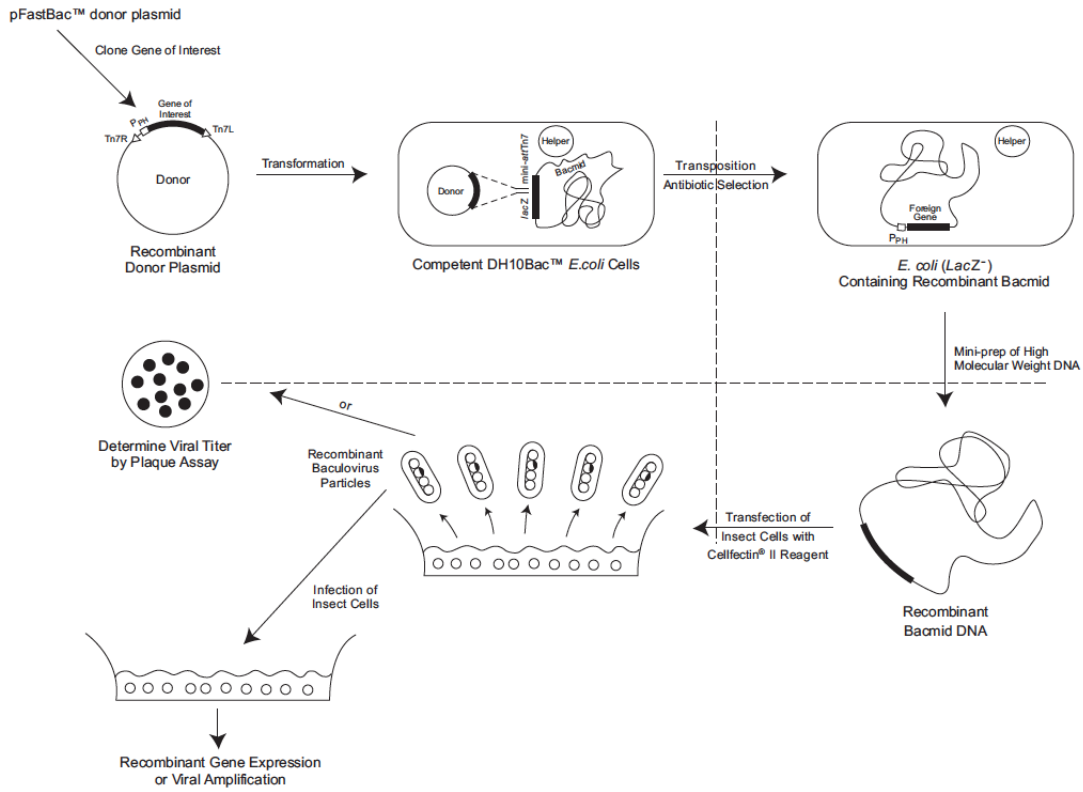


**Figure 16.** Generation of recombinant baculovirus and expression of gene of interest using baculovirus expression system and Sf9 insect cells [from Bac-to-Bac Baculovirus Expression System User Manual]

Recombinant JCPyV and BKPyV VLPs recapitulate the three-dimensional morphology of PyV virions as shown by electron microscopy and functionally by mediating hemagglutination and host cell binding (71, 335). These specific properties cannot, or can only partly, be mimicked by VP1 monomers and pentamers, respectively. Study on antibody responses in kidney transplant patients revealed significantly higher IgG ELISA levels for BKPyV VLPs in comparison to BKPyV VP1 monomers (352). In the same study the importance of the three-dimensional antigen structure was experimentally confirmed by denaturation, which caused a drop in anti-BKPyV VLP ELISA levels, whereas anti-BKPyV VP1 levels were hardly affected (352). This indicates that the respective antibody binding activities are distinguishable in humans and suggests a lower sensitivity and specificity for VP1 compared with VLPs (352). There is a greater potential for VP1 monomers and pentamers to detect cross-reacting antibodies. It has been shown indirectly by western blot on GST and GST-VP1 fusion proteins of BKPyV and JCPyV by using hyperimmune rabbit serum against BKPyV. Rabbit serum

showed strong cross-reactivity with GST-JCPyV VP1 fusion protein, and vice versa, anti-JCPyV VLP rabbit serum reacted also with GST- BKPyV VP1 chimeric protein (353). In conclusion, although seroprevalence determined with VLP-based ELISA suggest the absence of cross-reactivity between BKPyV-specific and JCPyV-specific antibodies, cross-reactivity may occur against denatured VP1 (western blot) or in assays applying monoclonal antibodies (353). VP1 cross-reactivity may therefore complicate a routine interpretation of serological results and demand additional confirmatory experiments (354).

# 4 Aims of the Thesis

The aims of the thesis are:

1. Use of virus-like particles as a tool to study the fate of primary JCPyV and BKPyV viremia.
2. Optimization of VLP-based ELISA for JCPyV and BKPyV IgG detection.
3. Development of preadsorption inhibition assay in order to precisely define JCPyV and BKPyV IgG serostatus for samples with ambiguous ELISA results.
4. Application of optimized JCPyV/BKPyV VLP-based ELISA in clinical case studies.
5. Investigation of prognostic value of ELISA utilizing as antigen either BKPyV VP1 VLPs or BKPyV LTag.

# 5 Results

## 5.1 Efficient Uptake of Blood-Borne BK and JC Polyomavirus-Like Particles in Endothelial Cells of Liver Sinusoids and Renal Vasa Recta

The renourinary tract is a well-known major persistence site for JCPyV and BKPyV. However, the initial routes of primary infection with both viruses are not well defined. Also, the fate of JCPyV and BKPyV primary viremia are unclear. JCPyV and BKPyV replication is highly specific to the human host which precludes studies of those viruses in animal model. However, α2,6-linked and α2,3-linked sialic acid structures serving as receptors for JCPyV and BKPyV, respectively, are commonly found in vertebrates, including mice. Therefore we decided to use a mouse model to investigate the fate of BKPyV and JCPyV in peripheral blood and their cellular site of uptake. Under these circumstances the mouse model simulates a non-immune host. We utilized JCPyV and BKPyV virus-like particles (VLPs) as a model system for native JCPyV and BKPyV, respectively. VLPs are multisubunit protein structures with identical overall structure to their corresponding native viruses. It is known that overexpression of major capsid protein 1 (VP1) of either JCPyV or BKPyV leads to self-assembly into VLPs, which recapitulate the three-dimensional morphology of native virus. Four different VLPs were used in the study: (1) JCPyV wild-type-VP1 VLPs; (2) BKPyV wild-type-VP1 VLPs; (3) JCPyV L55F-VP1 VLPs and (4) JCPyV S269F-VP1 VLPs. The last two carry mutations in VP1 which have been found exclusively in patients with PML. These amino acid substitutions close to binding sites for sialic acid structures enable viral interactions with cellular receptors and hence viral infectivity. Moreover, both mutants lack the ability to trigger hemagglutination which suggests that L55F and S269F mutations may influence the cell tropism of JCPyV in human by abrogating the ability to bind to sialylated molecules on a variety of peripheral cell types. Therefore we investigated if the distribution and clearance of JCPyV L55F-VP1 VLPs and JCPyV S269F-VP1 VLPs are different in comparison to JCPyV wild-type-VP1 VLPs.

OPEN ACCESS Freely available online

PLOS ONE

# Efficient Uptake of Blood-Borne BK and JC Polyomavirus-Like Particles in Endothelial Cells of Liver Sinusoids and Renal Vasa Recta

**Jaione Simon-Santamaria[1], Christine Hanssen Rinaldo[2,3], Piotr Kardas[4], Ruomei Li[1], Ivana Malovic[1], Kjetil Elvevold[1], Peter McCourt[1], Bård Smedsrød[1], Hans H. Hirsch[4,5]☯, Karen Kristine Sørensen[1]*☯**

**1** Department of Medical Biology, UiT – The Arctic University of Norway, Tromsø, Norway, **2** Department of Microbiology and Infection Control, University Hospital of North Norway, Tromsø, Norway, **3** Department of Clinical Medicine, UiT - The Arctic University of Norway, Tromsø, Norway, **4** Department of Biomedicine, University of Basel, Basel, Switzerland, **5** Divisions of Infectious Diseases and Hospital Epidemiology, University Hospital of Basel, Basel, Switzerland

## Abstract

Liver sinusoidal endothelial cells (LSECs) are specialized scavenger cells that mediate high-capacity clearance of soluble waste macromolecules and colloid material, including blood-borne adenovirus. To explore if LSECs function as a sink for other viruses in blood, we studied the fate of virus-like particles (VLPs) of two ubiquitous human DNA viruses, BK and JC polyomavirus, in mice. Like complete virions, VLPs specifically bind to receptors and enter cells, but unlike complete virions, they cannot replicate. $^{125}$I-labeled VLPs were used to assess blood decay, organ-, and hepatocellular distribution of ligand, and non-labeled VLPs to examine cellular uptake by immunohisto- and -cytochemistry. BK- and JC-VLPs rapidly distributed to liver, with lesser uptake in kidney and spleen. Liver uptake was predominantly in LSECs. Blood half-life (~1 min), and tissue distribution of JC-VLPs and two JC-VLP-mutants (L55F and S269F) that lack sialic acid binding affinity, were similar, indicating involvement of non-sialic acid receptors in cellular uptake. Liver uptake was not mediated by scavenger receptors. In spleen, the VLPs localized to the red pulp marginal zone reticuloendothelium, and in kidney to the endothelial lining of vasa recta segments, and the transitional epithelium of renal pelvis. Most VLP-positive vessels in renal medulla did not express PV-1/Meca 32, suggesting location to the non-fenestrated part of vasa recta. The endothelial cells of these vessels also efficiently endocytosed a scavenger receptor ligand, formaldehyde-denatured albumin, suggesting high endocytic activity compared to other renal endothelia. We conclude that LSECs very effectively cleared a large fraction of blood-borne BK- and JC-VLPs, indicating a central role of these cells in early removal of polyomavirus from the circulation. In addition, we report the novel finding that a subpopulation of endothelial cells in kidney, the main organ of polyomavirus persistence, showed selective and rapid uptake of VLPs, suggesting a role in viremic organ tropism.

**Citation:** Simon-Santamaria J, Rinaldo CH, Kardas P, Li R, Malovic I, et al. (2014) Efficient Uptake of Blood-Borne BK and JC Polyomavirus-Like Particles in Endothelial Cells of Liver Sinusoids and Renal Vasa Recta. PLoS ONE 9(11): e111762. doi:10.1371/journal.pone.0111762

**Editor:** Jianming Qiu, University of Kansas Medical Center, United States of America

**Received** June 23, 2014; **Accepted** September 30, 2014; **Published** November 6, 2014



**Data Availability:** The authors confirm that all data underlying the findings are fully available without restriction. The authors confirm that all data underlying the findings are fully available without restriction. All relevant data are within the Supporting Information files.

**Funding:** The work was supported by a grant from The Tromsø Research Foundation (Tromsø, Norway) to BS, and an institutional grant of the University of Basel (Basel, Switzerland) to HHH. The funders had no role in study design, data collection and analysis, decision to publish, or preparation of the manuscript.

**Competing Interests:** The authors have declared that no competing interests exist.

* Email: karen.sorensen@uit.no

☯ These authors contributed equally to this work.

## Introduction

The mucosal surfaces of the respiratory, oral-pharyngeal and gastrointestinal tracts are constantly exposed to a multitude of different viruses, only some of which eventually cause infection and disease [1]. Similarly to bacteria, viruses are likely to leak from the gut to the portal vein, and many of these viruses end up in the liver [2–8]. Some picornaviruses such as hepatitis A virus initially replicate in the intestinal mucosal surface and cause acute hepatitis when reaching the liver. Other viruses such as cytomegalovirus, Epstein-Barr virus, adenovirus, parvovirus B19, and polyomavirus cause only limited liver damage, if at all.

The liver has a critical role in pathogen detection and host defense, and contains the single largest number of macrophages, the highest concentration of natural killer cells and natural killer T cells, and the largest reticuloendothelial network in the body [9]. Of the various liver cells involved in host defense, liver sinusoidal endothelial cells (LSECs), which line the numerous sinusoids of this organ, are the least known. However, studies over the last three decades have revealed that these cells are highly active scavenger cells, removing large amounts of soluble waste macromolecules and nanoparticulate material from blood each day [10]. Thus, LSECS clearly play an important role as sentinel cells of the immune system due to: **1**) their location exposing them to 25–30% of cardiac output; **2**) their expression of several molecules involved in innate immunity such as various scavenger receptors [11–13]), the mannose receptor [14,15], toll-like receptors 2–4, 7 and 9 [16–19], and **3**) their capacity to produce cytokines and other molecules to alert their environment [16,19]. Furthermore, LSECs express Fc gamma-receptor IIb2 [20,21],

which mediates endocytosis of soluble immune complexes, and other receptors involved in virus uptake such as L-SIGN [22] and LSECtin [23]. Ligands eliminated from blood mainly by LSECs, and to a lesser by Kupffer cells (resident liver macrophages), include connective tissue turnover products, lysosomal enzymes [13,15,24–26]), modified plasma proteins and lipoproteins [27–30], soluble IgG immune complexes [31], yeast mannan [32], and adenovirus/adenoviral vectors [7,33]. Differently to macrophages, LSECs operate essentially via clathrin-mediated endocytosis, and not by phagocytosis, and the cells are equipped with an endocytic machinery capable of super-efficient uptake and degradation of the internalized ligands [10,34]. We have previously shown that this high scavenging activity of LSECs is conserved among all land-based vertebrates (amphibians, reptiles, birds, mammals) suggesting that this is a general mechanism for how soluble macromolecular waste material, and small colloidal particles, such as viruses, are cleared from blood [10,35].

Cellular uptake of virus has traditionally been studied in the context of productive infection with disease-forming virus in permissive cells. Apart from the recently reported central role of LSECs in clearing blood-borne adenovirus and adenoviral vectors [7,33], little is actually known about the role of LSECs in the uptake of virus. To explore the hypothesis that these cells act as general virus scavengers, we have studied the circulatory fate of virus-like particles (VLPs) of two non-enveloped, human DNA viruses; polyomavirus BK and JC (BKV and JCV), in mice. These viruses are approximately 40–45 nm in diameter, and are taken up in their permissive host cells via caveolin-mediated and clathrin-mediated endocytosis, respectively [36]. The VLPs represent a well-established model for endocytosis studies [37,38]. These particles are empty virus capsids consisting of 72 capsomers of polyoma viral protein 1 (VP1), which mediate the virus binding to sialic acid receptors during infection of susceptible cells [39].

BKV and JCV infect most people early in life and establish lifelong persistent infections in the renourinary tract with asymptomatic episodes of viral reactivation and shedding in urine. While reactivation of BKV may result in severe diseases in the kidney graft and bladder of kidney- and hematopoietic stem cell transplant patients [40], JCV may lead to severe demyelinating brain disease, progressive multifocal leukoencephalopathy (PML) in immunocompromised individuals, and in patients treated with novel immunomodulatory or depleting therapies for autoimmune diseases [41]. Following respiratory or gastrointestinal transmission, BKV and JCV colonize the renourinary tract as the major site of persistence. To reach the renourinary tract, a viremic phase has been postulated, but the fate of BKV and JCV when they first appear in the circulation is currently unknown. Like most polyomavirus, BKV and JCV replication is highly specific to the human host, which hampered studies of replicative disease in animal models. However, the alpha(2,3)-linked and alpha(2,6)-linked sialic acid receptors used by BKV and JCV, respectively, are widespread in vertebrates, including mice. This encouraged us to study the fate of BK- and JC-VLPs in the blood and their cellular site of uptake in a mouse model similar to other recent studies [37,42].

Here we present evidence for a central role of LSECs in the initial uptake of polyomavirus from blood. Despite the fact that mouse is not a permissive host for BKV and JCV, LSEC endocytic functions and receptor expression are highly similar between mammalian species, including humans [10,11,15,43–45], arguing that human LSECs are likely to also take up these virus particles when they first appear in the circulation. In addition, we found that the BK- and JC-VLPs rapidly distributed to a distinct population of endothelial cells in kidney medulla. These endothelial cells also avidly endocytosed a scavenger receptor ligand, suggesting that they represent a subpopulation of endothelial cells with extraordinarily high endocytic activity.

## Materials and Methods

### Ethics statement

All animal experiments were approved by the Norwegian National Animal Research Authority (NARA) (approval IDs: ID-1912, ID-2775, ID-4720, ID-4894). The substances used for mouse anesthesia were either 1) a combination of tiletamine hydrochloride (Zoletil forte vet, Virbac) and xylazine (Narcoxyl vet, Intervet), or 2) a combination of fentanyl/fluanisone (Hypnorm, VetaPharma) and midazolam (Dormicum, Roche). The mice were euthanized in 100% $CO_2$, while anesthetized as described above.

### Animals

Wild-type C57BL/6 male mice were obtained from Charles River laboratory (France). Mannose-receptor knock-out ($MR^{-/-}$) C57BL/6 mice [46] were kindly provided by Professor Michel Nussenzweig, The Rockefeller University, New York, NY. The $MR^{-/-}$ status was tested by polymerase chain reaction [46]. The animals were housed in rooms specially designed for mice, with 12 h/12 h day-night cycle, and free access to water and food (standard chow, Scanbur BK, Nittedal, Norway).

### Chemicals and reagents

Liberase TM (collagenase) was from Roche Applied Science (Oslo, Norway), Iodogen™ from Pierce Chemicals (Rockford, IL), and carrier-free Na125I from PerkinElmer Norge AS (Oslo, Norway). Bovine serum albumin was from MP Biomedicals (Solon, OH), bovine collagen type I (Vitrogen 100) from Cohesion Technologies (Palo Alto, CA), and Percoll™ and PD-10 columns (Sephadex G-25) from GE Healthcare (Uppsala, Sweden). Roswell Park Memorial Institute (RPMI) 1640 cell culture medium (supplemented with 20 mM sodium bicarbonate, 0.006% penicillin, and 0.01% streptomycin) was from Sigma-Aldrich (St Louis, MO), and Falcon cell culture plates from BD Biosciences (San Jose, CA). Draq5 was from Biostatus limited (Leicestershire, UK). Antibodies and suppliers are listed in Table 1.

### Cells

Hepatic non-parenchymal liver cells (NPCs) were prepared by collagenase (Liberase) perfusion of mouse livers, followed by low-speed differential centrifugation to remove hepatocytes, and density sedimentation of the NPCs on 25%–45% Percoll gradients to collect LSEC and Kupffer cells, as described in [47]. Purified LSECs (>90% purity) were obtained after a panning step (8 min, 37°C), to remove Kupffer cells. Primary cell cultures were established on glass cover slides (mixed LSEC and Kupffer cells), and in Falcon plates (LSECs), pre-coated with 2.7 μg/ml collagen type I and maintained in serum-free RPMI-1640 medium at 37°C at 5% $CO_2$. The cultures were washed 40 min after seeding, and allowed to continue spreading for approximately 1 h before use. Seeding of $3\times10^5$ LSEC/$cm^2$ gave confluent monolayers, with approximately $1.5\times10^5$ cells per $cm^2$.

### Virus-like particles (VLPs)

BK- and JC-VLPs were prepared as described previously [48]. Briefly, BK- and JC-VLPs were isolated from Sf9 insect cells infected with recombinant baculovirus encoding Dunlop BK-VP1 or Mad-1 JC-VP1 capsid protein. Recombinant baculoviruses containing PML variants of JC VP1 sequences L55F or S269F

**Table 1.** Antibodies and lectins used in the study.

| Antigen | Host | Clone | Isotype | Source | Dilution |
|---|---|---|---|---|---|
| BK-VP1 | Rabbit | Antiserum | - | [53] | 1:1600 |
| Mannose receptor (CD206) | Goat | Polyclonal | IgG | R&D Systems, AF2534 | 1 μg/ml |
| F4/80 | Rat | Cl:A31 | IgG2b | AbD Serotec, MCA497G | 10 μg/ml |
| CD31 | Rat | MEC13.3 | IgG2a | Biolegend, 102502 | 5 μg/ml |
| CD68 | Rat | FA-11 | IgG2a | Abcam, ab53444 | 10 μg/ml |
| CD163 | Rat | ED2 | IgG1 | AbD Serotec, MCA342GA | 10 μg/ml |
| Meca 32 | Rat | - | IgG2a | Antibodies online ABIN298904 | 10 μg/ml |
| Biotinylated *Sambucus nigra* agglutinin | - | - | - | Vector Laboratories B-1305 | 10 μg/ml |
| Biotinylated *Maackia amurensis II* hemagglutinin | - | - | - | Vector Laboratories B-1265 | 10 μg/ml |

Secondary antibodies: Alexa488-, Alexa546-, or Alexa555- anti-rat, anti-rabbit or anti-goat IgG (H+L), raised in donkey, goat, or rabbit, all diluted 1:500 (Life Technologies; Catalog No: A11006, A11008, A11055, A11081, A11010, A21431, A21434, A21428).
Positive lectin labeling was visualized by Alexa555-streptavidin, diluted 1:200 (Life Technologies; Catalog No S-21381).
doi:10.1371/journal.pone.0111762.t001

were obtained by site specific mutagenesis PCR using the following primers: L55F-Fwd (5′-ACC CAG ATG AGC ATT TTA GGG GTT TTA G-3′) and L55F-Rev (5′-CTA AAA CCC CTA AAA TGC TCA TCT GGG T-3′), S269F-Fwd (5′-TAA CAG ATC TGG TTT CCA GCA GTG GAG A-3′) and S269F-Rev (5′-TCT CCA CTG CTG GAA ACC AGA TCT GTT A-3′), respectively. Infected Sf9 cells were disrupted by sonication and glass mortar and pestle treatment. VLPs were purified from cellular lysate by CsCl gradient and stored in buffer consisting of 150 mM NaCl, 10 mM Tris-HCl pH 7.4 and 1.0 mM $CaCl_2$. The 3-dimensional structure and integrity of VLPs was confirmed by transmission electron microscopy (**Figure 1**). In short, JC-VLPs or BK-VLPs in 0.9% NaCl were placed on discharged pallodium coated mesh grids for 2 min; then washed twice with double distilled water, and once with freshly made 2% uranyl acetate. Another drop of 2% uranyl acetate was added for 10 sec. The grids were gently washed on drops of double distilled water and air dried before electron microscopy. The images were recorded in a FEI CM100 TEM transmission electron microscope (FEI, OR, USA), operating at 80 kV, and equipped with Veleta digital CCD camera (Olympus, Germany).

## Ligand labeling procedures

VLPs in phosphate buffered saline (PBS) were labeled with carrier-free $Na^{125}I$, using Iodogen as described by the manufacturer (Pierce Chemicals), and separated from unbound $^{125}I$ on a PD-10 column. The resulting specific radioactivity was approximately $4-7\times10^6$ cpm per μg protein. $^{125}I$-VLPs for injections were mixed with 0.9% NaCl to a final concentration of approximately 0.5 μg protein/100 μl (= dose injected per mouse).

Fluorescein isothiocyanate-labeled formaldehyde-denatured bovine serum albumin (FITC-FSA) was prepared by incubating FSA and FITC in sodium carbonate buffer (0.5 mol/L, pH 9.5) at a protein-dye ratio of 4:1 at 4°C overnight, and dialyzed against PBS.

## Blood clearance and organ distribution of radiolabeled VLPs

$^{125}I$-BK-VLP, $^{125}I$-JC-VLP, $^{125}I$-JC-$VLP_{L55F}$, or $^{125}I$-JC-$VLP_{S269F}$ (approximately 0.5 μg protein) were injected into the tail vein of anaesthetized mice (n = 3–5 per group). Immediately thereafter blood samples (5 μl) were collected over short time intervals from the tail tip, mixed with 0.3 ml of 13 mM citric acid, after which 0.3 ml 2% bovine serum albumin in water and 0.6 mL of 20% (wt/vol) trichloroacetic acid were added to the samples to precipitate non-degraded protein. Acid-soluble radioactivity represented degraded ligand [25]. To test if the higher doses of VLPs injected for immunohistochemistry would influence blood clearance and organ distribution, non-labeled JC-VLPs (15 μg = dose used for immunohistochemistry) were injected simultaneously with $^{125}I$-JC-VLPs (0.5 μg). This did not change the blood clearance or organ distribution pattern of the radiolabeled ligand. In some

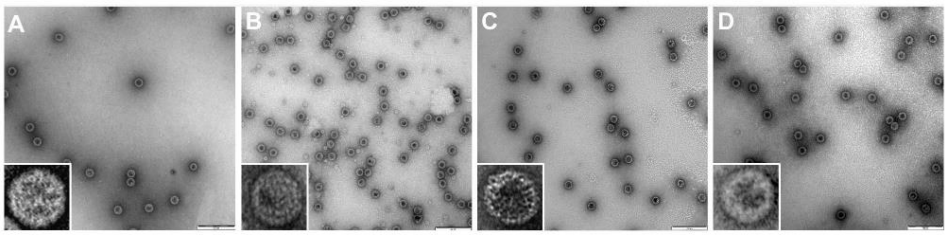


**Figure 1. Electron microscopy of BK- and JC-virus like particles (VLPs).** The figure show transmission electron micrographs of negatively stained BK- and JC-VLPs constructed from BK-VP1 or JC-VP1 proteins: A) BK-VP1 VLPs (Dunlop strain); B) JC-VP1-Mad-1 VLPs; C) JC-VP1-L55F VLPs; D) JC-VP1-S269F VLPs. Scale bars: 200 nm.
doi:10.1371/journal.pone.0111762.g001

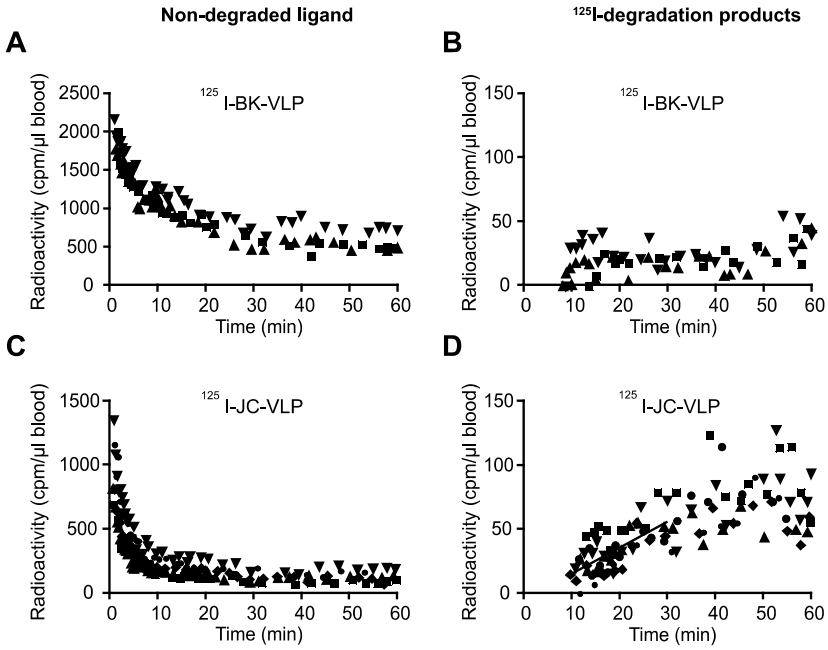


**Figure 2. Blood clearance and subsequent in vivo degradation of BK- and JC-virus like particles (VLPs).** Mice were injected intravenously with approximately 0.5 µg of $^{125}$I-BK-VLPs (n = 3; A, B), or $^{125}$I-JC-VLPs (n = 5; C, D), and blood samples taken at the indicated time points and analyzed for $^{125}$I-labeled degradation products and intact ligand [15]. Panels A and C show decrease of intact ligand in blood as a function of time. Panels B and D show increase in degradation products released into the blood with time. Results are given as cpm per µl blood. Different symbols refer to separate animals. cpm, counts per minute. The slope of line drawn in panel D represents the average rate of release of degradation products in the 10–30 min period after ligand injection where this release followed approximate first order kinetics.
doi:10.1371/journal.pone.0111762.g002

animals FSA (0.8 mg protein in100 µl 0.9% NaCl) was injected immediately before the administration of radiolabeled ligand to check for inhibition of blood clearance.

At the end of the monitoring period (10 min or 60 min) the anaesthetized animals were euthanized with 100% $CO_2$. The abdomens and thoraces were opened, and the animals were perfused via the left cardiac ventricle (outlet via the right atrium) with PBS to remove free tracer from the vasculature before the organs were excised and analyzed for radioactivity. The amount of tracer recovered was considered the sum of radioactivity of individual organs and carcass without organs.

## Hepatocellular distribution of $^{125}$I-VLPs

$^{125}$I-BK-VLP, $^{125}$I-JC-VLP, $^{125}$I-JC-VLP$_{L55F}$, or $^{125}$I-JC-VLP$_{S269F}$ (approximately 0.5 µg protein) was injected into the tail vein of anaesthetized mice (n = 3 per group). Ten minutes after the injection the animals were euthanized with 100% $CO_2$ and liver cells isolated by collagenase perfusion of liver via the portal vein, before separating the dispersed liver cells into hepatocytes and NPCs [47]. All steps during cell isolation and separation, except the liver perfusion step, were carried out on ice/below 4°C. Radioactivity in the hepatocyte and NPC fractions was measured in a Packard Gamma Counter. Cell numbers were assessed by cell counting in a hemocytometer.

**Table 2.** Rate of blood clearance of BK- or JC virus-like particles (VLPs) in mouse.

| Ligand | $t_{1/2}$ α (min)* | $t_{1/2}$ β (min)* | Fraction (%) eliminated in α phase | Fraction (%) eliminated in β phase |
|---|---|---|---|---|
| $^{125}$I-BK-VLP | 2.06±0.90 | 42.85±9.51 | 39.18±6.30 | 60.82±6.30 |
| $^{125}$I-JC-VLP | 1.17±0.11 | 46.08±37.20 | 75.70±3.84 | 24.30±3.84 |
| $^{125}$I-JC-VLP$_{L55F}$ | 1.28±0.26 | 25.16±12.76 | 79.21±2.75 | 20.80±2.75 |
| $^{125}$I-JC-VLP$_{S269F}$ | 1.06±0.30 | 41.81±7.62 | 70.92±11.60 | 29.08±11.60 |
| $^{125}$I-BK-VLP+FSA | 0.91±0.71 | 33.5±7.69 | 56.17±26.73 | 43.89±26.73 |
| $^{125}$I-JC-VLP+FSA | 1.04±0.11 | 31.13±8.50 | 85.62±2.78 | 14.37±2.78 |

N = 3 in all groups except $^{125}$I-JC-VLP where n = 5. Results are given as mean ± SD.
*$t_{1/2}$ α and $t_{1/2}$ β were calculated as described in [52].
doi:10.1371/journal.pone.0111762.t002

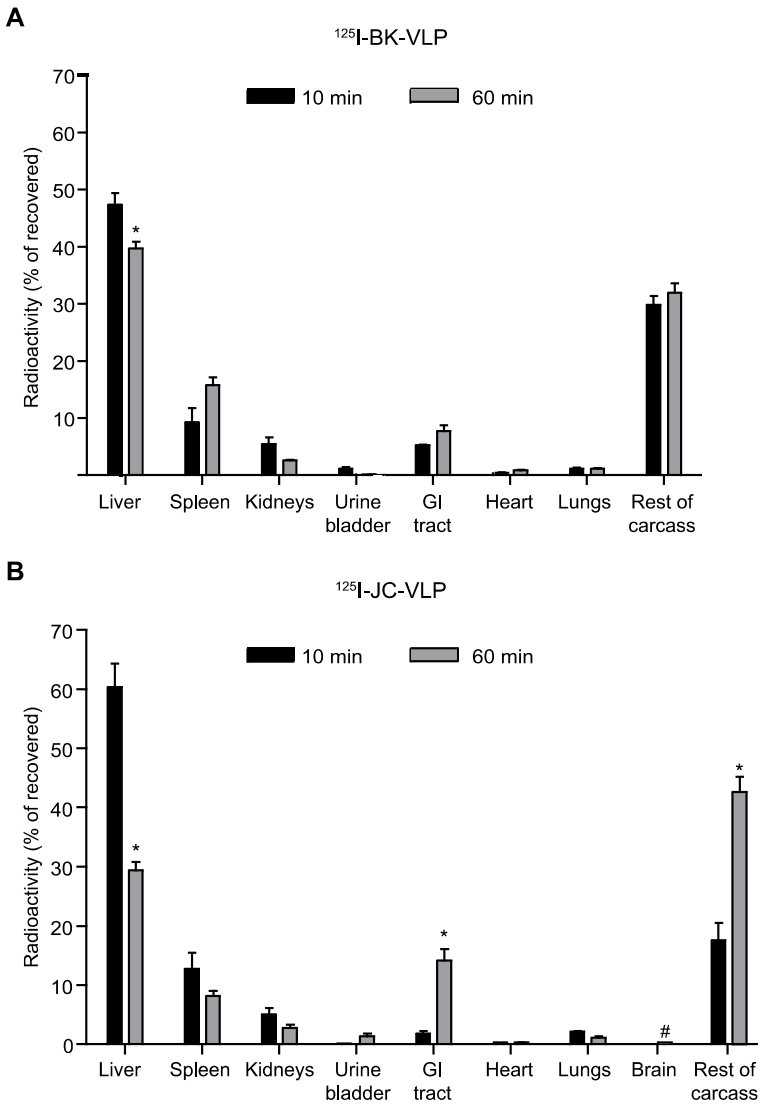


**Figure 3. Anatomical distribution of $^{125}$I-labelled BK- and JC-VLPs.** Mice were injected intravenously with $^{125}$I-labelled BK-VLPs (A) or JC-VLPs (B), euthanized after 10 min (black bars; n = 3) or 60 min (grey bars; n = 3 in A; n = 5 in B), and organs and tissues analyzed for radioactivity. The mice used in the circulatory half-life study (Figure 2) were included in this anatomical distribution study (60 min values). Total recovered radioactivity in all tissues at the given time points was taken as 100%. Error bars represent SEM. *Statistically significant difference ($p<0.01$) between tissue radioactivity at 10 min versus 60 min. # Brain radioactivity was measured at 60 min, only. GI tract, gastrointestinal tract (stomach and intestines including mesenterium).
doi:10.1371/journal.pone.0111762.g003

## Immunohistochemistry and lectin histochemistry

Non-labeled BK-VLPs or JC-VLPs (13–18 µg protein per mouse) was injected into the tail vein of anaesthetized mice (n = 3–5 per ligand). The animals were euthanized after 7–15 min, then perfused with PBS through the left cardiac ventricle to remove blood and thereafter with 4% paraformaldehyde (PFA) in PBS with 0.02 M sucrose. The perfusion fixed tissues were dehydrated, paraffin embedded and sectioned. In some animals, FITC-FSA (50 µg protein per mouse) was injected into the tail vein 5 min after injection of 10 µg JC-VLP, JC-VLP$_{L55F}$, or JC-VLP$_{S269F}$, and the mice euthanized 10 min thereafter, before perfusion fixation and tissue preparation for immunohistochemistry as described above. Antigen retrieval was achieved by 30 min microwaving in citrate buffer, pH 6. Blocking buffer was 5% goat serum or 1% BSA in TBS and 0.05 M Tween 20, pH 8.4. Sections were incubated overnight (37°C) with primary antibodies (**Table 1**) or non-immune IgG diluted in blocking buffer, washed and incubated with secondary antibody in blocking buffer for 1 h at room temperature. Nuclear stain was Draq5 (diluted 1:1000 in PBS). Sections were analysed in a Zeiss LSM 510 confocal laser scanning microscope (Carl Zeiss, Germany).

**Lectin histochemistry on tissue sections.** Biotinylated lectins, *Sambuccus nigra* agglutinin (SNA), and *Maackia amurensis* hemagglutinin (MAH), were purchased from Vector Labo-

**Table 3.** Liver uptake of BK- and JC-VLPs from blood takes place in NPCs.

| | Ratio of radioactivity in NPCs versus hepatocytes after injection of $^{125}$I-BK-VLPs | | Ratio of radioactivity in NPCs versus hepatocytes after injection of $^{125}$I-JC-VLPs |
|---|---|---|---|
| Mouse 1 | 6.5: 1 | Mouse 1 | 22.1: 1 |
| Mouse 2 | 6.3: 1 | Mouse 2 | 29.8: 1 |
| Mouse 3 | 26.5: 1 | Mouse 3 | 22.3: 1 |
| Average | 13.1: 1 | Average | 24.8: 1 |

The mice were injected intravenously with $^{125}$I-labelled VLPs, approximately 0.5 μg per animal, and euthanized after 10 min. Liver cells were then isolated by *in situ* perfusion with collagenase, and separated by low-speed differential centrifugation and subsequent density centrifugation on a Percoll gradient [47]. Radioactivity (counts per minute) was measured in the purified hepatocyte fraction, and in the NPC fraction enriched in LSECs and Kupffer cells.
doi:10.1371/journal.pone.0111762.t003

ratories (Vector Laboratories Inc, CA, USA), and Alexa555-streptavidin from Life Technologies (**Table 1**). SNA recognizes alpha(2,6)-linked sialic acids, and MAH recognizes alpha(2,3)-linked sialic acids [49]. Lectin labeling of paraffin tissue sections of liver, kidney and spleen were done according to the instructions from Vector Laboratories.

### Endocytosis experiments in isolated liver cells

**Confocal microscopy.** Primary NPC cultures, enriched in LSECs with approximately 10–20% Kupffer cells, were established on collagen coated glass cover slides. Since LSECs rapidly lose their *in vivo* uptake functions after isolation [50] endocytosis experiments were performed under serum-free conditions within 4 h of plating. Antibody markers for LSECs and Kupffer cells are listed in **Table 1**. The cells were incubated with BK-VLP, JC-VLP, or BKV for 30 min-1 h, washed, fixed in 4% PFA in PBS/0.02 M sucrose for 15 min, immune labeled, and subjected to confocal laser scanning microscopy.

**Immune EM.** Purified LSECs (approximately 1.5 million cells in 8 $cm^2$ Falcon wells) were incubated with 2.06E+10 genomic equivalents of CsCl gradient purified BKV in 1 ml serum-free RPMI 1640 medium for 2 h, washed in PBS and fixed in 4% formaldehyde in 200 mM Hepes buffer, pH 7.5, overnight, embedded in gelatin and 2.3 M sucrose, and snap frozen in liquid nitrogen. Immune labeling of ultrathin cryosections was performed as described [51]. Positive BK-VP1 labeling was detected by protein A-conjugated 10 nm gold complexes. The dried sections were examined in a JOEL JEM 1010 transmission electron microscope (JOEL, Tokyo, Japan) operating at 80 kV. Control experiments were included in parallel by omission of the primary antibody.

### Statistics and pharmacokinetic analyses

The statistical calculations (Mann-Whitney U test, ANOVA two-way analysis of variance) were performed with GraphPad Prism (GraphPad Software Inc. San Diego, CA). Clearance kinetics were analyzed as described [52].

## Results

### Removal of blood-borne BK- and JC-virus like particles (VLPs) was rapid, with JC-VLPs being cleared more efficiently than BK-VLPs

BK-VLPs and JC-VLPs were radiolabeled and injected via the tail vein. The rate of blood clearance of $^{125}$I-BK-VLP and $^{125}$I-JC-VLP is shown in **Figure 2A, C**. Semi-logarithmic decay plots revealed a biphasic pattern of elimination from blood, with an initial rapid $t_{1/2}$ α of 1–2 min for both ligands (**Table 2**). During this early phase the uptake from blood of $^{125}$I-BK-VLP and $^{125}$I-JC-VLP were 39% and 76%, respectively, revealing a considerably more effective initial blood clearance of JC-VLP than BK-VLP. After 60 min approximately 30% of the BK-VLP associated radioactivity was still in the circulation (**Figure 2A**), suggesting that BK-VLPs may interact with some unknown blood factor(s) protecting them from being taken up. In contrast, only 10% of JC-VLP associated radioactivity was left in blood after 30 min (**Figure 2C**).

Intracellular degradation of $^{125}$I-labeled proteins normally generates $^{125}$I-tagged low molecular mass degradation products that are released from the cells, and can be measured in blood following trichloroacetic precipitation of intact proteins [25]. Acid soluble $^{125}$I-degradation products appeared in blood 10 min after injection of the radiolabeled VLPs (**Figure 2B, D**). In agreement with the more efficient blood clearance of JC-VLPs, more degradation products were released to blood after injection of $^{125}$I-JC-VLPs than after $^{125}$I-BK-VLP injection in the 60 min monitoring period.

### BK- and JC-VLPs distributed to liver, with a minor uptake in spleen and kidney

To minimize the escape of label from the site of uptake due to intracellular ligand degradation, organ distribution of radiolabeled ligands was measured already 10 min after injection. At this point, the majority of the $^{125}$I-BK-VLP (48%) and $^{125}$I-JC-VLP (60%) associated radioactivity was found in liver, whereas spleen and kidneys contained 9% and 5% of the $^{125}$I-BK-VLPs, and 12% and 5% of the $^{125}$I-JC-VLPs, respectively (**Figure 3**).

To investigate the kinetics of organ distribution the VLPs following administration, the liver-associated radioactivity was followed from 10 to 60 min after injection. For $^{125}$I-BK-VLP, liver-associated radioactivity decreased only slightly (**Figure 3A**), which may reflect that cellular uptake and degradation overlap due to the slower blood clearance of BK-VLP. In contrast, for $^{125}$I-JC-VLP, the liver-associated radioactivity decreased from 60% to 30% of total recovered radioactivity during the same time period (**Figure 3B**), indicating effective hepatocellular degradation of JC-VLP. A corresponding increase of radioactivity in the gastrointestinal tract (including mesenterium and lymph nodes) and the rest of carcass in the same period was judged to be caused by redistribution of degradation products, which is commonly noted following administration of $^{125}$I-labeled ligands [26].

To measure the relative contribution of different liver cells in the VLP uptake mice injected intravenously with $^{125}$I-labelled BK- or JC-VLPs were sacrificed after 10 min for liver cell isolation and separation into hepatocytes and NPCs, the latter consisting mainly of LSECs and some Kupffer cells, as described in Materials and

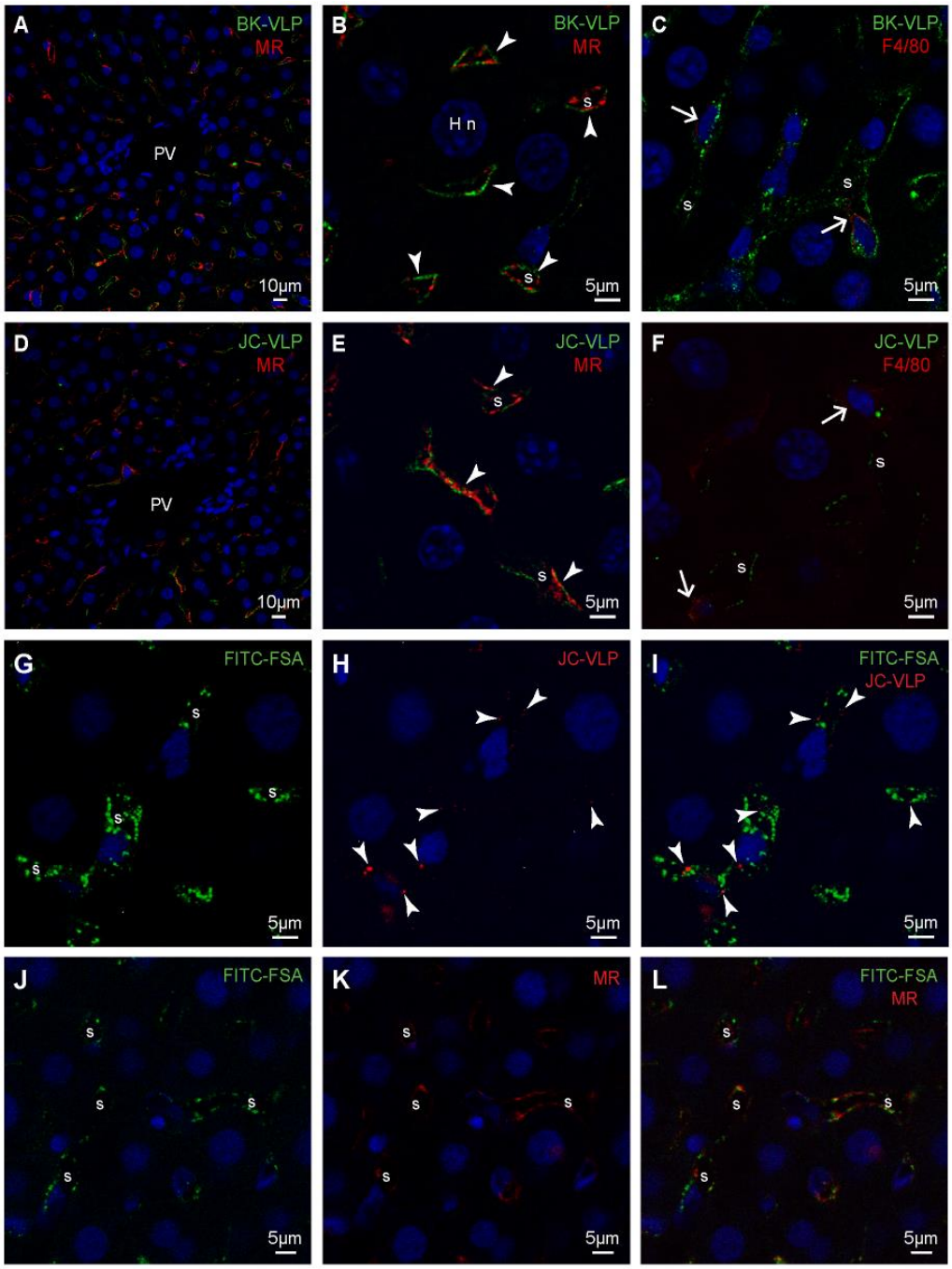


**Figure 4. Liver cell distribution of BK- and JC-VLPs after uptake from blood.** Panels A–F: Mouse livers were perfusion fixed 15 min after intravenous injection of BK-VLPs (A–C), or JC-VLPs (D–F). Paraffin embedded tissue sections were double immune labeled using a rabbit antiserum against BK-VP1 [53], and antibodies against the mannose receptor (MR), which is an LSEC marker in mouse liver [26], or F4/80 (Kupffer cell marker). Antibodies are listed in Table 1. The VP1 staining (green), indicative of BK-/JC-VLP uptake, showed a typical LSEC pattern (A, D, overview; B, E, close ups), as evidenced by similar localization of green VP1 and red MR staining along the sinusoids (arrowheads in B, E; overlap of red and green fluorescence is shown in yellow). Some BK- and JC-VLP uptake was also observed in F4/80 positive (red) Kupffer cells (arrows in C, F). PV, portal vein; S, sinusoid; Hn, nucleus of hepatocyte. Panels G–L: In G–L, FITC-labeled formaldehyde-denatured serum albumin (FITC-FSA) was injected into the tail vein 5 min after intravenous injection of JC-VLPs to functionally label the endothelium of the liver sinusoids [54,62]. Ten min thereafter the animals were euthanized, tissues perfusion fixed, paraffin embedded and prepared for immune histochemistry. Panels G-I show the distribution of FITC-FSA (green) and JC-VLP (red, arrowheads) in liver sinusoids (s). Panels J–L show similar distribution of FITC-FSA (green) and MR expression (red) in the sinusoids, s.
doi:10.1371/journal.pone.0111762.g004

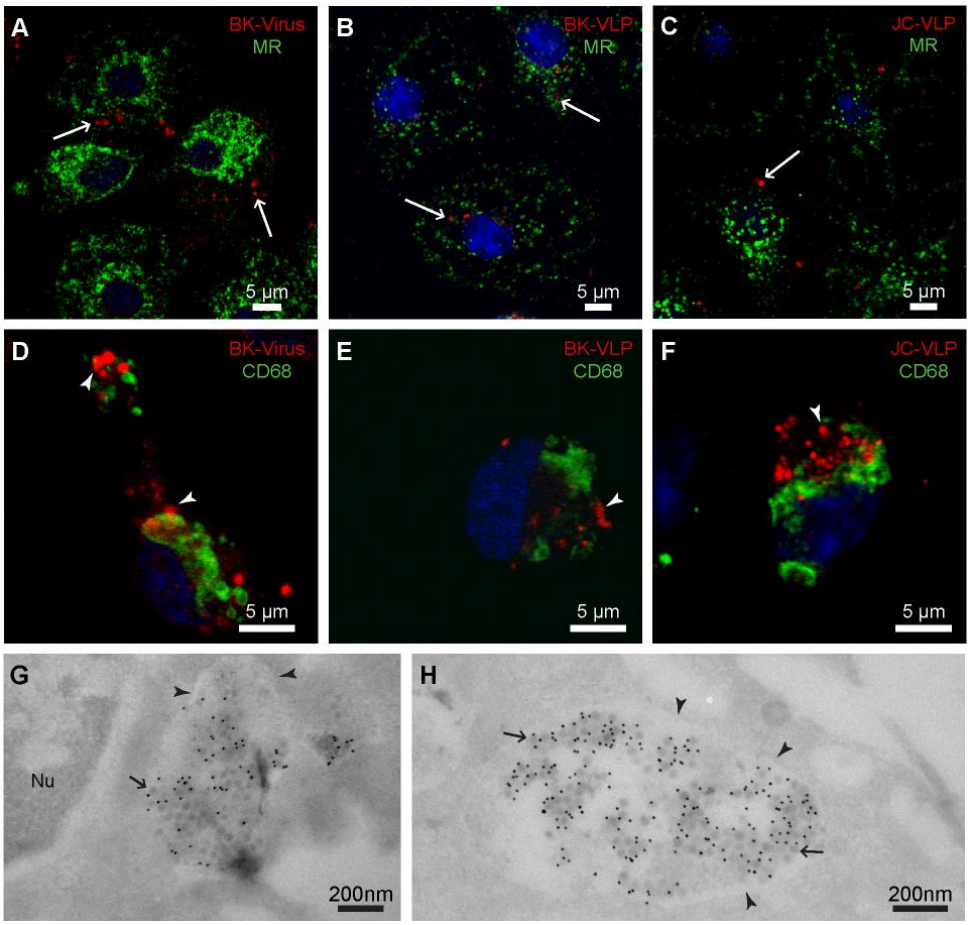


**Figure 5. In vitro endocytosis of BK- and JC-VLPs, and BK virions in liver sinusoidal cells.** Freshly isolated non-parenchymal liver cells (mixed LSEC and Kupffer cell cultures) were incubated at 37°C for 30 min with BK virions (A, D), or for 1 h with 10 µg/ml BK-VLPs (B, E), or JC-VLPs (C, F), fixed, and double immune labeled with a rabbit anti-BK-VP1 antiserum (red fluorescence) and antibodies against the mannose receptor (MR; LSEC marker; shown in green), or CD68 (Kupffer cell marker; green). Antibodies are listed in Table 1. Uptake of BK virions and BK-/JC-VLPs was observed both in isolated LSECs (arrows, A–C) and Kupffer cells (arrow heads, D–F). Panels G–H: Cryo-immune electron microscopy of BK virion uptake in LSEC membrane-bound vesicles. Purified LSEC cultures were incubated with BK virions for 2 h at 37°C. Positive BK-VP1 staining was visualized by protein-A-10 nm gold particles (black dots). Arrowheads points to vesicular membranes, and arrows to virus particles. Nu, nucleus.
doi:10.1371/journal.pone.0111762.g005

Methods. The liver radioactivity was mainly associated with the NPC fraction (**Table 3**).

## The liver uptake of BK- and JC-VLPs took place mainly in the sinusoidal endothelium

To identify the cellular distribution of VLPs in liver, non-labeled BK-VLPs or JC-VLPs were injected intravenously, and organs harvested after 7–15 min, fixed, paraffin embedded, and processed for immunohistochemistry using a rabbit antiserum against BK-VP1 [53] (**Table 1**) that cross-reacts with JC-VP1.

In liver, BK- and JC-VLP staining was observed along the hepatic sinusoids, colocalizing with cells expressing the mannose receptor (LSEC marker) (**Figure 4A, B, D, E; Figure S1**), or in cells that had endocytosed the scavenger receptor ligand FITC-FSA, a functional LSEC marker [30,54] (**Figure 4G–I**). In C57BL/6 mouse liver, the mannose receptor is expressed in LSECs but not in Kupffer cells [26]. Some uptake of BK- and JC-VLPs was also seen in F4/80 positive Kupffer cells (**Figure 4C, F**), whereas no BK- or JC-VLP positive staining was observed in hepatocytes, endothelial cells of portal venules or arteries, bile ducts or other liver structures.

To characterize in greater detail the cells involved in the hepatic uptake of polyomavirus, freshly isolated liver NPCs were incubated with infectious BKV, non-labeled BK-VLPs, or JC-VLPs for various time periods (30 min–1 h), immune labeled and subjected to confocal microscopy (**Figure 5A–F**). Both LSECs and Kupffer cells took up BK- and JC-VLPs, and BKV *in vitro*. Results were confirmed by double labeling with anti-BK-VP1 antiserum and antibodies against the mannose receptor (LSEC marker in liver [26]; **Figure 5A–C; Figure S2**) or CD68 (Kupffer cell marker; **Figure 5D–F**). Cryo-immune electron microscopy of purified LSEC cultures incubated with infectious BKV for 2 h showed virus accumulation in membrane-bound compartments (**Figure 5G, H**).

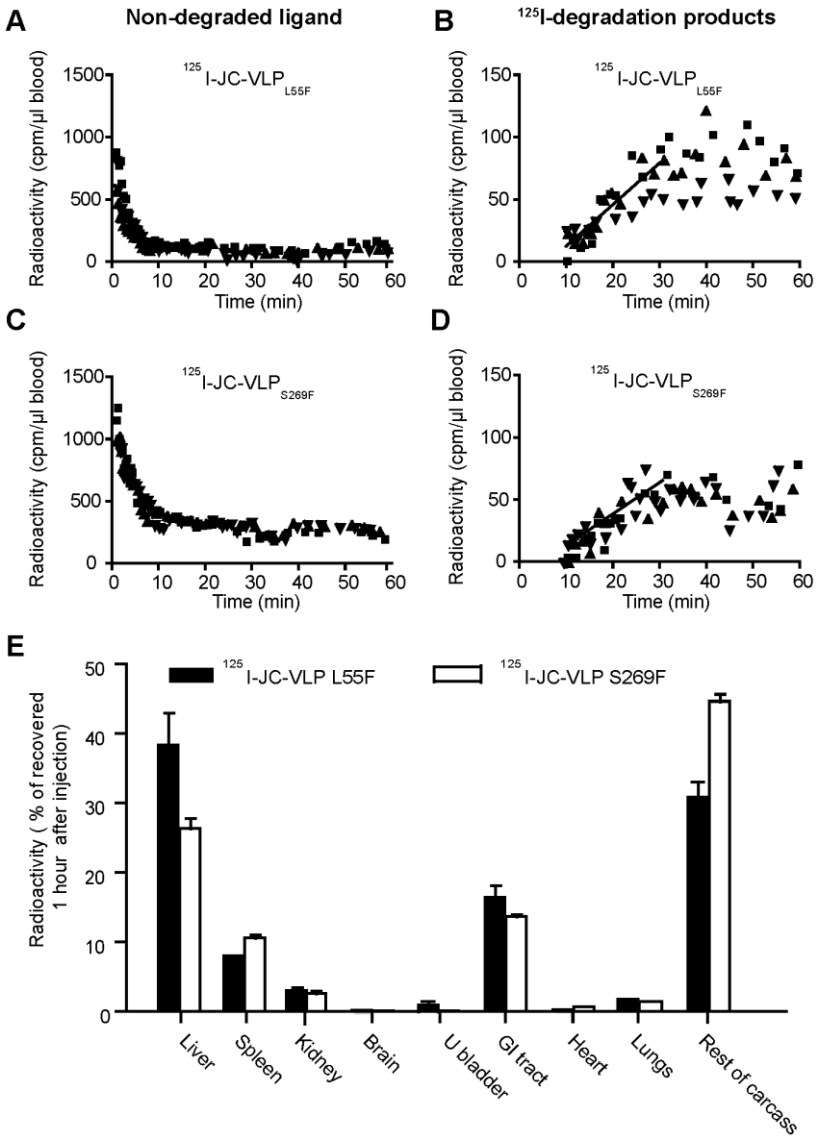


**Figure 6. Blood clearance and organ distribution of mutant JC-VLPs.** Mice were injected intravenously with $^{125}$I-JC-VLP$_{L55F}$ (n = 3, A–B), or $^{125}$I-JC-VLP$_{S269F}$ (n = 3, C–D), and blood samples taken at the indicated time points and analyzed for $^{125}$I-labeled degradation products and intact ligand [15]. Panels A and C show the decrease of intact ligand in blood as a function of time. Panels B and D show the increase in degradation products released into the blood with time. Different symbols refer to separate animals, and cpm to counts per minute. The slopes of the lines drawn in B and D represent the average release rate of degradation products in the 10–30 min period after ligand injection where this release followed approximate first order kinetics. E) Tissue distribution 60 min post injection. The animals in A–D were sacrificed after 60 min, and organs and tissues

analyzed for radioactivity. Recovered radioactivity in all tissues at this time point was taken as 100%. Error bars represent SEM. GI tract, gastrointestinal tract (stomach and intestines including mesenterium); U bladder, urine bladder. F) Hepatocellular distribution (±SD) of $^{125}$I-labeled JC-VLP mutants 10 min after intravenous injection; liver tissue was dispersed by collagenase perfusion, and radioactivity was measured in hepatocyte and non-parenchymal cell (NPC) fractions, respectively. G) Cellular distribution of JC-VLP$_{S269F}$ (anti-VP1 staining) 15 min after VLP injection. Uptake of JC-VLP$_{S269F}$ (red fluorescence; arrowheads) is seen along the sinusoids (s).
doi:10.1371/journal.pone.0111762.g006

## Liver uptake of blood-borne VLPs was not dependent on sialic acids

It is reported that BKV and JCV enter their natural host cells via carbohydrate receptors [55]. While BKV binds to alpha(2,3)-linked sialic acids on (for instance) gangliosides [56], JCV binds to alpha(2,6)-linked glycan lactoseries tetrasaccharide c (LSTc) [57]. To test whether blood clearance of JCV in mice is dependent on alpha(2,6)-linked sialic acids, we examined the elimination from blood of two JC-VLP variants occurring frequently in PML patients, namely JC-VLP$_{L55F}$ and JC-VLP$_{S269F}$ (**Figure 6A–D, Table 2**), which had been shown to no longer hemagglutinate red blood cells and to have lost their respective sialic acid receptor binding properties [58]. These VLPs were constructed from mutant forms of the JCV capsid protein VP1, in which one amino acid in the sialic acid binding loop of VP1 had been substituted. The data show that $^{125}$I-JC-VLP$_{L55F}$ and $^{125}$I-JC-VLP$_{S269F}$ were removed from the circulation in a similar manner as the JC-VLPs made from Mad-1 JC-VP1 (named here as JC-VLP) (**Table 2**). After 60 min nearly all $^{125}$I-JC-VLP$_{L55F}$, and 80% of the $^{125}$I-JC-VLP$_{S269F}$ were eliminated from blood (**Figure 6A, C**). Similarly to the JC-VLPs, acid soluble $^{125}$I-degradation products appeared in the circulation already after 10 min (**Figure 6B, D**).

Organ distribution of $^{125}$I-JC-VLP$_{L55F}$ and $^{125}$I-JC-VLP$_{S269F}$ 60 min post injection (**Figure 6E**) was similar to that of JC-VLP (**Figure 3B**), with the highest radioactivity measured in liver. Notably, radioactivity in the brain was negligible. Hepatocellular distribution studies, monitoring radioactivity in hepatocytes and NPCs separated10 min after injection of radiolabeled ligands, showed that the uptake of $^{125}$I-JC-VLP$_{L55F}$ and $^{125}$I-JC-VLP$_{S269F}$ was predominantly in the NPC fraction (**Figure 6F**). Immunohistochemistry revealed an LSEC-like pattern of distribution along the sinusoids (**Figure 6G**), as with JC-VLP (**Figure 4**). Of note, lectin histochemistry for SNA and MAH revealed that all hepatic endothelia expressed alpha(2,6)-linked-sialic acids and alpha(2,3)-linked sialic acids (**Figure S3**), whereas BK-VLPs and JC-VLPs (Mad-1 and mutants) distributed only to sinusoids (**Figures 4, and 6**), suggesting that these sialic acids are not essential for liver uptake.

## The scavenger receptor ligand formaldehyde-denatured serum albumin (FSA) reduced the rate of intracellular degradation of JC-VLP, but did not interfere with VLP uptake in liver

LSECs mediate their effective blood clearance of most known ligands via a limited set of endocytosis receptors of broad ligand specificity [10]. To study if LSEC scavenger receptors were involved in the uptake of circulating BK-VLPs or JC-VLPs, a high dose of FSA (0.8 mg/mouse) was injected immediately prior to the injection of $^{125}$I-labeled VLPs. FSA is a soluble scavenger receptor ligand and is reported to distribute mainly to the LSEC after intravenous administration [59]. No effect was observed on the blood clearance kinetics of $^{125}$I-BK-VLP (**Table 2**) or $^{125}$I-JC-VLP (**Figure S4, Table 2**). However, the release of $^{125}$I-JC-VLP degradation products to the blood (**Figure S4-B**) was slightly reduced by simultaneous FSA injection compared to injection of only $^{125}$I-JC-VLP (**Figure 2D**). This resulted in significantly more liver-associated radioactivity after 60 min (**Figure S4-C**) compared to injection of $^{125}$I-JC-VLP alone (**Figure 3B**), suggesting that metabolic turnover, but not uptake was rate limiting following targeting of the same cell by FSA and JC-VLP.

To investigate if the clearance of the VLPs was mediated by the mannose receptor, a C-type lectin with broad ligand binding properties and highly expressed in mouse, rat and human LSECs [15,26,43], mannose receptor deficient mice [46] were injected with $^{125}$I-JC-VLPs (**Figure S5**). These mice showed similar clearance and organ distribution of JC-VLPs as wild type mice (**Figures 2B, 3B**), indicating that the rapid JC-VLP blood clearance was not mediated by the mannose receptor pathway.

## Extrahepatic clearance of blood-borne BK- and JC-VLPs took place in endothelial cells of kidney vasa recta segments, and in reticuloendothelial cells of spleen red pulp marginal zone

The organ distribution studies of radiolabelled ligands showed a minor, but significant uptake in kidney and spleen. This prompted us to examine the VLP uptake in these organs by immunohistochemistry.

In kidney, BK- and JC-VLP uptake was specifically associated with microvessels of renal medulla (**Figure 7A–D**). Staining intensity of positive vessels was distinct and strong. However, VLP uptake was not seen in all medullary vessels, suggesting discrimination between different segments of vasa recta. Most of the VLP staining did not overlap with staining for Meca 32 (syn. PV-1, a component of fenestral diaphragms) (**Figure 8A–F**), which label endothelial cells of fenestrated segments of vasa recta [60,61]. This suggests that the BK- and JC-VLP uptake took place in non-fenestrated endothelial cells, which are located in descending segments of the vasa recta. Endothelial cells that took up VLPs also rapidly and selectively endocytosed FITC-FSA (**Figure 8G–I**), which in liver is a functional marker for LSECs [30,54,59,62]. FITC-FSA uptake in kidney was seen in medullary vessels only, and the uptake showed little overlap with Meca 32 staining (**Figure 8J–L**). The distribution pattern of JC-VLP and FITC-FSA in kidney medullary vessels almost completely overlapped, suggesting the presence of a highly endocytically active endothelium in these vessels.

BK- and JC-VLPs also distributed to the transitional epithelium of the renal pelvis (**Figure 7G, H**), whereas glomeruli and tubular structures of the nephron were negative in all mice (**Figure 7E, F**) except for one animal injected with BK-VLP, which showed positive staining of a few glomeruli (not shown). Lectin histochemistry for SNA and MAH showed positive labeling of all endothelia in kidney (**Figure S3**).

In spleen, the BK- and JC-VLPs distributed to the marginal zone that separates the lymphocyte rich white pulp from the red pulp (**Figure 9, and Figure S6**). The VP1 labeling showed a net-like staining pattern in this region. Double immune labeling for VP1 and the macrophage marker F4/80 (**Figure 9A–C**), or CD31 (**Figure 9D–F**), which is expressed by many endothelial cells, revealed scattered co-localisation of VLPs with CD31 and F4/80 positive cells, suggesting that the marginal zone reticulo-endothelial network of macrophages and endothelial cells are involved in VLP uptake in the spleen. Staining for the macrophage

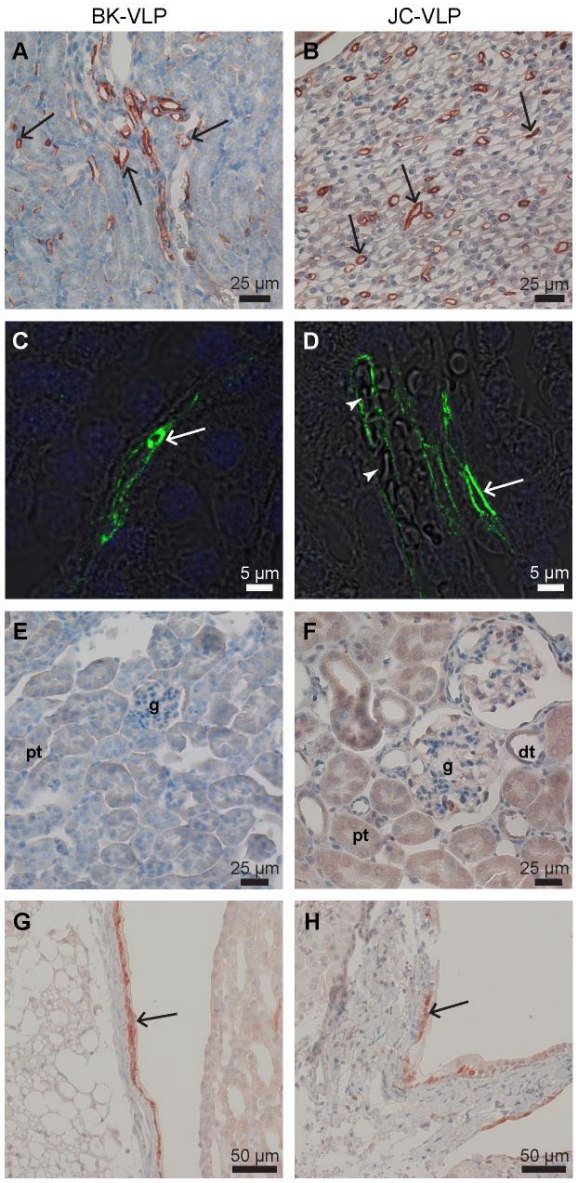


**Figure 7. Kidney distribution of intravenously administered BK- and JC-VLPs.** Mouse tissues were perfusion fixed 7 or 15 min after injection of BK-VLPs (A, C, E, G), or JC-VLPs (B, D, F, H). Paraffin sections were labeled using a rabbit anti-BK-VP1 antiserum [53]. VP1-labeling was visualized using HRP polymer/DAB reaction (brown color), or Alexa488-goat-anti-rabbit (green fluorescence). Specific uptake of VLPs was seen in the endothelial lining of microvessels in kidney medulla (arrows in A–D; with arrowheads in D pointing to blood filled medullary capillaries), whereas glomeruli (E, F), and tubular structures were negative (A–F). Epithelial cells in the transitional epithelium of renal pelvis also showed positive VP1 staining (arrows in G, H). g, glomerulus; pt, proximal tubulus; dt, distal tubulus.
doi:10.1371/journal.pone.0111762.g007

antigen CD163 [63] did not co-localize with VP1 staining (**Figure 9G–I**), indicating VLP uptake only in subsets of spleen red pulp macrophages. Some of the JC-VLP uptake in spleen co-localized with FITC-FSA which also distributed to the reticulo-endothelium of the spleen red pulp marginal zone (**Figure 9J–L**).

## Discussion

Clinical models of BKV and JCV infection demonstrating replicative pathologies with close correlation to nephropathy, cystitis or multifocal leukoencephalopathy are currently lacking. However, these viruses are recognized and taken up by cells from non-permissive hosts, including mice [37,42], allowing us to study their cellular site of uptake in a mouse model. Primary infection with these viruses is believed to occur during early childhood, but their initial infection route or organ distribution is not well known. Using well characterized VLPs, we present evidence that LSECs are highly effective in clearing a large fraction of blood-borne BKV and JCV particles. Moreover, we observed that BK and JC VLPs are efficiently taken up in some microvessels of renal medulla and the spleen marginal zone reticuloendothelium. By effectively acting as a virion sink in the absence of specific antibodies, LSECs may play a key role in the mostly asymptomatic course of primary BKV and JCV infection, leaving only little virus to escape and reach the renal medulla (and possibly the spleen), an important site of BKV and JCV persistence [40,41]. LSECs represent a highly specialized type of scavenger endothelium preserved across different vertebrate species including rodents and humans [10,45]. Several signature characteristics are the same in LSECs across mammals: Cell morphology and endocytosis receptor expression in human LSECs are identical to that of rodents and pig [10,11,15,43,44], and the scavenger function of rat, mouse, and pig LSECs is strikingly similar [64]. It is therefore likely that our present findings on the efficient LSEC endocytosis of polyoma VLPs in mice reflect the fate of these viruses also in human livers.

The observed biphasic pattern of polyoma VLP clearance from blood, with a rapid α-phase and a slower β-phase is comparable to the clearance kinetics of many macromolecules and colloids that are efficiently eliminated via receptor-mediated endocytosis in the LSECs [15,25,26]. There were, nevertheless, some interesting differences between the BK-VLP and JC-VLP clearance patterns. While JC-VLPs were almost completely removed from the circulation within 10 minutes, the α-phase was less dominant in the elimination of BK-VLPs, suggesting a rapid saturation of BK binding/uptake receptors or interaction of BK-VLPs with blood factors (proteins or cells), delaying the blood clearance. Interestingly, in their natural host cells BKV is reported to be internalized via caveolin-mediated endocytosis whereas JCV enters via clathrin-mediated endocytosis [36]. This could also be an explanation of our results, because LSECs have well-developed clathrin-mediated endocytosis machinery, and rely heavily on this type of endocytosis to maintain their signature scavenging activity [34,65].

Our hypothesis is that LSECs protect against virus infections, due to their very efficient endocytosis and high catabolic activity which rapidly destroy internalized material [10]. Our *in vivo* data indicate that at least JC-VLPs are rapidly degraded in the liver, as reported for other macromolecules taken up by the LSECs [10,26]. In this context, it is of interest to note that BKV viremia is readily detectable in transplant patients with BKV-associated diseases, while JCV viremia is only rarely detected in patients with JCV-associated diseases [66] [67].

However, degradation of VLPs is not a proof of cellular destruction of infective virus, and to establish whether BKV or JCV uptake in LSECs will lead to destruction of all internalized virus particles, or allow for endosomal escape and intracellular

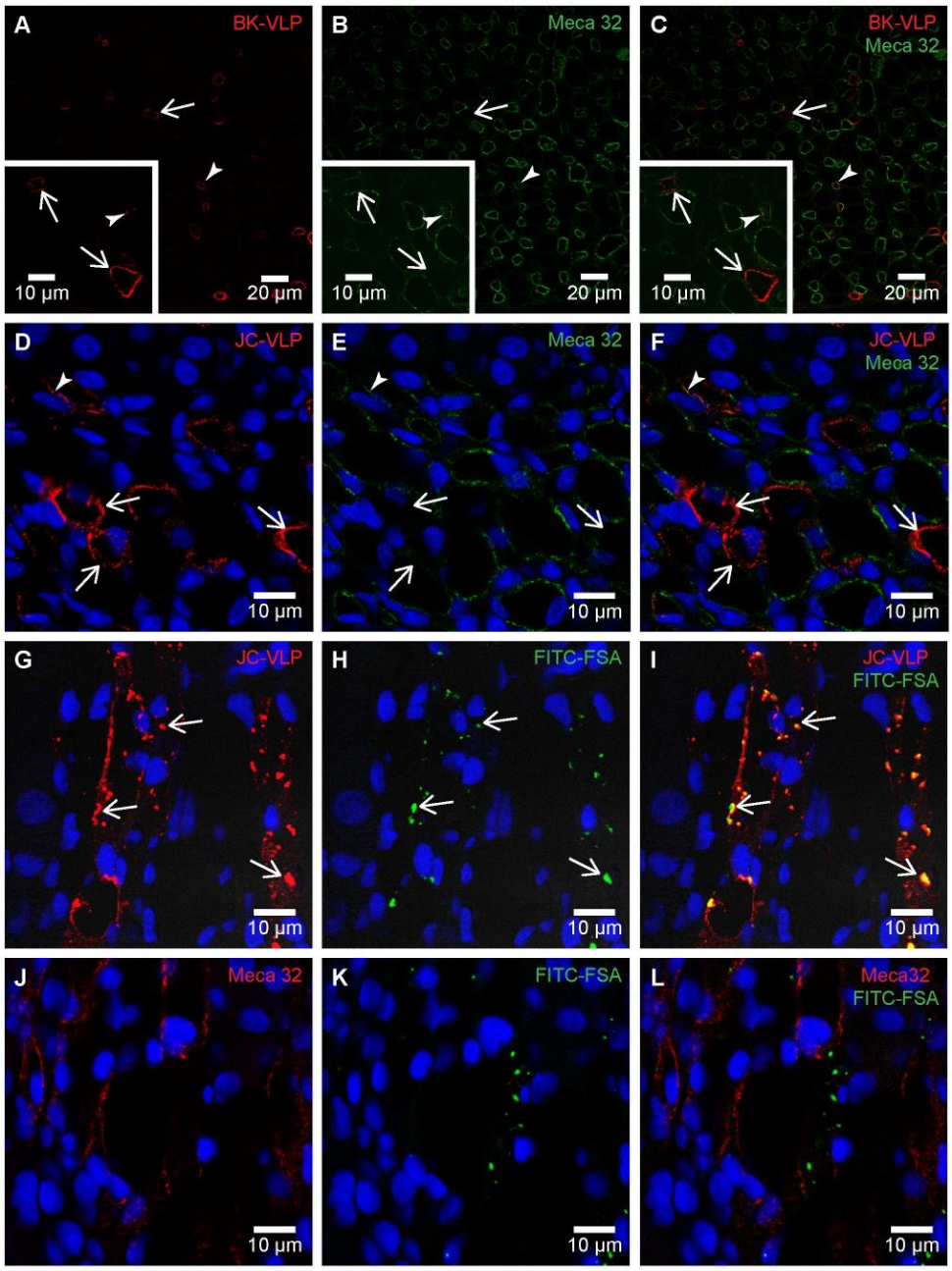


**Figure 8. Polyoma VLP and FITC-FSA uptake in renal medullary endothelial cells.** Panels A–F: Mouse tissues were perfusion fixed 7 min after intravenous injection of BK-VLP (A–C), or JC-VLP (D–F), and paraffin sections double immune labeled with anti-BK-VP1 (red) and anti-Meca 32 (green). Panels A–C: Arrows indicate endothelial uptake of BK-VLPs in Meca 32 negative vessels, and arrow heads to BK-VLP uptake in Meca 32 positive vessels. Panels D–F: Arrows indicate endothelial uptake of JC-VLPs in Meca 32 negative vessels, and arrow heads to JC-VLP uptake in Meca 32 positive vessels. Most BK-VLP or JC-VLP-positive vessels were Meca 32 negative or showed only weak Meca32 staining. Panels G–L: Tail vein injection of JC-VLPs was followed by injection of the scavenger receptor ligand FITC-FSA in the opposite tail vein and tissues perfusion fixed 15 min after the VLP administration. Paraffin sections were immune labeled with either anti-BK-VP1 (red; G–I) or anti-Meca 32 (red; J–L). G–I) The JC-VLP uptake in medullary vessel endothelia totally overlapped with FITC-FSA uptake (arrows). J–L) FITC-FSA uptake occurred mainly in Meca 32 negative vessels.
doi:10.1371/journal.pone.0111762.g008

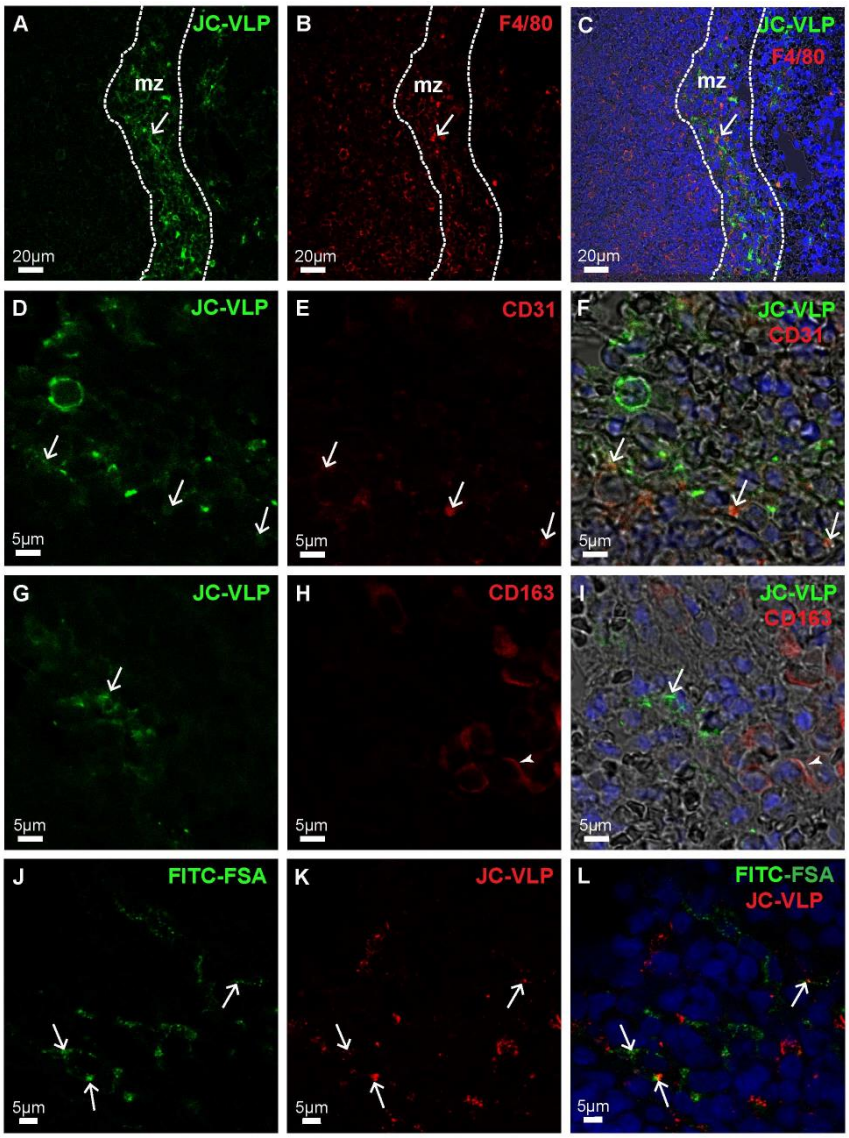


**Figure 9. JC-VLP uptake in spleen.** Panels A–I: Mouse tissues were perfusion fixed 7 min after intravenous injection of JC-VLPs. Paraffin sections of spleen were double immune labeled using a rabbit antiserum against BK-VP1 [53] (reacts also with JC-VP1), and antibodies against F4/80 (A–C), CD31 (D–F) or CD163 (G–I). Antibodies are listed in Table 1. The VP1 staining pattern (green) showed that the uptake of VLPs was concentrated in the red pulp marginal zone, mz (A), and here partly co-localized with F4/80 (C, arrow), and CD31 (F, arrows), but not with CD163 (I; arrow indicates VP1, and arrow head to CD163 staining). The F4/80 (B, C), CD31 (E, F), and CD163 (H, I) staining patterns are all shown in red. Panels J–L: In J–L, tail vein injection of JC-VLPs was followed by injection of FITC-FSA in the opposite tail vein and tissues perfusion fixed 15 min after the VLP administration. Both JC-VLP (K; red fluorescence) and FITC-FSA (J; green fluorescence) distributed to the reticuloendothelial network of the spleen red pulp marginal zone (L; arrows point to overlap of JC-VLP staining and FITC-FSA uptake).
doi:10.1371/journal.pone.0111762.g009

replication of a fraction of the internalized virions would require further studies. However, *in vitro* model systems are currently lacking that recapitulate the known *in vivo* physiological activity of human LSECs, hence impeding such studies.

In addition to a major hepatic uptake, a minor, but significant BK-/JC-VLP uptake was also measured in spleen red pulp and kidney medulla. The spleen red pulp is known to harbor scavenger type of endothelia [10] and could thereby serve as a secondary site of BKV and JCV clearance. Of note, the rapid and specific uptake of polyoma virus or VLPs in kidney medullary vessels has to our knowledge not been reported before, and may reveal novel insights into the infection route of BKV and JCV. It is notable, however, that clinical recommendations emphasize the importance of medullary tissue for a sensitive tissue diagnosis of BK polyoma-virus-associated nephropathy in kidney transplant recipients [68]. Moreover, BKV infection of endothelial cells has been reported in a patient with AIDS and a renal transplant recipient [69,70]. The kidney uptake reported in the present study was associated with

the endothelial lining of distinct vasa recta segments. Most of the VLP-positive vessels did not express PV-1/Meca32, suggesting location of VLPs in the non-fenestrated, or descending part of vasa recta [61]. The VLP positive endothelial cells also efficiently endocytosed a functional LSEC marker and scavenger receptor ligand, FITC-FSA, suggesting high endocytic activity of these cells compared to other renal endothelia. Whether this uptake will aid in persistence or clearance of the infectious virus remains to be revealed.

The brain, which is the main site for JCV pathology (PML) [41], was not readily identified by the intravenously injected VLPs, as judged by the extremely low levels of radioactivity accumulating in this organ. This apparent lack of uptake in brain may be explained partly by the intact blood-brain and blood-cerebrospinal fluid barrier of adult mammals. However, the steps in colonization of the brain by JCV are not well characterized and it is still unclear if this occurs during primary viremia or during reactivation [41], if it requires replication competent JCV as opposed to VLPs, or access via other cell types including B-lymphocytes and/or hematopoietic progenitor cells [71]. In addition to the usually distinct VP1 amino acid mutations found [58], virus causing PML bear a rearranged non-coding control region that increases the replication potential [72].

We tested the *in vivo* fate of VLPs of the two of the most frequently identified JCV mutants, namely JC-VLP$_{L55F}$ and JC-VLP$_{S269F}$, both of which have lost their ability to bind alpha(2,6)-linked sialic acid residues on gangliosides, used by JCV for cellular entry [41,58]. The rate of blood clearance was rapid, and organ distribution after 60 min was almost similar for Mad-1 and mutant JC-VLPs, suggesting that their blood clearance by scavenger cells did not depend on binding to alpha(2,6)-linked sialic acid receptors.

The high scavenging capacity of LSECs for most ligands is mediated by a limited set of high affinity endocytosis receptors [10]. Together with the mannose receptor, the scavenger receptors stabilin-1 and stabilin-2 are considered the main endocytic workhorses of these cells [10,65], and are responsible for the uptake of a wide range of macromolecules, including oxidized LDLs, hyaluronan, chondroitin sulphate, procollagen propeptides, and advanced glycation end products [13,30,65]. Many serum proteins that are phosphorylated as a consequence of platelet activation and blood coagulation are also recognized by the LSEC scavenger receptors [73]. Recent data suggest that the VP1 molecules of BKV contain posttranslational modifications including phosphate groups [74]. FSA, a well-known ligand for the scavenger/stabilin receptors [30,59] was unable to alter the clearance kinetics of blood-borne VLPs, suggesting that the LSEC scavenger receptors were not involved in the hepatic uptake of the particles. However, intracellular degradation of JC-VLPs in liver was significantly impaired. Together, these data suggest traffic of FSA and JC-VLP to the same degradation compartments, but via different receptors. However, we cannot exclude binding to different sites of the same endocytosis receptor, as non-reciprocal cross-competition is described for binding of FSA and hyaluronan to scavenger receptors/stabilin-2 in LSECs [11,13,25]. Mice deficient in the mannose receptor [46] showed similar clearance and organ distribution of BK/JC-VLPs as wild-type mice with normal expression of mannose receptor in LSECs. Although this is consistent with the fact that polyomavirus VLPs including BKV and JCV are not glycosylated [74], it should be noted that the mannose receptor has binding sites for non-glycosylated residues in addition to acting as a lectin [10,75].

## Conclusions

Mouse LSECs were identified as efficient scavengers of BK- and JC-VLPs. Despite this efficient clearance mechanism, the VLPs still reached the kidney which is a key organ of BKV and JCV persistence in humans. Of note, the kidney was targeted by VLPs, i.e. in the absence of virus replication. Here we identified uptake predominantly in endothelial cells of the non-fenestrated segments of vasa recta, which also possessed high endocytic activity towards the scavenger receptor ligand FITC-FSA, a hitherto unknown function of these renal endothelial cells. A better understanding of LSEC-mediated polyomavirus clearance may shed light into the role of these cells in the development of polyomavirus-associated diseases. Moreover, this may permit the development of strategies to harness this process for immunocompromised subjects at risk of polyoma virus replication.

## Supporting Information

**Figure S1 Liver distribution of BK- and JC-VLPs – details of Figure 4B and 4E.** The figure shows the green and red channels, white field (WF) image, and merged image of immune labeled paraffin sections of liver from mice injected with BK-VLPs (A–D), or JC-VLPs (E–H). The livers were perfusion fixed 15 min after intravenous injection, and sections labeled with rabbit antiserum to BK-VP1 (cross-reacts with JC-VP1), and an antibody to the mannose receptor (MR; LSEC marker [26]). The staining patterns of VLPs (A, E; green) and MR (B, F; red) were similar (overlay in D, H), and localized exclusively to sinusoids (s; arrowheads), whereas hepatocytes (outlined in C, D, G, H) were negative. Hn, hepatocyte nucleus.
(TIFF)

**Figure S2 Uptake of JC-VLPs in LSECs in vitro – Z-stack.** Freshly isolated LSECs were incubated at 37°C for 1 h with 10 μg/ml JC-VLPs, fixed, and double immune labeled with rabbit anti-serum to BK-VP1 (red), and an antibody to an LSEC marker (the mannose receptor, MR; green). Draq5 was used to stain the cell nucleus. The panel shows the images of a Z-stack recorded by confocal laser scanning microscopy. Every image shows the same cell at different depth (Z axis) with 0.3 μm distance from the previous optical image, recorded from a given 0 μm (A) to 1.2 μm depth (E). The intensity of the Draq5 staining increased gradually from A to D, meaning that the images were taken from a layer close to the cell plasma membrane in A, towards the center of the cell in D. Positive VP1 staining (red) can be seen in all images, indicating cellular uptake of VLPs. The MR is a constitutively recycling endocytosis receptor in LSECs [14] and MR staining is strongest towards the periphery of the cell.
(TIFF)

**Figure S3 Lectin histochemistry of liver, kidney and spleen.** Panels A–H: Paraffin sections of liver (A, B), kidney medulla (C, D), kidney cortex (E, F), and spleen (G, H) were labeled with biotinylated agglutinins: *Maackia amurensis II* (MAH; A, C, E, G) that binds to alpha(2,3)-linked sialic acid, and *Sambucus nigra* (SNA; B, D, F, H) that binds to alpha(2,6)-linked sialic acid. Lectin binding to sialic acids was visualized by Alexa555-streptavidin. Both type of lectins bound to all endothelia in liver (A, B), and kidney (C–F). In spleen (G–H), the lectin staining pattern was more diffuse than in the two other organs. PV, portal vein; CV, central vein; g, glomerulus.
(TIFF)

**Figure S4 Effects of the scavenger receptor ligand FSA on uptake and intracellular degradation of JC-VLP.** Panels A–C: Rate of blood clearance, and subsequent organ

distribution of $^{125}$I-JC-VLP in mice injected with a saturating dose (0.8 mg/mouse) of the scavenger receptor ligand FSA immediately prior to the injection of $^{125}$I-JC-VLP (dose: 0.5 μg/mouse). Blood samples were taken at the indicated time points in A, B and analyzed for $^{125}$I-labeled degradation products and intact ligand [15]. A, B) The graph in A shows decrease of intact ligand in blood as a function of time, whereas the graph in B shows increase in degradation products released into the blood with time. Results are given in cpm per μl blood. Different symbols refer to separate animals (n = 3). cpm, counts per minute. The slope of the line drawn in B represents the average release rate of degradation products in the 10–30 min period after ligand injection where this release followed approximate first order kinetics. C) Organ distribution of radioactivity 60 min after the intravenous administration of $^{125}$I-JC-VLP and FSA. *Significantly more radioactivity (p-value $<0.01$) was recovered in liver after 60 min following competitive inhibition with FSA (Figure S4-C; 44%), than after injection with $^{125}$I-JC-VLP alone (Figure 3B; 30%). U bladder, urine bladder; GI tract, gastrointestinal tract; FSA, formaldehyde denatured serum albumin.
(EPS)

**Figure S5 Blood clearance and tissue distribution of $^{125}$I-JC-VLPs in MR$^{-/-}$ mice.** C57BL/6 MR$^{-/-}$ mice (n = 2) were injected intravenously with approximately 0.5 μg of $^{125}$I-JC-VLP, and blood samples taken at the time points indicated in A and B and analyzed for $^{125}$I-labeled degradation products and intact ligand [15]. After 60 min, the animals were euthanized, then perfused free of blood, and radioactivity measured in tissues and organs. A) Kinetics of decrease of intact $^{125}$I-labeled ligand in blood. B) Increase in $^{125}$I-degradation products released into the blood with time. Results in A and B are given in counts per minute (cpm) per μl blood. C) Organ distribution of radioactivity 60 min after injection of ligand. Recovered radioactivity in organs and tissues at this time point was taken as 100%.
(EPS)

**Figure S6 Uptake of blood-borne BK-VLPs in spleen.** The figure shows the distribution of BK-VLPs in spleen 15 min after intravenous injection. Paraffin sections were stained with anti-BK-VP1 (Table 1) and Alexa488-goat-anti-rabbit antibody (green fluorescence). The VLPs were taken up in the reticuloendothelial network in the spleen red pulp marginal zone (mz, arrowheads). rp, red pulp; wp, white pulp.
(TIF)

## Acknowledgments

We thank Wenche Helen Bakkelund, Randi Olsen and Helga-Marie Bye, Department of Medical Biology, University of Tromsø, for skilled technical assistance with histology sectioning and immune electron microscopy.

## Author Contributions

Conceived and designed the experiments: JSS CHR RL IM KE PM BS HHH KKS. Performed the experiments: JSS RL PK IM KKS. Analyzed the data: JSS CHR RL IM BS HHH KKS. Contributed reagents/materials/analysis tools: CHR PK BS HHH KKS. Wrote the paper: JSS CHR HHH KKS. Provided critical evaluation of the manuscript, and read and approved the final version of the manuscript: JSS CHR PK RL IM KE PM BS HHH KKS.

## References

1. Virgin HW (2014) The Virome in Mammalian Physiology and Disease. Cell 157: 142–150.
2. Zhang L, Dailey PJ, He T, Gettie A, Bonhoeffer S, et al. (1999) Rapid clearance of simian immunodeficiency virus particles from plasma of rhesus macaques. J Virol 73: 855–860.
3. Mims CA (1959) The response of mice to large intravenous injections of ectromelia virus. II. The growth of virus in the liver. Br J Exp Pathol 40: 543–550.
4. Alemany R, Suzuki K, Curiel DT (2000) Blood clearance rates of adenovirus type 5 in mice. J Gen Virol 81: 2605–2609.
5. Inchley CJ (1969) The activity of mouse Kupffer cells following intravenous injection of T4 bacteriophage. Clin Exp Immunol 5: 173–187.
6. Green NK, Herbert CW, Hale SJ, Hale AB, Mautner V, et al. (2004) Extended plasma circulation time and decreased toxicity of polymer-coated adenovirus. Gene Ther 11: 1256–1263.
7. Ganesan LP, Mohanty S, Kim J, Clark KR, Robinson JM, et al. (2011) Rapid and Efficient Clearance of Blood-borne Virus by Liver Sinusoidal Endothelium. PLoS Pathog 7: e1002281.
8. Funk GA, Gosert R, Hirsch HH (2007) Viral dynamics in transplant patients: implications for disease. Lancet Infect Dis 7: 460–472.
9. Jenne CN, Kubes P (2013) Immune surveillance by the liver. Nat Immunol 14: 996–1006.
10. Sorensen KK, McCourt P, Berg T, Crossley C, Couteur DL, et al. (2012) The scavenger endothelial cell: a new player in homeostasis and immunity. Am J Physiol Regul Integr Comp Physiol 303: R1217–1230.
11. Politz O, Gratchev A, McCourt PA, Schledzewski K, Guillot P, et al. (2002) Stabilin-1 and -2 constitute a novel family of fasciclin-like hyaluronan receptor homologues. Biochem J 362: 155–164.
12. Malerod L, Juvet K, Gjoen T, Berg T (2002) The expression of scavenger receptor class B, type I (SR-BI) and caveolin-1 in parenchymal and nonparenchymal liver cells. Cell Tissue Res 307: 173–180.
13. McCourt PA, Smedsrod BH, Melkko J, Johansson S (1999) Characterization of a hyaluronan receptor on rat sinusoidal liver endothelial cells and its functional relationship to scavenger receptors. Hepatology 30: 1276–1286.
14. Magnusson S, Berg T (1989) Extremely rapid endocytosis mediated by the mannose receptor of sinusoidal endothelial rat liver cells. Biochem J 257: 651–656.
15. Malovic I, Sorensen KK, Elvevold KH, Nedredal GI, Paulsen S, et al. (2007) The mannose receptor on murine liver sinusoidal endothelial cells is the main denatured collagen clearance receptor. Hepatology 45: 1454–1461.
16. Martin-Armas M, Simon-Santamaria J, Pettersen I, Moens U, Smedsrod B, et al. (2006) Toll-like receptor 9 (TLR9) is present in murine liver sinusoidal endothelial cells (LSECs) and mediates the effect of CpG-oligonucleotides. J Hepatol 44: 939–946.
17. Uhrig A, Banafsche R, Kremer M, Hegenbarth S, Hamann A, et al. (2005) Development and functional consequences of LPS tolerance in sinusoidal endothelial cells of the liver. J Leukoc Biol 77: 626–633.
18. Hosel M, Broxtermann M, Janicki H, Esser K, Arzberger S, et al. (2012) Toll-like receptor 2-mediated innate immune response in human nonparenchymal liver cells toward adeno-associated viral vectors. Hepatology 55: 287–297.
19. Wu J, Meng Z, Jiang M, Zhang E, Trippler M, et al. (2010) Toll-like receptor-induced innate immune responses in non-parenchymal liver cells are cell type-specific. Immunology 129: 363–374.
20. Mousavi SA, Sporstol M, Fladeby C, Kjeken R, Barois N, et al. (2007) Receptor-mediated endocytosis of immune complexes in rat liver sinusoidal endothelial cells is mediated by FcgammaRIIb2. Hepatology 46: 871–884.
21. Ganesan LP, Kim J, Wu Y, Mohanty S, Phillips GS, et al. (2012) FcgammaRIIb on liver sinusoidal endothelium clears small immune complexes. J Immunol 189: 4981–4988.
22. Seckert CK, Renzaho A, Tervo HM, Krause C, Deegen P, et al. (2009) Liver sinusoidal endothelial cells are a site of murine cytomegalovirus latency and reactivation. J Virol 83: 8869–8884.
23. Li Y, Hao B, Kuai X, Xing G, Yang J, et al. (2009) C-type lectin LSECtin interacts with DC-SIGNR and is involved in hepatitis C virus binding. Mol Cell Biochem 327: 183–190.
24. Smedsrod B, Melkko J, Risteli L, Risteli J (1990) Circulating C-terminal propeptide of type I procollagen is cleared mainly via the mannose receptor in liver endothelial cells. Biochem J 271: 345–350.
25. Melkko J, Hellevik T, Risteli L, Risteli J, Smedsrod B (1994) Clearance of NH2-terminal propeptides of types I and III procollagen is a physiological function of the scavenger receptor in liver endothelial cells. J Exp Med 179: 405–412.
26. Elvevold K, Simon-Santamaria J, Hasvold H, McCourt P, Smedsrod B, et al. (2008) Liver sinusoidal endothelial cells depend on mannose receptor-mediated recruitment of lysosomal enzymes for normal degradation capacity. Hepatology 48: 2007–2015.
27. Smedsrod B, Melkko J, Araki N, Sano H, Horiuchi S (1997) Advanced glycation end products are eliminated by scavenger-receptor-mediated endocytosis in hepatic sinusoidal Kupffer and endothelial cells. Biochem J 322 (Pt 2): 567–573.
28. Svistounov D, Oteiza A, Zykova SN, Sorensen KK, McCourt P, et al. (2013) Hepatic disposal of advanced glycation end products during maturation and aging. Exp Gerontol 48: 549–556.
29. Van Berkel TJ, De Rijke YB, Kruijt JK (1991) Different fate in vivo of oxidatively modified low density lipoprotein and acetylated low density

lipoprotein in rats. Recognition by various scavenger receptors on Kupffer and endothelial liver cells. J Biol Chem 266: 2282–2289.
30. Li R, Oteiza A, Sorensen KK, McCourt P, Olsen R, et al. (2011) Role of liver sinusoidal endothelial cells and stabilins in elimination of oxidized low-density lipoproteins. Am J Physiol Gastrointest Liver Physiol 300: G71–81.
31. Skogh T, Blomhoff R, Eskild W, Berg T (1985) Hepatic uptake of circulating IgG immune complexes. Immunology 55: 585–594.
32. Asumendi A, Alvarez A, Martinez I, Smedsrod B, Vidal-Vanaclocha F (1996) Hepatic sinusoidal endothelium heterogeneity with respect to mannose receptor activity is interleukin-1 dependent. Hepatology 23: 1521–1529.
33. Jacobs F, Wisse E, De Geest B (2010) The role of liver sinusoidal cells in hepatocyte-directed gene transfer. Am J Pathol 176: 14–21.
34. Kjeken R, Mousavi SA, Brech A, Gjoen T, Berg T (2001) Fluid phase endocytosis of [125I]iodixanol in rat liver parenchymal, endothelial and Kupffer cells. Cell Tissue Res 304: 221–230.
35. Seternes T, Sorensen K, Smedsrod B (2002) Scavenger endothelial cells of vertebrates: a nonperipheral leukocyte system for high-capacity elimination of waste macromolecules. Proc Natl Acad Sci U S A 99: 7594–7597.
36. Neu U, Stehle T, Atwood WJ (2009) The Polyomaviridae: Contributions of virus structure to our understanding of virus receptors and infectious entry. Virology 384: 389–399.
37. Suzuki S, Sawa H, Komagome R, Orba Y, Yamada M, et al. (2001) Broad distribution of the JC virus receptor contrasts with a marked cellular restriction of virus replication. Virology 286: 100–112.
38. Goldmann C, Petry H, Frye S, Ast O, Ebitsch S, et al. (1999) Molecular cloning and expression of major structural protein VP1 of the human polyomavirus JC virus: formation of virus-like particles useful for immunological and therapeutic studies. J Virol 73: 4465–4469.
39. Tsai B, Qian M (2010) Cellular entry of polyomaviruses. Curr Top Microbiol Immunol 343: 177–194.
40. Hirsch HH (2005) BK virus: opportunity makes a pathogen. Clin Infect Dis 41: 354–360.
41. Hirsch HH, Kardas P, Kranz D, Leboeuf C (2013) The human JC polyomavirus (JCPyV): virological background and clinical implications. APMIS 121: 685–727.
42. Tan CS, Broge TA Jr, Seung E, Vrbanac V, Viscidi R, et al. (2013) Detection of JC virus-specific immune responses in a novel humanized mouse model. PLoS One 8: e64313.
43. Martens JH, Kzhyshkowska J, Falkowski-Hansen M, Schledzewski K, Gratchev A, et al. (2006) Differential expression of a gene signature for scavenger/lectin receptors by endothelial cells and macrophages in human lymph node sinuses, the primary sites of regional metastasis. J Pathol 208: 574–589.
44. Lalor PF, Lai WK, Curbishley SM, Shetty S, Adams DH (2006) Human hepatic sinusoidal endothelial cells can be distinguished by expression of phenotypic markers related to their specialised functions in vivo. World J Gastroenterol 12: 5429–5439.
45. Esbach S, Pieters MN, van der Boom J, Schouten D, van der Heyde MN, et al. (1993) Visualization of the uptake and processing of oxidized low-density lipoproteins in human and rat liver. Hepatology 18: 537–545.
46. Lee SJ, Evers S, Roeder D, Parlow AF, Risteli J, et al. (2002) Mannose receptor-mediated regulation of serum glycoprotein homeostasis. Science 295: 1898–1901.
47. Smedsrod B (2012) Protocol for the preparation of mouse liver Kupffer cells and liver sinusoidal endothelial cells. Munin open research archive: University of Tromsø, Tromsø, Norway. pp. Available: http://hdl.handle.net/10037/14575.
48. Bodaghi S, Comoli P, Bosch R, Azzi A, Gosert R, et al. (2009) Antibody responses to recombinant polyomavirus BK large T and VP1 proteins in young kidney transplant patients. J Clin Microbiol 47: 2577–2585.
49. Brinkman-Van der Linden EC, Sonnenburg JL, Varki A (2002) Effects of sialic acid substitutions on recognition by Sambucus nigra agglutinin and Maackia amurensis hemagglutinin. Anal Biochem 303: 98–104.
50. Martinez I, Nedredal GI, Oie CI, Warren A, Johansen O, et al. (2008) The influence of oxygen tension on the structure and function of isolated liver sinusoidal endothelial cells. Comp Hepatol 7: 4.
51. Slot JW, Geuze HJ (2007) Cryosectioning and immunolabeling. Nat Protoc 2: 2480–2491.
52. Hellevik T, Bondevik A, Smedsrod B (1996) Intracellular fate of endocytosed collagen in rat liver endothelial cells. Exp Cell Res 223: 39–49.
53. Rinaldo CH, Myhre MR, Alstad H, Nilssen O, Traavik T (2003) Human polyomavirus BK (BKV) transiently transforms and persistently infects cultured osteosarcoma cells. Virus Res 93: 181–187.
54. Xie G, Wang L, Wang X, DeLeve LD (2010) Isolation of periportal, midlobular, and centrilobular rat liver sinusoidal endothelial cells enables study of zonated drug toxicity. Am J Physiol Gastrointest Liver Physiol 299: G1204–1210.
55. Olofsson S, Bergstrom T (2005) Glycoconjugate glycans as viral receptors. Ann Med 37: 154–172.
56. Neu U, Allen SA, Blaum BS, Liu Y, Frank M, et al. (2013) A structure-guided mutation in the major capsid protein retargets BK polyomavirus. PLoS Pathog 9: e1003688.
57. Neu U, Maginnis MS, Palma AS, Stroh LJ, Nelson CD, et al. (2010) Structure-function analysis of the human JC polyomavirus establishes the LSTc pentasaccharide as a functional receptor motif. Cell Host Microbe 8: 309–319.
58. Gorelik L, Reid C, Testa M, Brickelmaier M, Bossolasco S, et al. (2011) Progressive multifocal leukoencephalopathy (PML) development is associated with mutations in JC virus capsid protein VP1 that change its receptor specificity. J Infect Dis 204: 103–114.
59. Blomhoff R, Eskild W, Berg T (1984) Endocytosis of formaldehyde-treated serum albumin via scavenger pathway in liver endothelial cells. Biochem J 218: 81–86.
60. Stan RV, Kubitza M, Palade GE (1999) PV-1 is a component of the fenestral and stomatal diaphragms in fenestrated endothelia. Proc Natl Acad Sci U S A 96: 13203–13207.
61. Pannabecker TL, Dantzler WH (2007) Three-dimensional architecture of collecting ducts, loops of Henle, and blood vessels in the renal papilla. Am J Physiol Renal Physiol 293: F696–704.
62. Elvevold K, Smedsrod B, Martinez I (2008) The liver sinusoidal endothelial cell: a cell type of controversial and confusing identity. Am J Physiol Gastrointest Liver Physiol 294: G391–400.
63. Lau SK, Chu PG, Weiss LM (2004) CD163: a specific marker of macrophages in paraffin-embedded tissue samples. Am J Clin Pathol 122: 794–801.
64. Elvevold KH, Nedredal GI, Revhaug A, Smedsrod B (2004) Scavenger properties of cultivated pig liver endothelial cells. Comp Hepatol 3: 4.
65. Hansen B, Longati P, Elvevold K, Nedredal GI, Schledzewski K, et al. (2005) Stabilin-1 and stabilin-2 are both directed into the early endocytic pathway in hepatic sinusoidal endothelium via interactions with clathrin/AP-2, independent of ligand binding. Exp Cell Res 303: 160–173.
66. Egli A, Infanti L, Dumoulin A, Buser A, Samaridis J, et al. (2009) Prevalence of polyomavirus BK and JC infection and replication in 400 healthy blood donors. J Infect Dis 199: 837–846.
67. Drachenberg CB, Hirsch HH, Papadimitriou JC, Gosert R, Wali RK, et al. (2007) Polyomavirus BK versus JC replication and nephropathy in renal transplant recipients: a prospective evaluation. Transplantation 84: 323–330.
68. Hirsch HH, Randhawa P, Practice ASTIDCo (2013) BK polyomavirus in solid organ transplantation. Am J Transplant 13 Suppl 4: 179–188.
69. Petrogiannis-Haliotis T, Sakoulas G, Kirby J, Koralnik IJ, Dvorak AM, et al. (2001) BK-related polyomavirus vasculopathy in a renal-transplant recipient. N Engl J Med 345: 1250–1255.
70. Vallbracht A, Lohler J, Gossmann J, Gluck T, Petersen D, et al. (1993) Disseminated BK type polyomavirus infection in an AIDS patient associated with central nervous system disease. Am J Pathol 143: 29–39.
71. Ferenczy MW, Marshall LJ, Nelson CD, Atwood WJ, Nath A, et al. (2012) Molecular biology, epidemiology, and pathogenesis of progressive multifocal leukoencephalopathy, the JC virus-induced demyelinating disease of the human brain. Clin Microbiol Rev 25: 471–506.
72. Gosert R, Kardas P, Major EO, Hirsch HH (2010) Rearranged JC virus noncoding control regions found in progressive multifocal leukoencephalopathy patient samples increase virus early gene expression and replication rate. J Virol 84: 10448–10456.
73. Hansen B, Melkko J, Smedsrod B (2002) Serum is a rich source of ligands for the scavenger receptor of hepatic sinusoidal endothelial cells. Mol Cell Biochem 229: 63–72.
74. Fang CY, Chen HY, Wang M, Chen PL, Chang CF, et al. (2010) Global analysis of modifications of the human BK virus structural proteins by LC-MS/MS. Virology 402: 164–176.
75. Napper CE, Drickamer K, Taylor ME (2006) Collagen binding by the mannose receptor mediated through the fibronectin type II domain. Biochem J 395: 579–586.

In conducted study, we observed distribution of both JCPyV VLPs and BKPyV VLPs mostly in the liver, but also at lower level in kidney and spleen. Moreover, liver uptake was predominantly observed in liver sinusoidal endothelial cells (LSECs). Surprisingly, there was no significant difference in tissue distribution between wild-type JCPyV VLPs and JCPyV VLP mutants (L55F and S269F). Also, the blood half-time was similar for all of them. With a view to the lack of sialic acid binding activity in mutant VLPs, this indicates involvement of other non-sialic acid receptors in cellular uptake. While all types of JCPyV VLPs were almost completely removed from the circulation within 10 minutes, it took significantly longer time for BKPyV VLPs. This suggests either higher stability of BKPyV VLPs in comparison to 3 variants of JCPyV VLPs or a rapid saturation of BKPyV binding receptors. Another reason for a delay of BKPyV VLPs clearance from the blood could be unspecific interactions of BKPyV VLPs with blood factors. To maintain signature scavenging activity LSECs rely on clathrin-mediated endocytosis. It is also known that in natural host cells BKPyV is internalized via caveolin-mediated, whereas JCPyV- via clathrin-mediated endocytosis. This could also explain the higher blood half-time for BKPyV VLPs in comparison to JCPyV VLPs.
Further studies would be required to establish whether JCPyV or BKPyV uptake in LSECs would lead to destruction of all internalized virus particles. Additionally, a better understanding of LSEC-mediated polyomavirus clearance could lead to better understanding of development mechanism of polyomavirus-associated diseases. This may also allow to develop the strategies to arrest this process for immunocompromised subjects at risk of high-level polyomavirus replication. Another important subject would be to investigate organ distribution, LSEC uptake and clearance of VLPs preincubated with either murine or human antibodies and to compare them with non-preincubated VLPs.

Due to morphological identity with authentic virus, virus-like particles are widely used as an antigen to detect virus-specific antibodies. Numerous studies showed that use of VLPs, rather than VP1 monomers or pentamers, for detection of specific antibodies makes the testing more sensitive and specific. Therefore majority of serological tests, including enzyme-linked immunosorbent assays (ELISA) utilize VLPs as the antigen.

## 5.2 Inter- and Intralaboratory Comparison of JC Polyomavirus Antibody Testing Using Two Different Virus-Like Particle-Based Assays

Because of more frequent application of immunosuppression, the risk of developing JCPyV- and BKPyV-associated diseases (PML for JCPyV and PyVAN and PyVHC for BKPyV) has increased drastically in the last decades. The risk of PML development is estimated to be 100-fold higher for JCPyV-seropositive patients in comparison to JCPyV-seronegatives. Most cases of PyVAN and PyVHC have been tested as positive for BKPyV at the moment of disease diagnosis. Moreover, positive JCPyV or BKPyV serostatus indicates not only past exposure, but also viral persistence which is associated with a risk of high-level viral replication in case of immunosuppression. Therefore, investigation of JCPyV and BKPyV infection has been receiving significantly more attention. However, correct identification of IgG positive and negative results could be problematic due to lack of universal standardized ELISA procedure.
In conducted study we reviewed and optimized virus-like particle (VLP)-based ELISA for JCPyV IgG detection. Moreover we developed the preadsorption inhibition assay in order to precisely define JCPyV serostatus for samples with ambiguous ELISA results.

CVI
Journals.ASM.org

# Inter- and Intralaboratory Comparison of JC Polyomavirus Antibody Testing Using Two Different Virus-Like Particle-Based Assays

**Piotr Kardas,[a] Mohammadreza Sadeghi,[b] Fabian H. Weissbach,[a] Tingting Chen,[b] Lea Hedman,[b,c] Eeva Auvinen,[b,c] Klaus Hedman,[b,c] Hans H. Hirsch[a,d,e]**

Transplantation and Clinical Virology, Department Biomedicine (Haus Petersplatz), University of Basel, Basel, Switzerland[a]; Department of Virology, Haartman Institute, University of Helsinki, Helsinki, Finland[b]; Department of Virology and Immunology, Helsinki University Central Hospital Laboratory Services, Helsinki, Finland[c]; Infectious Diseases and Hospital Epidemiology, University Hospital Basel, Basel, Switzerland[d]; Division of Infection Diagnostics, Department Biomedicine (Haus Petersplatz), University of Basel, Basel, Switzerland[e]

**JC polyomavirus (JCPyV) can cause progressive multifocal leukoencephalopathy (PML), a debilitating, often fatal brain disease in immunocompromised patients. JCPyV-seropositive multiple sclerosis (MS) patients treated with natalizumab have a 2- to 10-fold increased risk of developing PML. Therefore, JCPyV serology has been recommended for PML risk stratification. However, different antibody tests may not be equivalent. To study intra- and interlaboratory variability, sera from 398 healthy blood donors were compared in 4 independent enzyme-linked immunoassay (ELISA) measurements generating >1,592 data points. Three data sets (Basel1, Basel2, and Basel3) used the same basic protocol but different JCPyV virus-like particle (VLP) preparations and introduced normalization to a reference serum. The data sets were also compared with an independent method using biotinylated VLPs (Helsinki1). VLP preadsorption reducing ≥35% activity was used to identify seropositive sera. The results indicated that Basel1, Basel2, Basel3, and Helsinki1 were similar regarding overall data distribution ($P = 0.79$) and seroprevalence (58.0, 54.5, 54.8, and 53.5%, respectively; $P = 0.95$). However, intra-assay intralaboratory comparison yielded 3.7% to 12% discordant results, most of which were close to the cutoff (0.080 < optical density [OD] < 0.250) according to Bland-Altman analysis. Introduction of normalization improved overall performance and reduced discordance. The interlaboratory interassay comparison between Basel3 and Helsinki1 revealed only 15 discordant results, 14 (93%) of which were close to the cutoff. Preadsorption identified specificities of 99.44% and 97.78% and sensitivities of 99.54% and 95.87% for Basel3 and Helsinki1, respectively. Thus, normalization to a preferably WHO-approved reference serum, duplicate testing, and preadsorption for samples around the cutoff may be necessary for reliable JCPyV serology and PML risk stratification.**

Seroprevalence studies indicate that by early adulthood, JC polyomavirus (JCPyV) has infected approximately half of the general population (1, 2). Thereafter, JCPyV asymptomatically persists in renourinary tract and is intermittently shed into the urine (2–4). In immunocompromised patients, JCPyV can cause progressive multifocal leukoencephalopathy (PML), a demyelinating disease of the brain, with typically fatal outcome (5, 6). PML results from lytic JCPyV replication in subcortical oligodendrocytes that generate neuronal myelin sheaths. Progressive demyelination followed by neuronal dysfunction and cell death underlies the radiological and clinical features of PML (1, 5, 6). Despite some promising *in vitro* data (7), there is currently no specific antiviral therapy, and the outcome of PML depends largely on mounting JCPyV-specific immune functions that suppress JCPyV replication (1, 6, 8, 9). PML had been a frequent complication of HIV and AIDS patients in the era before combination antiretroviral therapy, affecting 1% to 8% of the patients at risk (10, 11). The availability of combination antiretroviral therapy (cART) has decreased the incidence of PML and significantly improved PML outcome (10, 12). Recently, an increasing number of PML cases were observed among multiple sclerosis (MS) patients treated with natalizumab. Natalizumab is a monoclonal antibody blocking α4β1 integrin and thereby homing of inflammatory cells to MS lesions (13–15). Practically all MS patients were found to be JCPyV seropositive at the time of natalizumab treatment, indicating that most, if not all, cases of PML were in fact caused by JCPyV reactivation (16). Thus, the risk of PML after 24 months of natalizumab therapy can be as high as 1:100 in JCPyV-seropositive patients but less than 1:10,000 in JCPyV-seronegative MS patients compared to less than 1:500,000 in the general population per year (1). Therefore, screening of MS patients for JCPyV antibodies may provide a relevant PML risk stratification tool and inform decisions regarding follow-up and treatment modalities (17, 18).

JCPyV antibodies can be detected by different techniques, including virus neutralization, hemagglutination inhibition of red blood cells, indirect immunofluorescence using JCPyV protein-expressing cells, and the enzyme-linked immunosorbent assay (ELISA) (1, 19). However, neutralization, while being functionally important, has some limitations, including the absence of a defined cutoff and the inability to detect specific, nonneutralizing antibodies. Hemagglutination inhibition assays generally show low sensitivity and do not allow reliable measurement of low antibody titers and detection of antibodies against JCPyV with typical PML-associated mutations in the sialic acid-binding region of

**Received** 17 July 2014 **Returned for modification** 1 September 2014
**Accepted** 16 September 2014
**Published ahead of print** 24 September 2014
**Editor:** M. F. Pasetti
Address correspondence to Hans H. Hirsch, hans.hirsch@unibas.ch.

doi:10.1128/CVI.00489-14
The authors have paid a fee to allow immediate free access to this article.

the mutant VP1 gene (20, 21). While ELISA is the most widely used technique, the different assays vary in performance, serum dilutions, empirically derived cutoffs, and antigen preparations. Although the major viral capsid protein VP1 is frequently used, preparations of monomer, pentamer, or virus-like particles (VLPs) have been reported, which together with differences in serum dilutions and cutoffs are likely to affect reliability and commutability of results (1, 19). We previously investigated the seroprevalence of JCPyV antibodies in 400 healthy blood donors from Basel, Switzerland. Although our overall results corresponded well to reports from other studies (22), including those on MS patients (23), as reviewed in reference 1, the interpretation of results around the cutoff is usually difficult. Particularly the implications of a false-negative result for patient counseling regarding the PML risk under natalizumab therapy or conversely the withholding of therapy for a patient with a false-positive result prompted us to work out an improved protocol integrating the option of preadsorption reduction testing. The Basel assay was compared with an independent ELISA from Helsinki using biotinylated JC VP1 VLPs. The results indicate that more than 90% of sera can be reliably assayed and that approximately 10% of sera with IgG levels around the cutoff need confirmatory testing by preadsorption reduction assay.

## MATERIALS AND METHODS

**Study participants and samples.** Serum samples ($n = 398$) were obtained from citrate-anticoagulated blood collected from 398 healthy blood donors at the time of blood donation in Basel, Switzerland (IRB 267/06), and were described previously (2). The sera had been stored frozen at −20°C until thawed and aliquoted for retesting in both participating laboratories. At the time of blood donation, the donors tested negative for infections with human immunodeficiency virus (HIV), hepatitis B virus (HBV), hepatitis C virus (HCV), and *Treponema pallidum*.

**Isolation and purification of recombinant JCPyV VLPs.** The preparation of JCPyV VLP in Basel was described previously (2). Briefly, the JCPyV Mad-1 VP1 gene was inserted into the respective site of the baculovirus using the Bac-to-Bac baculovirus expression system (Invitrogen, Basel, Switzerland) and transfected into *Spodoptera frugiperda* Sf9 cells (American Type Culture Collection [ATCC], Manassas, VA) in suspension according to the manufacturer's protocol. Pellets of infected Sf9 cells were resuspended in phosphate-buffered saline (PBS) containing 0.1 mM $CaCl_2$ and complete EDTA-free protease inhibitors (Roche, Basel, Switzerland), followed by sonication and centrifugation at 10,000 × *g* for 10 min to separate cytoplasmic VLPs in supernatants from the cell nuclei pellet. The supernatant was filtered with a 0.45-μm-pore paper filter and run on a 40% sucrose cushion at 70,000 × *g* for 3 h. The pellet was resuspended in PBS containing complete EDTA-free protease inhibitors and 0.25% deoxycholic acid, incubated in a water bath at 37°C for 1 h, and then chilled on ice for 5 min. Then an equal volume of 4 M NaCl with 0.1 mM $CaCl_2$ was added, and the mixture was incubated on ice for 30 min and centrifuged afterwards at 3,220 × *g* for 20 min. Intranuclear VLPs were isolated by resuspension of the nuclear pellet in a mixture of 10 mM Tris-HCl (pH 8), 500 mM NaCl, 1 mM $MgCl_2$, 1 mM $CaCl_2$, and 0.1% NP-40 and homogenization with glass mortar and pestle. After sonication and centrifugation at 17,000 × *g* for 1 h 30 min, VLPs were purified by CsCl ultracentrifugation at 150,000 × *g* for 24 h (Optima XPN-90 ultracentrifuge with an SW55 Ti rotor; Beckmann Coulter, Indianapolis, IN). Fractions were collected using the Beckman Coulter fraction recovery system, and those containing VLPs were pooled and ultracentrifuged at 300,000 × *g* for 2 h (SW55 Ti rotor) and stored in buffer A (150 mM NaCl, 10 mM Tris-HCl [pH 7.4], 1.0 mM $CaCl_2$) at −80°C. The three-dimensional structure and purity of VLPs were confirmed by sodium dodecyl sulfate–polyacrylamide gel electrophoresis (SDS-PAGE) and Coomassie staining as well as transmission electron microscopy.

The preparation of the JCPyV VLPs in Helsinki was also based on the JCPyV Mad-1 DNA sequence, but the major virus capsid protein VP1 coding region (nucleotides [nt] 1469 to 2533) was chemically synthesized and optimized for *S. frugiperda* usage (GenScript). VLPs were produced in insect cells using the Bac-to-Bac system (Invitrogen, Carlsbad, CA) as recommended by the manufacturer's instructions. Sf9 cells were infected and harvested at 4 to 5 days after infection by a 2-step lysis procedure (24), resuspending the cell pellet in buffer 1 (20 mM Tris-HCl [pH 7.5], 150 mM NaCl, 1% Triton) at +4°C for 10 min, followed by 10 min of centrifugation at 10,000 × *g*. The supernatant was removed, and the pellet was resuspended in sonication buffer (10 mM Tris-HCl [pH 8.0], 500 mM NaCl, 1 mM $CaCl_2$, 1 mM $MgCl_2$, 0.01% Triton) supplemented with a proteinase inhibitor cocktail (complete EDTA free; Roche, Mannheim, Germany). After three 20-s sonications and centrifugation at 15,000 × *g* for 40 min, the supernatant diluted in 20 mM Tris (pH 7.5) was layered on top of 1.52 g/cm$^3$ cesium chloride. After ultracentrifugation (Beckman L-70) in a Beckman SW28 Ti rotor at 23,000 × *g* at 10°C for 4 h, fractions were studied by SDS-PAGE. Those rich in VP1 and VLPs by electron microscopy (EM) were pooled and dialyzed against PBS. For use as an antigen, the VLPs were biotinylated with the EZ-Link Sulfo-NHS-LC-biotinylation kit (Pierce, Rockford, IL) as described previously (24).

**ELISA.** The Basel ELISA was essentially done as described previously (2). In brief, microtiter plates were coated with JCPyV VLPs (100 ng/well) overnight at 4°C followed by being washed five times with washing buffer (0.1% Tween 20). The wells were then incubated with blocking buffer (150 mM NaCl, 10 mM Tris-HCl [pH 7.4], 1 mM $CaCl_2$, 4% bovine serum albumin [BSA], 0.1% Tween 20) for 2 h at 25°C and then washed five times with washing buffer. Serum samples were diluted 1:400 in blocking buffer, and 100 μl was added per well. After 1 h of incubation at 25°C, the wells were washed again (5 times) and incubated for 1 h at 25°C with 100 μl/well of 1:10,000-diluted Fc-specific goat anti-human IgG conjugated with peroxidase (Sigma-Aldrich, Buchs, Switzerland). The wells were washed five times and incubated at 25°C for 30 min with 100 μl of freshly prepared 0.4 mg/ml *o*-phenylenediamine (Sigma-Aldrich, Buchs, Switzerland). The color reaction was stopped by adding 50 μl of 1 M sulfuric acid per well, and the optical density at 492 nm ($OD_{492}$) was measured using a Safire II plate reader (Tecan, Maennedorf, Switzerland). All results were recorded as blank well subtraction. The cutoff defining a positive serologic response was an $OD_{492}$ of 0.110, as reported previously (2, 25, 26).

Normalization of IgG activities (normalized OD [nOD]) was obtained by parallel testing of an internal laboratory reference serum at a dilution yielding an OD of close to 1.0 on every ELISA plate. The nOD was obtained by dividing the OD of the patient sample by the OD of the reference serum.

The Helsinki JCPyV IgG ELISA was conducted essentially as described for the human polyomaviruses MCPyV and TSPyV (24, 27). Briefly, streptavidin plates (Thermo Fisher Scientific, Waltham, MA) with the biotinylated VLPs attached (120 ng/well) were coated with a sample diluent (Ani Labsystems). The serum samples diluted 1:200 were applied in duplicate, and the absorbances at 492 nm were recorded with blank-plate subtraction. The cutoff values were calculated according to samples ($n = 170$) with absorbances below a provisional threshold of 0.150. Utilizing the mean (0.048) and standard deviation (SD) (0.036), the cutoffs for JCPyV IgG presence and absence were set at mean + 4 SD (0.192) and mean + 3 SD (0.156), respectively.

In summary, the most significant differences between assays from Basel and Helsinki1, respectively, were the type and concentration of coating antigen (nonmodified VLPs at 100 ng/well versus biotinylated VLPs at 120 ng/well) and the serum dilution (400-fold versus 200-fold).

**JCPyV VLP preadsorption assay.** ELISA plates were coated with 25 ng/well JCPyV VLPs overnight at 4°C. The serum samples were diluted 1:100 in blocking buffer (nonpreadsorbed) or in blocking buffer containing 25 ng

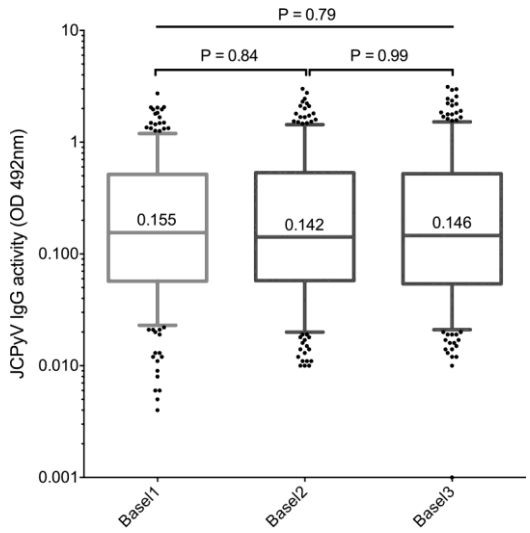


**FIG 1** Intralaboratory comparison of JCPyV VLP IgG activity ($OD_{492}$) by ELISA in 398 health blood donors. Basel1 shows the IgG activity results as reported previously; Basel2 shows results of retesting using a newly prepared VLP batch; Basel3 shows results of retesting together with the internal normalization control using reference serum (Basel3). IgG activity corresponds to an optical density at 492 nm without or with normalization ($OD_{492}$/$nOD_{492}$) as described in Materials and Methods. Boxes span the interquartile range (IQR) with the 25th and the 75th percentiles. The number in the box indicates the median, the whiskers indicate the 5th and 95th percentile range, and dots indicate outliers below and above the range. *P* values were calculated by the Kruskal-Wallis test and Mann-Whitney U test.

JCPyV VLPs per 100 μl (preadsorbed). After incubating without agitation at 25°C for 1 h, 100 μl of diluted serum or serum-VLP mixture was transferred into previously blocked (for 2 h at 25°C) JCPyV VLP-coated wells, and the standard ELISA protocol was followed (described above). Mock and preadsorbed samples were tested in parallel. The results were reported as the percentage of IgG OD activity reduction after preadsorption with JCPyV VLPs according to $[(OD_{nonpreadsorbed} - OD_{preadsorbed})/OD_{nonpreadsorbed}] \times 100$. To investigate the possible contribution of BKPyV antibodies (cross-reactivity), the preadsorption assay was performed in parallel with BK VP1 VLPs using 14 JCVPyV-positive sera ($0.08 < nOD < 0.25$ and preadsorption inhibition of ≥35%).

**Study design and statistical analysis.** All 398 healthy blood donor sera were investigated independently in two research centers: in Basel (according to a previously published ELISA protocol [Basel1]), with a new VLP preparation [Basel2] and an improved protocol with an OD normalization step [Basel3]) and in Helsinki (Helsinki1). The results of all four testing series were compared as intralaboratory intra-assay (Basel1 versus Basel2), intralaboratory interassay (Basel2 versus Basel3), and interlaboratory interassay (Basel2/Basel3 versus Helsinki1) comparisons. Discordant results were further investigated in preadsorption experiments, wherein the serum dilutions were tested in parallel by ELISA either directly or after prior preincubation with VLPs. Samples showing a decrease in IgG activity of ≥35% were regarded as JCPyV-seropositive sera. For the statistical analysis, GraphPad Prism 6.0 was used. Data with a nonnormal distribution as indicated by Kolmogorov-Smirnov Z test were analyzed by using the Kruskal-Wallis test or Mann-Whitney U test. Categorical data were analyzed using Pearson's $\chi^2$ test. Evaluation of agreement between different ELISA measurements was performed using Bland-Altman analysis. The specificity and sensitivity of the assays were calculated with MedCalc easy-to-use statistical software (www.medcalc.org). A two-sided *P* value of $<0.05$ was considered statistically significant.

## RESULTS

**Intralaboratory comparison of JCPyV VLP-based IgG serology.** For an intralaboratory comparison, 398 stored sera from 400 healthy blood donors that had been tested and reported previously (Basel1) (2) were compared with a second single measurement using a newly prepared batch of JCPyV VLPs (Basel2). As shown in Fig. 1, there was no significant difference in the overall distribution of the IgG activity ($P = 0.79$) or in the median values. Applying the previously established cutoff of 0.110, 58.0% were higher and called seropositive in the data set Basel1, 54.5% in Basel2, and 54.8% in Basel3 (Table 1). Thus, there were slightly more JCPyV-seropositive sera by Basel1 than by Basel2 or Basel3, but the difference was statistically not significant ($P = 0.95$, $\chi^2$ test).

In the absence of a "gold standard," the results were further investigated using the Bland-Altman analysis (Fig. 2). For Basel1 versus Basel2, overall slightly higher values were seen for Basel2, yielding a bias value of ΔOD of −0.027 (Fig. 2A). The 95% confidence interval (CI) was large, ranging from −0.690 to 0.635 and mostly due to differences in the higher-IgG-activity sera. Below an OD of 0.25 (arbitrarily defined by 2× the cutoff of 0.110 + the mean of the blank), and particularly below the cutoff OD of 0.110, the difference was minimal. The data suggest that variations in higher-titer sera with an OD of >0.25 contributed significantly to the intralaboratory variability. Restricting the Bland-Altman analysis to OD values of <0.25 revealed a mean bias of ΔOD of 0.033 and a more narrow 95% CI (−0.219 to 0.286 [data not shown]). Thus, variability appeared to be less for OD values below 0.25, but they had an impact on the qualitative interpretation of when to call a serum JCPyV seropositive.

Therefore, the intralaboratory discordance of the qualitative outcomes of both assays was examined (Table 2). Among 48 discordant results (12% of 398 sera), a majority of 33 (69%) sera were close to the cutoff and therefore likely to result from assay variations. Conversely, 15 were found to be highly discordant (with one positive result equal to or higher than an OD of 0.25) and unlikely to reflect mere assay variations. Independent retesting of these sera indicated that they most likely resulted from technical errors, including mislabeling or pipetting (data not shown).

To assess the reliability of the assay further, all 398 sera were tested again in single measurements, but in the presence of a JCPyV-positive reference serum yielding an OD value of close to 1.0 for normalization (data set Basel3). The overall distribution of the normalized OD values was not significantly different from those of Basel1 and Basel2 (Fig. 1), but the qualitative results seemed closer to those of Basel2 (Table 1). The Bland-Altman analysis of Basel1 versus Basel3 was similar to that of Basel1 versus Basel2, with a bias of ΔOD of −0.046 and a large 95% CI from

**TABLE 1** Intralaboratory comparison of qualitative JCPyV IgG results[a]

| Assay | No. of sera with JCPyV IgG serostatus[b]: | |
|---|---|---|
| | Seropositive | Seronegative |
| Basel1 | 231 | 167 |
| Basel2 | 221 | 177 |
| Basel3 | 218 | 180 |

[a] Sera from 398 healthy blood donors were tested. The cutoff of 0.110 was used for JCPyV serostatus determination.
[b] $P = 0.95$, calculated by $\chi^2$ test.

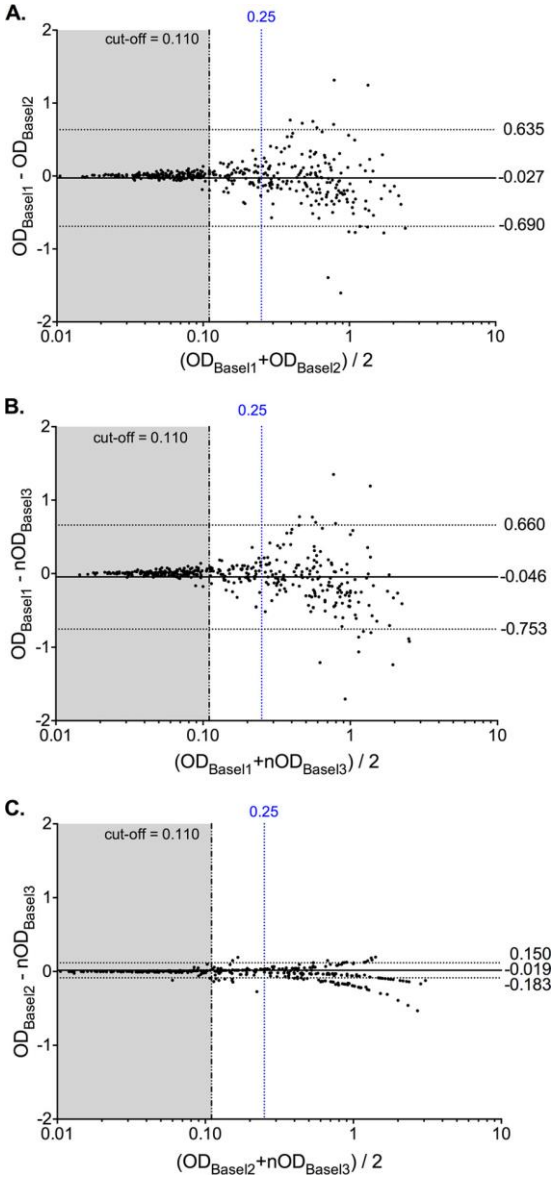


**FIG 2** Intralaboratory comparison of JCPyV serology results using Bland-Altman analysis. (A) Basel1 versus Basel2. (B) Basel1 versus Basel3. (C) Basel2 versus Basel3. In each panel, the solid horizontal line represents the overall median bias, and dashed horizontal lines indicate the 95% confidence interval. The black vertical dashed line indicates the assay cutoff at an OD of 0.110, and the blue vertical dashed line indicates an OD of 0.25.

−0.753 to 0.660 (Fig. 2B). There were 52 (13% of 398 sera) discordant results between Basel1 and Basel3, of which 36 (69%) were close to the cutoff (Table 2). In contrast, the Bland-Altman analysis of Basel2 versus Basel3 showed very good agreement with a bias of ΔOD of −0.019 and a narrower 95% CI from −0.183 to 0.150 (Fig. 2C). Only 25 results (6% of 398 sera) were qualitatively discordant, 23 (92%) of them being close to the cutoff (Table 2). Restricting the Bland-Altman analysis to an OD of <0.25 confirmed that the intralaboratory variation around the cutoff was also reduced (not shown). The results indicated that the intralaboratory variability was significantly improved by standardized testing and normalization and that the results close to the cutoff (e.g., below an OD of 0.25) would benefit from independent confirmatory testing.

**Interlaboratory comparison of serological IgG reactivity to JCPyV VLPs.** For an independent interlaboratory interassay comparison, the 398 sera were tested in another laboratory using independently prepared, codon-optimized and biotinylated JCPyV VLPs (see Materials and Methods). The overall distribution of OD results of data set Helsinki1 was not significantly different from that from Basel3 (median, 0.208; $P = 0.12$) (Fig. 3A). Using the cutoff OD of 0.156 determined for this assay, the JCPyV IgG seroprevalence in Helsinki1 was 53.5% and not significantly different from seroprevalence in Basel2 (54.5%) and Basel3 (54.8%) ($P = 0.92$, calculated by $\chi^2$ test).

The Bland-Altman analysis of Basel3 versus Helsinki1 revealed, however, a large bias of ΔOD of −0.278 and a 95% CI from −1.223 to 0.667 (Fig. 3B). This indicated that the overall OD values were higher for Helsinki1, which appeared to result mostly from sera with higher JCPyV IgG titers leading to a corresponding downward shape of the data points (Fig. 3B). Restriction of the Bland-Altman analysis to data points of an OD of <0.25 supported the notion that the differences were smaller around the critical cutoffs of 0.110 and 0.156 of either assay (Fig. 3C). Only 15 (4%) of 398 samples were discordant, 14 of them (93%) being close to the respective cutoff (Table 3). This emphasized the role of assay standardization and the need for an independent confirmatory assay for results close to the respective cutoff.

**Preadsorption assay to determine serostatus of discordant samples.** Discordant samples were tested using VLP preadsorption as a competition step to distinguish JCPyV-specific IgG-positive samples from those with unspecific antibodies (see Materials and Methods). The preincubation with soluble JCPyV VLPs is expected to bind JCPyV-specific antibodies and to reduce the remaining activity of the OD in the following ELISA. To estimate the specific reduction, the serum samples of the 398 healthy blood donors, which included 76 individuals with documented urinary JCPyV shedding detected by PCR as reported previously (2), were compared in the preadsorption assay. OD values obtained for nonpreadsorbed sera served as the reference to calculate reduction of IgG activity. Examination of the distribution of results for the 76 JCPyV-positive donors with proven urinary JCPyV shedding showed that preadsorption reduced the OD activity by ≥35% (Fig. 4A). Therefore, a reduction of ≥35% was chosen to define

**TABLE 2** Discordant results in intralaboratory testing of 398 healthy blood donors

| Discordant result[a] | No. of discordant samples | | |
|---|---|---|---|
| | Basel1 vs Basel2 | Basel1 vs Basel3 | Basel2 vs Basel3 |
| −/+ | 8 | 9 | 12 |
| −/++ | 9 | 10 | 1 |
| +/− | 25 | 27 | 11 |
| ++/− | 6 | 6 | 1 |
| Total | 48 | 52 | 25 |

[a] −, seronegative at an OD of <0.110; +, seropositive at 0.11 < OD < 0.25; ++, seropositive at an OD of >0.25.

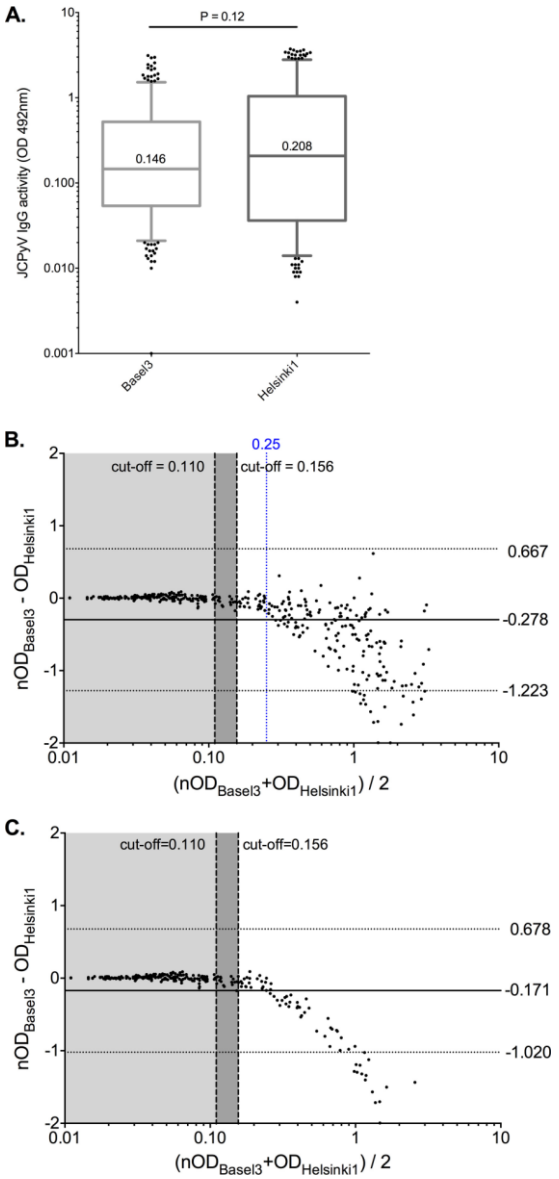


**FIG 3** JCPyV serology results using the biotinylated VLPs (Helsinki1). (A) Overall serology results of 398 healthy blood donors (Helsinki1) as described in Materials and Methods and in the legend to Fig. 1. (B) Bland-Altman analysis comparing Basel3 versus Helsinki1. (C) Bland-Altman analysis comparing Basel3 versus Helsinki1 restricted to data points of an OD of <0.25 in the Basel3 assay. The solid horizontal line represents the overall median bias, and dashed horizontal lines indicate the 95% confidence interval. The left vertical black dashed line indicates the assay cutoff OD of 0.110 of the Basel assays, the right vertical black dashed line indicates the assay cutoff OD of 0.156 of the Helsinki1 assay, and the blue vertical dashed line indicates the OD of 0.25.

the JCPyV-seropositive status for sera between an OD of 0.08 (cutoff − blank OD, 0.110 to 0.03) and an OD of 0.25.

To investigate how much cross-reactivity of BKPyV antibody contributed to the OD values close to the cutoff, a set of 14 JCPyV-positive sera with activity of 0.08 < nOD < 0.25 and preadsorption inhibition of ≥35% were also preadsorbed with BKPyV VLPs. The results revealed an average reduction by BK VLP preadsorption of only 7.87%, which is significantly different from the 50.96% for JCPyV VLPs (Fig. 4B) ($P < 0.0001$, $t$ test).

**TABLE 3** Discordant results in interlaboratory testing of 398 healthy blood donors

| Discordant result[a] | No. of discordant samples | |
|---|---|---|
| | Basel2 vs Helsinki1 | Basel3 vs Helsinki1 |
| −/+ | 14 | 5 |
| −/++ | 4 | 0 |
| +/− | 19 | 9 |
| ++/− | 3 | 1 |
| Total | 40 | 15 |

[a] −, seronegative at an OD of <0.110; +, seropositive at 0.11 < OD < 0.25; ++, seropositive at an OD of >0.25.

Preadsorption testing of the samples discordant between Basel3 and Helsinki1 indicated false-positive results for 1 (0.05%)

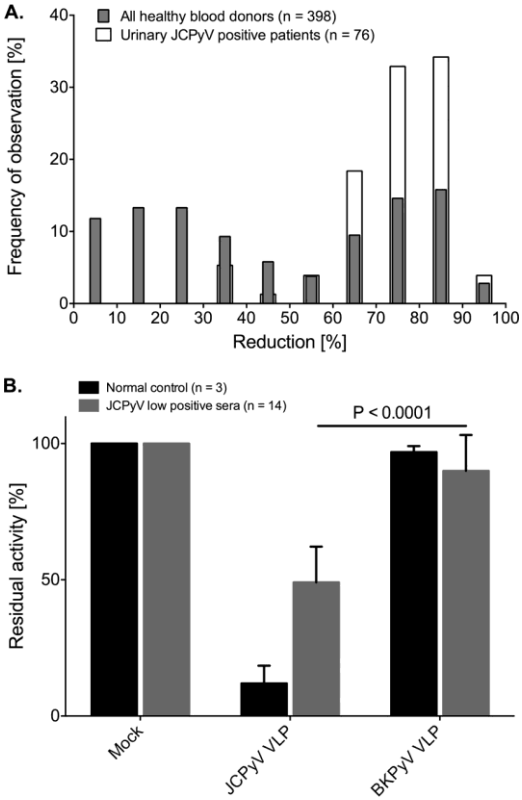


**FIG 4** Distribution of OD reductions in healthy blood donors and 76 patients shedding JCPyV in urine after preincubation with JCPyV VLPs and contribution of cross-reactive BKPyV antibodies to JCPyV-specific activity. (A) The histogram indicates the percentage of individuals with the corresponding degree of reduction of IgG activity after preadsorption with JCPyV VLPs as described in Materials and Methods. The results for 76 patients with JCPyV DNA-positive urine samples are shown (white bars), as are the results for 398 healthy blood donors (gray bars). Assuming that all urinary JCPyV DNA-positive patients are also JCPyV seropositive, a 35% reduction was determined for definition of serum samples with JCPyV-specific antibody titers. (B) A bar chart presents the remaining activity of JCPyV-specific antibodies for 14 low-JCPyV sera after preincubation with either JCPyV or BKPyV VLPs. The $P$ value was calculated by $t$ test.

TABLE 4 Determination of JCPyV serological results[a]

| Basel3 result | Helsinki1 result | Preadsorption result | Final serostatus | False-positive result | False-negative result |
|---|---|---|---|---|---|
| Positive | Positive | Positive | Positive | | |
| Positive | Negative | Positive | Positive | | Helsinki1 |
| Positive | Negative | Negative | Negative | Basel3 | |
| Negative | Negative | Negative | Negative | | |
| Negative | Positive | Negative | Negative | Helsinki1 | |
| Negative | Positive | Positive | Positive | | Basel3 |

[a] Samples were defined as positive if the OD was above the cutoff (0.11 for Basel3 and 0.156 for Helsinki1) and if preadsorption reduced the OD by ≥35% for an OD of ≥0.08.

TABLE 5 Summary of JCPyV serological results

| Result | No. of results for: Basel3 | Helsinki1 |
|---|---|---|
| True positive | 217 | 209 |
| False positive | 1 | 4 |
| True negative | 179 | 176 |
| False negative | 1 | 9 |
| Total | 398 | 398 |

and 4 (1.00%) donors, respectively, as well as false-negative results for 1 (0.05%) and 9 (2.26%) cases (Tables 4 and 5). The numbers of true-positive and true-negative results, respectively, were 217 and 179 in Basel3 and 209 and 176 in Helsinki1. Accordingly, the specificities of the Basel3 and Helsinki1 assays were 99.44% and 97.78%, respectively, whereas the sensitivities corresponded to 99.54% and 95.87%, respectively.

## DISCUSSION

Serological studies of JCPyV infection have recently gained increasing interest as predictors of the risk of developing PML in MS patients treated with natalizumab. In fact, a positive JCPyV serostatus, together with other factors, such as treatment history and duration of natalizumab exposure, has been proposed for identification of MS patients with a 100-fold-increased risk of PML. Given this impact of JCPyV serology, we critically reviewed the intra- and interlaboratory variation of two independently developed assays on a previously described population of Swiss healthy blood donors. The results demonstrate that the overall test performance of VLP-based ELISAs is good for describing the seroprevalence of this population from an epidemiological point of view. Approximately 54% to 58% of healthy adults are JCPyV seropositive, in line with other studies, including those done in MS patients (reviewed in detail recently in reference 1). Although no statistically significant differences in intra-assay and interassay variability were revealed on the population level, qualitative differences were seen in the identification of the individual JCPyV serostatus. The present study demonstrated that both the intra- and interassay variability caused approximately 10% discordant results. Two different sources of discordance became apparent. The first consisted typically of discordance at ODs higher than 0.25 in one of the comparators, was almost exclusively due to technical errors, such as labeling and pipetting, and could be resolved by retesting. In practice, this pitfall occurs typically when testing large series by single measurements and can be tackled by testing samples in duplicates or triplicates.

Not unexpectedly, the second and more frequent cause of discordance resulted from sera with a low IgG activity close to the cutoff of the assays. As indicated in this study, approximately 10% of sera were in this IgG activity range of ODs of less than 0.250 to 0.080. In this critical range, the overall assay variability was small according to the Bland-Altman analysis, but it nevertheless resulted in qualitatively different calls of the serostatus. Repeat testing is therefore unlikely to satisfactorily resolve this discordance, and other testing formats are needed. As shown here, introduction of normalization to a reference serum improved the overall assay performance by reducing the rate of discordance. Therefore, the use of reference sera for normalization seems to be a valuable option for assay standardization. Since discordances in this low OD range could still be caused by false-positive (e.g., cross-reactive) or false-negative (e.g., low IgG activities) results, the role of introducing a preadsorption step was investigated. By examining 398 sera with or without JCPyV VLP preadsorption, a 35% reduction was defined as a specific confirmatory value for JCPyV-seropositive sera. Preadsorption with BKPyV VLPs reduced the OD values by only 7.87%, indicating that cross-reactive antibodies to BKPyV contributed little, in agreement with earlier observations (2). Therefore, discordances between the Basel3 and Helsinki1 data sets could be resolved by preadsorption reduction, indicating the specificities of the Basel3 and Helsinki1 assays as 99.44% and 97.78%, respectively, and the sensitivities as 99.54% and 95.87%.

The investigation of JCPyV infection can employ detection of viral DNA or measurement of anti-JCPyV antibodies. However, previous studies revealed that in some cases, JCPyV DNA PCR is neither a sensitive indicator of JCV infection nor a specific predictor of PML, as demonstrated by some PML patients who had no detectable viral DNA in urine or blood samples (28, 29 [reviewed in detail recently in reference 1]). More recently, HLA class II DRB1*04:01 was reported to be associated with low JCPyV-specific T-cell responses and absence of detectable urinary viral shedding, albeit with normal JCPyV-specific antibodies (30). In another study, HLA-DRB1*15 was found to be associated with a negative JCPyV serostatus in MS patients, as measured by a commercial assay (31). The authors propose that serological assays might underestimate JCPyV infection status, with potential consequences for MS patients falsely identified as not exposed to JCPyV (32). We conclude that an improved serological assay with preadsorption for antibody activities around the cutoff is a critical first analysis to classify patients concerning JCPyV exposure. Further studies are needed to establish whether HLA-DRB typing is required to better stratify MS patients with critical HLA types.

Despite the obvious advantages of neutralization, ELISA has become the most versatile method for detection of anti-JCPyV antibodies (19, 20). It can utilize VP1 in the form of monomers, pentamers, or VLPs (1). However, ELISA with VLPs as the coating antigen has been shown to be more sensitive and specific than VP1 in the monomer or pentamer form (25, 33). For MS patients, there is a commercially available STRATIFY JCV DxSelect kit based on a second-generation ELISA for detection of JCPyV antibodies in humans (34). Clearly, screening, normalization with widely accepted reference sera, and preadsorption testing for specific reduction are important issues. In this context, it should be emphasized that a WHO-approved international reference serum would

be most valuable, as has been shown for other infections and vaccination serologies.

In summary, our findings demonstrate that serological assays for JCPyV IgG need to take into account whether epidemiological questions or individual risk assessments are to be addressed. No significant statistical differences were seen in the overall characteristics of four independent test series of 398 sera from healthy blood donors. Qualitatively, approximately 90% of the results were concordant between the data sets. For 10% of results, confirmatory testing was needed.

According to the results described here, the following points deserve consideration in laboratory testing of sera with unknown JCPyV serostatus by VLP-based ELISA. (i) At least duplicate testing should be performed to avoid technical errors. (ii) Normalization using a reference serum may improve IgG activity measurement. (iii) There should be repeat testing in preadsorption assay of sera in the low OD range around the cutoff (e.g., from OD 0.08 to 0.25 for the assay described here). (iv) There should be quality assessment programs with appropriate training of laboratory personnel involved in ELISA testing of patient samples. (v) Finally, clinical interpretation of negative JCPyV serology data may require the knowledge of the patients' HLA types.

## ACKNOWLEDGMENTS

The expert technical assistance of Jacqueline Samaridis, TCV Laboratory, Basel, with the preparation of the JCPyV VLPs and the ELISA is gratefully acknowledged.

The work at Helsinki was supported by the Academy of Finland (project 1122539), the Sigrid Jusélius Foundation, and the Helsinki University Central Hospital Research and Education, and Research and Development Funds. The Basel group was supported by an institutional grant from the University of Basel to H.H.H.

P.K. expressed and purified JC polyomavirus VP1 virus-like particles, carried out the ELISA, analyzed the data, and wrote the manuscript. M.S., instructed by T.C., expressed, purified, and biotinylated the Helsinki JC-VP1 VLPs, analyzed the data, and participated in the manuscript writing. F.W. expressed and purified JC polyomavirus VP1 virus-like particles and carried out the ELISA. L.H. accounted for the Helsinki serodiagnostics, designing and carrying out the ELISA and analyzing the data. E.A. conceived the collaborative work and participated in the Helsinki assay design and data analysis. K.H. conceived and coordinated the study in Helsinki and participated in data analysis and manuscript writing. H.H.H. designed the study, supervised the procedures, analyzed the data, interpreted the data, and wrote the manuscript.

## REFERENCES

1. **Hirsch HH, Kardas P, Kranz D, Leboeuf C.** 2013. The human JC polyomavirus (JCPyV): virological background and clinical implications. APMIS **121:**685–727. http://dx.doi.org/10.1111/apm.12128.
2. **Egli A, Infanti L, Dumoulin A, Buser A, Samaridis J, Stebler C, Gosert R, Hirsch HH.** 2009. Prevalence of polyomavirus BK and JC infection and replication in 400 healthy blood donors. J. Infect. Dis. **199:**837–846. http://dx.doi.org/10.1086/597126.
3. **Polo C, Perez JL, Mielnichuck A, Fedele CG, Niubo J, Tenorio A.** 2004. Prevalence and patterns of polyomavirus urinary excretion in immunocompetent adults and children. Clin. Microbiol. Infect. **10:**640–644. http://dx.doi.org/10.1111/j.1469-0691.2004.00882.x.
4. **Chesters PM, Heritage J, McCance DJ.** 1983. Persistence of DNA sequences of BK virus and JC virus in normal human tissues and in diseased tissues. J. Infect. Dis. **147:**676–684. http://dx.doi.org/10.1093/infdis/147.4.676.
5. **Ferenczy MW, Marshall LJ, Nelson CD, Atwood WJ, Nath A, Khalili K, Major EO.** 2012. Molecular biology, epidemiology, and pathogenesis of progressive multifocal leukoencephalopathy, the JC virus-induced demyelinating disease of the human brain. Clin. Microbiol. Rev. **25:**471–506. http://dx.doi.org/10.1128/CMR.05031-11.
6. **Tan CS, Broge TA, Jr, Seung E, Vrbanac V, Viscidi R, Gordon J, Tager AM, Koralnik IJ.** 2013. Detection of JC virus-specific immune responses in a novel humanized mouse model. PLoS One **8:**e64313. http://dx.doi.org/10.1371/journal.pone.0064313.
7. **Gosert R, Rinaldo CH, Wernli M, Major EO, Hirsch HH.** 2011. CMX001 (1-O-hexadecyloxypropyl-cidofovir) inhibits polyomavirus JC replication in human brain progenitor-derived astrocytes. Antimicrob. Agents Chemother. **55:**2129–2136. http://dx.doi.org/10.1128/AAC.00046-11.
8. **Khanna N, Wolbers M, Mueller NJ, Garzoni C, Du Pasquier RA, Fux CA, Vernazza P, Bernasconi E, Viscidi R, Battegay M, Hirsch HH.** 2009. JC virus-specific immune responses in human immunodeficiency virus type 1 patients with progressive multifocal leukoencephalopathy. J. Virol. **83:**4404–4411. http://dx.doi.org/10.1128/JVI.02657-08.
9. **Alstadhaug K, Croughs T, Henriksen S, Leboeuf C, Sereti I, Hirsch H, Rinaldo CH.** 2014. Treatment of progressive multifocal leukoencephalopathy with interleukin. JAMA Neurol. **71:**1030–1035. http://dx.doi.org/10.1001/jamaneurol.2014.825.
10. **Khanna N, Elzi L, Mueller NJ, Garzoni C, Cavassini M, Fux CA, Vernazza P, Bernasconi E, Battegay M, Hirsch HH,** for the Swiss HIV Cohort Study. 2009. Incidence and outcome of progressive multifocal leukoencephalopathy in 20 years of the Swiss HIV Cohort Study. Clin. Infect. Dis. **48:**1459–1466. http://dx.doi.org/10.1086/598335.
11. **Berger JR, Kaszovitz B, Post MJ, Dickinson G.** 1987. Progressive multifocal leukoencephalopathy associated with human immunodeficiency virus infection. A review of the literature with a report of sixteen cases. Ann. Intern. Med. **107:**78–87.
12. **Clifford DB, Yiannoutsos C, Glicksman M, Simpson DM, Singer EJ, Piliero PJ, Marra CM, Francis GS, McArthur JC, Tyler KL, Tselis AC, Hyslop NE.** 1999. HAART improves prognosis in HIV-associated progressive multifocal leukoencephalopathy. Neurology **52:**623–625. http://dx.doi.org/10.1212/WNL.52.3.623.
13. **Langer-Gould A, Atlas SW, Green AJ, Bollen AW, Pelletier D.** 2005. Progressive multifocal leukoencephalopathy in a patient treated with natalizumab. N. Engl. J. Med. **353:**375–381. http://dx.doi.org/10.1056/NEJMoa051847.
14. **Kleinschmidt-DeMasters BK, Tyler KL.** 2005. Progressive multifocal leukoencephalopathy complicating treatment with natalizumab and interferon beta-1a for multiple sclerosis. N. Engl. J. Med. **353:**369–374. http://dx.doi.org/10.1056/NEJMoa051782.
15. **Van Assche G, Van Ranst M, Sciot R, Dubois B, Vermeire S, Noman M, Verbeeck J, Geboes K, Robberecht W, Rutgeerts P.** 2005. Progressive multifocal leukoencephalopathy after natalizumab therapy for Crohn's disease. N. Engl. J. Med. **353:**362–368. http://dx.doi.org/10.1056/NEJMoa051586.
16. **Bloomgren G, Richman S, Hotermans C, Subramanyam M, Goelz S, Natarajan A, Lee S, Plavina T, Scanlon JV, Sandrock A, Bozic C.** 2012. Risk of natalizumab-associated progressive multifocal leukoencephalopathy. N. Engl. J. Med. **366:**1870–1880. http://dx.doi.org/10.1056/NEJMoa1107829.
17. **Kappos L, Bates D, Edan G, Eraksoy M, Garcia-Merino A, Grigoriadis N, Hartung HP, Havrdova E, Hillert J, Hohlfeld R, Kremenchutzky M, Lyon-Caen O, Miller A, Pozzilli C, Ravnborg M, Saida T, Sindic C, Vass K, Clifford DB, Hauser S, Major EO, O'Connor PW, Weiner HL, Clanet M, Gold R, Hirsch HH, Radu EW, Sorensen PS, King J.** 2011. Natalizumab treatment for multiple sclerosis: updated recommendations for patient selection and monitoring. Lancet Neurol. **10:**745–758. http://dx.doi.org/10.1016/S1474-4422(11)70149-1.
18. **Sorensen PS, Bertolotto A, Edan G, Giovannoni G, Gold R, Havrdova E, Kappos L, Kieseier BC, Montalban X, Olsson T.** 2012. Risk stratification for progressive multifocal leukoencephalopathy in patients treated with natalizumab. Mult. Scler. **18:**143–152. http://dx.doi.org/10.1177/1352458511435105.
19. **Cinque P, Dumoulin A, Hirsch HH.** 2010. Diagnosis of polyomavirus infection, replication and disease, p 401–424. *In* Jerome K (ed), Laboratory diagnosis of viral infections, 4th ed. Informa Healthcare, New York, NY.
20. **Hamilton RS, Gravell M, Major EO.** 2000. Comparison of antibody titers determined by hemagglutination inhibition and enzyme immunoassay for JC virus and BK virus. J. Clin. Microbiol. **38:**105–109.
21. **Gorelik L, Reid C, Testa M, Brickelmaier M, Bossolasco S, Pazzi A,**

**Bestetti A, Carmillo P, Wilson E, McAuliffe M, Tonkin C, Carulli JP, Lugovskoy A, Lazzarin A, Sunyaev S, Simon K, Cinque P.** 2011. Progressive multifocal leukoencephalopathy (PML) development is associated with mutations in JC virus capsid protein VP1 that change its receptor specificity. J. Infect. Dis. **204:**103–114. http://dx.doi.org/10.1093/infdis/jir198.

22. **Viscidi RP, Khanna N, Tan CS, Li X, Jacobson L, Clifford DB, Nath A, Margolick JB, Shah KV, Hirsch HH, Koralnik IJ.** 2011. JC virus antibody and viremia as predictors of progressive multifocal leukoencephalopathy in human immunodeficiency virus-1-infected individuals. Clin. Infect. Dis. **53:**711–715. http://dx.doi.org/10.1093/cid/cir507.
23. **Gorelik L, Lerner M, Bixler S, Crossman M, Schlain B, Simon K, Pace A, Cheung A, Chen LL, Berman M, Zein F, Wilson E, Yednock T, Sandrock A, Goelz SE, Subramanyam M.** 2010. Anti-JC virus antibodies: implications for PML risk stratification. Ann. Neurol. **68:**295–303. http://dx.doi.org/10.1002/ana.22128.
24. **Chen T, Hedman L, Mattila PS, Jartti T, Ruuskanen O, Soderlund-Venermo M, Hedman K.** 2011. Serological evidence of Merkel cell polyomavirus primary infections in childhood. J. Clin. Virol. **50:**125–129. http://dx.doi.org/10.1016/j.jcv.2010.10.015.
25. **Bodaghi S, Comoli P, Boesch R, Azzi A, Gosert R, Leuenberger D, Ginevri F, Hirsch HH.** 2009. Antibody responses to recombinant polyomavirus BK large T and VP1 proteins in pediatric kidney transplant patients. J. Clin. Microbiol. **47:**2577–2585. http://dx.doi.org/10.1128/JCM.00030-09.
26. **Ginevri F, Azzi A, Hirsch HH, Basso S, Fontana I, Cioni M, Bodaghi S, Salotti V, Rinieri A, Botti G, Perfumo F, Locatelli F, Comoli P.** 2007. Prospective monitoring of polyomavirus BK replication and impact of pre-emptive intervention in pediatric kidney recipients. Am. J. Transplant. **7:**2727–2735. http://dx.doi.org/10.1111/j.1600-6143.2007.01984.x.
27. **Kumar A, Kantele A, Jarvinen T, Chen T, Kavola H, Sadeghi M, Hedman K, Franssila R.** 2012. Trichodysplasia spinulosa-associated polyomavirus (TSV) and Merkel cell polyomavirus: correlation between humoral and cellular immunity stronger with TSV. PLoS One **7:**e45773. http://dx.doi.org/10.1371/journal.pone.0045773.
28. **Koralnik IJ, Boden D, Mai VX, Lord CI, Letvin NL.** 1999. JC virus DNA load in patients with and without progressive multifocal leukoencephalopathy. Neurology **52:**253–260. http://dx.doi.org/10.1212/WNL.52.2.253.
29. **Tornatore C, Berger JR, Houff SA, Curfman B, Meyers K, Winfield D, Major EO.** 1992. Detection of JC virus DNA in peripheral lymphocytes from patients with and without progressive multifocal leukoencephalopathy. Ann. Neurol. **31:**454–462. http://dx.doi.org/10.1002/ana.410310426.
30. **Jelcic I, Aly L, Binder TM, Jelcic I, Bofill-Mas S, Planas R, Demina V, Eiermann TH, Weber T, Girones R, Sospedra M, Martin R.** 2013. T cell epitope mapping of JC polyomavirus-encoded proteome reveals reduced T cell responses in HLA-DRB1*04:01$^{+}$ donors. J. Virol. **87:**3393–3408. http://dx.doi.org/10.1128/JVI.02803-12.
31. **Sundqvist E, Buck D, Warnke C, Albrecht E, Gieger C, Khademi M, Lima Bomfim I, Fogdell-Hahn A, Link J, Alfredsson L, Sondergaard HB, Hillert J, Oturai AB, Hemme B, Kockum I, Olsson T.** 2014. JC polyomavirus infection is strongly controlled by human leucocyte antigen class II variants. PLoS Pathog. **10:**e1004084. http://dx.doi.org/10.1371/journal.ppat.1004084.
32. **Berger JR, Houff SA, Gurwell J, Vega N, Miller CS, Danaher RJ.** 2013. JC virus antibody status underestimates infection rates. Ann. Neurol. **74:**84–90. http://dx.doi.org/10.1002/ana.23893.
33. **Chang D, Fung CY, Ou WC, Chao PC, Li SY, Wang M, Huang YL, Tzeng TY, Tsai RT.** 1997. Self-assembly of the JC virus major capsid protein, VP1, expressed in insect cells. J. Gen. Virol. **78:**1435–1439.
34. **Lee P, Plavina T, Castro A, Berman M, Jaiswal D, Rivas S, Schlain B, Subramanyam M.** 2013. A second-generation ELISA (STRATIFY JCV DxSelect) for detection of JC virus antibodies in human serum and plasma to support progressive multifocal leukoencephalopathy risk stratification. J. Clin. Virol. **57:**141–146. http://dx.doi.org/10.1016/j.jcv.2013.02.002.

Validation and optimization of VLP-based ELISA was performed by investigation of JCPyV-specific IgG response in 400 healthy blood donors. The same set of samples was in parallel tested in independent ELISA in Helsinki. Comparison of both data sets revealed discordance for 10% samples, which showed low IgG activity close to respective cutoffs of the assays. By introduction of normalization of results the overall assay performance has improved, resulting in decrease of discordance rate. To precisely define JCPyV serostatus for samples with discordant ELISA results, we developed a preadsorption inhibition assay. Decrease in IgG activity has been measured after preincubation with JCPyV VLPs in solution. The 35% decrease in the signal has been determined as the cutoff for the preadsorption ihibition assay. Moreover, we also analyzed JCPyV IgG seropositive samples after preadsorption with BKPyV VLPs and therefore excluded impact of cross-reactive antibodies in total JCPyV IgG signal.

In conclusion, we confirmed that VLP-based ELISA with normalization step can serve as a reliable tool for JCPyV IgG serology. Additionally, the preadsorption assay can help with unequivocal determination of JCPyV serostatus for samples with low IgG levels close to cutoff. For testing of sera with unknown JCPyV IgG serostatus the following points should be taken under consideration: (1) sample should be tested at least in duplicate; (2) normalization using reference serum should be always performed - additional quality control, when the expected signal for reference serum is known; (3) sample with low IgG activity close to cutoff should be additionally tested in preadsorption inhibition assay; (4) training of a person performing the testing would be beneficial.

## 5.3 Optimizing JC and BK Polyomavirus IgG Testing for Seroepidemiology and Patient Counseling

In the previous study 10% of VLP-based ELISA results were discordant in the interlaboratory comparison with results from independent ELISA testing. All of them showed low IgG activity against JCPyV VLPs. To avoid misinterpretation of serostatus for samples with low antibody responses, we reinvestigated the performance of our optimized VLP-based ELISA by investigation of serum sample at 100-, 200- and 400-fold serial dilutions, in contrast to only one 400-fold dilution used in the previous study. Moreover, we adapted our ELISA for BKPyV IgG detection, by utilizing BKPyV VLPs as a coating antigen.

Journal of Clinical Virology 71 (2015) 28–33

Contents lists available at ScienceDirect

Journal of Clinical Virology

journal homepage: www.elsevier.com/locate/jcv

# Optimizing JC and BK polyomavirus IgG testing for seroepidemiology and patient counseling

Piotr Kardas [a], Céline Leboeuf [a], Hans H. Hirsch [a,b,c,*]

[a] Transplantation & Clinical Virology, Department Biomedicine — Haus Petersplatz, University of Basel, Basel, Switzerland
[b] Infection Diagnostics, Department Biomedicine — Haus Petersplatz, University of Basel, Basel, Switzerland
[c] Infectious Diseases and Hospital Epidemiology, University Hospital Basel, Basel, Switzerland

ARTICLE INFO

*Article history:*
Received 28 May 2015
Received in revised form 20 July 2015
Accepted 26 July 2015

*Keywords:*
Polyomavirus
Antibody
BK virus
JC virus
PML
Nephropathy
Cystitis
Multiple sclerosis
Natalizumab
ELISA
Screening
Transplantation

ABSTRACT

*Background:* Polyomavirus JC (JCPyV) and BK (BKPyV) can cause significant diseases in immunocompromised patients including nephropathy, hemorrhagic cystitis, and leukoencephalopathy. Recently, JCPyV and BKPyV IgG have been explored as risk predictors in multiple sclerosis and transplant patients, but sensitivity, specificity and quantification issues limit current performance.
*Objective:* To improve JCPyV and BKPyV-specific antibody testing.
*Study design:* Healthy blood donor sera ($N = 400$) were tested at dilutions 1:100, 1:200, and 1:400 for JCPyV- and BKPyV-specific IgG using VP1 virus-like particle (VLP)-based ELISAs normalized to a laboratory reference serum. Normalized optical density 492 nm greater or equal 0.1 in all 3 dilutions was regarded as reactive. Sera with discordant reactivity in at least one dilution were retested after VLP preadsorption.
*Results:* At dilutions 1:100, 1:200, and 1:400, IgG reactivity was 74%, 60% and 53% for JCPyV, and 93%, 86% and 74% for BKPyV, respectively. At these dilutions, JCPyV-VLP preadsorption identified 56, 4 and 0 false-positives and 0, 4 and 27 false-negatives, respectively. Dilution-dependent sensitivity was 100%, 98%, and 89%, and specificity 65, 98%, and 100%, respectively. For sera diluted 100-, 200-, and 400-fold, BKPyV-VLP preadsorption identified 28, 1 and 0 false-positives, and 0, 0 and 46 false-negatives, and sensitivity was 100%, 100%, 86%, and specificity 50%, 98%, 100%, respectively.
*Conclusion:* For seroepidemiology studies, normalized JCPyV and BKPyV IgG ELISA at 1:200 serum dilution provides optimal sensitivity and specificity with the lowest false-positive and false-negative rate. For individual risk assessment, dilutions of 100, 200, and 400 combined with preadsorption for low-reactive sera may be most appropriate.



## 1. Background

JC polyomavirus (JCPyV) and BK polyomavirus (BKPyV) were identified in 1971 as the first of now more than 12 human polyomavirus (HPyV) species [1]. Most humans have been exposed to HPyVs as evidenced by seroprevalence rates ranging from 30% to more than 90% [2–5]. For JCPyV and BKPyV, it has been demonstrated early on that both viruses are transmitted during childhood without specific signs or symptoms, and thereafter persist in the renourinary tract. In fact, ongoing JCPyV and BKPyV replication is detectable as asymptomatic viruria in 10–30% of healthy blood donors at the time of blood donation [3]. In immunocompromised patients, JCPyV and BKPyV replication may eventually progress to significant organ disease. Thus, JCPyV can cause progressive multifocal leukoencephalopathy (PML) in patients with HIV-AIDS, malignancies, organ transplants or with autoimmune diseases receiving potent therapies [6–8]. BKPyV can cause polyomavirus-associated nephropathy (PyVAN) after kidney transplantation or hemorrhagic cystitis (PyVHC) after allogeneic hematopoietic stem cell transplantation [9]. PML is a demyelinating disease affecting typically the white matter of the brain due to cytopathic replication of JCPyV in myelin sheath-producing oligodendrocytes and possibly other cells [8]. Although, JCPyV-specific T-cells are viewed as key to control and outcome of PML [10–12], higher JCPyV-specific IgG levels may correlate with survival [11,13]. However, JCPyV-specific IgG also serve as marker of latent JCPyV infec-

*Abbreviations:* BKPyV, BK polyomavirus; ELISA, enzyme-linked immunosorbent assay; HPyV, human polyomavirus; Ig, immunoglobulin; JCPyV, JC polyomavirus; MS, multiple sclerosis; PML, progressive multifocal leukoencephalopathy; nOD, normalized optical density; PyVHC, polyomavirus-associated hemorrhagic cystitis; PyVAN, polyomavirus-associated nephropathy; VLP, virus-like particle; VP1, viral capsid protein 1.

* Corresponding author at: Department Biomedicine, University of Basel, Petersplatz 10, CH-4009 Basel, Switzerland.
*E-mail address:* hans.hirsch@unibas.ch (H.H. Hirsch).

http://dx.doi.org/10.1016/j.jcv.2015.07.305
1386-6532/

tion and have been associated with a 100-fold increased risk of PML in multiple sclerosis (MS) patients receiving prolonged natalizumab treatment after failure of other therapies [14,15]. PML treatment in the absence of effective antivirals focuses on improving immune control over JCPyV replication by alleviating the underlying immunodeficiency.

PyVAN results from high-level cytopathic BKPyV replication in renal tubular epithelial cells causing tubular denudation, inflammation, and chronic allograft failure with tubular atrophy and interstitial fibrosis [16–18]. Current strategies to avert PyVAN aim at identifying patients with BKPyV viremia and judiciously reducing maintenance immunosuppression [19]. Subsequent increases in BKPyV-specific T-cell responses are associated with clearance BKPyV replication [20–22]. Risk factors for BKPyV viremia and nephropathy include high-dose steroids for acute rejection, HLA mismatches, tacrolimus-mycophenolate combinations as compared to cyclosporine-mycophenolate, and older recipient age [18,19,23]. An increased risk of BKPyV replication has been reported for patients with low or absent BKPyV IgG when receiving a kidney transplant from a donor with high BKPyV IgG level [24–26]. Given this growing clinical need to reliably determine JCPyV- and BKPyV-IgG serology in individual patients, we realized that our current virus-like particle (VLP)-based ELISA required normalization to a positive reference serum, at least duplicate testing to identify technical errors, and the differentiation of specific from unspecific IgG by preadsorption reduction assays for activities around the cut-off [27]. These aspects should be conveniently accommodated in a semi-quantitative serological screening for both viruses.

## 2. Objective

To improve testing of serostatus and semi-quantitative antibody level of JCPyV and BKPyV virus-like particle (VLP)-based ELISAs, we explored three serial dilutions of sera from healthy blood donors, and used VLP preadsorption reduction to evaluate discordant reactivities.

## 3. Study design

### 3.1. Samples

Four hundred sera were available for JCPyV-IgG testing, and 399 for BKPyV-IgG testing, obtained from healthy blood donors as described previously [3]. All sera were stored at −20 °C and only aliquots of the samples were thawed and stored at 4 °C during testing period.

### 3.2. Production and purification of JCPyV and BKPyV VP1 VLPs

JCPyV and BKPyV VP1 VLPs have been described previously [27]. Briefly, the recombinant baculovirus vector containing either JCPyV Mad-1 VP1 or BKPyV Dun-lop VP1 gene was generated using Bac-to-Bac Baculovirus expression system (Invitrogen, Basel, Switzerland) and transfected into insect *Spodoptera frugiperda* Sf9 cells (American Type Culture Collection [ATCC], Manassas, VA) in suspension according to manufacturer's protocol. VP1 VLPs were purified from cell lysates by CsCl ultracentrifugation.

### 3.3. Normalized ELISA performance

ELISAs were essentially performed as described previously [27], Briefly, microtiter plates (Sigma–Aldrich, Buchs, Switzerland) were coated with JCPyV VP1- or BKPyV VP1-VLPs (25 ng/well) overnight at 4 °C followed by 5 washes with $H_2O$ + 0.1% Tween 20 (washing buffer). The wells were then incubated with blocking buffer (150 mM NaCl, 10 mM Tris–HCl [pH 7.4], 1 mM $CaCl_2$, 4% bovine serum albumine [BSA], 0.1% Tween 20) for 2 h at 25 °C. Each serum sample was serially diluted 1:100, 1:200 and 1:400 in blocking buffer and 100 μL was added per well. After 1 h-incubation at 25 °C, the wells were washed five times with washing buffer and incubated for 1 h at 25 °C with 100 μL/well of 1:10,000-diluted Fc-specific goat anti-human IgG conjugated with peroxidase (Sigma–Aldrich, Buchs, Switzerland). Then, the wells were washed five times with washing buffer and incubated for 30 min at 25 °C with 100 μL of freshly prepared 0.4 mg/mL *o*-phenylenediamine (Sigma–Aldrich, Buchs, Switzerland). The color reaction was stopped with 50 μL 1 M sulfuric acid per well, and the optical density (OD) was measured at 492 nm using Safire II plate reader (Tecan, Maennedorf, Switzerland). All results were recorded after blank well subtraction. To compare results across plates, $OD_{492}$ values were normalized (nOD) by dividing the $OD_{492}$ of the tested serum by the $OD_{492}$ of a diluted internal laboratory reference serum with an $OD_{492}$ of close 1.0. The cutoff defining a positive serological response was nOD ≥ 0.100 for each of the three dilutions and abbreviated accordingly as nOD100, nOD200, nOD400.

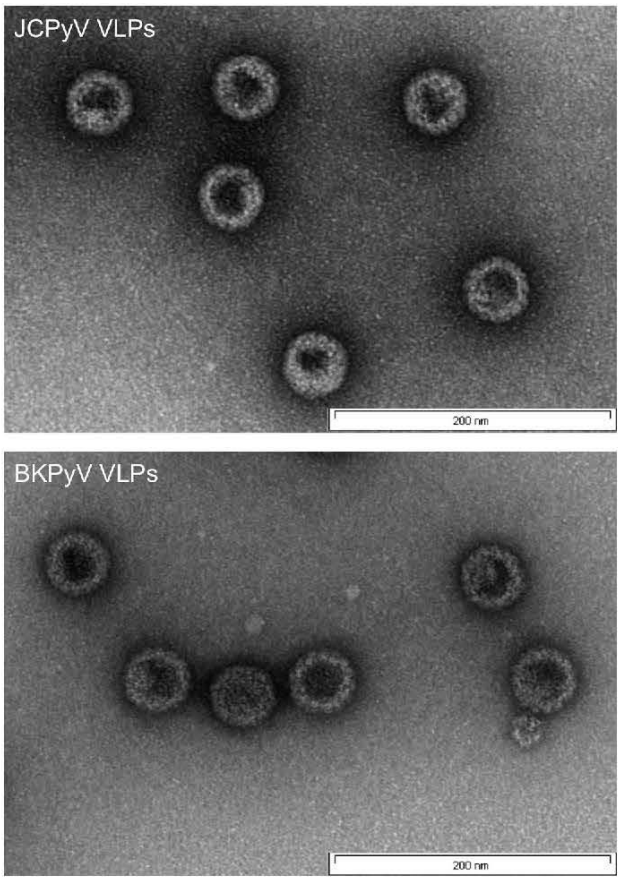


**Fig. 1.** JCPyV and BKPyV virus-like particles used as antigens in normalized ELISA and preadsorption assay.
Transmission electron micrographs of negatively stained JCPyV and BKPyV VLPs consisting of the major capsid protein VP1, expressed in baculovirus-Sf9 cell system. White bar in the lower right corner of each micrograph represents 200 nm.

### 3.4. Preadsorption assay with JCPyV- and BKPyV-VLPs

Preadsorption assays were conducted as reported previously [27]. Briefly, ELISA plates were coated with 25 ng/well of either

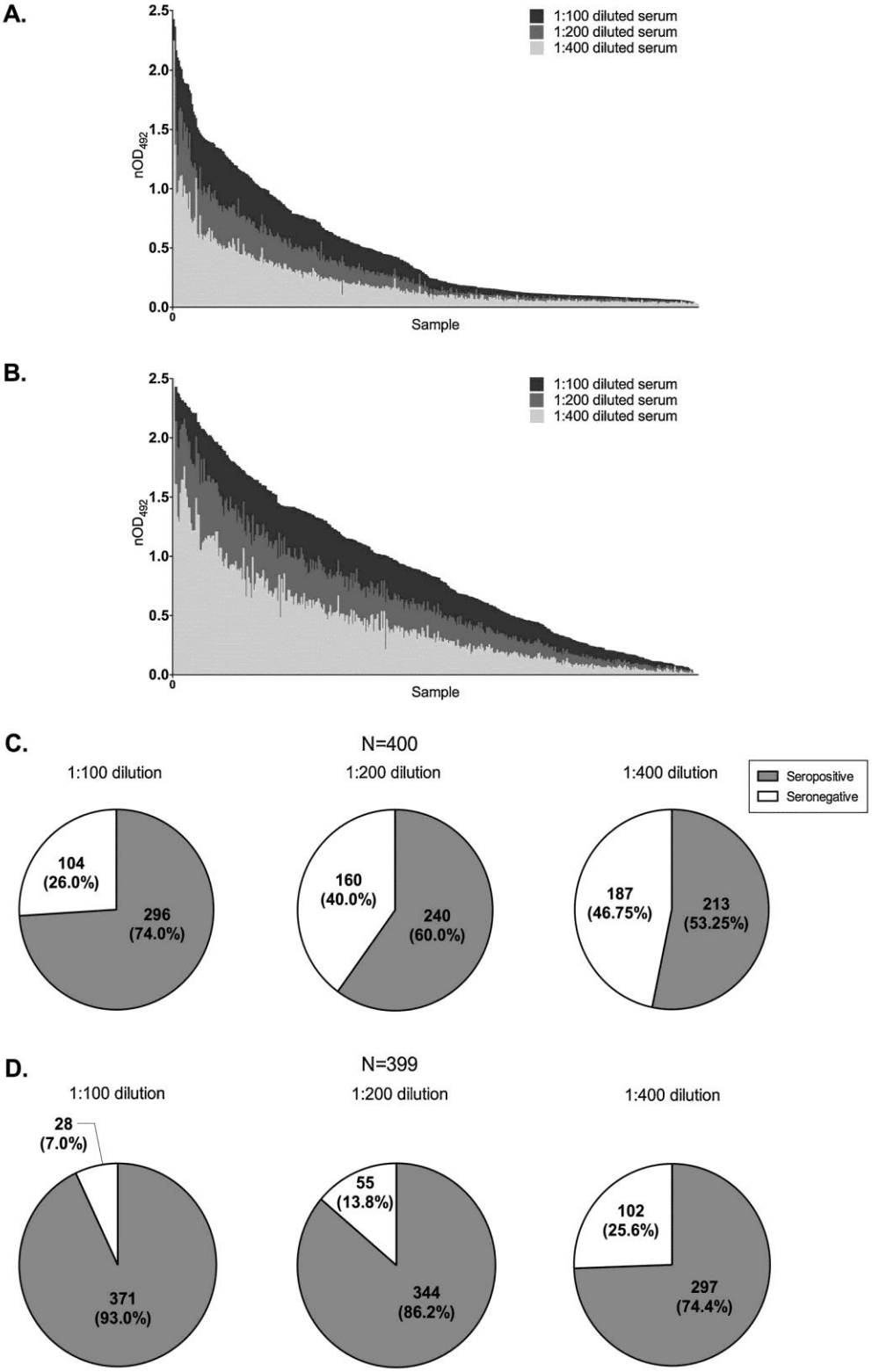


**Fig. 2.** JCPyV and BKPyV normalized OD (nOD) ELISA of serial serum dilutions. Sera from healthy blood donors were tested in 100-fold (black), 200-fold (dark grey) and 400-fold (light grey) dilution. (A) nOD for JCPyV ($n = 400$) (B) nOD for BKPyV ($n = 399$), in a descending order of the nOD at 1:100 dilution. (C) JCPyV seroprevalence according nOD $\geq 0.100$ at indicated serum dilution. (D) BKPyV seroprevalence according nOD $\geq 0.100$ at indicated serum dilution.

JCPyV or BKPyV VP1 VLPs overnight at 4 °C. The sera diluted 1:100 either in blocking buffer (non-preadsorbed) or in blocking buffer containing VLPs at final concentration of 25 ng VLP per 100 μL (preadsorbed) were incubated at 25 °C for 1 h. The preadsorbed samples were then tested by ELISA in parallel with non-preadsorbed samples. The results were reported as percentage of OD reduction after preadsorption with VLPs calculated according to the following formula: [(OD non-preadsorbed − OD preadsorbed)/OD non-preadsorbed] × 100. A reduction equal or greater than 35% was used to discriminate IgG-positive from IgG-negative samples as described previously [27]. As detailed elsewhere, JCPyV-specific normalized IgG activity by preadsorption with VLP were compared to unadsorbed nOD activity was determined in 76 healthy blood donors, who served as true positives due to documented urinary JCPyV shedding and showed a preadsorption reduction of at least 35% by JCPyV-, but not BKPyV-VLPs [27].

### 3.5. Statistical analysis

Numerical data for VP1 mutant ELISA were analyzed with Mann-Whitney *U*-test. Sensitivity and specificity of the assays utilizing different serum dilutions were calculated with MedCalc software (www.medcalc.org) and GraphPad Prism 6.0. Two-sided $P < 0.05$ was considered as statistically significant.

## 4. Results

### 4.1. Comparing normalized VLP ELISA at 100-, 200-, and 400-fold dilution

JCPyV and BKPyV virus-like particles (VLPs) have a 40–45 nm diameter similar to the infectious virions, and were checked for purity and morphology (Fig. 1).

To compare the antibody levels, serial dilutions of 100-, 200-, and 400-fold were prepared from sera obtained from 400 healthy blood donors. The serum dilutions were tested together with an internal laboratory reference serum, to which the optical density at 492 nm was normalized (nOD). The nODs of the three dilutions were sorted according to descending order of the values obtained for the 1:100 diluted sera (Fig. 2). The nODs for either JCPyV-VLPs (Fig. 2A) or BKPyV-VLPs (Fig. 2B) ranged from very high values around nOD 2.3, and then steadily declined. Below nOD 0.15, the values leveled off and the differences became minimal between the dilutions.

The nOD1:100 for JCPyV IgG ranged from 2.425 and 0.021, with a median of 0.185 (interquartile range [IQR]: 0.089 and 0.747). The JCPyV nOD1:200 ranged from 1.966 to 0.020 (median: 0.153, IQR: 0.072 and 0.500) and the nOD1:400 from 1.400 to 0.022 (median: 0.102, IQR: 0.052 and 0.294). The decline in nOD was faster for JCPyV IgG than for BKPyV IgG indicating that the overall JCPyV antibody levels were lower than the BKPyV antibody levels in a larger proportion of the tested donors. Indeed, the nODs for BKPyV IgG were higher showing a nOD1:100 from 2.844 to 0.021, with a median of 0.825 (IQR: 0.316 and 1.380). The BKPyV nOD1:200 ranged from 2.319 to 0.003 (median 0.532, IQR: 0.179 and 0.971) and the nOD1:400 from 1.827 and 0.003 (median 0.309, IQR: 0.094 and 0.619). Thus, the serial dilution provided a semi-quantitative assessment of the antibody levels and are in line with a wider exposure of the general population to BKPyV than JCPyV, regardless of the actual dilution and cut-off definition.

To develop categorical results of seropositive and –negative JCPyV- and BKPyV-specific IgG responses, nOD ≥ 0.100 were used to define reactivity categories for each serum dilution. As expected, the number of reactive sera declined with increasing dilution. For JCPyV IgG, 296 sera were reactive at the 1:100 (74%), but only 240 (60%) sera were reactive at the 1:200 dilution, and 213 (53%) sera at the 1:400 dilution (Fig. 2C). Similarly, BKPyV IgG seroreactivity declined with increasing dilutions, yet at a higher level, being positive in 371 (93%), 344 (86%) and 297 (74%) samples, at the 100-, 200-, and 400-fold dilution, respectively (Fig. 2D).

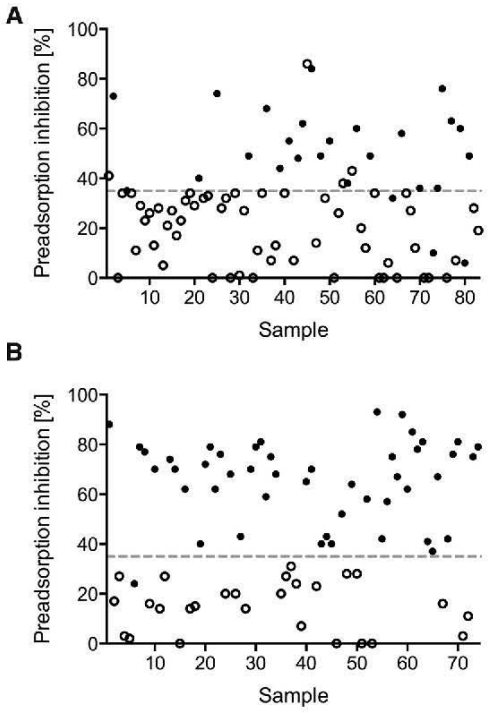


**Fig. 3.** Pre-adsorption reduction for discordant sera (A) 83 sera JCPyV positive in dilution 1:100 and negative in 1:400 dilution were tested by preadsorption reduction to distinguish false-positive and false–negative results for JCPyV (summarized in Table 1). (B) 74 sera BKPyV positive in dilution 1:100 and negative in 1:400 dilution were tested by VLP-preadsorption reduction to distinguish false-positive and false–negative results for BKPyV (summarized in Table 1).

### 4.2. Preadsorption reduction assay

Concordant nODs results at all three dilutions were obtained for JCPyV-IgG in 317 (79%) healthy blood donors, being reactive with nODs ≥ 0.1 in 213 (53%) and non-reactive in 104 (26%) sera (nOD < 0.1). For 83 (21%) sera, a discordant serostatus was observed in one or two dilutions (nOD1:100 median 0.132, IQR 0.112 and 0.160; nOD1:200 median 0.090, IQR: 0.076 and 0.103; nOD1:400 median 0.061, IQR: 0.053 and 0.071), all being non-reactive at the 1:400 dilution. To distinguish between false-positive and false-negative reactivity, the 83 sera were tested by JCPyV VLP preadsorption using as a cutoff the 35% reduction in nOD1:100 (Fig. 3A) described previously [27]. The results indicated that at dilution 1:200, 27 (33%) sera could be confirmed as containing specific anti-JCPyV IgG, 56 (67%) were in fact false-positive, but there were no false-negatives. At dilution 1:200, the JCPyV seroreactive sera contained 4 (5%) false-positives and 4 (5%) false-negatives of the 83 discordant sera, whereas at dilution 1:400, 27 (33%) sera were missed as false-negative, but there were no false-positives.

Concordant nODs results at all three dilutions were obtained for BKPyV-IgG in 323 (81%) healthy blood donors, being reactive with nODs ≥ 0.1 in 297 (74%) and non-reactive with nODs < 0.1 in 28 (7%) sera. Discordant reactivity in one or two dilutions were observed in 74 (19%) sera (nOD1:100 median 0.189, IQR: 0.148 and 0.241; nOD1:200 median 0.111, IQR: 0.087 and 0.140; nOD1:400

**Table 1**
Impact of serum dilution on specificity and sensitivity of normalized ELISA JCPyV- and BKPyV serology.

| | Serum dilution | TP | FP | TN | FN | % Sensitivity (95% CI) | % Specificity (95% CI) |
|---|---|---|---|---|---|---|---|
| JCPyV | 1:100 | 240 | 56 | 104 | 0 | 100.00 (98.47–100.00) | 65.00 (57.07–72.36) |
| | 1:200 | 236 | 4 | 156 | 4 | 98.33 (95.79–99.54) | 97.50 (93.72–99.31) |
| | 1:400 | 213 | 0 | 160 | 27 | 88.75 (84.06–92.45) | 100.00 (97.72–100.00) |
| BKPyV | 1:100 | 343 | 28 | 28 | 0 | 100.00 (98.93–100.00) | 50.00 (36.34–63.66) |
| | 1:200 | 343 | 1 | 55 | 0 | 100.00 (98.93–100.00) | 98.21 (90.45–99.95) |
| | 1:400 | 297 | 0 | 56 | 46 | 86.59 (82.52–90.01) | 100.00 (93.63–100.00) |

TP: true-positive; FP: false-positive; TN: true-negative; FN: false-negative; CI: confidence interval.

median 0.063, IQR: 0.043 and 0.079). All 74 samples were reactive at 1:100 and non-reactive at 1:400 dilution. BKPyV-VLP preadsorption reduction revealed (Fig. 3B) that 46 (62%) could be confirmed as true-positive for anti-BKPyV IgG at 1:100 dilution, 28 (38%) were false-positive, but there were no false-negative results. At dilution 1:200, the BKPyV serostatus showed 1 (1.4%) false-positive and no false-negative reactivities, whereas at dilution 1:400, 46 (62%) sera were missed as false-negative, but there were no false-positives. These results and the dilution-dependent sensitivity and specificity are summarized in Table 1.

## 5. Discussion

The JCPyV and BKPyV serostatus is receiving increasing attention as potential predictor of the risk of developing PyV-associated diseases in specific clinical settings. This is due to the fact that a positive BKPyV- or JCPyV-serostatus indicates not only past exposure, but also viral persistence and the associated risk of progressing to high-level replication once immune control fails [11,13,28,29]. However, reliable identification of positive and negative IgG reactivity as well as a semi-quantitative, but still feasible assessment of antibody levels would be of major importance. In this study, we show that using lower serum dilutions can significantly increase the sensitivity of VLP ELISAs. In order to maintain specificity, however, true- and false-positive reactivity should be identified in a confirmatory test such as VLP-preadsorption. Three aspects emerge from our study:

First, the 1:200 dilution provided the best trade-off between sensitivity and specificity with respective values being 98.3% and 97.5% for JCPyV IgG, and 100% and 98% for BKPyV IgG. Thus, the 1:200 dilution in the normalized ELISA format may be the most time- and labor-effective for seroepidemiological studies of larger sample size, even when duplicate analyses are performed.

Second, the 1:100 dilution provided the highest sensitivity, and was not associated with false-negative seroreactivity. If combined with preadsorption reduction for confirmation, this approach might be the most suitable for individual patient counseling. JCPyV serology is currently recommended for better appreciating the PML risk in MS patients, since a false-negative seroreactivity may result in underestimating the risk, while a false-positive reactivity may result in withholding an effective treatment option. Indeed, our results indicate that one third of low JCPyV IgG reactivities could be confirmed by preadsorption reduction as true-positives that would have been missed otherwise.

Third, the 1:400 dilution provided a first semi-quantitative approximation of higher and lower JCPyV- and BKPyV-specific IgG levels as visualized by the convenient spread of the nODs present in a large number of healthy blood donors. Importantly, the 1:400 dilution had a specificity of 100%, while sensitivity only decreased to 87–89%. As relative antibody levels and their change over time should be explored in clinical settings, the 1:400 seems appropriate. The semi-quantitative serial dilution of 100-, 200-, and 400-fold evident in Figs. 2 and 3 could be supplemented by quantitative end-point dilution in specific clinical or academic settings, where true titers are desirable particularly for high antibody levels, including intrathecal antibodies or pretransplant serology [30–33].

Quantitative aspects of JCPyV-specific IgG have been associated with survival in HIV-AIDS patients with PML, which was also correlated with a higher JCPyV-specific T-cell response as measured by interferon-γ release assays. Such a quantitative relationship has not been established for MS patient counseling, as yet. Quantitative aspects of BKPyV IgG are currently emerging in kidney transplant donors and recipients [33], and may also be important for allogeneic stem cell transplant recipients [34,35]. An optimized testing format as described here would provide more reliable testing including quantifying relative antibody levels. Indeed, Bohl et al. reported that kidney transplant recipients with low antibody titers of less than 1:1280 were at increased risk of developing early BKPyV replication when receiving a graft from a BKPyV-seropositive donor with very high antibody levels [25]. In addition, cases of primary infection post-transplant may become evident [36]. As a note of caution, pretransplant dialysis may reduce the seroreactivity [37]. Recent data indicated that the age-dependent decline of BKPyV-specific IgG at a 1:400 dilution also corresponded to lower BKPyV-specific CD4 T-cell responses [28]. Interestingly, older recipients have been shown to be at increased risk for high-level BKPyV viruria, viremia and nephropathy after kidney transplantation [23,38].

We conclude that testing 100-, 200-, and 400-fold dilution series of sera in a normalized VLP ELISA provides a convenient first determination of JCPyV and BKPyV-specific antibody status and levels. Depending on the results, preadsorption reduction assays could be applied to low-level reactivities in order to rule out false-positives. Clearly, the normalized ELISA test format hinges on the availability of reference sera containing of defined JCPyV IgG and BKPyV IgG titers. To move this field forward, WHO-approved reference sera are urgently needed, which significantly enhance the reproducibility and permit elucidation of potential role of BK-and JCPyV serology in clinical practice.

## Conflict of interest

None declared.

## Funding

This study was funded by a personal appointment grant of the University of Basel to HHH.

## Ethical approval

All donors gave a written informed consent to the protocol (267/06) approved by the local review board of Basel.

Ethical approval was given; protocol (267/06) approved by the local review board

## Acknowledgements

We wish to thank Ms. Marion Wernli, Mr Fabian Weissbach, and Ms. Jacqueline Samaridis as well as all members of the Transplantation & Clinical Virology at the Department Biomedicine for support and helpful discussions.

## References

[1] C.H. Rinaldo, H.H. Hirsch, The human polyomaviruses: from orphans and mutants to patchwork family, APMIS 121 (2013) 681–684.
[2] W.A. Knowles, P. Pipkin, N. Andrews, A. Vyse, P. Minor, D.W. Brown, et al., Population-based study of antibody to the human polyomaviruses BKV and JCV and the simian polyomavirus SV40, J. Med. Virol. 71 (2003) 115–123.
[3] A. Egli, L. Infanti, A. Dumoulin, A. Buser, J. Samaridis, C. Stebler, et al., Prevalence of Polyomavirus BK and JC infection and replication in 400 healthy blood donors, J. Infect. Dis. 199 (2009) 837–846.
[4] J.M. Kean, S. Rao, M. Wang, R.L. Garcea, Seroepidemiology of human polyomaviruses, PLoS Pathog. 5 (2009) e1000363.
[5] J.T. Nicol, R. Robinot, A. Carpentier, G. Carandina, E. Mazzoni, M. Tognon, et al., Age-specific seroprevalences of merkel cell polyomavirus, human polyomaviruses 6, 7, and 9, and trichodysplasia spinulosa-associated polyomavirus, Clin. Vaccine Immunol. 20 (2013) 363–368.
[6] H.H. Hirsch, P. Kardas, D. Kranz, C.T. Leboeuf, J.C. human, The human JC polyomavirus (JCPyV): virological background and clinical implications, APMIS 121 (2013) 685–727.
[7] M.W. Ferenczy, L.J. Marshall, C.D. Nelson, W.J. Atwood, A. Nath, K. Khalili, et al., Molecular biology, epidemiology, and pathogenesis of progressive multifocal leukoencephalopathy, the JC virus-Induced demyelinating disease of the human brain, Clin. Microbiol. Rev. 25 (2012) 471–506.
[8] S. Gheuens, C. Wuthrich, I.J. Koralnik, Progressive multifocal leukoencephalopathy: why gray and white matter, Annu. Rev. Pathol. 8 (2013) 189–215.
[9] C.H. Rinaldo, G.D. Tylden, B.N.T. Sharma, B.K. polyomavirus, The human polyomavirus BK (BKPyV): virological background and clinical implications, APMIS 121 (2013) 728–745.
[10] I.J. Koralnik, P. Du, R.A. asquier, N.L. Letvin, JC virus-specific cytotoxic T lymphocytes in individuals with progressive multifocal leukoencephalopathy, J. Virol. 75 (2001) 3483–3487.
[11] N. Khanna, M. Wolbers, N.J. Mueller, C. Garzoni, P. Du, R.A. asquier, C.A. Fux, et al., JC virus-specific immune responses in human immunodeficiency virus type 1 patients with progressive multifocal leukoencephalopathy, J. Virol. 83 (2009) 4404–4411.
[12] I. Jelcic, I. Jelcic, W. Faigle, M. Sospedra, R. Martin, Immunology of progressive multifocal leukoencephalopathy, J. Neurovirol. (2015), PMID: 25740538.
[13] R.P. Viscidi, N. Khanna, C.S. Tan, X. Li, L. Jacobson, D.B. Clifford, et al., JC virus antibody and viremia as predictors of progressive multifocal leukoencephalopathy in human immunodeficiency virus-1-infected individuals, Clin. Infect. Dis. 53 (2011) 711–715.
[14] G. Bloomgren, S. Richman, C. Hotermans, M. Subramanyam, S. Goelz, A. Natarajan, et al., Risk of natalizumab-associated progressive multifocal leukoencephalopathy, N Engl. J. Med. 366 (2012) 1870–1880.
[15] P.S. Sorensen, A. Bertolotto, G. Edan, G. Giovannoni, R. Gold, E. Havrdova, et al., Risk stratification for progressive multifocal leukoencephalopathy in patients treated with natalizumab, Mult. Scler. 18 (2012) 143–152.
[16] I. Binet, V. Nickeleit, H.H. Hirsch, O. Prince, P. Dalquen, F. Gudat, et al., Polyomavirus disease under new immunosuppressive drugs: a cause of renal graft dysfunction and graft loss, Transplantation 67 (1999) 918–922.
[17] P.S. Randhawa, S. Finkelstein, V. Scantlebury, R. Shapiro, C. Vivas, M. Jordan, et al., Human polyoma virus-associated interstitial nephritis in the allograft kidney, Transplantation 67 (1999) 103–109.
[18] H.H. Hirsch, W. Knowles, M. Dickenmann, J. Passweg, T. Klimkait, M.J. Mihatsch, et al., Prospective study of polyomavirus type BK replication and nephropathy in renal-transplant recipients, N Engl. J. Med. 347 (2002) 488–496.
[19] H.H. Hirsch, P. Randhawa, BK polyomavirus in solid organ transplantation, Am. J. Transplant. 13 (Suppl 4) (2013) 179–188.
[20] S. Binggeli, A. Egli, S. Schaub, I. Binet, M. Mayr, J. Steiger, et al., Polyomavirus BK-specific cellular immune response to VP1 and large T-antigen in kidney transplant recipients, Am. J. Transplant. 7 (2007) 1131–1139.
[21] P. Comoli, S. Basso, H.H. Hirsch, A. Azzi, Fontana, M. Cioni, et al., Humoral and Cellular Immunity to Polyomavirus BK Large T. and VP1 Antigens after Pediatric Kidney Transplantation 2009, American Congress of Transplantation, Boston, MA, USA, 2009, pp. 283.
[22] T. Schachtner, K. Muller, M. Stein, C. Diezemann, A. Sefrin, N. Babel, et al., BK virus-specific immunity kinetics: a predictor of recovery from polyomavirus BK-associated nephropathy, Am. J. Transplant. 11 (2011) 2443–2452.
[23] H.H. Hirsch, F. Vincenti, S. Friman, M. Tuncer, F. Citterio, A. Wiecek, B.K. et al. Polyomavirus, Replication in de novo kidney transplant patients receiving tacrolimus or cyclosporine: a prospective, randomized, multicenter study, Am. J. Transplant. 13 (2013) 136–145.
[24] F. Ginevri, S. De, R. antis, P. Comoli, N. Pastorino, C. Rossi, G. Botti, B.K. Polyomavirus, et al., Infection in pediatric kidney-allograft recipients: a single-center analysis of incidence, risk factors, and novel therapeutic approaches, Transplantation 75 (2003) 1266–1270.
[25] D.L. Bohl, G.A. Storch, C. Ryschkewitsch, M. Gaudreault-Keener, M.A. Schnitzler, E.O. Major, et al., Donor origin of BK virus in renal transplantation and role of HLA C7 in susceptibility to sustained BK viremia, Am. J. Transplant. 5 (2005) 2213–2221.
[26] P. Sood, S. Senanayake, K. Sujeet, R. Medipalli, S.K. Van-Why, D.C. Cronin, et al., Donor and recipient BKV-specific IgG antibody and posttransplantation BKV infection: a prospective single-center study, Transplantation 95 (2013) 896–902.
[27] P. Kardas, M. Sadeghi, F.H. Weissbach, T. Chen, L. Hedman, E. Auvinen, et al., Inter- and intralaboratory comparison of JC polyomavirus antibody testing using two different virus-like particle-based assays, Clin. Vaccine Immunol. 21 (2014) 1581–1588.
[28] T. Schmidt, C. Adam, H.H. Hirsch, M.W. Janssen, M. Wolf, J. Dirks, et al., BK polyomavirus-specific cellular immune responses are age-dependent and strongly correlate with phases of virus replication, Am. J. Transplant. 14 (2014) 1334–1345.
[29] L. Aly, S. Yousef, S. Schippling, I. Jelcic, P. Breiden, J. Matschke, et al., Central role of JC virus-specific $CD^{4+}$ lymphocytes in progressive multi-focal leucoencephalopathy-immune reconstitution inflammatory syndrome, Brain 134 (2011) 2687–2702.
[30] F. Weber, C. Goldmann, M. Kramer, F.J. Kaup, M. Pickhardt, P. Young, et al., Cellular and humoral immune response in progressive multifocal leukoencephalopathy, Ann. Neurol. 49 (2001) 636–642.
[31] J. Kuhle, R. Gosert, R. Buhler, T. Derfuss, R. Sutter, O. Yaldizli, et al., Management and outcome of CSF-JC virus PCR-negative PML in a natalizumab-treated patient with MS, Neurology 77 (2011) 2010–2016.
[32] K. Alstadhaug, T. Croughs, S. Henriksen, C. Leboeuf, I. Sereti, H. Hirsch, et al., Treatment of P Rogressive Multifocal Leukoencephalopathy with Interleukin 7, JAMA Neurology, 2014, pp. E1–E5.
[33] D.L. Bohl, D.C. Brennan, C. Ryschkewitsch, M. Gaudreault-Keener, E.O. Major, G.A. Storch, BK virus antibody titers and intensity of infections after renal transplantation, J. Clin. Virol. 43 (2008) 184–189.
[34] M. Koskenvuo, A. Dumoulin, I. Lautenschlager, E. Auvinen, L. Mannonen, V.J. Anttila, et al., BK polyomavirus-associated hemorrhagic cystitis among pediatric allogeneic bone marrow transplant recipients: treatment response and evidence for nosocomial transmission, J. Clin. Virol. 56 (2013) 77–81.
[35] M. Koskenvuo, I. Lautenschlager, P. Kardas, E. Auvinen, L. Mannonen, P. Huttunen, et al., Diffuse gastrointestinal bleeding and BK polyomavirus replication in a pediatric allogeneic haematopoietic stem cell transplant patient, J. Clin. Virol. 62 (2015) 72–74.
[36] I. Lautenschlager, T. Jahnukainen, P. Kardas, J. Lohi, E. Auvinen, L. Mannonen, et al., A case of primary JC polyomavirus infection-associated nephropathy, Am. J. Transplant. 14 (2014) 2887–2892.
[37] S. Bodaghi, P. Comoli, R. Boesch, A. Azzi, R. Gosert, D. Leuenberger, F. Ginevri, H.H. Hirsch, Antibody responses to recombinant polyomavirus BK large T. and VP1 proteins in pediatric kidney transplant patients, J. Clin. Microbiol. 47 (2009) 2577–2585.
[38] E. Ramos, C.B. Drachenberg, J.C. Papadimitriou, O. Hamze, J.C. Fink, D.K. Klassen, et al., Clinical course of polyoma virus nephropathy in 67 renal transplant patients, J. Am. Soc. Nephrol. 13 (2002) 2145–2151.

With this study we presented that also BKPyV VLPs can be utilized in our normalized ELISA for BKPyV IgG detection. By testing 400 healthy donor samples at 100-, 200 and 400-fold dilutions we showed, that 100-fold dilution provides the highest sensitivity for both JCPyV and BKPyV testings and no false-negative results. Taking this dilution and supporting it with preadsorption inhibition assay might be the most suitable for testing individual patients. Although at 200-fold serum dilution sensitivity went down to 98.3% for JCPyV IgG and stayed at 100% for BKPyV IgG, the best trade-off between sensitivity and specificity was achieved. Thus, 200-fold dilution in normalized VLP-based ELISA might be the most appropriate for seroepidemiological studies of large sample size. 400-fold serum dilution might give first approximation of high and low JCPyV and BKPyV IgG levels. Of note, specificity was equal to 100%, whereas sensitivity decreased to 87% - 89%. Depending on the results, preadsorption reduction assays could be applied to low-level antibody sear in order to rule out false-positives.

Although we showed that normalized ELISA is a specific and sensitive assay for detection of antibodies against either JCPyV or BKPyV, officially approved reference serum is needed in order to enhance reproducibility and permit clarification of PyV serology potential in clinical practice.

In immunocompetent individuals JCPyV or BKPyV infection is not definite and may be subclinical or unspecific. Both viruses can cause serious diseases only when immune functions are impaired. This applies to immunocompromised patients, including those with HIV-AIDS and patients with hematologic malignancies, solid cancers, organ transplantation, and autoimmune diseases treated with immunomodulators. Among these patients the risk of high-level JCPyV or BKPyV replication, followed by development of PyV-associated disease, is higher because their immune control fails to control viral replication. The most common disease caused by JCPyV is PML, whereas two most common BKPyV-associated diseases are PyVAN and PyVHC. Unfortunately there is currently no specific antiviral therapy for any of those and treatment is usually focused on regaining immune functions controlling virus replication. Therefore, sensitive and specific testing for antibodies against JCPyV and BKPyV in immunocompromised individuals is needed. The following 4 case report studies cover examples of immunocompromised individuals undergoing the treatment with different immunosuppressive drugs. Normalized ELISA was utilized to investigate their JCPyV and BKPyV serostatus in order to support the diagnosis of PyV-associated diseases.

## 5.4 Progressive Multifocal Leukoencephalopathy in Common Variable Immunodeficiency: Mitigated Course Under Mirtazapine and Mefloquine

J. Neurovirol.
DOI 10.1007/s13365-015-0340-4

# Progressive multifocal leukoencephalopathy in common variable immunodeficiency: mitigated course under mirtazapine and mefloquine

Rebekka Kurmann[1,9] &Christian Weisstanner[2,9] &Piotr Kardas[3] &Hans H. Hirsch[3,4] & Roland Wiest[2,9] &Bernhard Lämmle[5,8,9] &Hansjakob Furrer[6,9] &Renaud Du Pasquier[7,10] & Claudio L. Bassetti[1,9] &Mathias Sturzenegger[1,9] &Heinz Krestel[1,9]

Received: 2 January 2015 / Revised: 31 March 2015 / Accepted: 2 April 2015


**Abstract** Demonstration of survival and outcome of progressive multifocal leukoencephalopathy (PML) in a 56-year-old patient with common variable immunodeficiency, consisting of severe hypogammaglobulinemia and CD4+ T lymphocytopenia, during continuous treatment with mirtazapine (30 mg/day) and mefloquine (250 mg/week) over 23 months. Regular clinical examinations including Rankin scale and Barthel index, nine-hole peg and box and block tests, Berg balance, 10-m walking tests, and Montreal Cognitive Assessment (MoCA) were done. Laboratory diagnostics included complete blood count and JC virus (JCV) concentration in cerebrospinal fluid (CSF). The noncoding control region (NCCR) of JCV, important for neurotropism and neurovirulence, was sequenced. Repetitive MRI investigated the course of brain lesions. JCV was detected in increasing concentrations (peak 2568 copies/ml CSF), and its NCCR was genetically rearranged. Under treatment, the rearrangement changed toward the archetype sequence, and later JCV DNA became undetectable. Total brain lesion volume decreased (8.54 to 3.97 $cm^3$) and atrophy increased. Barthel (60 to 100 to 80 points) and Rankin (4 to 2 to 3) scores, gait stability, and box and block (7, 35, 25 pieces) and nine-hole peg (300, 50, 300 s) test performances first improved but subsequently worsened. Cognition and walking speed remained stable. Despite initial rapid deterioration, the patient survived under continuous treatment with mirtazapine and mefloquine even though he belongs to a PML subgroup that is usually fatal within a few months. This course was paralleled by JCV clones with presumably lower replication capability before JCV became undetectable. Neurological deficits were due to PML lesions and progressive brain atrophy.

**Keywords** CD4+ T lymphocytopenia - Idiopathic primary hypogammaglobulinemia - Mefloquine - Mirtazapine - Progressive multifocal leukoencephalopathy - Noncoding control region

Electronic supplementary material The online version of this article (doi:10.1007/s13365-015-0340-4) contains supplementary material, which is available to authorized users.

* Heinz Krestel
heinz-krestel@bluewin.ch

1 Department of Neurology, Inselspital, Bern University Hospital, Freiburgstrasse 10, 3010 Bern, Switzerland

2 University Institute of Diagnostic and Interventional Neuroradiology, Inselspital, Bern University Hospital, Bern, Switzerland

3 Transplantation & Clinical Virology, Department Biomedicine (Haus Petersplatz), University of Basel, Basel, Switzerland

4 Infectious Diseases & Hospital Epidemiology, University Hospital Basel, Basel, Switzerland

5 Department of Hematology, Inselspital, Bern University Hospital, Bern, Switzerland

6 Department of Infectious Diseases, Inselspital, Bern University Hospital, Bern, Switzerland

7 Department of Neurology, Lausanne University Hospital, Lausanne, Switzerland

8 Center for Thrombosis and Hemostasis, Mainz University Medical Center, Mainz, Germany

9 University of Bern, Bern, Switzerland

10 Department of Clinical Neurosciences, University of Lausanne, Lausanne, Switzerland

Published online: 28 April 2015

## Introduction

Progressive multifocal leukoencephalopathy (PML) is caused by JC polyomavirus (JCPyV or JC virus (JCV)) infection of the central nervous system. PML risk factors are HIV infection, immunosuppressive therapy after organ and stem cell transplantation, and immunomodulatory agents used in the treatment of autoimmune disorders (Steiner and Berger 2012; Weber 2008; Gheuens et al. 2011; Bellizzi et al. 2013).

JCV can have a strong neurotropism, not only lytically infecting oligodendrocytes and, to a lesser extent, astrocytes, but can also spread to gray matter (Bellizzi et al. 2013; Elphick et al. 2004; Wüthrich and Koralnik 2012). JCV enters cells via N-linked glycoprotein with α-(2,6)-linked sialic acid and the serotoninergic 5-HT-2A receptor, two components of a putative JCV receptor. JCV is internalized with the 5-HT-2A receptor by clathrin-mediated endocytosis (Bellizzi et al. 2013; Elphick et al. 2004). The archetype JCV is not associated with PML. Increased virulence and neurotropism of JCV are associated with genetic rearrangement mainly in its hypervariable noncoding control region (NCCR) (Bellizzi et al. 2013). The NCCR of the archetype JCV contains a bidirectional promoter, the viral origin of replication, enhancers, and six regions termed box A to F which contain binding sites for host transcription factors and the viral large T antigen. The NCCR is involved in virus replication, and its genetic rearrangement has been associated with poor PML outcome (Bellizzi et al. 2013; Hirsch et al. 2013). Impairment of the host immune system with CD4+ and CD8+ T lymphocytopenia, NCCR rearrangement, activation/upregulation of transcription factors binding to recombined NCCR, and migration of JCV—freely or via B lymphocytes—are conditions that, in combination, will lead to PML (Bellizzi et al. 2013).

As yet, no specific treatment exists against JCV. Of the several compounds tested, we would like to focus on mirtazapine and mefloquine. Mirtazapine can pass the blood–brain barrier (BBB) and inhibits central noradrenergic, serotoninergic, and histaminergic receptors. Its binding to the 5-HT-2A receptor is believed to block JCV entry into cells (Elphick et al. 2004). Mefloquine equally passes the BBB and is believed to accumulate in the brain in significantly higher concentrations than in plasma due to its long plasma half-life, lipophilicity, and inhibition of an ATP-binding cassette (ABC) transporter called multidrug resistance protein 1 (MDR-1) that is an efflux pump at the BBB. Mefloquine's assumed anti-JCV activity is inhibition of DNA replication by binding to the T antigen, a JCV helicase (Brickelmaier et al. 2009). PML treatment with mirtazapine or mefloquine was mainly described in patients with HIV, organ transplant, dermatomyositis, polycythemia vera, sarcoidosis, systemic lupus erythematosus, and idiopathic CD4+ T lymphocytopenia (Loyaga-Rendon et al. 2013; Delgado-Alvarado et al. 2013; Hohlfeld et al. 2012; Verma et al. 2007; Vulliemoz et al. 2006; Beppu et al. 2012; Naito et al. 2012; Clifford et al. 2013; Cettomai and McArthur 2009). Combined treatment with mefloquine and mirtazapine has been reported in PML cases in the context of HIV infection, multiple sclerosis (MS) (Gheuens et al. 2011; Iannetta et al. 2013; Moenster and Jett 2012; Schröder et al. 2010), and in one seemingly immunocompetent PML patient (Christakis et al. 2013). One case series compared the effect of mirtazapine to mirtazapine and mefloquine in 34 HIV-negative patients with PML (Gheuens et al. 2011), including nine patients who had hematological disorders including Waldenstrom macroglobulinemia, common variable immunodeficiency (CVID), and idiopathic CD4+ or CD8+ T lymphocytopenia. Combined treatment did not improve 1-year survival of the 34 patients compared to mirtazapine alone. Neither survival rate nor presence or lack of therapeutic effect was presented for the subgroup with hematological disorders and, in particular, for the patients with CVID or idiopathic CD4+ or CD8+ T lymphocytopenia.

CVID encompasses a diagnostic group of approximately 150 different primary immunodeficiencies, which have a common set of features including hypogammaglobulinemia, but which have different underlying causes (Salzer et al. 2012). Late-onset combined immune deficiency (LOCID) is a CVID subgroup, defined by the additional occurrence of opportunistic infections and/or a CD4+ T cell count < 200 x $10^6$ cells/L (Malphettes et al. 2009).

The overall 1-year survival rate of HIV-negative PML patients is around 50 % (Marzocchetti et al. 2009), with dramatic variations depending on the underlying immunocompromising disorder. The 1-year survival rate of PML patients with CVID or LOCID is not well known. HIV-negative PML patients with CVID or idiopathic CD4+ or CD8+ T lymphocytopenia were reported to survive at least 1 year under mirtazapine alone or in combination with mefloquine, but their numbers were not specified (Gheuens et al. 2011). Further PML cases with constitutive immunodeficiency were reported: three were CVID patients and three most likely fulfilled (according to us) the LOCID criteria (Supplementary Table 1) or had Good's syndrome (Squintani et al. 2010). None was treated with mirtazapine and/or mefloquine, but with different compounds, or did not receive treatment. Survival was less than 10 months or not reported.

We present an adult patient with CVID and CD4+ T lymphocytopenia (i.e., LOCID) who contracted PML and was treated with mirtazapine and mefloquine since October 2012. His regular follow-up included clinical examination and measurements of motor performance, cognition, brain lesion volume, and JCV DNA quantification in cerebrospinal fluid (CSF). The NCCR of JCV was DNA-sequenced, as it is typically rearranged in PML with deletion and/or duplication of archetype sequence elements. This patient is still alive without active PML signs 23 months after diagnosis, has residual neurological deficits, and has a reasonable quality of life.

## Patient and methods

Our study complies with the Declaration of Helsinki and was approved by the local ethics committee of Bern. Written informed consent was obtained. The 56-year-old patient was followed up at ~3 monthly intervals between September 2012 and August 2014, when he was last seen, with general clinical and neurological examinations, assessments of Rankin scale and Barthel index (disability, independence in daily activities), Berg balance test (for static and dynamic balance abilities), 10-m walking test, Montreal Cognitive Assessment (MoCA, cognition), and nine-hole peg and box and block tests (manual fine and coarse motor skills performed with right hand under physiotherapist supervision). Laboratory diagnostics included differential blood count; serum protein electrophoresis; and quantification of IgG, IgM, and IgA concentrations, absolute B lymphocyte as well as CD4+ and CD8+ T lymphocyte counts. From DNA isolated out of CSF, (i) the JCV copy number was determined by quantitative polymerase chain reaction (PCR) and (ii) the NCCR of JCV was selectively amplified by PCR. PCR products were separated on agarose gel, excised, and sequenced as previously described (Hirsch et al. 2013). Repetitive cerebral MRIs were performed and segmented manually slice by slice on high-resolution fluid-attenuated inversion recovery (FLAIR) sequences (pulse parameters: TR/TE of 8500/89 ms, TI 2500 ms; matrix size 512 × 512) in order to determine the cerebral lesion volumes, using a slice thickness of 1 $mm^3$ and the open source Software 3-D Slicer Version 4.2.2.3 (www.slicer.org).

## Results

### PML diagnosis in September 2012

The patient first noticed persistent diplopia, worse on gaze to the right shortly after a severe sinusitis in June 2012. Over the next 2 months, gait disturbance, coordination problems of the right arm and leg, and severe fatigue appeared.

At first admission in September 2012, neurological examination showed a complex pretectal syndrome (abduction deficit of the right eye, hypotropia and esotropia of the right eye, and a vertical gaze palsy), mild right-sided hemiparesis (including facial palsy), and right-sided hemi-ataxia including gait ataxia. Cranial MRI (T2-weighted and FLAIR images) showed hyperintense confluent lesions in the left-sided medial thalamus, hypothalamus, mesencephalon, and tegmentum pontis (Fig. 1). Further lesions were found in the colliculus superior and inferior, medulla oblongata, right gyrus frontalis medius, and in the right cerebellar hemisphere with the latter two lesions enhancing with gadolinium (not shown). CSF contained six mononuclear cells per microliter, protein 0.61 g/l, glucose 2.85 mmol/l, lactate 1.6 mmol/l, and no oligoclonal bands. The cytological analysis was negative for neoplastic cells. Cultures of CSF were negative for general bacterial growth, *Mycobacterium tuberculosis*, and *Cryptococcus neoformans*. Serology was negative for various neurotropic bacteria and viruses including HIV. PCR with DNA from CSF was negative for *Mycoplasma pneumoniae*, *Tropheryma whipplei*, *Listeria monocytogenes*, *Mycobacterium tuberculosis*, herpes simplex 1 and 2, varicella zoster, cytomegalovirus, Epstein-Barr virus, enteroviruses, and human herpesvirus 6 but showed 1167 copies/ml and, a week later, 2568 copies/ml of JCV DNA (Table 1, Fig. 2). Together with the neurological deficits, the MRI lesion pattern, and the positive JCV DNA PCR, the diagnosis of PML was established. The diagnosis of CVID was based on familial severe hypogammaglobulinemia (his 2 sisters were also affected) and a history of immune thrombocytopenia (ITP), autoimmune hemolytic anemia (AIHA), and pseudo T cell lymphoma. The patient first presented with hepatosplenomegaly at the age of 3 years and was diagnosed with AIHA 2 years later (Roth et al. 1975). He suffered from lifelong recurrent sinopulmonary infections. For their efficient prevention, he was regularly and successfully treated with intravenous immunoglobulins (IvIgG). Blood analysis at the time of PML diagnosis showed hypogammaglobulinemia (IgG 3.19 g/l, under replacement therapy with IvIgG 30 g every 4 weeks; IgM <0.05 g/l; IgA <0.06 g/l), as well as a severe depletion of CD4+ T (97/μl) and B lymphocytes (0/μl). Our patient belongs to the only 10 % of CVID patients with very low B cell counts. In contrast, the CD8+ T cell count was normal (Table 1). His immunodeficiency matches the definition of LOCID. PCR amplification and sequencing of the NCCR of JCV DNA from September 3, 2012, revealed a genetic rearrangement. Four sequences were obtained with a common signature deletion *del*($C_{54–55}D_{1–64}$) of most of the D box, starting in the end of the C box (variants V1C120903, V2C120903, V1C120907, and V2C120907), together with partial duplications of the sequence boxes A, B, and C whereas two variants with continuous duplications (V1C121205 and V2C121205) were identified in the last CSF sample with lower JCV loads (Fig. 2).

The patient's condition rapidly deteriorated with progression of right-sided hemiataxia, gait ataxia, pretectal oculomotor syndrome, and onset of dysarthria. In October 2012, we started treatment with mirtazapine 30 mg daily and mefloquine (250 mg daily for 3 days, then 250 mg weekly) and as of then continued therapy.

### Follow-up examinations over the course of 23 months

Between September 2012 and August 2014, the Barthel (60 to 100 to 80) and Rankin (4 to 2 to 3) scores first improved and then fell to a level still better compared to treatment start. The

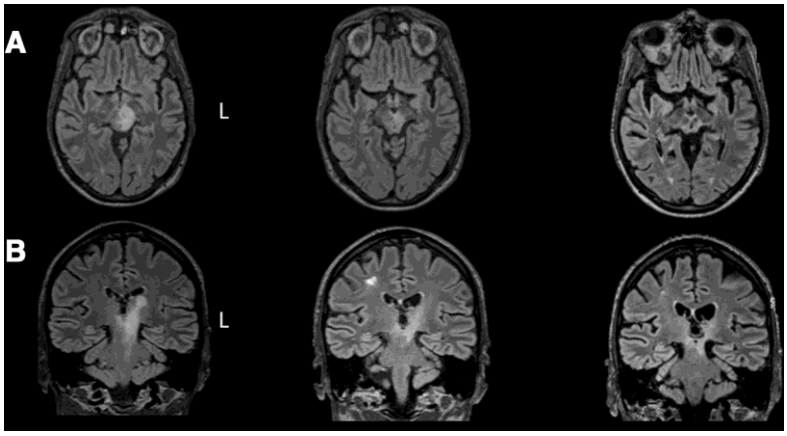


**Fig. 1** Brain MRI, depicting axial (**a**) and coronal (**b**) fluid attenuated inversion recovery (FLAIR) sections on different time points: *left column* on September 2012, *middle column* on June 2013, and *right column* on September 2013. Note the typical PML affection of midline structures and subcortical white matter (U fibers) as, e.g., seen in **b** in the *left* and *middle column*, respectively. Also, note shrinking of total lesion volume, as well as progressive brain atrophy from *middle* to *right column*. *L* left. Cerebral MRIs from January, May, and August 2014 are not depicted because the increase in brain atrophy and decrease in lesion volume were quantified and given numerically in the "Results" section and Table 1, respectively

nine-hole peg test (300, 50, 300 s) and the box and block test (7, 35, 25 pieces during follow-up) showed first an improvement of manual skills and then a deterioration due right-sided ataxia in this right hander. On the Berg balance test, which was not accomplishable at the time of diagnosis, the patient scored independent with a tendency to worsen. His walking speed over 10 m remained unaltered (1.0–1.25 m/s) (Table 1; reference ranges for all tests in respective figure legend). B cell counts were always 0/μl. The hypogammaglobulinemia (varying IgG concentrations due to monthly IvIgG replacement) and the CD4+/CD8+ T cell counts remained essentially unchanged (Table 1). In CSF from September 7, 2012, 2568 JCV copies/ml were found with NCCR sequences that still contained the common signature deletion *del*($C_{54–55}D_{1–64}$) but different partial duplications of the boxes C, D, and E than on September 3 (Fig. 2). While under mirtazapine and mefloquine for about 2 months, JCV concentration decreased to 363 copies/ml on 5 December 2012. Now, the signature deletion of box D was lost and a less complex NCCR rearrangement was found interrupting the continuity of the D box at $D_{35}$ by inserting the sequences $B_{20–23}$, $C_{1–55}$, and $D_{1–35}$ (Table 1, Fig. 2). JCV DNA was not detectable by PCR as of March 2013. The patient's cognitive performance (MoCA) showed a slight deficit which remained stable (Table 1). Over the course of 23 months, total brain lesion volume decreased from 8.54 to 3.97 $cm^3$, as did the midline-lesion volume (hypothalamic, mesencephalic, pontine) from 7.31 to 0.50 $cm^3$. The midline-lesion volume was assumed to be responsible for the oculomotor deficit, dysarthria, and the motor symptoms (Table 1). While the midline-lesion volume decreased upon treatment initiation, the total lesion volume first increased due to appearance of new subcortical lesions and then decreased (Table 1, Fig. 1). Brain atrophy visibly increased between PML onset in September 2012 until September 2013 (Fig. 1). Between September 2013 and August 2014, brain atrophy further advanced and was quantified by a decrease in volume of gray matter (735 to 640 $cm^3$, 13 %) and white matter (436 to 411 $cm^3$, 6 %).

In September 2013, the patient reported ongoing improvement and no treatment side effects. Ambulation was possible without walking aid for ~1000 m. Hemiparesis, hemiataxia, and gait ataxia had improved. Dysarthria and the pretectal syndrome persisted at a stable level. His manual fine and coarse motor skills showed a tendency to worsen. In January 2014, he contracted community-acquired pneumonia and his performance could not be tested. Afterward, gait balance, right-handed manual skills, and dysarthria were worse without signs of active PML (MRI, CSF). As of then, performance remained largely stable except for manual fine motor skills (Table 1).

## Discussion

We present a patient meeting definite diagnostic certainty for PML (Berger et al. 2013) acquired on the basis of CVID, respectively, an especially severe subcategory, LOCID. The time point of JCV infection cannot be determined with certainty: would earlier sera have been available, they might have been positive for JCV antibodies due to repeated IvIgG infusions. Alternatively, even with an earlier infection, they might have been negative because of a severely defective humoral immune response caused by the severe B cell depletion. Our

**Table 1** Barthel index, Rankin scale, and nine-hole peg and box and block tests (given is the average of three performances with the right hand for each test), Berg balance, and 10-m walking tests

| Assessments | Diagnosis | Tx start | Follow-up | | | | | | | |
|---|---|---|---|---|---|---|---|---|---|---|
| | Sept 2012 | Oct 2012 | Dec 2012 | Jan2013 | Mar 2013 | Jun2013 | Sept2013 | Jan2014 | May2014 | Aug 2014 |
| Barthel index | | 60 | 75 | 100 | 100 | 100 | 100 | [b] | 65 | 80 |
| Rankin scale | | 4 | 4 | 3 | 2 | 2 | 2 | | 3 | 3 |
| Nine-hole peg (s) | | Not possible | 73 | 81 | 50 | 52 | 90 | | 240 | Not possible |
| Box and block (pieces) | | 7 | 21 | 22 | 26 | 35 | 30 | | 25 | 25 |
| Berg balance (points) | | Not possible | Not possible | | | 52 | 50 | | 40 | 40 |
| Ten-minute walking test (m/s) | | Not possible | Not possible | 1.25 | 1.00 | 1.00 | 1.11 | | 1.0 | 1.0 |
| Total lesion volume ($cm^3$) | 8.54 | 7.04 | 11.50 | 16.76 | 14.68 | 7.11 | 6.31 | 6.30 | 5.36 | 3.97 |
| Midline-lesion volume ($cm^3$) | 7.31 | 5.96 | 5.27 | 3.28 | 3.12 | 2.56 | 1.25 | 1.21 | 0.87 | 0.50 |
| JCV DNA copies/ml CSF | 1167/2568 | No LP | 363 | No LP | 0 | 0 | No LP | 0 | No LP | No LP |
| Leukocytes (cells/μl) | 3300 | 2400 | 1800 | 1400 | 2000 | 1900 | 1900 | [b] | 1700 | 2200 |
| Lymphocytes (cells/μl) | 850 | 940 | 650 | 730 | 880 | 550 | 900 | | 613 | 525 |
| CD4+ T (cells/μl) | | 88 | 111 | 99 | 109 | 102 | 134 | | 88 | 80 |
| CD8+ T (cells/μl) | | 531 | 549 | 485 | 551 | 446 | 606 | | 352 | 291 |
| B lymphocytes (cells/μl) | | 0 | 0 | 0 | 0 | 0 | 0 | | 0 | 0 |
| IgG (g/l)[a] | 3.19 | 15.30 | 8.68 | | | | 7.58 | | 8.00 | 9.09 |
| IgM (g/l) | <0.05 | <0.05 | 0.12 | | | | <0.05 | | 0.09 | <0.03 |
| IgA (g/l) | <0.06 | <0.06 | 0.07 | | | | <0.06 | | 0.05 | <0.05 |
| Thrombocytes (cells/μl) | 128,000 | 165,000 | 162,000 | 122,000 | 146,000 | 137,000 | 131,000 | | 157,000 | 137,000 |
| MoCA | | Other test[c] | 24/30 | 22/30 | 24/30 | 24/30 | 27/30 | | 26/30 | 26/30 |

In addition, brain MRI total and midline (hypothalamic and brainstem)-lesion volume, JCV DNA concentration in CSF, absolute CD4+ and CD8+ T as well as B cell counts, immunoglobulin concentrations (IgG, IgM, IgA) in serum, and Montreal Cognitive Assessment (MoCA) are given. Diagnosis, treatment start (Tx start) with mefloquine + mirtazapine, and follow-up assessments were made at given time points. Reference ranges: Barthel: 100 (points) indicate independency in grooming, toilet use, absence of incontinence, bathing, feeding, dressing, transfers, walking, and climbing stairs. Rankin: scale runs from 0 (no symptoms) to 6 (dead); 2 indicates slight disability. Nine-hole peg: normal sex/age-related cutoff for right hand ≤21 ± 5 s (Oxford Grice et al. 2003). Box and block: normal sex/age-related cutoff for right hand ≥74 ± 11 pieces (Mathiowetz et al. 1985). Berg balance: independency scores >40 and ≤56 points. Ten-minute walking (speed): healthy male adult, decade 50–60—1.39 m/s. MoCA—26–30 points for healthy adults. Lymphocytes (cells/μl)—B 72–460, CD4+ T 410–1590, and CD8+ T 137–823. Immunoglobulins (g/l)—IgG 6.50–13.50, IgA, 0.75–3.12, and IgM 0.56–3.52

*LP* lumbar puncture, *IgG/M/A* immunoglobulin G/M/A

[a] Under four weekly IvIgG substitutions

[b] No clinical parameters were collected because the patient suffered from community-acquired pneumonia in Jan 2014

[c] A moderate cognitive deficit in a different test battery using Consortium to Establish a Registry for Alzheimer's Disease (CERAD) and material and norm values for neuropsychological diagnostic (MNND) tests

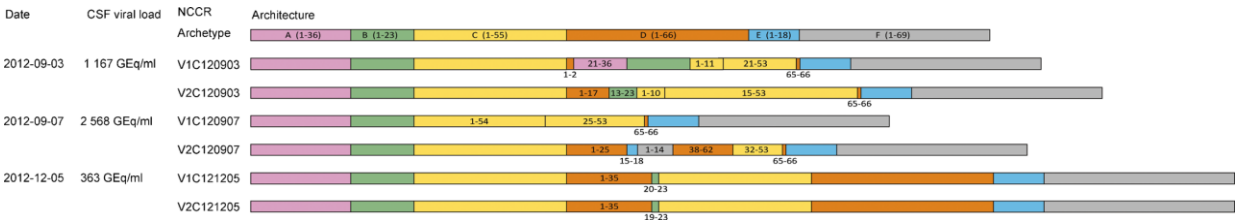


**Fig. 2** Schematic illustration of the JCV archetype noncoding control region (NCCR) and the rearranged NCCRs found in CSF at indicated time points. The NCCR of the archetype JCV is presented with six blocks *A-B-C-D-E-F* in *different colors* and with numbers (*in brackets*) indicating their size in base pairs. For the rearranged NCCRs, the size in base pairs is indicated only for those sequence blocks in which mutations were found. The date, viral load in CSF, and the archetype and variant (see "Results" section) JCV NCCR architectures are indicated. *CSF* cerebrospinal fluid, *GEq/ml* genome equivalents (or copies) per milliliter

patient was in fact positive for anti-JCV IgG. We believe that this was rather due to the IvIgG infusions.

Our patient is still alive almost 2 years after PML onset and tolerates well the long-term treatment with mefloquine and mirtazapine. Clinical improvement, already evident 2 months after treatment initiation, was paralleled by the reduction of the midline-lesion volume, while the total lesion volume increased up to the fourth treatment month due to the appearance of new lesions. After the fifth treatment month, no new lesions appeared and the known lesions were shrinking with subsequent brain atrophy predominantly at former lesion sites. Why new neuroradiological lesions appeared during the first 4 months under mirtazapine that is supposed to block JCV entry into cells remains unclear. It has to be taken into account that amplification of viral DNA in CSF does not fully reflect viral replication in brain tissue, as shown by the lower PCR sensitivity in CSF of AIDS patients with PML on antiretroviral therapy (Marzocchetti et al. 2005). Cognition remained stable, which is important as PML is usually paralleled with cognitive decline and brain atrophy. This is partly explained by the small subcortical- and large midline-lesion volume. Had he not contracted community-acquired pneumonia in January 2014, he might have been well at an overall better performance level. We did not find any cause, i.e., no active PML signs for his deterioration after pneumonia, and hence did not treat him with interleukin-7, a promising new agent for PML patients (Alstadhaug et al. 2014). His worse performance was mainly due to increased ataxia which might be due to increased brain atrophy at the former midline-lesion site.

It has to be left open whether mirtazapine and mefloquine contributed to the survival of our patient. In general, survival of HIV-negative patients with PML and comparable immune status (idiopathic CD4+ T lymphocytopenia, CVID, Good's syndrome) to our patient ranges between 2 and 3 months (longer for one patient in a vegetative state) without treatment and between 2 and 10 months under treatments including cidofovir, cytosine arabinoside, or interferon ((Squintani et al. 2010), Supplementary Table 1). Survival of PML patients with idiopathic CD4+ or CD8+ T lymphocytopenia or CVID (immune status of individuals not specified) under mirtazapine or mirtazapine + mefloquine (without information about assignment of treatment to individuals) was at least 1 year (Gheuens et al. 2011) and even 34 months in a patient with idiopathic CD4+ T lymphocytopenia (242/μl) under mirtazapine (and mefloquine for the first few months) (Delgado-Alvarado et al. 2013). It has to be kept in mind that the B cell deficiency in CVID and the B and CD4+ T cell deficiency in LOCID patients with PML cannot be modified except for substitution with IvIgG. This is unlike PML infections in patients with, e.g., HIV, MS under natalizumab therapy, or cancer under immunosuppression, in whom the underlying condition predisposing to PML often can be modulated or reverted resulting in improved immunocompetence and abatement of PML. IvIgG therapy can contribute to partial restoration of the CD4+ T cell compartment and the reduction of CD8+ T cell activation in CVID patients (Paquin-Proulx et al. 2013). It is, however, less likely that IvIgG played an important role in the immune defense of our patient, as it did not prevent JCV infection and PML onset.

The NCCR rearrangements identified in our patient were insofar compatible with the literature, as deletions mainly affected the D box, while duplications were rather found in proximity to the origin of replication and the promoter of the early viral gene region (Hirsch et al. 2013). Although the NCCR architecture differed from so-called prototypes previously reported in PML, or in HIV patients with PML (Bellizzi et al. 2013), it becomes increasingly clear that NCCR rearrangements apparently are variable among different PML patients and frequently unique for an individual patient. It is therefore difficult to identify particular NCCR rearrangements that correlate with a poor PML outcome (Hirsch et al. 2013). Notably, different NCCR rearrangements were detected in our patient over time. It is tempting to speculate that this change toward the archetype NCCR, which is believed to be associated with lower virus replication, contributed to the patient's survival and absent detection of JCV DNA in CSF. The inherent limitation of this and other single cases in a highly variable disease is, of course, the difficulty of generalizing the evidence of the approaches to diagnosis and therapy to larger

populations. The observation of the parallelism between changes in the NCCR and disease evolution, however, may have pathogenetic implications, and further data of this type could help in comparing potential effects of different approaches to therapy on outcome.

Multiple reasons may underlie the mixed treatment results of mirtazapine, mefloquine, or both, particularly in PML patients with constitutional immunodeficiency. First, different diseases with variable degrees of immunodeficiency predisposing to PML cannot be well compared concerning their response to treatment. Second, the delay between PML symptom onset and treatment initiation, as well as the brain lesion volume at diagnosis, is important. As suggested (Cettomai and McArthur 2009), most significant clinical improvement may be achieved with therapy start close to PML symptom onset and little lesion volume. Third, the NCCR of JCV should be systematically sequenced in future PML treatment studies to learn whether NCCR reshuffling indeed affects survival and may be influenced by treatment. Brain atrophy may constitute a future problem, as its progression in the absence of active PML is unclear and treatment options except for physiotherapy are missing.

**Acknowledgments** We thank the nurses, physiotherapists, and residents of our neurological ward for their support with clinical data collection.

**Contributors** RK, MS, and HK were involved in diagnosis and treatment of the patient. RK, MS, and HK designed the study. RK, CW, and PK conducted the examinations and laboratory studies. RK, BL, MS, and HK drafted the manuscript. RW, HF, RDP, and HHH intellectually contributed to data interpretation and the manuscript. The version to be published was approved by all of the authors. HK accepts full responsibility for the data as guarantor.

**Funding** No extra funds were used in this study.

**Conflict of interest** The authors declare that they have no conflict of interest.

**Patient consent** Obtained.

## References

Alstadhaug KB, Croughs T, Henriksen S et al (2014) Treatment of progressive multifocal leukoencephalopathy with interleukin 7. JAMA Neurol 71:1030–1035

Bellizzi A, Anzivino E, Rodio DM et al (2013) New insights on human polyomavirus JC and pathogenesis of progressive multifocal leukoencephalopathy. Clin Dev Immunol 10:839719

Beppu M, Kawamoto M, Nukuzuma S et al (2012) Mefloquine improved progressive multifocal leukoencephalopathy in a patient with systemic lupus erythematosus. Intern Med 51:1245–1247

Berger JR, Aksamit AJ, Clifford DB et al (2013) PML diagnostic criteria: consensus statement from the AAN Neuroinfectious Disease Section. Neurology 80:1430–1438

Brickelmaier M, Lugovskoy A, Kartikeyan R et al (2009) Identification and characterization of mefloquine efficacy against JC virus in vitro. Antimicrob Agents Chemother 53:1840–1849

Cettomai D, McArthur JC (2009) Mirtazapine use in human immunodeficiency virus-infected patients with progressive multifocal leukoencephalopathy. Arch Neurol 66:255–258

Christakis PG, Okin D, Huttner AJ et al (2013) Progressive multifocal leukoencephalopathy in an immunocompetent patient. J Neurol Sci 326:107–110

Clifford DB, Nath A, Cinque P et al (2013) A study of mefloquine treatment for progressive multifocal leukoencephalopathy: results and exploration of predictors of PML outcomes. J Neurovirol 19:351–358

Delgado-Alvarado M, Sedano MJ, González-Quintanilla V et al (2013) Progressive multifocal leukoencephalopathy and idiopathic CD4 lymphocytopenia. J Neurol Sci 327:75–79

Elphick GF, Querbes W, Jordan JA et al (2004) The human polyomavirus, JCV, uses serotonin receptors to infect cells. Science 306:1380–1383

Gheuens S, Bord E, Kesari S et al (2011) Role of CD4+ and CD8+ T-cell responses against JC virus in the outcome of patients with progressive multifocal leukoencephalopathy (PML) and PML with immune reconstitution inflammatory syndrome. J Virol 85:7256–7263

Hirsch H, Kardas P, Kranz D et al (2013) The human polyomavirus (JCPyV): virological background and clinical implications. Acta Pathol Microbiol Immunol Scand 121:685–727

Hohlfeld SK, Günthard HF, Zeitz J et al (2012) Progressive multi-focal leukoencephalopathy as a rare lethal complication in untreated sarcoidosis. BMJ Case Rep. doi: 10.1136/bcr.03.2011.4036

Iannetta M, Bellizzi A, Lo Menzo S et al (2013) HIV-associated progressive multifocal leukoencephalopathy: longitudinal study of JC virus non-coding control region rearrangements and host immunity. J Neurovirol 19:274–279

Loyaga-Rendon RY, Taylor DO, Koval CE (2013) Progressive multifocal leukoencephalopathy in a heart transplant recipient following rituximab therapy for antibody-mediated rejection. Am J Transplant 13:1075–1079

Malphettes M, Gérard L, Carmagnat M et al (2009) Late-onset combined immune deficiency: a subset of common variable immunodeficiency with severe T cell defect. Clin Infect Dis 49:1329–1338

Marzocchetti A, Di Giambenedetto S, Cingolani A et al (2005) Reduced rate of diagnostic positive detection of JC virus DNA in cerebrospinal fluid in cases of suspected progressive multifocal leukoencephalopathy in the era of potent antiretroviral therapy. J Clin Microbiol 43:4175–4177

Marzocchetti A, Tompkins T, Clifford DB et al (2009) Determinants of survival in progressive multifocal leukoencephalopathy. Neurology 73:1551–1558

Mathiowetz V, Volland G, Kashman N et al (1985) Adult norms for the box and block test of manual dexterity. Am J Occup Ther 39:386–391

Moenster RP, Jett RA (2012) Mirtazapine and mefloquine therapy for progressive multifocal leukoencephalopathy in a patient infected with human immunodeficiency virus. Am J Health Syst Pharm 69:496–498

Naito K, Ueno H, Sekine M et al (2012) Akinetic mutism caused by HIV-associated progressive multifocal leukoencephalopathy was successfully treated with mefloquine: a serial multimodal MRI Study. Intern Med 51:205–209

Oxford Grice K, Vogel KA, Le V et al (2003) Adult norms for a commercially available nine hole peg test for finger dexterity. Am J Occup Ther 57:570–573

Paquin-Proulx D, Santos BA, Carvalho KI et al (2013) IVIg immune reconstitution treatment alleviates the state of persistent immune activation and suppressed CD4 T cell counts in CVID. PLoS ONE 8, e75199

Roth P, Morell A, Hunziker HR et al (1975) Schweiz med Wschr 105:1584–1585

Salzer U, Warnatz K, Peter HH (2012) Common variable immunodeficiency—an update. Arthritis Res Ther 14:223

Schröder A, Lee DH, Hellwig K et al (2010) Successful management of natalizumab-associated progressive multifocal leukoencephalopathy and immune reconstitution syndrome in a patient with multiple sclerosis. Arch Neurol 67:1391–1394

Squintani G, Ferrari S, Bazzoli E et al (2010) Progressive multifocal leukoencephalopathy in a patient with Good's syndrome. Int J Infect Dis 14:e444–e447

Steiner I, Berger JR (2012) Update on progressive multifocal leukoencephalopathy. Curr Neurol Neurosci Rep 12:680–686

Verma S, Cikurel K, Koralnik IJ et al (2007) Mirtazapine in progressive multifocal leukoencephalopathy associated with polycythemia vera. J Infect Dis 196:709–711

Vulliemoz S, Lurati-Ruiz F, Borruat FX et al (2006) Favourable outcome of progressive multifocal leucoencephalopathy in two patients with dermatomyositis. J Neurol Neurosurg Psychiatry 77:1079–1082

Weber T (2008) Progressive multifocal leukoencephalopathy. Neurol Clin 26:833–854

Wüthrich C, Koralnik IJ (2012) Frequent infection of cortical neurons by JC virus in patients with progressive multifocal leukoencephalopathy. J Neuropathol Exp Neurol 71:54–65

## 5.5 A Case of Primary JC Polyomavirus Infection–Associated Nephropathy

American Journal of Transplantation 2014; 14: 2887–2892
Wiley Periodicals Inc.



doi: 10.1111/ajt.12945

Case Report

# A Case of Primary JC Polyomavirus Infection–Associated Nephropathy

**I. Lautenschlager[1], T. Jahnukainen[2], P. Kardas[3], J. Lohi[4], E. Auvinen[1], L. Mannonen[1], A. Dumoulin[3], H. H. Hirsch[3,5,*] and H. Jalanko[2]**

[1]*Department of Virology, Helsinki University Hospital (HUSLAB) and University of Helsinki, Helsinki, Finland*
[2]*Pediatric Nephrology and Transplantation, Children's Hospital Helsinki University Hospital and University of Helsinki, Helsinki, Finland*
[3]*Transplantation and Clinical Virology, Department of Biomedicine, University of Basel, Basel, Switzerland*
[4]*Department of Pathology, Helsinki University Hospital and University of Helsinki, Helsinki, Finland*
[5]*Infectious Diseases and Hospital Epidemiology, University Hospital Basel, Basel, Switzerland*
[*]*Corresponding author: Hans H. Hirsch, hans.hirsch@unibas.ch*

**A 15-year-old boy with a posterior urethral valve received a deceased donor kidney transplant (KT) in March 2011. Basiliximab induction followed by tacrolimus-based triple medication was used as immunosuppression. Eleven months after KT, the graft function deteriorated and the biopsy demonstrated interstitial nephritis suggestive of acute rejection. BK polyomavirus (BKPyV) surveillance in urine and plasma was negative. The patient received methylprednisolone pulses and anti-thymocyte globulin. Immunohistochemistry was positive for simian virus 40 (SV40) large T-antigen (LTag) in the biopsies, and quantitative polymerase chain reaction for JC polyomavirus (JCPyV) indicated high viral loads in urine and borderline levels in plasma. Immunosuppression was reduced and follow-up biopsies showed tubular atrophy and interstitial fibrosis. Two years after KT, antibody-mediated rejection resulted in graft loss and return to hemodialysis. Retrospective serologic work-up indicated a primary JCPyV infection with seroconversion first for IgM, followed by IgG, but no indication of BKPyV infection. In the SV40 LTag positive biopsies, JCPyV deoxyribonucleic acid (DNA) with archetype noncoding control region was detected, while BKPyV DNA was undetectable. To the best of our knowledge, this is the first reported case of primary JCPyV infection as the cause of PyV-associated nephropathy in KT.**

**Abbreviations: ABMR, antibody-mediated rejection; ATG, anti-thymocyte globulin; AZA, azathioprine; BKPyV, BK polyomavirus; BK-PyVAN, BKPyV-associated nephropathy; CMV, cytomegalovirus; CsA, cyclosporine; DNA, deoxyribonucleic acid; DSA, donor-specific antibodies; EBV, Epstein-Barr virus; Egfr, estimated GFR; HE, hematoxylin; IFTA, interstitial fibrosis and tubular atrophy; IHC, immunohistochemistry; IS, immunosuppression after induction therapy; ISH, *in situ* hybridization; IVIG, intravenous gammaglobulin infusions; JCPyV, JC polyomavirus; JC-PyVAN, JCPyV-associated nephropathy; JCV, JC virus; KT, kidney transplant; LTag, large T-antigen; MFI, mean fluorescence intensity; MP, methylprednisolone; MPA, mycophenolic acid; ND, under detection level; pCr, plasma creatinine concentration; PCR, polymerase chain reaction; PE, plasma exchange; PyV, polyomavirus; PyVAN, polyomavirus-associated nephropathy; SV40, simian virus 40; Tac, tacrolimus; VLP, virus-like particles**

**Received 24 June 2014, revised 17 July 2014 and accepted for publication 24 July 2014**

## Introduction

Polyomavirus-associated nephropathy (PyVAN) remains a challenging infectious complication after kidney transplant (KT) and is typically caused by uncontrolled BK polyomavirus (BKPyV) replication. However, a few cases of PyVAN have been attributed to JC polyomavirus (JCPyV) (1–4). Although JCPyV viruria is common in healthy blood donors as well as in KT recipients, JCPyV-associated nephropathy (JC-PyVAN) is considered to be a rare complication with a mostly benign course. Accordingly, routine screening for JCPyV replication is not recommended after KT (4).

## Case Report

A 15-year-old boy with a posterior urethral valve received a deceased donor KT in March 2011 (cytomegalovirus [CMV] D+/R−; Epstein–Barr virus [EBV] D+/R+). Basiliximab induction was given on days 0 and 4, accompanied by tacrolimus (target trough level 10–12 ng/mL), azathioprine, and methylprednisolone (MP). The plasma creatinine concentration (pCr) decreased to 1.33 mg/dL within 3 days. Three months posttransplant, the estimated GFR (eGFR) was 52 mL/min/1.73 $m^2$ and a protocol biopsy showed no signs of rejection. Six months posttransplant,

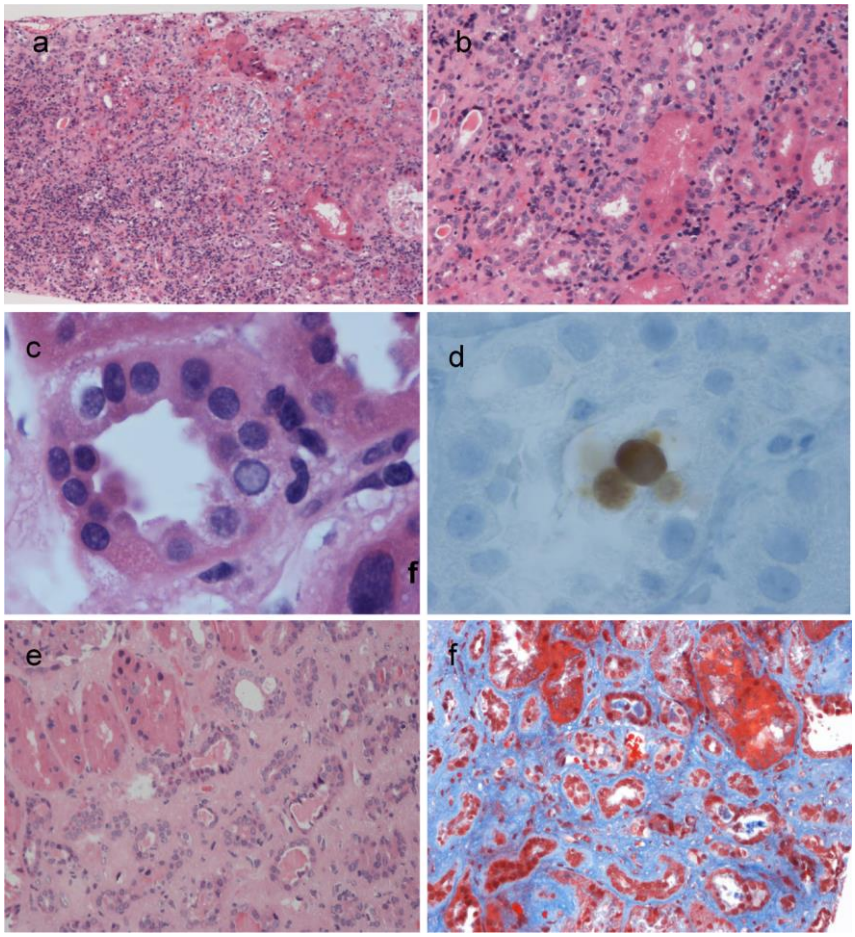


**Figure 1: Kidney allograft biopsy.** (a) Interstitial nephritis with focal inflammatory infiltrates (hematoxylin [HE] staining, magnification ×100). (b) A close view of interstitial inflammation demonstrating mainly lymphocyte infiltration, some eosinophils and plasma cells, and some tubulitis (HE staining, magnification ×200). (c) A tubular cell located polyomavirus inclusion in (HE staining, magnification ×1000). (d) Simian virus 40 positive nuclear staining of tubular cells (magnification ×1000). (e) Tubular atrophy and fibrosis in a follow-up biopsy (HE staining, magnification ×200). (f) Interstitial fibrosis (bright blue color) (trichrome staining, magnification ×200).

pCr had increased to 1.67 mg/dL, and azathioprine was changed to mycophenolic acid (MPA). Nine months posttransplant, the patient presented with primary CMV infection and disease, which was successfully treated with valganciclovir. Screening for BKPyV deoxyribonucleic acid (DNA) in plasma was performed every 3 months during the first year posttransplant according to a standard protocol and remained negative.

Eleven months posttransplant, pCr increased to 5.56 mg/dL. BKPyV DNA was not detected in plasma or urine, but JCPyV DNA was positive in urine. CMV, EBV and other viral nucleic acid tests were negative. Allograft biopsy demonstrated florid interstitial inflammation (i3) with mixed cellularity: lymphocytes, some with blast morphology, predominated together with plasma cells and eosinophils, and tubulitis (t3) (Figure 1). Interstitial nephritis suggestive of acute cellular rejection was graded IB according to the Banff criteria (5,6) (see Table 1). The patient received MP pulses with a moderate decrease in pCr. The follow-up biopsy demonstrated a similar histological pattern and antithymocyte globulin (ATG) was given because steroid-resistant rejection was suspected. Immunoperoxidase staining with an mAb against simian virus 40 (SV40) large T-antigen (LTag), which also reacts with the LTag of BKPyV and JCPyV, was positive indicating PyV nephropathy (Figure 1). However, urine and plasma were repeatedly negative for BKPyV DNA, while urine was positive for JCPyV DNA by polymerase chain reaction (PCR) (7,8). Another biopsy taken 12 months posttransplant demonstrated persisting interstitial nephritis and borderline rejection. BKPyV PCR in plasma and urine remained

**Table 1:** JCV viral loads in urine and plasma in relation to plasma creatinine concentration and biopsy finding

| Time from KT (days) | Urine JCV-DNA (cps/mL) | Plasma JCV-DNA (cps/mL) | pCr (mg/dL) | Immunosuppression | DSA | Biopsy finding (Banff criteria) | SV40 staining | C4d staining |
|---|---|---|---|---|---|---|---|---|
| 324 | | ND | 5.66 | Tac 5–7 ng/mL | neg | Interstitial nephritis, acute cellular rejection susp. (grade IB) | pos | neg |
| | | | | MPA 400 mg/m$^2$ b.i.d. | | | | |
| | | | | MP pulses 10 mg/kg once daily ×3 | | | | |
| | | | | Oral MP 0.12 mg/kg eod | | | | |
| +4 | 7.53 $\log_{10}$ | | 4.03 | Tac 6–8 ng/mL | neg | Interstitial nephritis, acute rejection, borderline (grade IA) | pos | neg |
| | | | | MPA 400 mg/m$^2$ b.i.d. | | | | |
| | | | | Oral MP 0.12 mg/kg eod | | | | |
| +10 | 7.78 $\log_{10}$ | | | | | | | |
| +37 | | 200 | 2.67 | ATG 100 mg/d ×8 | neg | Interstitial nephritis, acute rejection, borderline (borderline rejection) | pos | neg |
| | | | | Tac 6–8 ng/mL | | | | |
| | | | | AZA 1 mg/kg/d | | | | |
| | | | | Oral MP | | | | |
| +59 | | | 2.96 | | | IFTA (no rejection) | neg | neg |
| +136 | | 279 | | | | | | |
| +167 | | 318 | | Tac 6–8 ng/mL | | | | |
| | | | | Oral MP 0.1 mg/kg/d | | | | |
| +221 | 7.81 $\log_{10}$ | | 2.82 | Tac 5–6 ng/mL | neg | IFTA (no rejection) | neg | neg |
| | | | | Oral MP 0.1 mg/kg/d | | | | |
| +226 | | ND | 2.52 | | | | | |
| +351 | 6.97 $\log_{10}$ | ND | 2.65 | | | | | |
| +397 | 5.91 $\log_{10}$ | ND | 3.85 | Tac 4–5 ng/mL | pos | | | |
| | | | | Oral MP 0.1 mg/kg/d | | | | |
| +485 | ND | ND | 5.18 | Tac 4–6 ng/mL | | | | |
| | | | | AZA 1 mg/kg/d | | | | |
| | | | | Oral MP 1 mg/kg/d | | | | |
| | | | | PE, IVIG | | | | |
| +505 | 3.80 $\log_{10}$ | ND | 5.94 | Dialysis | pos | Glomerular sclerosis, IFTA (antibody mediated rejection) | neg | pos |

ATG, anti-thymocyte globulin; AZA, azathioprine; b.i.d., twice daily; cps, copies; d, daily; DSA, donor-specific antibodies; eod, every other day; IFTA, interstitial fibrosis and tubular atrophy; IVIG, intravenous gammaglobulin infusions; JCV, JC virus; KT, kidney transplantation; MP, methylprednisolone; MPA, mycophenolic acid; ND, under detection level; neg, negative; PE, plasma exchange; pCr, plasma creatinine concentration; pos, positive; SV40, simian virus 40; Tac, tacrolimus target level ng/mL.

negative. Quantitative JCPyV PCR indicated high viral load in urine (7.53 $\log_{10}$ cps/mL), and low values around the limit of detection in plasma. The SV40 staining was positive in all three biopsies (Table 1). Immunosuppression was reduced, and the pCr gradually decreased from 2.96 to 2.52 mg/dL. Also, the urine JCPyV load decreased (Table 1). Follow-up biopsies showed tubular atrophy and interstitial fibrosis, and negative staining for SV40 LTag (Figure 1).

Two years posttransplant, pCr started to increase gradually up to 5.0 mg/dL. The patient was on reduced immunosuppression with low-dose tacrolimus (trough levels 3.1–6.0 ng/mL) and every other day MP (0.1 mg/kg). *De novo* donor-specific class II HLA antibodies were detected using single-antigen bead panels (One Lambda, Inc., Canoga Park, CA) with mean fluorescence intensity (MFI) of 11 080 for DQ4; 7 969 for DQ8; and 3 580 for DR53. The graft biopsy showed strong C4d positivity of peritubular capillaries and glomeruli and severe chronic changes, including glomerular sclerosis, glomerular basement membrane lamellation (transplant glomerulopathy), interstitial fibrosis and tubular atrophy, speaking for antibody-mediated chronic rejection and allograft nephropathy. Repeated donor-specific antibodies (DSA) evaluation revealed decline in DQ4 and DQ8 DSA levels (MFI 4819 and 6352, respectively) and increase in DR53 level (MFI 16 376). Staining for with SV40 remained negative. Despite intravenous MP pulses, extensive plasma exchange therapy and immunoglobulin infusions, the graft function did not recover and the patient became dialysis-dependent.

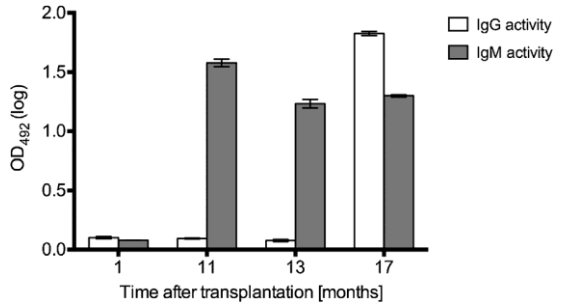


**Figure 2: JC polyomavirus (JCPyV)-specific antibody responses.** JCPyV IgG and IgM antibody response to JCPyV virus-like particles (VLP) analyzed by enzyme immune assay using a cut-off value of 0.11 $OD_{492\,nm}$ for sera diluted 1:400 as described previously (7).

Retrospective DNA extraction from the three biopsy samples showing positive SV40 LTag staining revealed JCPyV DNA by PCR. Sequencing of the JCPyV noncoding control region demonstrated an archetype architecture and no relevant point mutations as reported by others (1). BKPyV DNA was not found. Thus, a diagnosis of JCPyV-associated nephropathy JC-PyVAN was established. Testing of available plasma samples for JCPyV-specific antibodies using viral protein 1-derived virus-like particles (VLP) by enzymimmunoassay (9) revealed seroconversion for JCPyV IgM at 11 months posttransplant followed by IgG seroconversion at 16 months posttransplant (Figure 2). BKPyV-specific IgG antibodies were not detectable.

## Discussion

JCPyV replication with asymptomatic viruria is found in approximately one-third of the JCPyV-infected healthy blood donors (9) and is also common in KT recipients (10–13). However, only few studies have reported impaired kidney graft function in conjunction with JCPyV replication (14). Molecular studies of kidney allograft biopsies have detected the presence of JCPyV in the cases of documented PyVAN (15). Despite this frequent detection of JCPyV in the renourinary tract, JC-PyVAN is rare (1,2,4,16). In fact, since the first report of JC-PyVAN (3), less than a dozen cases have been published, all of which were adult KT recipients (17–19) (Table 2). Primary JCPyV infection is known to occur during childhood usually after BKPyV infection has occurred. The seroprevalence of JCPyV ranges from 24% in the age group of 10–14 years (20) to

**Table 2:** Previously reported JC-PyVAN cases

| | Kazory et al (3) | Wen et al (17) | Drachenberg et al (1) | Kantarci et al (18) | Aubert et al (19) | This report |
|---|---|---|---|---|---|---|
| Patients studied | 1 | 1 | 6 | 1 | 1 | 1 |
| Age (years) | 37 | 62 | 62 (mean) | 28 | 43 | 16 |
| Transplant type | Kidney | Kidney | Kidney | Kidney | Kidney | Kidney |
| Time of diagnosis | 6 years | 12 months | 29 months (mean) | 6 months | 29 months | 12 months |
| Prior rejection | No | Yes | Yes, 1 patient | Yes | No | No |
| IS | CsA, Aza, prednisone | Tac, MMF, MP | Tac, MMF, prednisone | Tac, MPA, MP | Tac, MMF, steroids | Tac, (Aza) MPA, MP |
| BKPyV screening | No | No | Yes | No | No | Yes |
| Decoy cells | Yes | n.t. | Yes | n.t. | n.t. | n.t. |
| BKPyV DNAuria | n.t. | n.t. | No | No | No | No |
| BKPyV DNAemia | No | n.t. | No | No | No | No |
| JCPyV DNAuria | n.t. | yes | Yes ($7.7\,log_{10}$ cps/mL) | Yes ($10.5\,log_{10}$ cps/mL) | Yes ($12\,log_{10}$ cps/mL) | Yes ($7.7\,log_{10}$ cps/mL) |
| JCPyV DNAemia | Yes | n.t. | No/low | No | Yes ($7\,log_{10}$ cps/mL) | no/low |
| Declining renal function | Yes | Yes | No | Yes | Yes | Yes |
| Biopsy results | | | | | | |
| Interstitial nephritis | Yes | Yes | Yes | Yes | Yes | Yes |
| Intranuclear inclusion | Yes | Yes | Yes | Yes | Yes | Yes |
| SV40LT staining | n.t. | n.t. | Yes | Yes | Yes | Yes |
| JCPyV detection | Yes (ISH) | Yes (IHC), (PCR) Archetype | Yes (PCR) Archetype NCCR | n.t. | Yes (PCR) | Yes (PCR) Archetype NCCR |
| Prior JCPyV antibodies | n.t. | n.t. | n.t. | n.t. | n.t | Negative |
| Origin of virus | Unknown | Unknown | Unknown | Unknown | Unknown | Primary infection |
| Treatment | ↓IS | ↓IS | ↓IS | ↓IS | ↓IS | ↓IS |
| Graft loss | Yes (PyVAN) | No | No | No | Yes (PyVAN) | Yes (ABMR) |

ABMR, antibody-mediated rejection; Aza, azathioprine; BKPyV, BK polyomavirus; cps, copies; CsA, cyclosporine A; DNA, deoxyribonucleic acid; IHC, immunohistochemistry; IS, immunosuppression after induction therapy; ISH, *in situ* hybridization; JCPyV, JC polyomavirus; JC-PyVAN, JCPyV-associated nephropathy; MMF, mycophenolate mofetil; MP, methylprednisolone; MPA, mycophenolic acid; NCCR, noncoding control region; n.t., not tested; SV40LT, simian virus 40 large T; Tac, tacrolimus.

50% in the age group of 9–11 years and adults (9,16,21). Although primary infections should occur in pediatric or adolescent KT recipients, this is, to the best of our knowledge, the first documented case of primary JCPyV infection leading to PyVAN.

While high copy numbers of JCPyV DNA were found in the urine of our patient, viremia was below or barely above the lower limit of detection, despite significant allograft involvement. This is in agreement with most previous reports on JC-PyVAN (1), with few exceptions (15). The clinical course of JC-PyVAN was described to be less severe than that of BKPyV-associated nephropathy (BK-PyVAN) and could be successfully managed by a reduction in the immunosuppression when detected early (1). Most data on JCPyV replication concern, however, adult KT patients who more often are JCPyV seropositive. Our patient was clearly seronegative and demonstrated a seroconversion first for IgM and followed by IgG, indicative of primary infection. The poor outcome of this case highlights the potential importance of JCPyV serostatus in pediatric and adolescent KT recipients. In line with the studies by others (22), PyV-specific serology of donor and recipients may help to identify patients at higher risk benefiting from a targeting screening modality. In addition, the absence of BKPyV in plasma and urine probably delayed a proper diagnosis at the time of the initial biopsies, especially in view of the pronounced inflammation interpreted as acute cellular rejection.

The histological picture of JC-PyVAN with significant interstitial inflammation and subsequent tubular atrophy and fibrosis in our patient corresponds to the findings in severe PyVAN cases described earlier (1). However, concomitant tubulitis, interstitial inflammation, and repetitively negative plasma BKPyV DNA raised a suspicion of severe acute rejection leading to MP pulses and ATG therapy. Although some response of the pCr was noticed, the renal allograft function remained impaired. Eventually, the diagnosis of JC-PyVAN was made by a positive JCPyV DNA finding in the biopsy and was confirmed by JCPyV serology. The low or undetectable JCPyV DNA in plasma points to the fact that molecular diagnostics of this analyte was not useful for diagnosis and follow-up.

The reduction of immunosuppression was initially followed by an improved renal allograft function and a decrease of urinary JCPyV viral load indicating a favorable response. During follow-up, however, the patient developed DSA and a clear-cut C4d positivity in the graft indicating an antibody-mediated rejection, which was not responsive to plasma exchanges and immunoglobulin infusions. At this advanced stage, therapy with anti-CD 20 antibodies (rituximab) or bortezomib was regarded as futile and dialysis was commenced.

Although this case suggests the possible interchangeable role of BK and JC in PyVAN of the KT, it is notable that JCPyV nephropathy appears to occur only in the absence of BKPyV co-infection (1). The reason for this difference is not clear given the fact that JCPyV replication and urinary shedding is typically more frequent in healthy individuals (9). Presumably, intrarenal JCPyV replication progressing to organ-invasive kidney disease is disadvantaged in comparison to BKPyV in the co-infected immunocompromised host. On the other hand, progressive multifocal leukoencephalopathy is almost exclusively caused by JCPyV replication in the brain, but some cases have been reported with similar presentation (23), where BKPyV, but not JCPyV, has been detected in the central nervous system (24). Whether this is due to differences in immune control or host cell factors is unknown, but a significant role of the viral noncoding control region in the infected host cell appears likely (16).

## Conclusions

This case of primary JCPyV infection illustrates that JC-PyVAN represents a diagnostic and therapeutic challenge requiring a high index of suspicion with high urine JCPyV viral loads as sole indicator. Our case points to the limitations of current guidelines, and emphasizes that blood JCPyV DNA findings are not reliable. So far, no therapy for JCPyV exists and the only option is to reduce immunosuppression. Although favorable outcomes have been reported in prospectively managed cases, our case was characterized by subsequent humoral rejection and graft failure. Further studies and experience are clearly needed to optimize the management of JCPyV-associated nephropathy, and the role of donor and recipient serology for BKPyV and JCPyV prior to KT may be valuable for targeting respective screening strategies (25).

## Acknowledgments

The study was supported by the grants of Helsinki University Hospital Funds (to IL and to HJ) and by an unrestricted appointment grant of the University of Basel (to HHH).

## Ethical Approval

The study was approved by the Institutional Review Board and the Ethics Committee of Helsinki University Hospital.

## Disclosure

The authors of this manuscript have no conflicts of interest to disclose as described by the *American Journal of Transplantation*.

## References

1. Drachenberg CB, Hirsch HH, Papadimitriou JC, et al. Polyomavirus BK versus JC replication and nephropathy in renal transplant recipients: A prospective evaluation. Transplantation 2007; 84: 323–330.

2. Delbue S, Ferraresso M, Ghio L, et al. Review on JC virus infection in kidney transplant recipients. Clin Dev Immunol 2013; 2013: 926391. doi: 10.1155/2013/926391
3. Kazory A, Ducloux D, Chalopin J-M, Angonin R, Fontanière B, Moret H. The first case of JC virus allograft nephropathy. Transplantation 2003; 76: 1653–1655.
4. Hirsch HH, Randhawa P. BK polyomavirus in solid organ transplantation. Am J Transplant 2013; 13 (Suppl 4): 179–188.
5. Racusen LC, Colvin RB, Solez K, et al. The Banff 97 working classification of renal allograft pathology. Kidney Int 1999; 55: 713–723.
6. Sis B, Mengel M, Haas M, et al. Banff '09 meeting report: Antibody mediated graft deterioration and implementation of Banff working groups. Am J Transplant 2010; 10: 464–471.
7. Hirsch HH, Mohaupt M, Klimkait T. Prospective monitoring of BK virus load after discontinuing sirolimus treatment in a renal transplant patient with BK virus nephropathy. J Infect Dis 2001; 184: 1494–1495.
8. Dumoulin A, Hirsch HH. Reevaluating and optimizing polyomavirus BK and JC real-time PCR assays to detect rare sequence polymorphisms. J Clin Microbiol 2011; 49: 1382–1388.
9. Egli A, Infanti L, Dumoulin A, et al. Prevalence of polyomavirus BK and JC infection and replication in 400 healthy blood donors. J Infect Dis 2009; 199: 837–846.
10. Helanterä I, Ortiz F, Auvinen E, et al. Polyomavirus BK and JC infections in well matched Finnish kidney transplant recipients. Transplant Int 2009; 22: 688–693.
11. Mengelle C, Kamar N, Mansuy JM, et al. JC virus DNA in the peripheral blood of renal transplant patients: A 1-year prospective follow-up in France. J Med Virol 2011; 83: 132–136.
12. Delbue S, Ferraresso M, Elia F, et al. Investigation of polyomaviruses replication in pediatric patients with nephropathy receiving rituximab. J Med Virol 2012; 84: 1464–1470.
13. Muller A, Beck B, Theilemann K, et al. Detection of polyomavirus BK and JC in children with kidney diseases and renal transplant recipients. Pediatr Infect Dis J 2005; 24: 778–781.
14. Kusne S, Vilchez RA, Zanwar P, et al. Polyomavirus JC urinary shedding in kidney and liver transplant recipients associated with reduced creatinine clearance. J Infect Dis 2012; 206: 875–880.
15. Randhawa P, Baksh F, Aoki N, Tschirhart D, Filkenstein S. JS virus infection in allograft kidneys. Analysis by polymerase reaction and immunohistochemistry. Transplantation 2001; 71: 1300–1303.
16. Hirsch HH, Kardas P, Kranz D, Leboeuf C. The human JC polyomavirus (JCPyV): Virological background and clinical implications. APMIS 2013; 121: 685–727.
17. Wen MC, Wang CL, Wang M, et al. Association of JC virus with tubulointerstitial nephritis in a renal allograft recipient. J Med Virol 2004; 72: 675–678.
18. Kantarci G, Eren Z, Dmirag A, et al. JC virus-associated nephropathy in a renal transplant recipients and comparative analysis of previous cases. Transplant Infect Dis 2011; 13: 89–92.
19. Aubert O, Galmiche L, Rozenberg F, et al. Post-transplant allograft dysfunction. Kidney Int 2013; 83: 765–767.
20. Stolt A, Sasnauskas K, Koskela P, Lehtinen M, Dillner J. Seroepidemiology of the human polyomaviruses. J Gen Virol 2003; 84: 1499–1504.
21. Knowles WA, Pipkin P, Andrews N, et al. Population-based study of antibody to human polyomaviruses BKV and JCV and the simian polyomavirus SV40. J Med Virol 2003; 71: 115–123.
22. Bohl DL, Storch GA, Ryschkewitsch C, et al. Donor origin of BK virus in renal transplantation and role of HLA C7 in susceptibility to sustained BK viremia. Am J Transplant 2005; 5: 2213–2221.
23. Hirsch HH. BK virus: Opportunity makes a pathogen. Clin Infect Dis 2005; 41: 354–360.
24. Hix JK, Braun WE, Isada CM. Delirium in a renal transplant recipient associated with BK virus in the cerebrospinal fluid. Transplantation 2004; 78: 1407–1408.
25. Hirsch HH, Babel N, Comoli P, et al. European perspective on human polyomavirus infection, replication and disease in solid organ transplantation. Clin Microbiol Infect 2014; 20 (Suppl 7): 74–88.

## 5.6 BK Polyomavirus-Specific Cellular Immune Responses Are Age-Dependent and Strongly Correlate With Phases of Virus Replication

American Journal of Transplantation 2014; 14: 1334–1345
Wiley Periodicals Inc.



doi: 10.1111/ajt.12689

# BK Polyomavirus-Specific Cellular Immune Responses Are Age-Dependent and Strongly Correlate With Phases of Virus Replication

**T. Schmidt[1], C. Adam[2], H. H. Hirsch[3,4], M. W. W. Janssen[1,5], M. Wolf[1], J. Dirks[1], P. Kardas[3,4], T. Ahlenstiel-Grunow[6], L. Pape[6], T. Rohrer[7], D. Fliser[2], M. Sester[1,*] and U. Sester[2]**

[1]*Department of Transplant and Infection Immunology, Institute of Virology, Saarland University, Homburg, Germany*
[2]*Department of Internal Medicine IV, Saarland University, Homburg, Germany*
[3]*Division of Transplantation & Clinical Virology, Department Biomedicine (Haus Petersplatz), University of Basel, Basel, Switzerland*
[4]*Division of Infectious Disease & Hospital Epidemiology, University Hospital Basel, Basel, Switzerland*
[5]*Department of Urology, Saarland University, Homburg, Germany*
[6]*Department of Pediatric Nephrology, Hannover Medical School, Hannover, Germany*
[7]*Department of Pediatrics, Saarland University, Homburg, Germany*
[*]*Corresponding author: Martina Sester, martina.sester@uks.eu*

**BK polyomavirus (BKPyV) infection is widespread and typically asymptomatic during childhood, but may cause nephropathy in kidney transplant recipients. However, there is only limited knowledge on BKPyV-specific immunity in children and adults, and its role in BKPyV-replication and disease posttransplant. We therefore characterized BKPyV-specific immunity from 122 immunocompetent individuals (1–84 years), 38 adult kidney recipients with (n = 14) and without BKPyV-associated complications (n = 24), and 25 hemodialysis (HD) patients. Blood samples were stimulated with overlapping peptides of BKPyV large-T antigen and VP1 followed by flow-cytometric analysis of activated CD4 T cells expressing interferon-γ, IL-2 and tumor necrosis factor-α. Antibody-levels were determined using enzyme-linked immunosorbent assay. Both BKPyV-IgG levels and BKPyV-specific CD4 T cell frequencies were age-dependent (p = 0.0059) with maximum levels between 20 and 30 years (0.042%, interquartile range 0.05%). Transplant recipients showed a significantly higher BKPyV-specific T cell prevalence (57.9%) compared to age-matched controls (21.7%) or HD patients (28%, p = 0.017). Clinically relevant BKPyV-replication was associated with elevated frequencies of BKPyV-specific T cells (p = 0.0002), but decreased percentage of cells expressing multiple cytokines (p = 0.009). In conclusion, BKPyV-specific cellular immunity reflects phases of active BKPyV-replication either after primary infection in childhood or during reactivation after transplantation. Combined analysis of BKPyV-specific T cell functionality and viral loads may improve individual risk assessment.**

**Keywords: BKPyV, CD4 T cell, cytokine profiling, flow-cytometry, IFNγ, interferon-γ, T cell**

**Abbreviations: BKPyV, BK polyomavirus; CFSE, carboxyfluorescein diacetate succinimidyl ester; CMV, cytomegalovirus; DMSO, dimethylsulfoxide; FCS, fetal calf serum; HD, hemodialysis; IFNγ, interferon-γ; IQR, interquartile range; PBMC, peripheral blood mononuclear cells; PBS, phosphate buffered saline; PyVAN, polyomavirus-associated nephropathy; RTx, renal transplant; SEB, *Staphylococcus aureus* enterotoxin B; TNF-α, tumor necrosis factor-α**

**Received 18 December 2013, revised 22 January 2014 and accepted for publication 29 January 2014**

## Introduction

The BK polyomavirus (BKPyV) is widespread in the human population with seroprevalences of more than 80% (1,2). After primary infection occurring largely during childhood, BKPyV establishes latency in the renourinary tract (3). While BKPyV-infection and reactivation in healthy individuals generally remain asymptomatic throughout life, they are a major cause of renal dysfunction in kidney transplant patients during immunosuppressive therapy. Up to 10% of all patients develop a polyomavirus-associated nephropathy (PyVAN) that results in allograft loss in 10–80% of cases (4–6). As occurrence of PyVAN is associated with preceding periods of high-level BKPyV-replication, routine assessment of viral load in urine and plasma is recommended after kidney transplantation where persistent viremia for more than 3 weeks indicates presumptive PyVAN (5).

Apart from direct viral load testing and renal allograft biopsy that may identify BKPyV as a causative agent for renal dysfunction after kidney transplantation, analysis of a patient's humoral and cellular immune response toward BKPyV may inform on the individual capacity for effective

virus control (7–12). Several studies on humoral immunity in renal transplant (RTx) recipients support a correlation of BKPyV-IgGs and a patient's history of BKPyV-exposure, although antibody titers seem to have limited value to predict PyVAN (9,13–16). In contrast, as with immunity toward other persistent pathogens (17–20), BKPyV-specific cellular immunity and its functionality may have potential to be used as a monitoring approach to predict BKPyV-replication or to guide the outcome of therapeutic interventions (7). Of note, viruria is observed not only in RTx recipients, but also in asymptomatic healthy individuals (21,22), which may indicate differences in immune-based control mechanisms. Until now, however, knowledge is limited about BKPyV-specific cellular immunity in asymptomatic immunocompetent individuals of different ages and how this immunity differs from RTx recipients with BKPyV-complications. In this study, BKPyV-specific cellular and humoral immune responses in immunocompetent individuals were characterized in early childhood, adolescents and adults and results were compared with those of adult RTx recipients with and without BKPyV-complications.

## Materials and Methods

### *Study subjects*

For the age-associated characterization of BKPyV-specific cellular immunity, we cross-sectionally analyzed CD4 T cells in whole blood samples of 122 immunocompetent individuals between 1 and 84 years of age (mean age 27.6 ± 21.2 years; 62 females; 56 and 66 individuals below and above the age of 18 years, respectively). In addition, to detect differences in BKPyV-specific immunity in individuals with an elevated risk for BKPyV-associated complications, 38 RTx recipients (mean age 55.2 ± 14.9 years), and 25 hemodialysis (HD) patients as pretransplant controls were recruited and compared to an age-matched subgroup of healthy controls (Table 1). All transplant recipients received an immunosuppressive drug regimen including anti-IL-2 receptor antibody induction, steroids and calcineurin inhibitors (34 on tacrolimus, 4 on cyclosporine A). In addition, all except two patients received an antiproliferative drug (33 on mycophenolate mofetile and 3 on azathioprine). Among transplant patients, 14 had confirmed clinically relevant BKPyV-replication (RTx-BKPyV positive), which was defined as (i) more than $10^4$ virus copies/mL plasma or more than $10^7$ virus copies/mL urine in at least two subsequent samples and/or (ii) more than $10^4$ virus copies/mL plasma or more than $10^7$ virus copies/mL urine in one sample combined with an increase in serum creatinine level that was not attributable to other causes and/or (iii) more than $10^3$ virus copies/mL plasma and more than $10^6$ virus copies/mL urine combined with an increase in serum creatinine level and responsiveness to reduction of immunosuppressive regimens and/or (iv) biopsy-proven PyVAN. The remaining 24 transplant recipients did not fulfill any of these criteria (RTx-BKPyV negative). The study was approved by the local ethics committee. All participants and in the case of children their parents gave informed consent.

### *Quantitation and phenotypic analysis of BKPyV-specific CD4 T cells*

Antigen-specific T cells from heparinized whole blood were stimulated for 6 h as described before (23,24), except that a mixture of overlapping 15-mer peptides derived from the BKPyV large T- and VP1-protein (Swiss-Prot ID P14999, 170 peptides and Swiss-Prot ID 14996, 88 peptides, respectively; JPT, Berlin, Germany; equal concentration of each peptide) were used as stimuli. In detail, the total amount of all peptides was dissolved in dimethylsulfoxide (DMSO) as recommended by the manufacturer, combined and further diluted with phosphate buffered saline (PBS) to a final concentration of 0.53 mg total peptides, 0.6% DMSO and 7.6% PBS/mL whole blood. As negative and positive controls, respectively, cells were stimulated with respective amounts of solvent (PBS and DMSO), irrelevant peptides derived from human actin (Swiss-Prot ID P68133, 92 peptides; JPT) or 2.5 μg/mL *Staphylococcus aureus* enterotoxin B (SEB; Sigma, Deisenhofen, Germany). Stimulations were carried out for a total of 6 h in the presence

**Table 1:** Characteristics of immunocompetent controls, hemodialysis patients and renal transplant recipients without (BKPyV negative) or with clinically relevant BKPyV-replication (BKPyV positive)

| | | | Transplant recipients | | |
|---|---|---|---|---|---|
| | Controls | Hemodialysis patients | BKPyV negative | BKPyV positive | p-Value |
| Number of individuals | 23 | 25 | 24 | 14 | |
| Age (years, mean ± SD) | 56.3 ± 16.0 | 61.3 ± 18.0 | 51.4 ± 15.8 | 61.8 ± 10.8 | 0.111 |
| Females (n, %) | 12 (52.2%) | 16 (64.0%) | 12 (50.0%) | 1 (7.1%) | 0.007 |
| Leukocyte counts/μL (mean ± SD) | 6957 ± 1913 | 6673 ± 1514 | 8722 ± 3890 | 7581 ± 2106 | 0.132 |
| % Lymphocytes (mean ± SD) | 31.8 ± 10.7 | 20.6 ± 5.7 | 22.4 ± 11.5 | 21.9 ± 11.3 | 0.003 |
| Immunosuppressive drugs | | | | | |
| IL-2R Ab; CNI (Tac/CyA); MMF; MP | | | 21 (19 Tac/2 CyA) | 12 (all Tac) | |
| IL-2R Ab; Tac; Aza; MP | | | 2 | 1 | |
| IL-2R Ab; CyA; MP | | | 1 | 1 | |
| Type of transplant | | | | | |
| Deceased donor | | | 22 | 12 | |
| Living donor | | | 2 | 2 | |
| Time since transplantation (months, median [IQR]) | n.a. | n.a. | 13.7 (35.5) | 10.3 (22.1) | 0.282 |
| Time since clinically relevant BKPyV-replication (months, median [IQR]) | n.a. | n.a. | n.a. | 8.5 (22.0) | |

BKPyV, BK polyomavirus; n.a., not applicable; SD, standard deviation; IQR, interquartile range; IL-2R Ab, interleukin-2 receptor antibody; CNI, calcineurin inhibitor; Tac, tacrolimus; CyA, cyclosporine A; MMF, mycophenolate mofetile; MP, methylprednisolone; Aza, azathioprine.

of 1 μg/mL anti-CD28 and anti-CD49d (BD, Heidelberg, Germany) and 10 μg/mL of brefeldin A (Sigma) were added for the last 4 h. Stimulated cells were treated with 2 mM EDTA for 15 min to disrupt cell–cell interactions, fixed and immunostained under permeabilizing conditions using titered amounts of anti-CD4, anti-CD69, anti-interferon-γ (IFNγ), anti-IL-2 and anti-tumor necrosis factor-α (TNF-α) (all from BD). CD4 T cells were analyzed on a FACS Canto II using FACS-Diva-software V6.1.3 (BD). For analyses of antigen-specific CD4 T cells, frequencies of activated CD4 T cells after stimulation with the antigen were subtracted for the negative control. For cytokine profiling, BKPyV-specific CD4 T cells in each individual were subdivided according to their cytokine expression, and the percentages of triple, double and single cytokine-expressing CD4 T cells were quantified. To ensure robust statistical analysis of T cell subpopulations, only samples with BKPyV-specific T cell frequencies above detection limit and a minimum of 20 cytokine-expressing cells were included.

#### *Quantitation of BKPyV-specific antibody responses*

BKPyV-specific IgG- and IgM-levels were quantified at a serum dilution of 1:400 using an enzyme-linked immunosorbent assay on the basis of virus-like particles as described before (2). The optical density at 492 nm ($OD_{492}$) obtained with PBS alone was taken as background and subtracted. The cut-off defining a positive serologic response was $OD_{492} = 0.110$ for BKPyV-specific IgG and IgM as established before (2,9,25,26).

#### *Analysis and quantitation of antigen-specific proliferation*

Antigen-specific proliferation was analyzed using carboxyfluorescein diacetate succinimidyl ester (CFSE) assay. Isolated peripheral blood mononuclear cells (PBMC) were stained with 5 μM CFSE according to the manufacturer's instruction (Life Technologies, Darmstadt, Germany). Thereafter, 600 000 PBMC/well (96-well format) were incubated overnight in medium (RPMI, 5% fetal calf serum [FCS], 1% glutamine, 1% penicillin/streptomycin) and stimulated as described above with BKPyV-peptides, DMSO (solvent, negative control) and SEB, respectively, in a total volume of 60 μL. The following day, cultures were supplemented with 240 μL of RPMI 5% FCS and incubated for a total of 7 days. SEB-treated cells were split 1:2 at Day 4. Prior to further staining, cells were treated with 2 mM EDTA for 15 min to disrupt cell–cell interactions, then co-stained using anti-CD3, anti-CD4 and anti-CD8 antibodies (all from BD) and analyzed using flow cytometry.

#### *Statistical analysis*

Statistical analysis was carried out using GraphPad Prism V5.04 (GraphPad, San Diego, CA). Comparison of continuous variables (BKPyV-specific CD4 T cell frequencies, antibody levels, and leukocyte counts and percentage of lymphocytes) from more than two groups was performed using the Friedman test for paired and the Kruskal–Wallis test for nonpaired values. Differences in age were analyzed using the one-way analysis of variance test. The chi-square test was used to analyze differences in sex. Correlation between BKPyV-specific CD4 T cell frequencies and antibody levels was done using Spearman's correlation.

## Results

### *BKPyV-specific CD4 T cells are detectable in whole blood samples of immunocompetent individuals*

Frequencies of CD4 T cells specific for BKPyV-VP1 and/or large T antigen were assessed directly from whole blood samples of a total of 122 healthy individuals between 1 and 84 years of age. An example of a 24-year-old individual is shown in Figure 1A. Antigen-specific CD4 T cells were identified using flow cytometry based on the induction of the activation marker CD69 and the cytokine IFNγ after specific stimulation. Stimulation with the solvent (DMSO) and the SEB served as negative and positive controls, respectively. The results for all 122 individuals are depicted in Figure 1B. Although frequencies were generally low, activated CD4 T cells were detectable after stimulation with

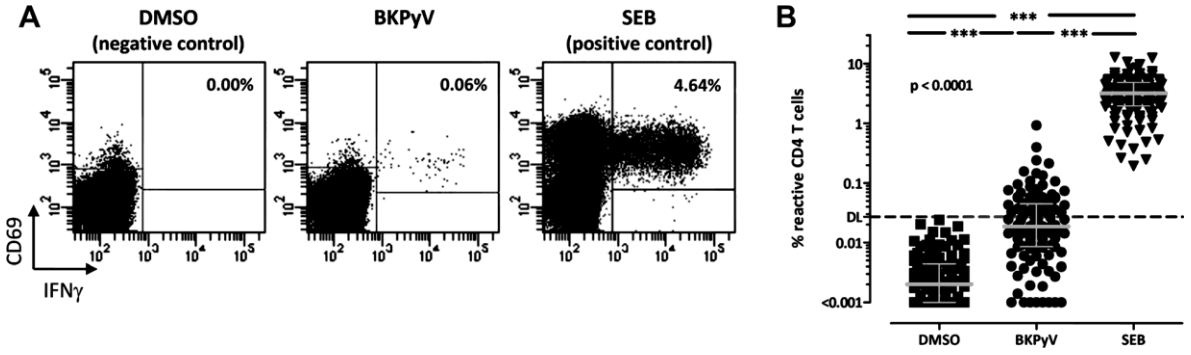


**Figure 1: Detection of BKPyV-specific CD4 T cells in blood samples of immunocompetent individuals.** Whole blood samples were stimulated with solvent (DMSO, negative control), overlapping 15-mer peptides derived from the BKPyV large T- and VP1-protein (BKPyV) and *Staphylococcus aureus* enterotoxin B (SEB; positive control), respectively, and reactive CD4 T cells (CD69+/IFNγ+) were analyzed using flow cytometry. Based on a pilot series of experiments, we did not have any evidence of a substantial induction of BKPyV-specific CD8 T cells after short-term stimulation and we have therefore restricted analysis of cytokine-producing cells to the CD4 T cell population. (A) Typical dotplots of one representative individual are shown. Numbers indicate the percentage of reactive CD4 T cells. (B) Frequencies of antigen-reactive CD4 T cells of all tested immunocompetent control persons (n = 122) are depicted. Bars indicate median values and IQR; the dashed line represents the detection limit of 0.027% BKPyV-specific CD4 T cells calculated based on the frequency distribution of all negative control stimulations. A similar detection limit (0.026%) was derived from a receiver operator characteristic analysis of 11 BKPyV-seronegative and 13-seropositive children below 10 years of age. Statistical analysis was performed using the Friedman test with Dunn's posttest. BKPyV, BK polyomavirus; DMSO, dimethylsulfoxide; IFNγ, interferon-γ; IQR, interquartile range.

BKPyV-peptides (median 0.018%, interquartile range [IQR] 0.036%, IFNγ-producing CD69+CD4 T cells) whereas the solvent alone did not induce any relevant response (median 0.002%, IQR 0.003%). In addition, a series of 12 samples showed that median T cell frequencies after stimulation with irrelevant peptides derived from human actin were rather low (0.0036%, IQR 0.0086%) and in the same range as with DMSO alone (0.0013%, IQR 0.0026%). As shown by the clear reactivity toward SEB (median 3.184%, IQR 2.867%), T cells from all individuals were generally able to produce IFNγ during the 6-h stimulation period. To more precisely assign the frequencies of CD4 T cells specifically reacting toward BKPyV, results obtained after stimulation with the BKPyV-peptides were corrected for the background values of the corresponding negative control. The frequency distribution from the negative control stimulation of all 122 individuals was also used to determine a detection limit of 0.027% BKPyV-specific CD4 T cells that enabled discrimination of background reactivities from a truly positive result. Interestingly, approximately one-third of all tested persons (42/122, 34.4%) showed BKPyV-specific CD4 T cell frequencies above this detection limit, indicating a clearly detectable BKPyV-specific cellular immune response. These results show that BKPyV-specific CD4 T cells may be detected directly from whole blood samples of immunocompetent healthy individuals. Moreover, as the solvent generally did not induce any unspecific reactivity, BKPyV-specific CD4 T cells are even detectable at lower frequencies.

### *BKPyV-specific cellular and humoral immunity is age-dependent and reaches a maximum between the age of 20 and 30 years*

In order to investigate potential variations of BKPyV-specific immunity with age in healthy individuals, frequencies of activated CD4 T cells after stimulation with BKPyV-peptides or SEB as well as levels of BKPyV-specific IgG and IgM antibodies were analyzed in different age groups (Figure 2). As expected, median frequencies of BKPyV-specific CD4 T cells were low in the youngest age group (0.010%, IQR 0.027% in children between 0 and 10 years) and were below detection limit in most samples. Thereafter, T cell levels steadily increased (median 0.018%, IQR 0.033%, in the age group between 10 and 20 years; Figure 2A, left panel), and reached a maximum between 20 and 30 years of age (median 0.042%, IQR 0.050%) with 68.4% of individuals above detection limit. In individuals above 30 years of age, median T cell frequencies decreased again. By contrast, activated CD4 T cells after polyclonal stimulation with SEB were detectable in all individuals (Figure 2A, right panel). Of note, SEB-reactive T cells were lowest in young children between 0 and 10 years (median 1.388%, IQR 1.958%) whereas there were no significant differences in T cell frequencies in the older age groups. As with CD4 T cell levels, BKPyV-specific IgG levels showed an age-dependent increase reaching maximum levels between 20 and 30 years (Figure 2B, left panel), and a strong correlation of the individual BKPyV-specific IgG levels and CD4 T cell frequencies was detected ($p < 0.0001$, $r = 0.5458$; Figure 2C). Of note, only 4 out of 122 individuals were seronegative but T cell positive including three adolescents who were all close to the detection limits. There were no significant differences in IgM levels between age groups and most samples had levels below detection limit (Figure 2B, right panel). Taken together, BKPyV-specific cellular and humoral immunity is highly prevalent in young individuals, reaches its maximum in young adults and then declines with increasing temporal distance from BKPyV primary infection.

### *BKPyV-specific cellular immune responses in immunocompetent individuals are dominated by multifunctional T cells*

To gain insight into the functionality of BKPyV-specific immune cells, cytokine expression profiles and proliferative activity were analyzed in more detail. Polyfunctional BKPyV-specific CD4 T cells were characterized by the combined expression of IFNγ, IL-2 and TNFα. In addition, the percentage of IL-2 positive or negative single or double cytokine-positive subpopulations were quantified (Figure 3). The majority of BKPyV-specific CD4 T cells were producing all three cytokines (62.3%; Figure 3B and C, left panels). The remaining cells showed reduced functionality with IL-2 negative (22.5%) or IL-2 positive (15.2%) phenotypes. In contrast, no dominant subpopulation was identified after polyclonal stimulation (Figure 3B and C, right panels). Unlike frequencies of the BKPyV-specific CD4 T cells, the cytokine expression profiles did not show any age-dependent differences (data not shown).

In addition to their capacity to produce cytokines, the proliferative activity of BKPyV-specific T cells was analyzed after 7 days of proliferation using CFSE. Representative dotplots of proliferating BKPyV-specific T cells with respective negative and positive controls are shown in Figure 4A. Analysis of BKPyV-induced proliferation in samples of 29 healthy individuals between 5 and 84 years revealed that the median percentage of proliferated CD4 T cells was highest between 20 and 40 years of age (3.89%, IQR 7.46%), whereas frequencies of proliferated cells were low in most samples from children and older adults (median 0.14%, IQR 4.95% and median 0.67%, IQR 4.44%, respectively; $p = 0.03$; Figure 4B, left panel). Proliferative activity of BKPyV-specific CD8 T cells was generally lower and did not differ significantly between the three age groups ($p = 0.39$; Figure 4C, left panel). Most CD4 and CD8 T cells were able to proliferate after polyclonal stimulation (Figure 4B and C, right panels). In general, there was a strong correlation between the proliferation of BKPyV-specific CD4 and CD8 T cells (Figure 4D, $r = 0.7334$, $p < 0.0001$). In summary, BKPyV-specific CD4 T cells in immunocompetent individuals show proliferative activity and are predominantly multifunctional in their cytokine expression profile.

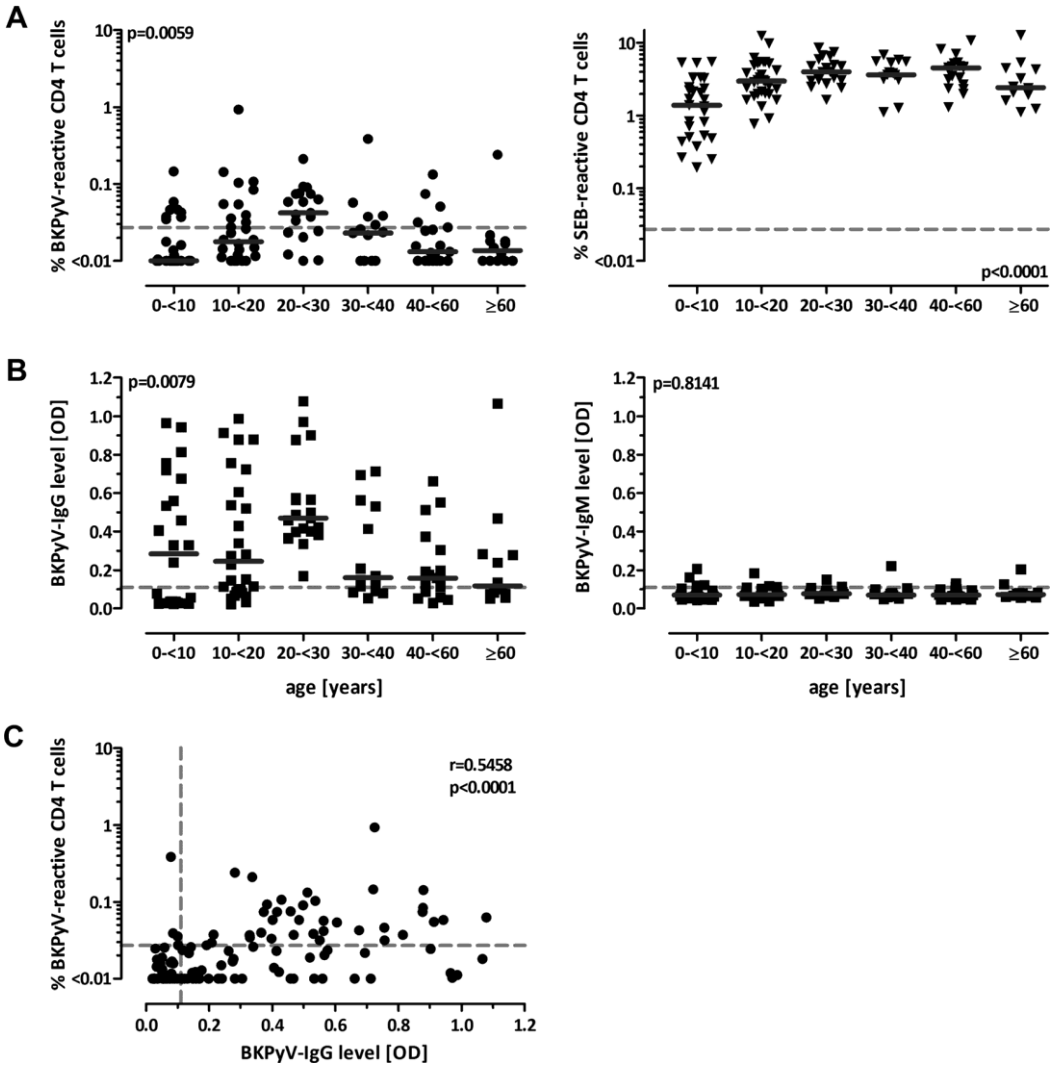


**Figure 2: BKPyV-specific cellular and humoral immunity shows age-dependent differences.** Scatterplots depict (A) frequencies of reactive CD4 T cells (CD69+/IFNγ+) after stimulation with BKPyV-peptides (left panel) or *Staphylococcus aureus* enterotoxin B (SEB; right panel) as well as (B) BKPyV-specific IgG (left panel) and IgM levels (right panel) in different age groups of immunocompetent individuals (n = 122 for cellular [A]; A and n = 116 for humoral immunity [B]). The correlation of BKPyV-specific CD4 T cell frequencies and IgG levels of all individuals where both tests were available (n = 116) is shown in (C). Dashed lines represent the detection limits for positive test results. Bars indicate median values. Statistical significance was assessed using Kruskal–Wallis test for (A) and (B); p- and r-values in (C) were calculated using Spearman correlation. Antibody levels are expressed as optical density at 492 nm ($OD_{492}$). BKPyV, BK polyomavirus; IFNγ, interferon-γ.

### *Clinically relevant BKPyV-replication events in RTx recipients are associated with a significant change in T cell functionality*

To assess potential changes in BKPyV-specific immunity related to BKPyV-associated complications, T cells and antibodies were characterized in 38 RTx recipients with (RTx-BKPyV positive, 13/14 males) or without confirmed clinically relevant BKPyV-replication (RTx-BKPyV negative, n = 24). Twenty-five HD patients served as pretransplant controls. BKPyV-specific CD4 T cells were found in 57.9% of all transplant recipients. This was significantly higher as compared to age-matched healthy controls (21.7%) or HD patients (28.0%, p = 0.017). Interestingly, frequencies of BKPyV-specific CD4 T cells were significantly higher in transplant recipients with clinically relevant BKPyV-replication (median 0.105%, IQR 0.140%) whereas respective T cell frequencies of age-matched healthy controls (median 0.016%, IQR 0.017%), HD patients (median 0.011%, IQR 0.031%) and transplant recipients without BKPyV-associated complications (median 0.014%, IQR

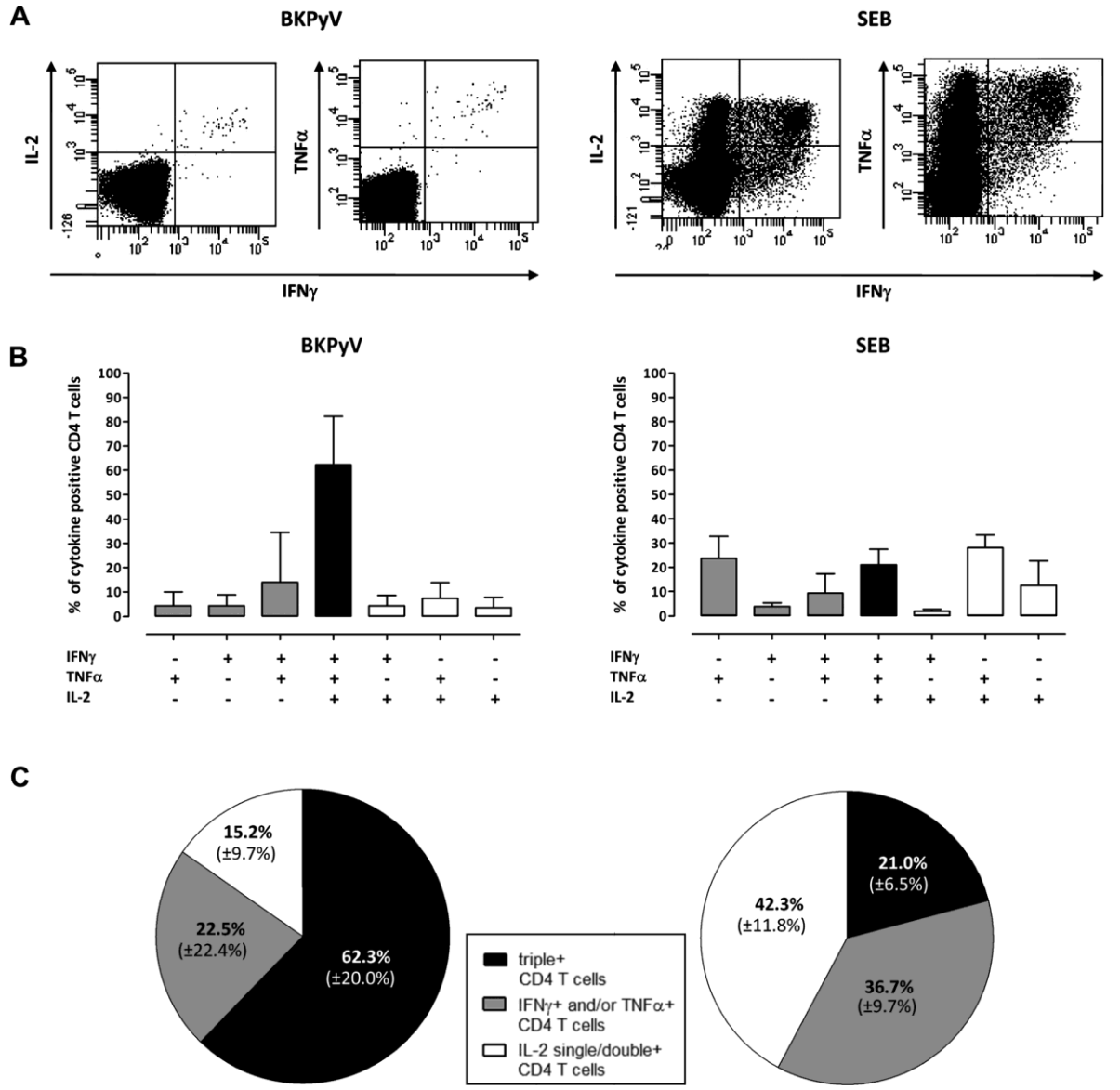


**Figure 3: BKPyV-specific CD4 T cells of immunocompetent individuals are predominantly co-expressing multiple cytokines.** The contribution of IFNγ-, IL-2- and TNFα-expressing CD4 T cells after stimulation with BKPyV-peptides (left panels) or *Staphylococcus aureus* enterotoxin B (SEB; right panels) is shown. (A) Typical dotplots of cytokine-expressing CD4 T cells of one representative individual. (B) Cytokine-expressing CD4 T cells are divided according to their expression of IFNγ, IL-2 and TNFα. This analysis was performed in all samples where at least 20 cytokine-producing CD4 T cells were detectable (n = 24). Bars represent subpopulations of single-, double- or triple-cytokine-producing cells among all BKPyV- or SEB-reactive CD4 T cells including means and SDs. (C) Subpopulations of cytokine-positive CD4 T cells are grouped according to their functional profile; cells expressing all three cytokines are depicted in black, cells lacking IL-2 expression in gray and cells expressing IL-2 alone or together with TNFα or IFNγ in white. Numbers indicate means and SDs of the respective subpopulations. BKPyV, BK polyomavirus; IFNγ, interferon-γ; TNF-α, tumor necrosis factor-α.

0.041%) were below detection limit (p = 0.0002; Figure 5A, left panel). In contrast, no differences were observed for SEB-reactive CD4 T cells (Figure 5A, right panel). As with CD4 T cell frequencies, levels of BKPyV-specific IgG and, to a lesser extent, IgM antibodies were significantly higher in the transplant patient group with recent BKPyV-episodes (p = 0.0019 for IgG, p = 0.0309 for IgM; Figure 5B).

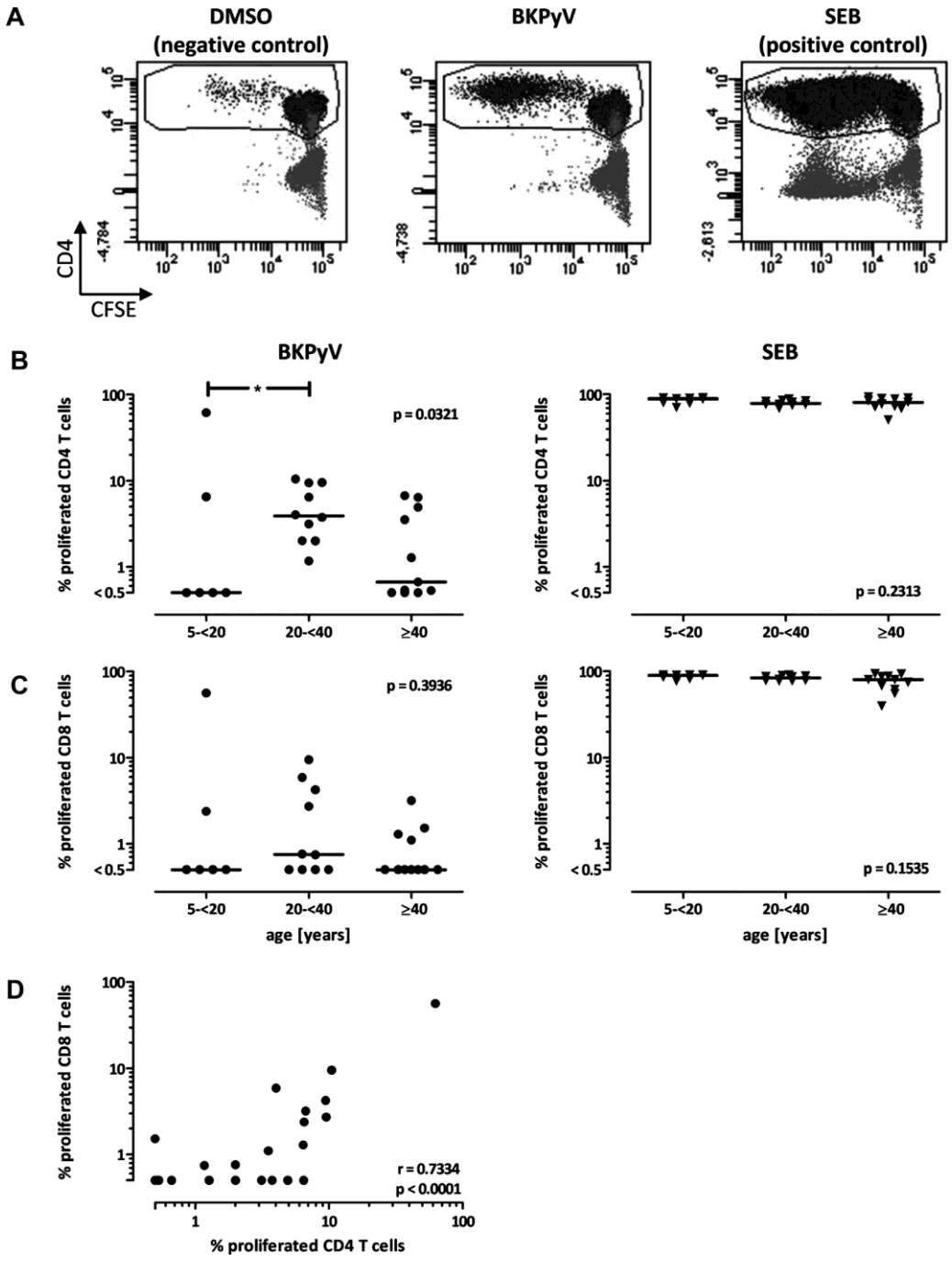


**Figure 4: Proliferative activity of BKPyV-specific T cells is highest in young adults.** Isolated PBMCs were labeled with the fluorescent dye carboxyfluorescein succinimidyl ester (CFSE) and stimulated with solvent (DMSO, negative control), BKPyV-peptides and the *Staphylococcus aureus* enterotoxin B (SEB; positive control), respectively. After 7 days of culture, proliferated T cells were quantified using flow cytometry. Typical dotplots of one representative individual are shown in (A) gated for CD4 T cells. Frequencies of proliferated CD4 (B) and CD8 (C) T cells after stimulation with BKPyV-peptides (left panel) or SEB (right panel) of the tested immunocompetent controls (n = 29) are depicted in three different age groups. Bars indicate median values. Statistical comparison of the different age groups was performed using the Kruskal–Wallis test with Dunn's posttest. Significant differences in posttest were indicated (*$p < 0.05$). Correlation of the proliferation activity of BKPyV-specific CD4 and CD8 T cells is shown in (D). The p- and r-values were calculated using Spearman's correlation. BKPyV, BK polyomavirus; DMSO, dimethylsulfoxide; PBMC, peripheral blood mononuclear cells.

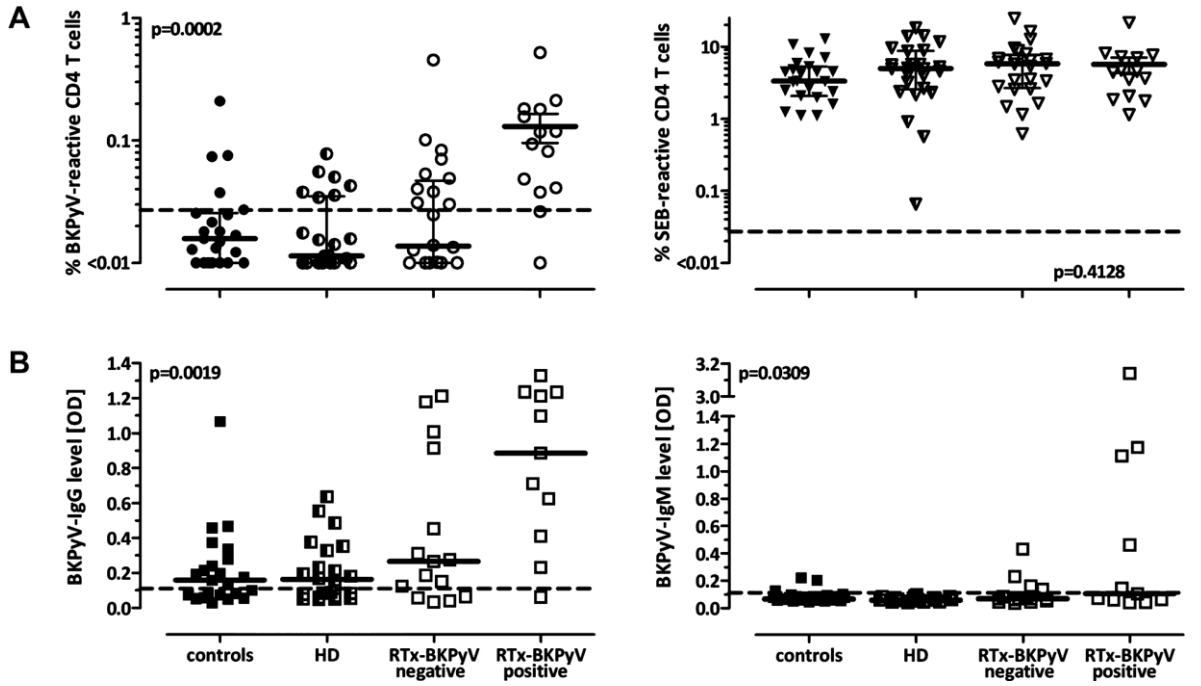


**Figure 5: Frequencies of BKPyV-specific immune responses strongly correlate with BKPyV-replication episodes in renal transplant (RTx) recipients.** BKPyV-specific immune responses were compared in age-matched cohorts of immunocompetent individuals (controls, n = 23), hemodialysis patients (HD; n = 25 [A] and 22 [B]) and RTx recipients either without (RTx-BKPyV negative, n = 24 [A]; A and 15 [B]) or with clinically relevant BKPyV-replication (RTx-BKPyV positive, n = 14 [A] and 11 [B]). Patients with clinically relevant BKPyV-replication had median (IQR) serum creatinine of 2.4 mg/dL (1.2), and median (IQR) peak viral load of 15 000 copies/mL (40 163) in plasma and $1.3 \times 10^9$ copies/mL ($4.2 \times 10^9$) in urine. Scatterplots depict (A) frequencies of reactive CD4 T cells after stimulation with BKPyV-antigen (left panel) or *Staphylococcus aureus* enterotoxin B (SEB; right panel) as well as (B) BKPyV-specific IgG (left panel) and IgM levels (right panel). Dashed lines represent the detection limits for positive test results. Bars indicate median values. Antibody levels are expressed as optical density at 492 nm ($OD_{492}$). Statistical significance was assessed using the Kruskal–Wallis test. BKPyV, BK polyomavirus; IQR, interquartile range.

When assessing the proliferative activity of BKPyV-specific T cells in the different patient and control groups, proliferation was measurable, although transplant patients received antiproliferative drugs as part of their immunosuppressive regimen. A higher percentage of proliferating CD4 and CD8 T cells was observed in RTx-BKPyV positive patients, although this did not reach statistical significance for CD4 T cells (Figure 6A and B). To assess the effect of BKPyV-reactivation episodes on the functionality of BKPyV-specific cells, cytokine expression profiles were characterized in all individuals with at least 20 cytokine-producing cells after whole blood stimulation with BKPyV-peptides. As shown in Figure 6C, patients with BKPyV-complications showed a loss of polyfunctional BKPyV-specific CD4 T cells producing all three cytokines, whereas respective profiles of SEB-induced cells were unaffected (Figure 6C, lower panel). When comparing the percentages of triple-cytokine-positive BKPyV-specific CD4 T cells, significant differences were found between the four groups ($p = 0.009$). The decrease in triple-positive cells was associated with a concomitant increase in cytokine-single positivity ($p = 0.002$).

Taken together, BKPyV-replication events in adult RTx recipients are associated with profound changes in BKPyV-specific immunity that are characterized by higher levels of BKPyV-specific antibodies and T cells with proliferative activity and lower levels of polyfunctional T cells.

## Discussion

BKPyV-replication is one of the main infectious complications in RTx recipients that causes premature decline in allograft function in more than 50% of cases (4–6). By contrast, BKPyV is not known to cause significant illness in immunocompetent individuals, although reactivation with low-level viruria may occur intermittently (21,22). In this study, we have performed a detailed quantitative and functional characterization of BKPyV-specific T cell responses in a large cohort of immunocompetent individuals across a wide age range and have shown that maximum levels of specific CD4 T cells occur between the ages of 20 and 30 years, and thereafter progressively decrease to below detection limit in most of the older age groups. In line

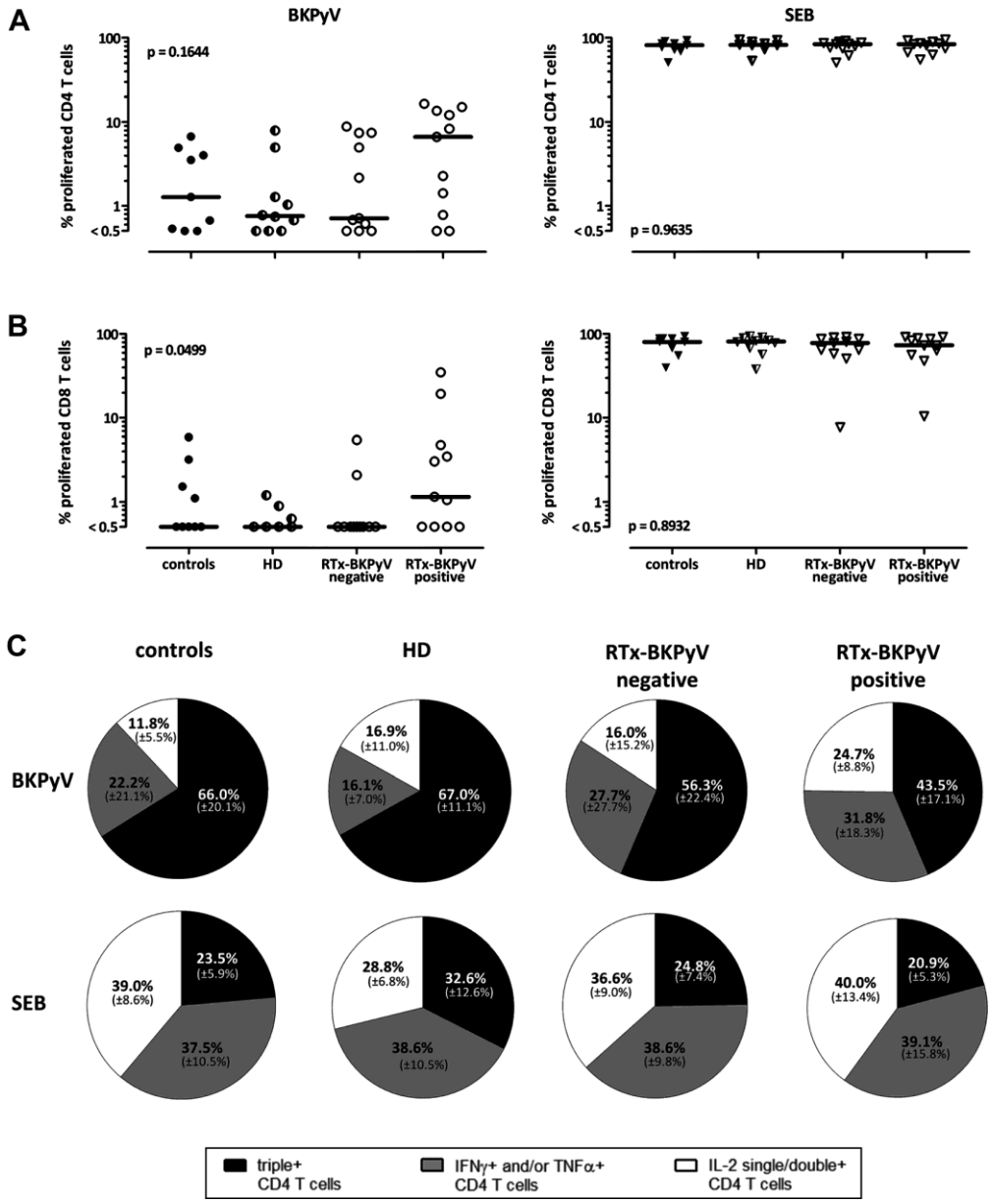


**Figure 6: Functional properties of BKPyV-specific T cells are associated with clinically relevant BKPyV-replication events.** Proliferative activity as well as cytokine expression profiles after whole blood stimulation was assessed in age-matched cohorts of immunocompetent individuals (controls), hemodialysis patients (HD) and renal transplant (RTx) recipients either without (RTx-BKPyV negative) or with clinically relevant BKPyV-replication (RTx-BKPyV positive). Frequencies of proliferated CD4 (A) and CD8 (B) T cells after stimulation with BKPyV-antigen (left panel) or SEB (right panel) are depicted for the tested individuals in the different groups (n = 9 [controls], 10 [HD], 11 [RTx-BKPyV negative], and 11 [RTx-BKPyV positive]). Bars indicate median values. (C) Pie charts represent the cytokine-expressing CD4 T cells after whole blood stimulation, divided into three groups according to their expression of IFNγ, IL-2 and TNFα. Cells expressing all three cytokines are depicted in black, cells with reduced cytokine expression but expressing IL-2 in white and IL-2 negative cells in gray. This analysis was performed in all samples where at least 20 cytokine-producing CD4 T cells were detectable (n = 17 [controls], 5 [HD], 8 [RTx-BKPyV negative] and 12 [RTx-BKPyV positive]). Percentages of all cytokine-producing CD4 T cells are shown as means of all tested individuals per group. Numbers indicate means and SDs. Statistical significance was assessed using the Kruskal–Wallis test with Dunn's posttest. The posttest detected no significant differences between groups. BKPyV, BK polyomavirus; IFNγ, interferon-γ; SEB, *Staphylococcus aureus* enterotoxin B; TNF-α, tumor necrosis factor-α.

with previous observations (1,2), this is largely paralleled by the increase and subsequent decline in BKPyV-specific antibodies. These results are of interest since they possibly relate to the increased vulnerability of older kidney transplant recipients to BKPyV-replication and disease that have been observed in large single-center studies (27), registry analyses (28) and, most recently, in a prospectively, randomized controlled clinical trial comparing tacrolimus versus cyclosporine-based maintenance immunosuppression (29). Conversely, the overall better responses of pediatric transplant recipients to reducing immunosuppression may be related to a higher number of BKPyV-specific T cells at transplantation and their age-dependent better proliferative expansion capacity. However, this may not apply to the rather rare BKPyV-negative patient experiencing primary infection posttransplant. We further demonstrate that RTx recipients with clinically relevant BKPyV-associated complications have significantly higher frequencies of specific CD4 T cells and antibodies as compared to age-matched healthy controls, HD patients and RTx recipients without BKPyV-associated complications. Notably, however, whereas BKPyV-specific CD4 T cells of immunocompetent individuals exhibit a predominantly multifunctional phenotype characterized by the expression of several cytokines in response to specific stimulation, kidney transplant patients with BKPyV-associated complications experience a significant loss of multifunctional CD4 T cells, which emphasizes the particular need for intact T cell functionality to control clinically relevant BKPyV-replication.

The age dependence in humoral immunity is in line with previous studies in either children or adults that show a low prevalence of BKPyV-specific antibodies in children (9,25,30) whereas in adults, maximum IgG levels were found in individuals between 20 and 40 years and decrease thereafter (1,2). In addition, association of BKPyV-replication with high titers of BKPyV-specific IgG and in particular IgM levels in RTx recipients has been reported earlier and the increase in mean antibody levels correlated with BKPyV-load posttransplant (9,11,13,31). In terms of cellular immunity, quantitative measures of frequencies and multifunctionality as well as cut-offs are not directly comparable as studies are heterogeneous in study design, readout, sample material, stimuli, stimulation time or investigated subgroups of patients (10). Nevertheless, as with antibodies, it appears that viral replication is associated with the induction of significant amounts of BKPyV-specific T cells (9,11,32). Moreover, there is evidence that T cells induced in transplant recipients seem to be predominantly directed toward structural antigens (VP1–3) (11,32). In these patients, T cell induction may have required higher levels of local or systemic viral replication than in immunocompetent individuals, where viruria only occurs intermittently at a low level (21,22), and where specific T cells gradually decreased to below detection limit with increasing time since primary infection. Thus, the level of specific immunity may directly mirror viral exposure through the extent of viral replication. As BKPyV has a tropism for renal tubular epithelial cells and uses the host polymerase for replication (4), viral replication should be directly linked to the regenerative activity of these cells. In immunocompetent individuals, this activity should be highest in the period of growth during childhood and throughout adolescence. In adults, an acute need for regeneration of tubular epithelial cells frequently arises in the context of ischemia and reperfusion injury following renal transplantation. This may lead to a concomitant increase in viral replication with potential systemic spread, especially in the presence of immunosuppressive drugs. As with BKPyV-specific immunity, an age-dependent decrease in antigen-specific T cell frequencies has also been observed with other persistent pathogens such as the varicella zoster virus (33,34), where subsequent virus exposure of elderly individuals by zoster vaccination led to the reinduction of a significant T cell response (34). Thus, challenge with the virus is needed to induce and maintain significant amounts of both specific T cell and humoral immune responses.

Although the frequencies of BKPyV-specific T cells are highest in temporal association with virus exposure in both young healthy individuals and immunocompromized patients with BKPyV-complications, their functionality was significantly different in the two groups. A significant loss of triple-cytokine expressing cells and a concomitant increase in single-cytokine positivity were only detected in RTx recipients with BKPyV-associated complications. Multifunctionality of T cells is known to be important for protection from a variety of clinically relevant pathogens such as *Mycobacterium tuberculosis*, influenza virus, human immunodeficiency virus, hepatitis C virus and cytomegalovirus (CMV) (19,20,35–39). In addition, a loss in multifunctionality is associated with cell-surface markers of exhaustion, although phenotypic analyses of exhaustion have not yet been performed in patients with BKPyV-associated complications. In our study, the loss in functionality appears to be specific for BKPyV-reactive T cells, as the functionality of SEB-reactive T cells, which include cells with other specificities, was not altered. In the case of BKPyV-infection, it is presently unclear whether functional impairment of specific T cells is a cause or an effect of increased BKPyV-replication. In patients with ongoing CMV replication, an anergic T cell phenotype characterized by restricted functionality and elevated expression of the inhibitory molecule programmed death-1 can be observed even before detectable viremia (19,40), which may imply a rather causative role of increased viremia. Nevertheless, impaired functionality of CMV-specific T cells in transplant recipients may also occur for a prolonged period even after virus control (19). In line with observations by others (12), this also seems to be the case for BKPyV-specific T cells. One might speculate that the quantitative increase of specific T cells in patients with BKPyV-related complications may act as a mechanism to compensate their reduced functionality. Indeed, a quantitative increase in BKPyV-specific cellular immunity in

response to reduction in immunosuppression, which is still the mainstay to effectively treat BKPyV-complications (29,41–42), was associated with control of viral replication in many cases (7,9,43).

A limitation of this study is its cross-sectional design. Thus, the data do not allow any conclusions to be drawn on potential changes in functionality prior to viremia or as an indicator for virus control thereafter. The clinical use of multifunctionality as a monitoring tool to guide therapeutic interventions is hampered by the fact that frequencies of BKPyV-specific T cells are generally low before and during the first weeks after transplantation. Therefore, unlike CMV-infection, where the frequencies of antigen-specific T cells are higher (19), it seems rather less feasible to use BKPyV-specific T cells as a parameter to predict BKPyV-complications prior to viremia. In contrast, as BKPyV-specific T cell levels increase in temporal association with virus replication and/or reduction in immunosuppression, cell numbers are sufficiently high to use loss of functionality as a correlate of impaired control. This is supported by the recent observation that high numbers of polyfunctional BKPyV-specific T cells were found in patients with a history of rapid BKPyV-clearance (12). Thus, cytokine profiling would enable immunological monitoring of viremic patients at risk for PyVAN. This would be of particular clinical value, as reduction of immunosuppression is recommended in all patients with confirmed BKPyV-viremia, although only a minority of these patients effectively proceed to PyVAN (42,44). Decreasing the number of patients who are targeted for reduction of immunosuppression would also minimize the overall risk for acute graft rejection. In technical terms, the flow-cytometric whole-blood assay is readily suitable for clinical use. Nevertheless, future studies in a longitudinal setting are needed to refine the areas of application as a parameter to distinguish patients with prompt resolution of viremia/viruria from those with delayed or no response and hence to early identify patients at high risk for PyVAN.

In summary, temporal association with BKPyV primary infection in young immunocompetent adults and periods of BKPyV-reactivation in RTx recipients is associated with highest frequencies of BKPyV-specific T cells. Conversely, older transplant recipients may be at increased risk for BKPyV-replication and disease due to declining cellular immunity. Despite quantitative similarities, young adults and patients with complications differ in functional characteristics of BKPyV-specific immunity. Thus, cytokine profiling may hold promise for the future as a tool for discrimination of immunologically controlled BKPyV-infection from uncontrolled virus replication and hence for predicting the risk of developing PyVAN.

## Acknowledgments

The authors acknowledge excellent technical assistance from Candida Guckelmus and Katharina Schmitt. Financial support was provided by grants from ''Zentrale Forschungskommission der Universität des Saarlandes,'' Novartis and Pfizer Pharma GmbH (to MS, TS, and US). The funding sources did not have any role in the study design, or in the acquisition or interpretation of the data.

## Disclosure

The authors of this manuscript have no conflicts of interest to disclose as described by the *American Journal of Transplantation*.

## References

1. Knowles WA, Pipkin P, Andrews N, et al. Population-based study of antibody to the human polyomaviruses BKV and JCV and the simian polyomavirus SV40. J Med Virol 2003; 71: 115–123.
2. Egli A, Infanti L, Dumoulin A, et al. Prevalence of polyomavirus BK and JC infection and replication in 400 healthy blood donors. J Infect Dis 2009; 199: 837–846.
3. Chesters PM, Heritage J, McCance DJ. Persistence of DNA sequences of BK virus and JC virus in normal human tissues and in diseased tissues. J Infect Dis 1983; 147: 676–684.
4. Hirsch HH, Steiger J. Polyomavirus BK. Lancet Infect Dis 2003; 3: 611–623.
5. Hirsch HH, Brennan DC, Drachenberg CB, et al. Polyomavirus-associated nephropathy in renal transplantation: Interdisciplinary analyses and recommendations. Transplantation 2005; 79: 1277–1286.
6. Vasudev B, Hariharan S, Hussain SA, Zhu YR, Bresnahan BA, Cohen EP. BK virus nephritis: Risk factors, timing, and outcome in renal transplant recipients. Kidney Int 2005; 68: 1834–1839.
7. Binggeli S, Egli A, Schaub S, et al. Polyomavirus BK-specific cellular immune response to VP1 and large T-antigen in kidney transplant recipients. Am J Transplant 2007; 7: 1131–1139.
8. Comoli P, Binggeli S, Ginevri F, Hirsch HH. Polyomavirus-associated nephropathy: Update on BK virus-specific immunity. Transpl Infect Dis 2006; 8: 86–94.
9. Ginevri F, Azzi A, Hirsch HH, et al. Prospective monitoring of polyomavirus BK replication and impact of pre-emptive intervention in pediatric kidney recipients. Am J Transplant 2007; 7: 2727–2735.
10. Babel N, Volk HD, Reinke P. BK polyomavirus infection and nephropathy: The virus-immune system interplay. Nat Rev Nephrol 2011; 7: 399–406.
11. Schachtner T, Muller K, Stein M, et al. BK virus-specific immunity kinetics: A predictor of recovery from polyomavirus BK-associated nephropathy. Am J Transplant 2011; 11: 2443–2452.
12. Trydzenskaya H, Sattler A, Muller K, et al. Novel approach for improved assessment of phenotypic and functional characteristics of BKV-specific T-cell immunity. Transplantation 2011; 92: 1269–1277.
13. Bohl DL, Brennan DC, Ryschkewitsch C, Gaudreault-Keener M, Major EO, Storch GA. BK virus antibody titers and intensity of infections after renal transplantation. J Clin Virol 2008; 43: 184–189.
14. Leuenberger D, Andresen PA, Gosert R, et al. Human polyomavirus type 1 (BK virus) agnoprotein is abundantly expressed but immunologically ignored. Clin Vaccine Immunol 2007; 14: 959–968.
15. Chen Y, Trofe J, Gordon J, et al. Interplay of cellular and humoral immune responses against BK virus in kidney transplant recipients with polyomavirus nephropathy. J Virol 2006; 80: 3495–3505.

16. Egli A, Dumoulin A, Köhli S, Hirsch HH. Polyomavirus BK after kidney transplantation—Role of molecular and immunologic markers. Trends Transpl 2009; 3: 18.
17. Sester M, Sester U, Gärtner B, et al. Levels of virus-specific CD4 T-cells correlate with cytomegalovirus control and predict virus-induced disease after renal transplantation. Transplantation 2001; 71: 1287–1294.
18. Sester M, Gärtner BC, Sester U. Monitoring of CMV specific T-cell levels after organ transplantation. J Lab Med 2008; 32: 121–130.
19. Sester U, Presser D, Dirks J, Gärtner BC, Köhler H, Sester M. PD-1 expression and IL-2 loss of cytomegalovirus-specific T cells correlates with viremia and reversible functional anergy. Am J Transplant 2008; 8: 1486–1497.
20. Sester U, Fousse M, Dirks J, et al. Whole-blood flow-cytometric analysis of antigen-specific CD4 T-cell cytokine profiles distinguishes active tuberculosis from non-active states. PLoS ONE 2011; 6: e17813.
21. Zhong S, Zheng HY, Suzuki M, et al. Age-related urinary excretion of BK polyomavirus by nonimmunocompromised individuals. J Clin Microbiol 2007; 45: 193–198.
22. Polo C, Perez JL, Mielnichuck A, Fedele CG, Niubo J, Tenorio A. Prevalence and patterns of polyomavirus urinary excretion in immunocompetent adults and children. Clin Microbiol Infect 2004; 10: 640–644.
23. Sester U, Gärtner BC, Wilkens H, et al. Differences in CMV-specific T-cell levels and long-term susceptibility to CMV infection after kidney, heart and lung transplantation. Am J Transplant 2005; 5: 1483–1489.
24. Schmidt T, Sester M. Detection of antigen-specific T cells based on intracellular cytokine staining using flow-cytometry. Methods Mol Biol 2013; 1064: 267–274.
25. Bodaghi S, Comoli P, Bosch R, et al. Antibody responses to recombinant polyomavirus BK large T and VP1 proteins in young kidney transplant patients. J Clin Microbiol 2009; 47: 2577–2585.
26. Prelog M, Egli A, Zlamy M, Hirsch HH. JC and BK polyomavirus-specific immunoglobulin G responses in patients thymectomized in early childhood. J Clin Virol 2013; 58: 553–558.
27. Ramos E, Drachenberg CB, Portocarrero M, et al. BK virus nephropathy diagnosis and treatment: Experience at the University of Maryland Renal Transplant Program. Clin Transpl 2002; 143–153.
28. Dharnidharka VR, Cherikh WS, Abbott KC. An OPTN analysis of national registry data on treatment of BK virus allograft nephropathy in the United States. Transplantation 2009; 87: 1019–1026.
29. Hirsch HH, Vincenti F, Friman S, et al. Polyomavirus BK replication in de novo kidney transplant patients receiving tacrolimus or cyclosporine: A prospective, randomized, multicenter study. Am J Transplant 2013; 13: 136–145.
30. Ali AM, Gibson IW, Birk P, Blydt-Hansen TD. Pretransplant serologic testing to identify the risk of polyoma BK viremia in pediatric kidney transplant recipients. Pediatr Transplant 2011; 15: 827–834.
31. Randhawa PS, Gupta G, Vats A, Shapiro R, Viscidi RP. Immunoglobulin G, A, and M responses to BK virus in renal transplantation. Clin Vaccine Immunol 2006; 13: 1057–1063.
32. Schachtner T, Stein M, Sefrin A, Babel N, Reinke P. Inflammatory activation and recovering BKV-specific immunity correlate with self-limited BKV replication after renal transplantation. Transpl Int 2013; doi: 10.1111/tri.12251 [Epub ahead of print].
33. Sadaoka K, Okamoto S, Gomi Y, et al. Measurement of varicella-zoster virus (VZV)-specific cell-mediated immunity: Comparison between VZV skin test and interferon-gamma enzyme-linked immunospot assay. J Infect Dis 2008; 198: 1327–1333.
34. Weinberg A, Lazar AA, Zerbe GO, et al. Influence of age and nature of primary infection on varicella-zoster virus-specific cell-mediated immune responses. J Infect Dis 2010; 201: 1024–1030.
35. Seder RA, Darrah PA, Roederer M. T-cell quality in memory and protection: Implications for vaccine design. Nat Rev Immunol 2008; 8: 247–258.
36. Kannanganat S, Ibegbu C, Chennareddi L, Robinson HL, Amara RR. Multiple-cytokine-producing antiviral CD4 T cells are functionally superior to single-cytokine-producing cells. J Virol 2007; 81: 8468–8476.
37. Schmidt T, Dirks J, Enders M, et al. CD4+ T-cell immunity after pandemic influenza vaccination cross-reacts with seasonal antigens and functionally differs from active influenza infection. Eur J Immunol 2012; 42: 1755–1766.
38. Kannanganat S, Kapogiannis BG, Ibegbu C, et al. Human immunodeficiency virus type 1 controllers but not noncontrollers maintain CD4 T cells coexpressing three cytokines. J Virol 2007; 81: 12071–12076.
39. Semmo N, Day CL, Ward SM, et al. Preferential loss of IL-2-secreting CD4+ T helper cells in chronic HCV infection. Hepatology 2005; 41: 1019–1028.
40. Dirks J, Tas H, Schmidt T, et al. PD-1 analysis on CD28 CD27 CD4 T cells allows stimulation-independent assessment of CMV viremic episodes in transplant recipients. Am J Transplant 2013; 13: 3132–3141.
41. Hirsch HH. BK virus: Opportunity makes a pathogen. Clin Infect Dis 2005; 41: 354–360.
42. Hirsch HH, Randhawa P, Practice ASTIDCo. BK virus in solid organ transplant recipients. Am J Transplant 2009; 9 (Suppl 4): S136–S146.
43. Comoli P, Hirsch HH, Ginevri F. Cellular immune responses to BK virus. Curr Opin Organ Transplant 2008; 13: 569–574.
44. Hirsch HH, Randhawa P. BK polyomavirus in solid organ transplantation. Am J Transplant 2013; 13 (Suppl 4): 179–188.

## 5.7 Diffuse Gastrointestinal Bleeding and BK Polyomavirus Replication in a Pediatric Allogeneic Haematopoietic Stem Cell Transplant Patient

Journal of Clinical Virology 62 (2015) 72–74

Contents lists available at ScienceDirect

Journal of Clinical Virology

journal homepage: www.elsevier.com/locate/jcv

Case Report

# Diffuse gastrointestinal bleeding and BK polyomavirus replication in a pediatric allogeneic haematopoietic stem cell transplant patient

M. Koskenvuo[a,*], I. Lautenschlager[b], P. Kardas[c], E. Auvinen[b], L. Mannonen[b], P. Huttunen[a], M. Taskinen[a], K. Vettenranta[a], H.H. Hirsch[c,d]

[a] Division of Hematology-Oncology and Stem Cell Transplantation, Children's Hospital, University of Helsinki, Finland
[b] Department of Virology, Helsinki University Hospital (HUSLAB) and University of Helsinki, Helsinki, Finland
[c] Transplantation & Clinical Virology, Department Biomedicine, University of Basel, Basel, Switzerland
[d] Infectious Diseases &Hospital Epidemiology, University Hospital Basel, Basel, Switzerland

ARTICLE INFO

*Article history:*
Received 10 September 2014
Received in revised form 4 November 2014
Accepted 8 November 2014

*Keywords:*
Hemorrhagic cystitis
BK virus
Polyoma
HSCT
Gastrointestinal
Bleeding

ABSTRACT

Patients undergoing haematopoietic stem cell transplantation (HSCT) are at high risk of severe gastrointestinal bleeding caused by infections, graft versus host disease, and disturbances in haemostasis. BK polyomavirus (BKPyV) is known to cause hemorrhagic cystitis, but there is also evidence of BKV shedding in stool and its association with gastrointestinal disease. We report putative association of BKPyV replication with high plasma viral loads in a pediatric HSCT patient developing hemorrhagic cystitis and severe gastrointestinal bleeding necessitating intensive care. The observation was based on chart review and analysis of BKPyV DNA loads in plasma and urine as well as retrospective BKPyV-specific IgM and IgG measurements in weekly samples until three months post-transplant. The gastrointestinal bleeding was observed after a >100-fold increase in the plasma BKPyV loads and the start of hemorrhagic cystitis. The BKPyV-specific antibody response indicated past infection prior to transplantion, but increasing IgG titers were seen following BKPyV replication. The gastrointestinal biopsies were taken at a late stage of the episode and were no longer informative of BK polyomavirus involvement. In conclusion, gastrointestinal complications with bleeding are a significant problem after allogeneic HSCT to which viral infections including BKPyV may contribute.



## 1. Why this case is important?

Bleeding complications are a significant clinical challenge after hematopoietic stem cell transplantation (HSCT), affecting different organs and may be the result of the underlying disease, specific treatment, or associated complications. Hemorrhagic cystitis illustrates this as a paradigm [1,2] by having an early onset prior to engraftment, being attributed mainly to urotoxic conditioning, now less prevalent following a widespread use of uroprophylaxis with hyperhydration and mesna, and changes in conditioning protocols. By contrast, hemorrhagic cystitis of late onset has been attributed to viral infections, particularly by the BK polyomavirus (BKPyV), affecting 5–15% of HSCT patients at or shortly after engraftment [3]. Reported risk factors for the BKPyV-associated hemorrhagic cystitis vary, but often include myeloablative conditioning, an unrelated donors, graft-versus-host disease (GvHD) of grades II–IV, and conditioning with cyclophosphamide, busulfan and/or total body irradiation [1,4,5].

Similarly, the gastrointestinal tract is a typical site of inflammation and bleeding in HSCT patients, resulting from mucositis, infection and GvHD. Interestingly, BKPyV DNA has been detected in the stools of 40% of hospitalized children, but at relatively low levels [6]. However, higher rates of BKPyV shedding have been reported after HSCT [7]. We present a case history of a pediatric patient having received an allogeneic HSCT and suffering from a severe gastrointestinal bleeding in conjunction with BKPyV replication.

## 2. Case description

An 8-year old girl presented with a precursor B acute lymphoblastic leukemia (BCP) in April of 2008. She was treated according to the Nordic NOPHO ALL-2008 protocol in the standard risk arm [8]. At the end of the leukemia treatment (maintenance phase) in October of 2010, a marrow relapse was diagnosed. A morphologic and molecular genetic remission was achieved after treatment according to the REZ-BFM-2002 (group S3) protocol. An

* Corresponding author at: Division of Hematology-Oncology and Stem Cell Transplantation Children's Hospital, University of Helsinki, Stenbäckinkatu 11, 00029 HUS, Helsinki, Finland. Tel.: +358 50 3624430; fax: +358 9 471 74707.
*E-mail address:* minna.koskenvuo@utu.fi (M. Koskenvuo).

http://dx.doi.org/10.1016/j.jcv.2014.11.016
1386-6532/

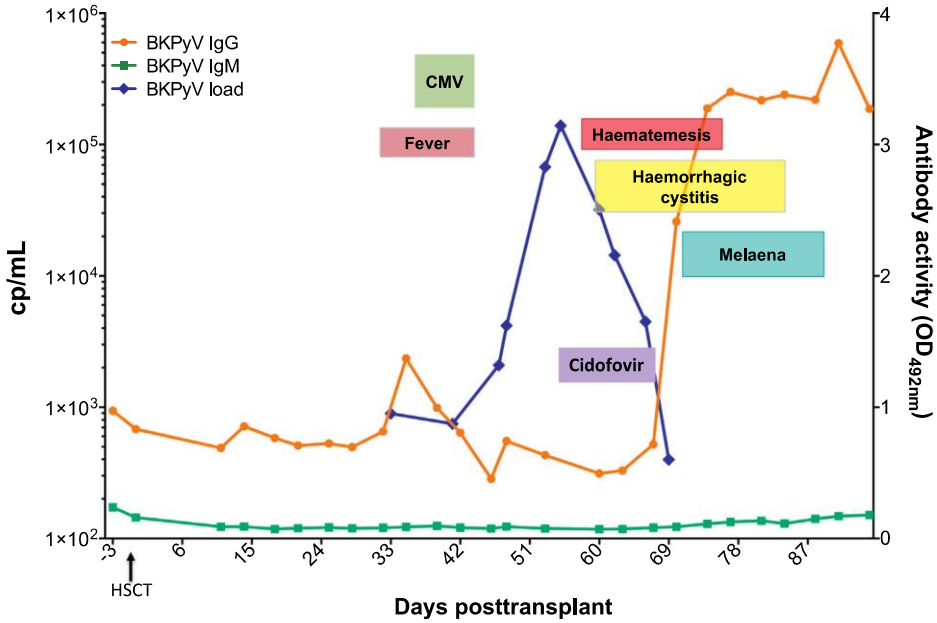


**Fig. 1.** BKPyV copy numbers in blood and IgG and IgM serological responses of the patient undergoing HSCT with haematemesis and gastrointestinal bleeding.

allogeneic HSCT was performed in March of 2011 using an HLA-matched (10/10) female unrelated donor (CMV and EBV positive). The myeloablative conditioning regimen consisted of thymoglobulin (ATG), cyclophosphamide at 120 mg/kg, etoposide at 60 mg/kg and total body irradiation (TBI) at 12 Gy (lungs 8 Gy).

The engraftment (neutrophil count > $0.5 \times 10^9$/L for 3 consecutive days) was documented at day +21 post-transplant. As GvHD prophylaxis, mycophenolic acid was administered, but switched to sirolimus on day +37 for suboptimal plasma levels. The patient became febrile on day +32 after transplantation and broad-spectrum bacterial antibiotics were started. The fever persisted and BKPyV was detected in plasma by PCR [8] on day +35 followed by a CMV reactivation with very low DNA copy numbers (270/ml plasma) on day +40. Intravenous ganciclovir was started and the plasma CMV turned negative.

On day +53, haematemesis started and oesophagogastroduodenoscopy (EGD) showed clots and diffuse bleeding from fundus. Bleeding time was normal and no venous thromboprophylaxis was used at the time the bleeding occurred. A Senstaken–Blakemore tube was placed and the patient was transferred to ICU for four days. Iv somastatin and cyclocapron were started to support hemostasis. In parallel, plasma BKPyV DNA load increased from 900 to 139′900 cp/ml by day +55. Intravenous cidofovir was started at 5 mg/kg once a week on day +55 and ganciclovir stopped. With microscopic haematuria and urine BKPyV loads up to $9.27 \times 10^7$/ml being detected intravesical cidofovir was administered weekly using the same dose 5 mg/kg for four weeks. On day +80, plasma EBV loads became detectable with a low copy number of 2700/ml. Preemptive rituximab 375 mg/m$^2$ was started, and plasma EBV loads turned negative after two weekly doses (Fig. 1).

On day +56, ascites was detected and drained with a peritoneal catheter. Ultrasound showed an inverse blood flow in the liver vessels. The liver enzymes stayed normal but the kidney function was slightly affected so that before the last cidofovir dose the serum creatinine concentration was 31 μmol/L, the creatinine clearance 1.5 ml/s/1.73 m$^2$, and cystatine C 0.99 mg/L. With the symptoms (haematemesis and gastrointestinal problems) peaking the patient needed frequent platelet and red blood cell transfusions and during the ICU treatment had seizures and minor neurological compromise. Yet, an MRI scan of the CNS was normal and the spinal tap showed no sign of infection. By the time of discharge from the ICU the patient was neurologically fully recovered and a transient hypernatremia remained as the cause of seizures.

On day +70 haematemesis, melena and diffuse bleeding from distal part of the colon occurred and another OGD and colonoscopy revealed that the distal part of the esophagus was inflamed and the colon diffusely hemorrhagic. There were no signs of acute radiation therapy induced changes like epithelial damage, regenerative atypia or increased number of eosinophils [9]. Furthermore, the biopsies revealed no sign of GvHD or infection (CMV, EBV, HSV, fungus).

## 3. Similar and contrasting cases in the literature

Gastrointestinal bleeding remains a potentially life-threatening complication following allogeneic HSCT [9]. In a recent autopsy series of adult patients, gastrointestinal bleeding was observed in 12% [9]. Although BKPyV is associated with hemorrhagic cystitis, less is known about its role with other bleeding problems [10,11]. One presumed route of BKPyV transmission is oral, and the exposure might lead to a gastrointestinal disease, like adenovirus. High BKPyV loads had been reported in the stools of patients with hemorrhagic cystitis, but their clinical significance could not be established in the adult population [1]. Kim et al. has reported on a case with a BKPyV infection with colonic ulcers with the viremia and uria coinciding with the marked gastrointestinal manifestations and the start of BKPyV [12]. There is evidence of other polyomaviruses like JCV associated with colorectal disorders in both immunocompetent and immunocompromised patients [13–17].

## 4. Discussion

Even in the face of a multitude of potential causes (e.g. poor engraftment, medication, and GvHD), viral infections remain prevalent even in the pediatric patient population and include at least cytomegalovirus, noro-, astro- or adenoviridae. In our patient, the bleeding was observed concomitantly with a massive increase

in plasma BKPyV and hemorrhagic cystitis. The observed CMV reactivation had responded to ganciclovir therapy and the contribution of GvHD had been ruled out. Sirolimus has been associated with platelet-independent problems in haemostasis, and even in our case the drug levels were transiently high (i.e. 36 μg/L), but returned to normal levels before sirolimus was withdrawn on day + 53 post-transplant [18]. In our patient the bleeding persisted despite the plasma levels of sirolimus were undetectable on day +70. BK viremia and viruria coincided with the massive gastrointestinal manifestations and the start of BK-PyVHC. Retrospective analyzed BKPyV-specific antibody response was inline with a significant exposure showing high IgG and IgM titers. Unfortunately, the biopsies were taken at a late stage and could no longer inform about BKPyV involvement. During the follow-up the BKPyV loads remained low for months.

In conclusion, gastrointestinal complications with bleeding are a significant problem after allogeneic HSCT with viral infections including BKPyV putatively contributing. Massive BK viremia has been associated with PyVHC, but, similar to adenovirus, may result in other replication foci including the GI tract, which needs to be addressed in future studies.

## Funding

The study was supported by the grants of Helsinki University Hospital Funds (to IL) and by an unrestricted appointment grant of the University of Basel (to HHH).

## Competing interests

None declared.

## Ethical approval

The study was approved by The Ethics Committee of Helsinki University Hospital.

## Author contributions

MK, PH, MT and KV were all involved in treating the patient and taking care of the post-transplant follow-up. MK collected the data and contributed to writing the manuscript. EA and LM were responsible for the virology analyses in Helsinki. PK performed serology experiments IL and HHH consulted on the case, provided laboratory analyses, interpreted the data and contributed to writing the manuscript.

## Acknowledgements

We thank the help of Pia Kiviluoma, RN, with all the practical help concerning the sample logistics.

## References

[1] Hirsch HH. Polyoma and papilloma virus infections after hematopoietic stem cell or solid organ transplantation. In: Bowden P, Ljungman P, Snydman DR, editors. Transplant Infections. third ed. New York, NY, USA: Lippincott Williams & Wilkins; 2010. p. 465–82.
[2] Dropulic LK, Jones RJ. Polyomavirus BK infection in blood and marrow transplant recipients. Bone Marrow Transplant 2008;41:11–8.
[3] Corczynska E, Turkiewicz D, Rybka K, Toporski J, Kalwak K, Dyla A, et al. Incidence, clinical outcome, and management of virus-induced hemorrhagic cystitis in children and adolescents after allogeneic hematopoietic cell transplantation. Biol Blood Marrow Transplant 2005;11:797–804.
[4] Giraud G, Priftakis P, Bogdanovic G, Remberger M, Dubrulle M, Hau A, et al. BK-viruria and haemorrhagic cystitis are more frequent in allogeneic haematopoietic stem cell transplant patients receiving full conditioning and unrelated-HLA-mismatched grafts. Bone Marrow Transplant 2008;41:737–42.
[5] Cheuk DK, Lee TL, Chiang AK, Ha SY, Lau YL, Chan GC. Risk factors and treatment of hemorrhagic cystitis in children who underwent hematopoietic stem cell transplantation. Transpl Int 2007;20:73–81.
[6] Vanchiere JA, Abudayyeh S, Copeland CM, Lu LB, Graham DY, Butel JS. Polyomavirus shedding in the stool of healthy adults. J Clin Microbiol 2009 Aug;47(8):2388–91.
[7] Wong AS, Cheng VC, Yuen KY, Kwong YL, Leung AY. High frequency of polyoma BK virus shedding in the gastrointestinal tract after hematopoietic stem cell transplantation: a prospective and quantitative analysis. Bone Marrow Transplant 2009 Jan;43(1):43–7.
[8] Koskenvuo M, Dumoulin A, Lautenschlager I, Auvinen E, Mannonen L, Anttila VJ, et al. BK polyomavirus-associated hemorrhagic cystitis among pediatric allogeneic bone marrow transplant recipients: treatment response and evidence for nosocomial transmission. J Clin Virol 2013;56:77–81.
[9] Zhang L, Xie XY, Wang Y, Wang YH, Chen Y, Ren ZG. Treatment of radioation-induced hemorrhagic gastritis with prednisolone: a case report. World J Gastroenterol 2012;18:7402–4.
[10] Labrador J, lopez-Anglada L, Perez-Lopez E, Lozano FS, Lopez-Corral L, Sanchez-Barba M, et al. Analysis of insidence, risk factors and clinical outcome of thromboembolic and bleeding events in 431 allogeneic hematopoietic stem cell transplantation recipients. Haematologica 2013;98(3):437–43.
[11] Khayyata S, Soubani AO, Bonnett M, Nassar H, Abidi MH, Al-Abbadi MA. The major autopsy findings in adult patients after hematopoietic stem cell transplantation. Ann Transplant 2007;12:11–8.
[12] Erard V, Kim HW, Corey L, Limaye A, Huang ML, Myerson D, et al. BK DNA viral load in plasma: evidence for an association with hemorrhagic cystitis in allogeneic hematopoietic cell transplant recipients. Blood 2005;106:1130–2.
[13] Gorczynska E, Turkiewicz D, Rybka K, Toporski J, Kalwak K, Dyla A, et al. Incidence, clinical outcome, and management of virus-induced hemorrhagic cystitis in children and adolescents after allogeneic hematopoietic cell transplantation. Biol Blood Marrow Transplant 2005;11:797–804.
[14] Kim GY, Nuovo G, Thomas F. BK virus and colonic ulcers. Clin Gastroenterol Hepatol 2004;2:175–7.
[15] Burke MT, Trnka P, Walsh M, Poole L, McTaggart SJ, Burke JR. Progressive multifocal leukoencephalopathy with gastrointestinal disease in a pediatric kidney transplant recipient. Pediatr Transplant 2013;17:119–24.
[16] Coelho TR, Gaspar R, Figueiredo P, Mendonca C, Lazo PA, Almeida L. Human JC polyomavirus in normal colorectal mucosa, hyperplastic polyps, sporadic adenomas, and adenocarcinomas in Portugal. J Med Virol 2013;85:2119–27.
[17] Bellizzi A, Barucca V, Di Nardo G, Fioriti F, Iebba V, Schippa S, et al. JC viral reactivation in a pediatric patient with Crohn's disease. Int J Immunopathol Pharmacol 2010;23:955–9.
[18] Rampino T, Marasa M, Malvezzi PM, Soccio G, Roscini E, Gamba G, et al. Platelet-independent defect in hemostasis associated with sirolimus use. Transplant Proc 2004;36:700–2.

Our normalized VLP-based ELISA was applied to investigate anti-JCPyV and anti-BKPyV antibodies in clinical case studies:

(1) Patient with definitive diagnosis for PML showed positive JCPyV IgG serostatus, which was in line with other PML symptoms including high level of JCPyV DNA detected in cerebrospinal fluid (CSF), NCCR mutations characteristic for PML and brain lesions shown by magnetic resonance imaging (MRI). However in this case positive JCPyV IgG serostatus might be unreliable since the patient has regularly received intravenous immunoglobulins (IvIgG). Two years after PML onset, the patient is still alive.

(2) Asymptomatic JCPyV viral shedding occurs in up to 30% of human population. However, only few reports describe JCPyV as a cause of PyVAN. This is the first case report study of JCPyV-VAN. Normalized JCPyV VLP-based ELISA was used for detection of anti-JCPyV IgG and IgM. Testing has been performed at several time points after kidney transplantation. Young boy was clearly seronegative and demonstrated a seroconversion first for IgM and followed by IgG, which indicates primary infection. The poor outcome of this case highlights the potential importance of JCPyV serostatus in pediatric and adolescent KT recipients. Our case underlines the limitations of current guidelines and proves that blood JCPyV DNA findings are not reliable. Further studies and better understanding are needed to optimize the management of JCPyV-associated nephropathy and the potential role of JCPyV and BKPyV serology for donor and recipient.

(3) Testing of 122 immunocompetent and 63 immunocompromised patients demonstrated age dependency of BKPyV IgG level, with the highest values between 20 and 30 years. Also maximum levels of specific CD4 T cells has been observed for the same age rang, and thereafter progressively decreased to below detection limit in most of the older age groups. This correlation suggests an increased vulnerability of older kidney transplant recipients to BKPyV-replication. Whereas BKPyV-specific CD4 T cells of immunocompetent individuals exhibited a multifunctional phenotype expressing several cytokines in response to stimulation, kidney transplant patients with BKPyV-associated complications showed a significant loss of multifunctional CD4 T cells. These results indicate the particular need for intact T cell functionality to control BKPyV replication. Despite quantitative similarities, young adults and patients with complications differed in functional characteristics of BKPyV-specific immunity. Therefore, cytokine profiling may be important as a tool for discrimination of immunologically controlled BKPyV-infection from uncontrolled virus replication and therefore could serve as risk predictor of PyVAN development.

(4) Pediatric allogeneic hematopoietic stem cell transplant patient was tested as positive for BKPyV IgG antibodies, which was in accordance with a significant BKPyV viruria and viremia and start of PyVHC. Gastrointestinal complications with bleeding are a significant problem after allogeneic HSCT with viral infections including BKPyV. Massive BKPyV viremia has been associated with PyVHC which can result in other replication foci including the GI tract. This has to be taken under consideration in future studies.

## 5.8 Antibody Response to BK Polyomavirus as a Prognostic Biomarker and Potential Therapeutic Target in Prostate Cancer

VLPs composed of VP1 and LTag are currently the most common antigens to detect specific anti-JCPyV and anti-BKPyV antibodies. Both proteins are good ELISA antigen candidates due to their immunogenicity and capability to stimulate B cell responses. Therefore we decided to use both proteins as antigens in ELISA for screening of BKPyV IgG response among 226 patients undergoing radical prostatectomy from primary prostate cancer. With this, we investigated whether the preoperative antibody responses to BKPyV LTag or VP1 were associated with the risk of biochemical recurrence of prostate cancer.

# Antibody response to BK polyomavirus as a prognostic biomarker and potential therapeutic target in prostate cancer

**Keller Etienne Xavier[1], Kardas Piotr[2], Acevedo Claudio[1], Sais Giovanni[1], Poyet Cédric[1], Banzola Irina[1], Mortezavi Ashkan[1], Seifert Burkhardt[3], Sulser Tullio[1], Hirsch H. Hans[2,4,*] and Provenzano Maurizio[1,*]**

[1] Oncology Research Unit, Division of Urology and Division of Surgical Research, University Hospital Zurich, CH-8091 Zurich, Switzerland

[2] Transplantation and Clinical Virology, Department Biomedicine (Haus Petersplatz), University of Basel, CH-4003 Basel, Switzerland

[3] Epidemiology, Biostatistics and Prevention Institute, University of Zurich, CH-8001 Zurich, Switzerland

[4] Infectious Diseases & Hospital Epidemiology, University Hospital Basel, CH-4031 Basel, Switzerland

[*] These authors contributed equally to this work

***Correspondence to***: *Maurizio Provenzano*, ***email***: *maurizio.provenzano@usz.ch*

***Keywords***: BK polyomavirus, prostate cancer, prognosis, antibody response, biochemical recurrence

***Received***: *December 03, 2014* ***Accepted***: *January 15, 2015* ***Published***: *January 31, 2015*



## ABSTRACT

**Infectious agents, including the BK polyomavirus (BKPyV), have been proposed as important inflammatory pathogens in prostate cancer. Here, we evaluated whether the preoperative antibody response to BKPyV large T antigen (LTag) and viral capsid protein 1 (VP1) was associated with the risk of biochemical recurrence in 226 patients undergoing radical prostatectomy for primary prostate cancer. Essentially, the multivariate Cox regression analysis revealed that preoperative seropositivity to BKPyV LTag significantly reduced the risk of biochemical recurrence, independently of established predictors of biochemical recurrence such as tumor stage, Gleason score and surgical margin status. The predictive accuracy of the regression model was denotatively increased by the inclusion of the BKPyV LTag serostatus. In contrast, the VP1 serostatus was of no prognostic value. Finally, the BKPyV LTag serostatus was associated with a peculiar cytokine gene expression profile upon assessment of the cellular immune response elicited by LTag. Taken together, our findings suggest that the BKPyV LTag serology may serve as a prognostic factor in prostate cancer. If validated in additional studies, this biomarker may allow for better treatment decisions after radical prostatectomy. Finally, the favorable outcome of LTag seropositive patients may provide a potential opportunity for novel therapeutic approaches targeting a viral antigen.**

## INTRODUCTION

Prostate cancer is the most commonly diagnosed solid malignancy among males in western countries (233'000 estimated new cases in 2014 in the US) [1]. Currently established prognostic clinicopathologic parameters insufficiently differentiate between indolent and aggressive prostate cancer, leading to both over- and undertreatment of this disease [2]. Hence, an increasing amount of gene and protein biomarkers are considered for a more individualized risk stratification, but their implementation in routine clinical practice is still under evaluation [3, 4]. Therefore, a novel biomarker addressing an established model of prostate carcinogenesis might serve as a clinically valuable prognostic factor and could uncover a therapeutic target allowing for an effective tumor control.

Chronic inflammation is considered to be one of the main factors contributing to prostate cancer development [5]. Among other inflammatory-related infectious agents, the human BK polyomavirus (BKPyV) has been proposed as an important pathogen involved in the transition of

**Table 1: Distribution of BKPyV VP1 by LTag serostatus**

| | LTag serostatus | | | |
|---|---|---|---|---|
| Characteristic | LTag- (*n*=103) | LTag+ (*n*=52) | LTag++ (*n*=51) | p |
| VP1 serostatus | | | | |
| VP1- | 22 (21%) | 13 (25%) | 12 (24%) | 0.87[a] |
| VP1+ | 81 (79%) | 39 (75%) | 39 (77%) | |

[a]Two-sided Pearson Chi-square test.

normal prostate glands towards overt prostate cancer [6]. This virus is ubiquitous in the human population and establishes a persistent asymptomatic infection in the urinary tract [7]. BKPyV replication is orchestrated by the viral regulatory protein large T antigen (LTag) and leads to lysis of permissive cells with the release of viral progeny. Such a lytic productive infection elicits an antibody response to the viral capsid protein 1 (VP1) in most healthy humans [8]. In the case of an abortive infection – where LTag expression is uncoupled from VP1 expression – LTag still exerts a substantial host cell stimulation that may transform into oncogenic activity by binding products of tumor suppressor genes, such as p53 and retinoblastoma proteins (pRB) [9]. In the context of the latter event, an antibody response against LTag can be elicited.

Investigating the antibody response to both BKPyV VP1 and LTag in prostate cancer patients could clarify the role of these antigens as key targets of cancer immune surveillance. In this study, we evaluated biochemical recurrence free survival (RFS) – as defined by the rate of patients without prostate specific antigen (PSA) relapse over time after radical prostatectomy (RP) – according to the preoperative BKPyV serostatus of primary prostate cancer patients. In addition, we verified the specificity of the antibody response to BKPyV LTag by analyzing the cell-mediated immune response to this antigen in selected patients. The final aim was to evaluate BKPyV serology as a potential prognostic biomarker for prostate cancer recurrence.

## RESULTS

All of the 206 patients available for analysis had an adenocarcinoma of the prostate and their clinicopathologic characteristics are summarized in Supplementary Table S1. In two patients, no prostate cancer was found in the prostatectomy specimen (pTx), although positive prostate biopsies were confirmed.

The immunoglobulin G (IgG) serological assay results and the selected cutoffs differentiating VP1 seronegative from (VP1-) seropositive patients (VP1+) as well as the cutoffs differentiating LTag seronegative (LTag-), borderline LTag seropositive (LTag+) and strongly LTag seropositive patients (LTag++) are reported in Figure 1. The LTag-cutoffs were defined as the 50$^{th}$ and the 75$^{th}$ percentile of all the LTag IgG ratio values (1.0226 and 1.1478, respectively), corresponding to the closest quartile to a ratio of 1 and to the next highest quartile, respectively. Accordingly, 159/206 (77%) patients were VP1+ (Fig. 1A), 52/206 (25%) LTag+ and 51/206 (25%) LTag++ (Fig. 1B). No association was found between VP1 and LTag serostatus (Table 1). When only VP1 and LTag seropositive patients were considered ($n$ = 78), a trend for

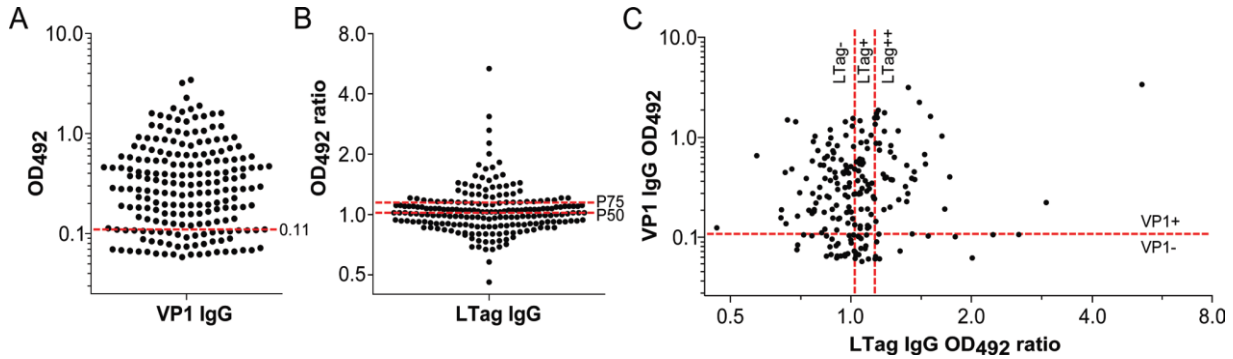


**Figure 1: Antibody activity against BKPyV VP1 and LTag in patients who underwent RP for primary prostate cancer (n = 206).** (A) Column scatter graph of the VP1 IgG optical density values at 492 nm ($OD_{492}$). The established cutoff ($OD_{492}$ = 0.11) defining VP1 seropositivity (VP1+) was marked by a red dashed line. (B) Column scatter graph of the LTag IgG $OD_{492}$ ratio values. Following cutoffs defined LTag seropositivity: overall 50$^{th}$ percentile (P50) $OD_{492}$ ratio (1.0226) for borderline seropositive patients (LTag+) and overall 75$^{th}$ percentile (P75) $OD_{492}$ ratio (1.1478) for strongly seropositive patients (LTag++) (red dashed lines). (C) Scatter plot correlating VP1 and LTag IgG activity. Quadrants were generated according to the selected VP1 and LTag cutoffs (red dashed lines).

**Table 2: Distribution of patient clinicopathologic characteristics by BKPyV serostatus**

| | BKPyV serostatus | | | | | | |
|---|---|---|---|---|---|---|---|
| Characteristic | VP1- (*n*=47) | VP1+ (*n*=159) | p | LTag- (*n*=103) | LTag+ (*n*=52) | LTag++ (*n*=51) | p |
| Age at operation | | | | | | | |
| <63 y | 19 (40%) | 74 (46%) | 0.46[a] | 47 (46%) | 25 (48%) | 21 (41%) | 0.77[a] |
| ≥63 y | 28 (60%) | 85 (54%) | | 56 (54%) | 27 (52%) | 30 (59%) | |
| PSA at diagnosis | | | | | | | |
| <10 ng/mL | 41 (87%) | 126 (79%) | 0.22[a] | 84 (82%) | 41 (79%) | 42 (82%) | 0.89[a] |
| ≥10 ng/mL | 6 (13%) | 33 (21%) | | 19 (18%) | 11 (21%) | 9 (18%) | |
| Tumor stage | | | | | | | |
| <pT3 | 36 (77%) | 124 (78%) | 0.84[a] | 78 (76%) | 39 (75%) | 43 (84%) | 0.42[a] |
| ≥pT3 | 11 (23%) | 35 (22%) | | 25 (24%) | 13 (25%) | 8 (16%) | |
| Nodal status | | | | | | | |
| pN0 | 26 (55%) | 86 (54%) | 0.82[b] | 53 (51%) | 32 (61%) | 27 (53%) | 0.50[b] |
| pN1 | 2 (4%) | 5 (3%) | | 3 (3%) | 3 (6%) | 1 (2%) | |
| Unknown | 19 (40%) | 68 (43%) | | 47 (46%) | 17 (33%) | 23 (45%) | |
| Gleason score | | | | | | | |
| 5-6 | 11 (23%) | 27 (17%) | 0.59[a] | 21 (20%) | 5 (10%) | 12 (24%) | 0.08[a] |
| 7 | 30 (64%) | 112 (70%) | | 68 (66%) | 37 (71%) | 37 (73%) | |
| 8-9 | 6 (13%) | 20 (13%) | | 14 (14%) | 10 (19%) | 2 (4%) | |
| Surgical margin | | | | | | | |
| R0 | 35 (75%) | 108 (68%) | 0.39[a] | 70 (68%) | 35 (67%) | 38 (75%) | 0.66[a] |
| R1 | 12 (25%) | 51 (32%) | | 33 (32%) | 17 (33%) | 13 (25%) | |

[a]Two-sided Pearson Chi-square test.
[b]Two-sided Fisher's exact test.

a moderate correlation between VP1 and LTag activity was found (Spearman's rho = 0.22, p = 0.05) (Fig. 1C).

The contingency table analysis did not provide any evidence for an association between the BKPyV serostatus and the clinicopathologic parameters (age at operation, PSA at diagnosis, tumor stage, nodal status, Gleason score and surgical margin status), other than a trend for a low proportion of Gleason score 5-6 in the LTag+ group and for a low proportion of Gleason score 8-9 in the LTag++ group (Table 2).

To search for an association between BKPyV serostatus and the clinical course of the disease after RP, we performed survival analyses based on time to biochemical recurrence (BR). To ensure the quality of our follow-up data, we analyzed the estimates of RFS before and after stratification for established predictors of BR. Over a median follow-up of 48 months (range = 13–70), a BR was documented in 43 patients. The overall estimated RFS was 87% (95% confidence interval [CI], 83–92) at 24 months and 77% (95% CI, 71–84) at 48 months after surgery (Supplementary Fig. S1). High tumor stage, high Gleason score and positive surgical margins were associated with significantly lower estimates of RFS ($p < 0.001$, $p < 0.001$ and $p = 0.001$, respectively), whereas no significant difference in the estimates of RFS was found for PSA stratification ($p = 0.31$) (Supplementary Fig. S2).

For VP1 serostatus stratification, no significant difference in the estimates of RFS was found ($p = 0.96$) (Fig. 2A). Higher IgG activity cutoffs, differentiating patients with a stronger antibody response to VP1, did not reveal any significant differences either (Supplementary Fig. S3). By contrast, LTag+ and LTag++ patients showed significantly higher estimates of RFS than LTag- patients ($p = 0.007$) (Fig. 2B). Notably, the estimated RFS at 48 months was 89% (95% CI, 79–99) for LTag++ patients, 85% (95% CI, 75–95) for LTag+ patients and 68% (95% CI, 57–78) for LTag- patients.

To further evaluate the predictive accuracy of the BKPyV VP1 and LTag serological assays for BR, time-dependent receiver operating characteristic (ROC) curve analyses were performed based on RFS at 12, 24, 36 and 48 months after surgery. For the VP1 IgG assay, the 95% CI of the area under the curve (AUC) persistently included the 0.50 limit, thus revealing no evidence for a prognostic potential (Fig. 3A). For the LTag IgG assay, the AUC reached 0.68 (95% CI, 0.57–0.79) at 48 months (Fig. 3B). The predictive accuracy of established predictors of BR yielded similar results; at 48 months, the AUC was 0.68 (95% CI, 0.57–0.78) for tumor stage, 0.67 (95% CI, 0.58-0.76) for Gleason score, 0.63 (95% CI, 0.54–0.73) for surgical margin status and 0.57 (95% CI, 46–69) for PSA level at diagnosis (Supplementary Fig. S4).

In the multivariate analysis, LTag+ and LTag++ patients maintained a significantly lower risk of BR than

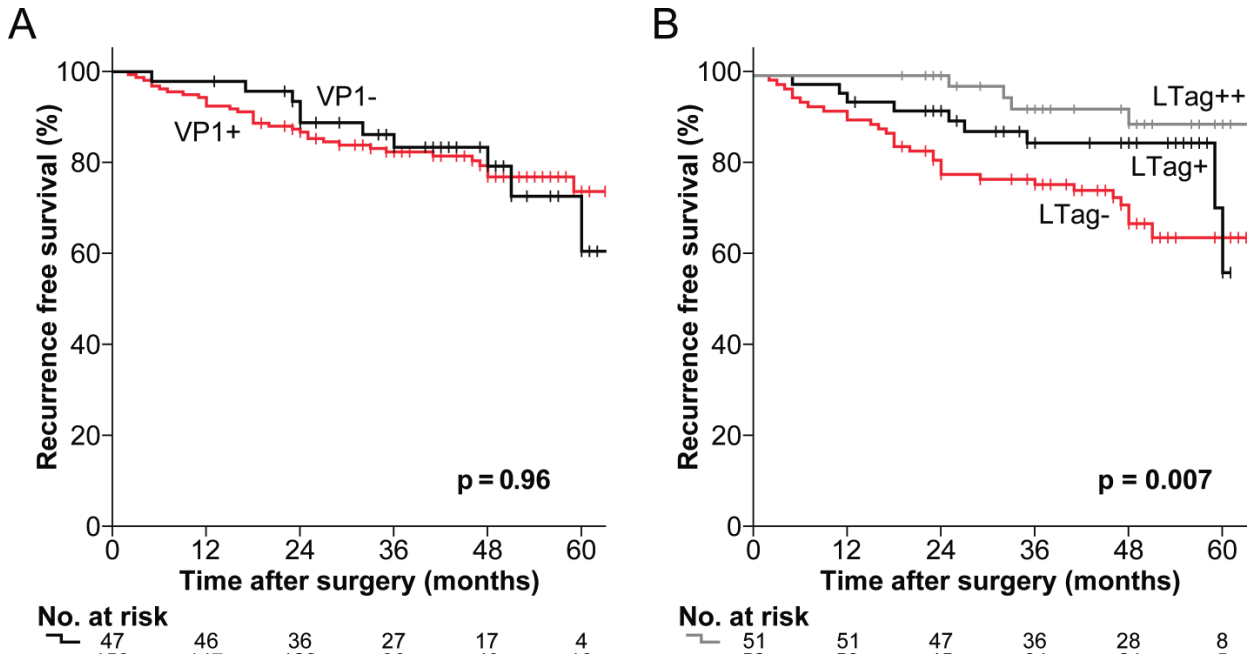


**Figure 2: Kaplan-Meier estimates of RFS by BKPyV serostatus in patients who underwent RP for primary prostate cancer.** (A) Estimates of RFS stratified by the established cutoff for VP1 seropositivity ($OD_{492}$ = 0.11) (black line = VP1- and red line = VP1+). (B) Estimates of RFS stratified by the 50th and the 75th percentile LTag IgG $OD_{492}$ ratio (1.0226 and 1.1478, respectively) (grey line = LTag++, black line = LTag+ and red line = LTag-). All p values were two-sided log-rank tests.

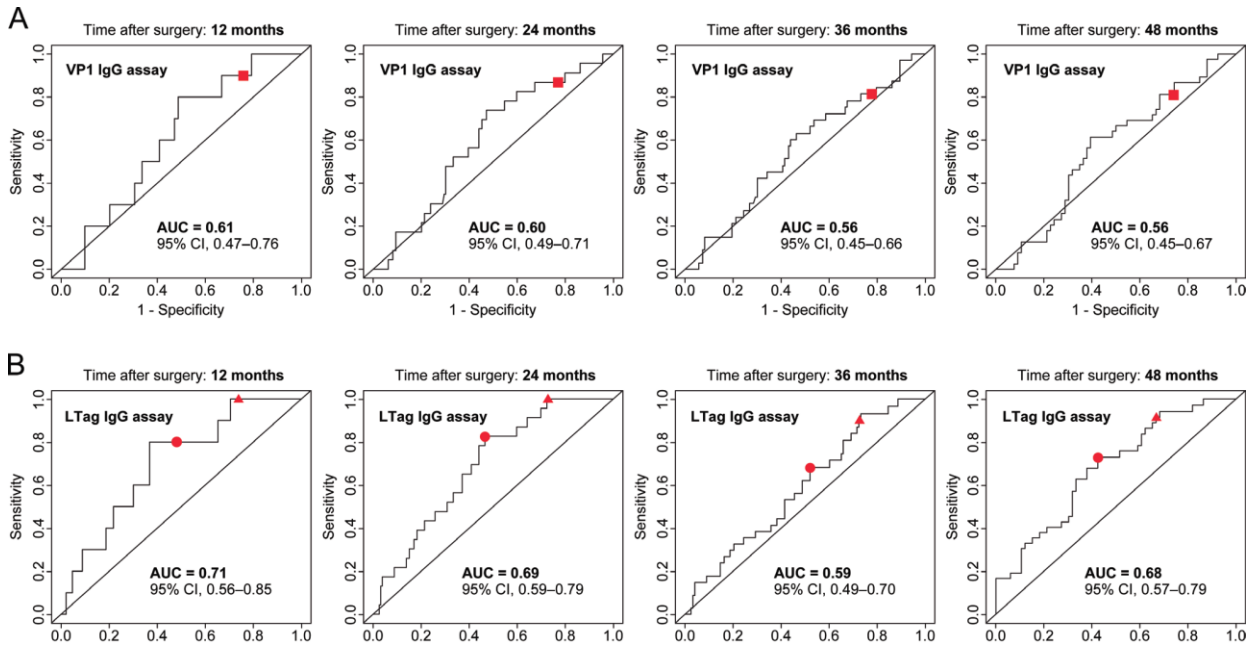


**Figure 3: Evaluation of the predictive accuracy of the BKPyV serological assays based on estimates of RFS in patients who underwent RP for primary prostate cancer.** (A) Time-dependent ROC curves for the VP1 IgG assay prediction of BR at 12, 24, 36 and 48 months after surgery. Curves were calculated based on continuous VP1 IgG activity levels, with the established cutoff ($OD_{492}$ = 0.11) symbolized by a red square. (B) Time-dependent ROC curves for the LTag IgG assay prediction of BR at 12, 24, 36 and 48 months after surgery. Curves were calculated based on continuous LTag IgG activity levels, with the overall 50th percentile LTag IgG $OD_{492}$ ratio (1.0226) and the overall 75th percentile LTag IgG $OD_{492}$ ratio (1.1478) cutoff symbolized by a red circle and a red triangle, respectively.

LTag- patients, independent of established predictors of this event (tumor stage, Gleason score and surgical margin status) (Table 3). The predictive accuracy of the Cox regression model – as quantified by the Harrell's concordance index – could be increased from 0.76 (95% CI, 0.68 – 0.83) to 0.79 (95% CI, 0.71 – 0.86) before and after inclusion of the BKPyV serostatus variable, respectively. PSA and VP1 serostatus did not reach the entry level criterion for the forward-stepwise Cox regression model and these parameters were therefore not included in the multivariate analysis.

The favorable prognosis of LTag seropositive patients prompted us to verify a finding that we previously reported, namely that the LTag serostatus was associated with a peculiar cellular immune response profile upon LTag antigen stimulation. For this purpose, we selected 12 age-, stage- and grade-matched patients with the aim of having 4 patients per LTag serostatus group (i.e. LTag-, LTag+ and LTag++). Patients' peripheral blood mononuclear cells (PBMCs) were *ex vivo* stimulated either with a BKPyV LTag peptide pool or with a CEF (cytomegalovirus, Epstein-Barr virus and influenza virus) peptide pool for the analysis of the gene expression of three specific cytokines: interferon gamma (IFN-γ), interleukin 10 (IL-10) and transforming growth factor β1 (TGF-β1). Comparisons were made between the group of LTag seronegative patients (LTag-, n = 4) and the group of LTag seropositive patients (LTag+/++, n = 8) (Fig. 4A). After LTag peptide pool stimulation, no evidence for differing IFN-γ gene expression levels was found between the LTag- group and the LTag+/++ group (p = 1.00). Notably, the LTag+/++ group showed significantly higher IL-10 gene expression levels than the LTag- group (p = 0.008), while higher TGF-β1 gene expression levels were observed in the LTag- group (p = 0.11) (Fig. 4A). In contrast, the CEF peptide pool stimulation showed no evidence for differing cytokine gene expression levels upon BKPyV LTag serostatus stratification (Fig. 4A).

To verify whether the observed *ex vivo* cellular immune responses of these 12 patients were indeed

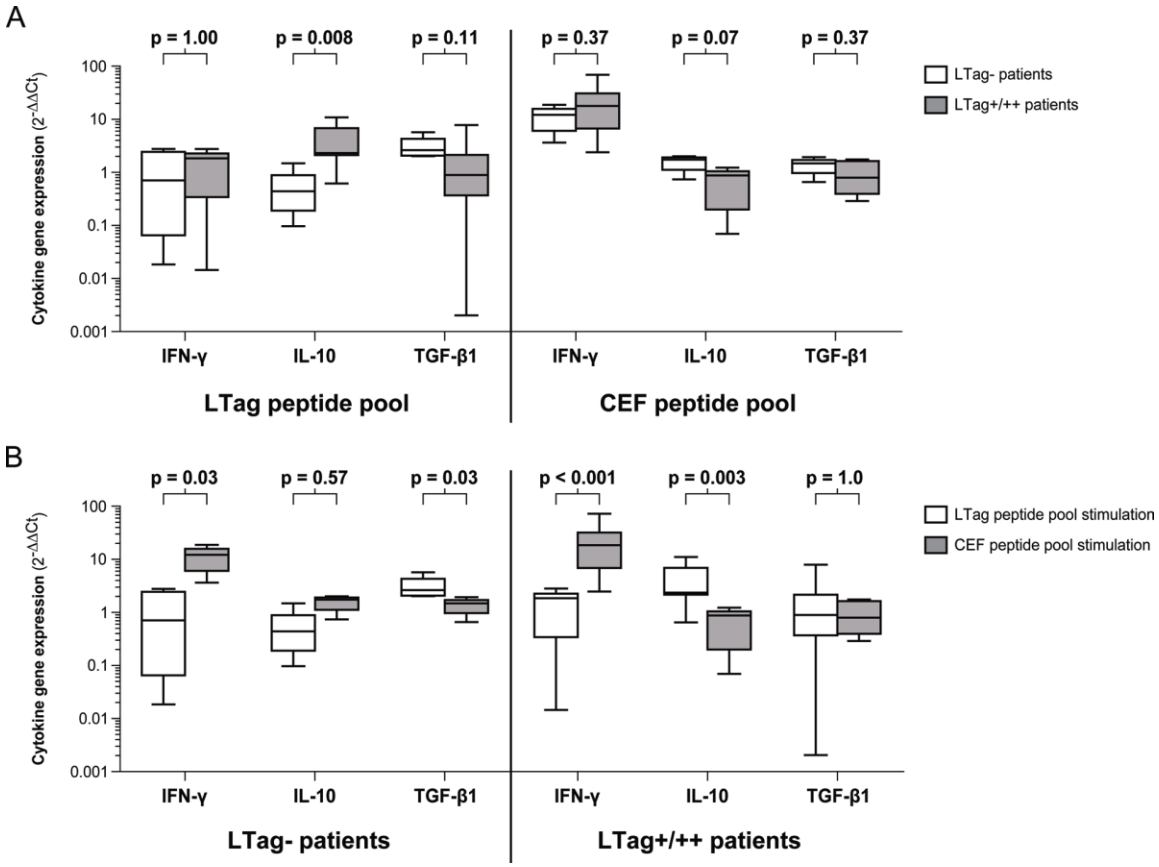


**Figure 4: Cytokine gene expression upon peptide pool stimulation of PBMCs from 12 selected age-, stage- and grade-matched prostate cancer patients.** (A) Box-and-whiskers plots comparing the IFN-γ, IL-10 and TGF-β1 gene expression levels between LTag seronegative patients (LTag-) and LTag borderline seropositive and strongly seropositive patients (LTag+/++) upon either LTag or CEF peptide pool stimulation. (B) Box-and-whiskers plots comparing the IFN-γ, IL-10 and TGF-β1 gene expression levels upon either LTag or CEF peptide pool stimulation in the group of LTag seronegative patients (LTag-) and in the group of LTag borderline seropositive and strongly seropositive patients (LTag+/++). Distributions of cytokine gene expression levels variables were compared by Mann-Whitney U tests. All p values were two-sided.

**Table 3: Multivariate Cox regression analysis of the risk of BR for BKPyV serostatus stratification, adjusting for established predictors of BR**

| Variable | Parameter | | | HR | (95% CI) | p[a] |
|---|---|---|---|---|---|---|
| BKPyV serostatus | LTag+ | vs. | LTag- | 0.44 | (0.21 – 0.93) | 0.032 |
| | LTag++ | vs. | LTag- | 0.25 | (0.09 – 0.71) | 0.009 |
| Tumor stage | pT≥3 | vs. | pT<3 | 3.5 | (1.8 – 6.8) | <0.001 |
| Gleason score | ≥7b | vs. | ≤7a | 2.1 | (1.1 – 3.7) | 0.034 |
| Surgical margin | R1 | vs. | R0 | 2.4 | (1.1 – 4.0) | 0.018 |

HR = hazard ratio

[a]All *P* values were two-sided.

specific to the BKPyV LTag, we compared the cytokine gene expression patterns induced by either the LTag or the CEF peptide pool. In both the LTag- and the LTag+/++ group, the CEF peptide pool stimulation induced considerably higher IFN-γ gene expression levels than the LTag peptide pool stimulation ($p = 0.03$ and $p < 0.001$, respectively) (Fig. 4B). Furthermore, after CEF peptide pool stimulation of the PBMCs from LTag+/++ patients, the IL-10 gene expression levels remained significantly lower than after LTag peptide pool stimulation ($p = 0.003$) (Fig. 4B). This confirms that the IL-10 elevation observed in LTag+/++ patients is indeed specific to the LTag peptide pool stimulation. Finally, in the LTag- group, a trend towards a higher TGF-β1 gene expression upon LTag-peptide pool stimulation was found ($p = 0.03$) (Fig. 4B).

## DISCUSSION

Cumulative evidence for a co-factorial role of the BKPyV in prostate carcinogenesis has emerged from prostate tissue analyses and immune response characterization studies in prostate cancer patients [10-12]. To our knowledge, this is the first study addressing the prognostic significance of the antibody response to BKPyV in prostate cancer patients.

In comparison to Merkel cell carcinoma patients, where high Merkel cell polyomavirus VP1 IgG levels were associated with a better progression-free survival [13], no evidence for an association between the BKPyV VP1 serostatus and the risk of prostate cancer recurrence was provided in this study. This finding underlines the notion that a productive BKPyV infection – leading to a strong VP1 IgG activity – is unlikely to reflect the oncogenic potential of the BKPyV, as permissive cells will be lysed upon release of the viral progeny [14].

Rather, the novelty of our investigation is the finding that an antibody response to the viral regulatory protein LTag is associated with the clinical course of prostate cancer patients after RP. Because the LTag may lead to the oncogenic transformation of BKPyV infected glandular prostate cells, an increased antibody activity against this oncogenic protein would be expected in cases with high risk of BR. Indeed, in cervical cancer patients, antibodies against human papillomavirus proteins E6 and E7, whose functions are similar to LTag, are markers of worse prognosis [15]. Differently, in this study, increasing estimates of RFS were found over increasing levels of preoperative BKPyV LTag IgG activity. Particularly, about 89% of all strongly LTag seropositive patients were free of BR at 48 months after RP, whereas only 68% of all LTag seronegative patients were BR-free at 48 months. This finding was highlighted in the multivariate analysis adjusting for the usually available patient clinicopathologic characteristics, which indicated that the risk of BR was lowered by at least 29% in strongly LTag seropositive patients and that even borderline seropositivity for BKPyV LTag led to a risk reduction of at least 7%. Of note, the addition of the BKPyV serostatus variable in the multivariate Cox regression model resulted in a denotative increase of the predictive accuracy of the model, thus suggesting the preoperative BKPyV serostatus as a potentially valuable biomarker for the prediction of BR after RP.

The almost equal distribution of the VP1 serostatus over the three levels of the LTag serostatus reveals that more than half of all VP1 seronegative patients must have had LTag antigens exposed to their immune system in the absence of a VP1 antigenic stimulation. This exemplifies that the uncoupled continuous expression of LTag with the lacking VP1 expression, typically occurring in abortively infected cells, can be effectively targeted by the immune system. However, to date, it is unknown whether the prostate is the main site for the antigenic exposition of BKPyV LTag to the immune system and the detection of LTag in areas of overt prostate cancer remains elusive and needs to be standardized [16]. Several studies

regarding the association between BKPyV and prostate cancer led to the common conclusion that the virus exerts its oncogenic activity at early stages of cancer development [10]. Particularly, LTag has frequently been detected in areas of proliferative inflammation atrophy (PIA), which is considered a precursor lesion leading to prostatic intraepithelial neoplasia and overt prostate cancer [17]. The absence of any association between the BKPyV serostatus and the usual patient clinicopathologic characteristics, such as tumor stage or Gleason score, underlines the concept that BKPyV has an etiological role only in precancerous and early stage cancer lesions surrounding tumor areas.

The cytoplasmic localization of LTag in complex with wild type p53 in abortively infected cells, as seen at the PIA level [10, 18], makes this antigen a suitable target for the generation of memory $CD8^+$ and $CD4^+$ T cells. Indeed, reactivation of HLA class I effector memory $CD8^+$ T cells and class II polyfunctional $CD4^+$ T cells with dual T-helper and T-cytotoxic properties was observed in BKPyV seropositive healthy subjects experiencing smoldering infections [19-21]. Furthermore, peculiar cellular immune response profile was recalled by the LTag stimulation of PBMCs in BKPyV seropositive prostate cancer patients [11].

Correspondingly, we assessed the cytokine gene expression of PBMCs upon *ex vivo* LTag peptide pool stimulation and could verify our previous findings. Notably, we were able to recall a strong IL-10 gene expression in LTag seropositive patients and additionally characterized a trend for an increased TGF-β1 gene expression in LTag seronegative patients. Both IL-10 and TGF-β1 are characteristic of type 1 T regulatory cells and are frequently reported as immunoregulatory cytokines impairing cancer immune surveillance [22-24]. Yet, IL-10 has also been found to induce effective antitumor immune responses in various studies [25]. The latter might explain why the LTag peptide pool stimulation would recall the expression of IL-10 in the favorable prognosis group of LTag seropositive patients. Hence, a favorable microenvironment allowing for effective immune-mediated tumor surveillance would explain the long-lasting absence of BR in most patients showing strong LTag seropositivity enrolled in this study.

We could verify the PBMCs' ability to recall a strong IFN-γ immune response upon stimulation with the immunogenic CEF peptide pool. In addition, no evidence for a significant increase in IL-10 or TGF-β1 cytokine gene expression levels was found after CEF peptide pool stimulation. This was in agreement with our expectations, as the CEF peptide pool is used for its ability to recall effector immune responses and stimulates CD8+ T cells to preferentially produce IFN-γ. Hereby, we not only attributed the specificity of our findings to the BKPyV, but also verified that the individual variability of the LTag-specific antibody activity was not due to individual differences of age-related decline of immune functions. The relative immunological integrity of the evaluated cohort is further attested by the overall VP1 seroprevalence of 77%, which is in agreement with previous age-stratified seroepidemiological studies on polyomaviruses in blood donors [26, 27].

On account of these findings, the elicitation of a functional immune response against the BKPyV LTag by therapeutic means might increase the amount of specific prostate-infiltrating T lymphocytes with effector functions or redirect existing effector T cells with an exhausted phenotype, thereby inducing a favorable local tumor immune microenvironment allowing for immune-mediated tumor surveillance and consequently lower the risk of BR after RP [28].

Although more than 200 prostate cancer patients were tested for BKPyV serostatus using subtype 1/b1 for VP1-based virus-like particles (VLP) generation – which is the most common BKPyV subtype among Caucasians [29] – the present study is not devoid of limitations. Particularly, patients' ethnicity and antigenically distinct BKPyV serotypes might represent possible confounding factors of our estimates of RFS [30, 31]. Moreover, a potential LTag-specific antibody cross-reactivity between the BKPyV and other human polyomaviruses – such as the endemic JC Polyomavirus (JCPyV) – might have contributed to the LTag IgG ratio values [32]. However, so far, no rationale for a role of polyomavirures other than the BKPyV has been demonstrated in prostate cancer [33]. Notably, in our prior investigations, we could not find any JCPyV-specific LTag sequences at indicative copy numbers in prostatic tissues, whereas BKPyV-specific LTag sequences were readily detectable in 42% of the PCa tissue specimens and 32% of the benign prostatic hyperplasia tissues [11]. Based on the findings reported by Bodaghi et al., the rise of IgG activity levels against BKPyV-specific LTag subdomain 1 (LTD1) is preceded by an extensive BKPyV viremia in immunocompromised kidney transplanted patient [34]. Accordingly, we consider it most plausible to assume that the IgG activity observed in our investigation reflects BKPyV LTag exposure to the immune system. Additional studies on human polyomaviruses' LTag IgG seroprevalence and its distribution over age groups in healthy populations would be needed for clarification.

Another limitation of our study is the absence of evidence for an association between the PSA levels at diagnosis and the risk of BR, the former being an established risk-predictor. This might be related to the relatively short follow-up or to the intrinsic imprecisions of PSA measurements, which were not standardized. Nevertheless, our findings are based on a representative prostate cancer patient cohort undergoing RP, as reflected by the significant and independent performance of other established predictors of BR, such as tumor stage, Gleason score and surgical margin status. Hence, the

reported results are intriguing enough to justify further characterization of the role of BKPyV in prostate cancer.

In conclusion, our investigation provides an unprecedented epidemiological evidence for an association between antibody responses to BKPyV LTag and the clinical course of prostate cancer. Particularly, we reveal that the preoperative LTag serology may be a valuable biomarker for the prediction of favorable prostate cancer prognosis after RP. If validated in additional studies, this biomarker may allow for better postoperative treatment decisions. Finally, this study suggests a promising opportunity for novel therapeutic approaches targeting a virus-related oncogenic antigen in early prostate cancer lesions.

## METHODS

### Study population

We evaluated a case series of 226 patients undergoing RP for primary prostate cancer in our institution between October 2007 and November 2011. A prospective observational tumor marker study design was used, according to Simon et al. [35]. Whole-mount prostatectomy sections were analyzed by the Institute of Surgical Pathology of the University Hospital of Zurich. Tumor grades and stages were assigned according to the International Society of Urological Pathology (ISUP 2005) [36] and Union for International Cancer Control (UICC 2002 and 2009) [37, 38], respectively. When no prostate cancer was found in the prostatectomy specimen (pTx), Gleason score at biopsy was reported. None of the patients had received neoadjuvant androgen-deprivation therapy.

The primary endpoint was time from surgery to BR, with censoring of patients without BR at the date of last follow-up. For this purpose, patients were routinely assessed by PSA measurements at 6 weeks, 3, 6 and 12 months postoperatively and annually thereafter. BR was defined as a rise in PSA levels ≥0.1 ng/mL after surgery. Serum PSA level testing was not standardized, since many patients were initially diagnosed and followed up in referral centers. Overall, 20 patients unfit for survival analyses were excluded for the following reasons: i) postoperative PSA measurements not available ($n$ = 4); ii) postoperative PSA nadir (PSA level drop <0.1 ng/mL) not reached ($n$ = 13); iii) administration of a second-line therapy at PSA levels <0.1 ng/mL ($n$ = 3). Local ethics committee approval and written informed consent from all patients were provided. This study was conducted following the Reporting Recommendations for Tumor Marker Prognostic Studies (REMARK) guidelines [39].

### Blood specimen collection and handling

Blood specimens were collected before surgery. Serum tubes were centrifuged at 1300 x g for 10 min at room temperature. After centrifugation, serum specimens (1 mL aliquots) were frozen within 2 hours after collection and stored at -80°C until use. PBMCs were isolated from venous blood by Ficoll-Hypaque density gradient centrifugation (Histopaque, Sigma-Aldrich, St. Louis, MO, USA) and stored in liquid nitrogen until use.

### Serological analysis

Serological assays were performed blinded to the patients' characteristics and outcome. Antibody responses to BKPyV were measured by enzyme immunoassays (EIA) based on two BKPyV antigens: the VP1 in the form of VLP and the N-terminal 133-aa LTag subdomain 1 (LTD1) conjugated with glutathione-S-transferase (GST-LTD1 fusion protein). These two antigens were produced as described previously [34]. Briefly, VLP were isolated from *Spodoptera frugiperda* Sf9 cells (American Type Culture Collection [ATCC], Manassas, VA, USA) infected with recombinant baculovirus encoding BKPyV subtype 1/b1 VP1 (Bac-to-Bac baculovirus expression system, Invitrogen, Carlsbad, CA, USA). Infected Sf9 cells were disrupted by sonication and glass mortar and pestle treatment. VLP were purified from cellular lysate by CsCl gradient. The 3-dimensional conformation of VLP was confirmed by transmission electron microscopy. For LTD1 expression, the recombinant baculovirus transfer plasmid was ligated with a pFastBac1-GST vector (Invitrogen, Carlsbad, CA, USA) allowing for single-step GST-fusion protein purification by glutathione-affinity chromatography (Glutathione Sepharose 4B, GE Healthcare, Piscataway, NJ, USA). Purified non-VLP expressing cell lysates and purified GST were used as negative controls.

After coating EIA wells with 100 ng of VLP or 25 ng of GST-LTD1 fusion proteins, BKPyV-specific VP1 or LTag IgG activity, respectively, was measured as an optical density value at 492 nm ($OD_{492}$) with a serum dilution of 1:400 using an automated plate reader (Tecan Group Ltd., Männedorf, Switzerland), as described previously [34]. For each antigen, all serum samples were analyzed on the same day. For VP1 IgG, we adopted the cutoff $OD_{492}$ = 0.11 after subtraction of purified non-VLP expressing cell lysates $OD_{492}$ value (negative control) to differentiate seronegative (VP1-) from seropositive patients (VP1+), as established elsewhere [8, 34, 40, 41]. For LTag IgG, the ratio of the GST-LTD1 IgG $OD_{492}$ value divided by its respective affinity-purified GST IgG $OD_{492}$ value (negative control) was calculated for each patient. This allowed for normalization of inter-individual variations of unspecific IgG binding to GST. Ideally, an LTag IgG ratio

of >1 would define a patient as seropositive. Therefore – and since a standard cutoff for the LTag IgG activity had not been defined at the time of this study execution –, we considered the quartile of all LTag IgG $OD_{492}$ ratio values closest to a ratio of 1 to differentiate between seronegative (LTag-) and borderline seropositive patients (LTag+) and the next highest quartile to discriminate strongly seropositive (LTag++) patients. This allowed for specific comparisons between seronegative (LTag-), borderline seropositive (LTag+) and strongly seropositive patients (LTag++).

### *Ex vivo* induction and cytokine gene expression by qRT-PCR

After thawing, PBMCs were stimulated with either a BKPyV LTag peptide pool, a positive control CEF (cytomegalovirus, Epstein-Barr virus and influenza virus) peptide pool, or a negative control HIV peptide pool (JPT Peptide Technology, Berlin, Germany), as previously described [11]. Quantitative gene amplification was performed by using a Corbett Rotor-Gene 3000 Instrument (Corbett Life Science, Sydney, Australia) with a TaqMan Universal PCR master mix reagents kit and "on demand" sets of primers and probes for cytokine gene expression of IFN-γ, IL-10 and TGF-β1 (Applied Biosystems, Rotkreuz, Switzerland), as previously described [42]. The negative control was used to compute cytokine gene expression fold changes. Finally, the normalized data were analyzed by the $2^{-\Delta\Delta Ct}$ method using β-Actin as an endogenous reference gene [43].

### Statistical analysis

Categorical variables were evaluated by contingency table analyses and Pearson Chi-square tests or Fisher's exact tests, as appropriate. Mann-Whitney U tests were run to determine differences between continuous independent variables. Association between continuous variables was assessed by Spearman's rank correlation coefficient. Estimates of RFS were calculated with the Kaplan-Meier method and were compared with the log-rank test. Based on these estimates of RFS, the predictive accuracy of the considered BKPyV seromarkers was evaluated by time-dependent ROC curves. A forward-stepwise multivariate Cox regression analysis (entry level at 0.05) was modeled to evaluate the antibody response to BKPyV as a predictor of BR, adjusting for established predictors of BR. Proportional hazard assumption was assessed for each variable with the plot of a log-negative-log survival distribution and by the plot of Schoenfeld's residuals over time. The predictive accuracy of the Cox regression model was estimated using the Harrell's concordance index. Owing to multiple comparisons, the two-sided significance level was set at 0.01, exception made for the multivariate Cox regression analysis. The latter represents a single test that includes confounding covariates, justifying a significance level of 0.05.

Column scatter graphs were generated with GraphPad Prism 5.04 (GraphPad Software, La Jolla CA, USA). Time-dependent ROC curves were estimated with the timeROC v0.2 package for R [44]. The Harrell's concordance index was based on forward-stepwise multivariate Cox regression analysis results using Stata 13.1 (Stata Corp., College Station, TX, USA). Analyses of all other variables were performed with IBM SPSS Statistics 22.0 (IBM Corp., Armond, NY, USA).

## ACKNOWLEDGMENTS

We wish to thank Prof. Dr. Giulio C. Spagnoli for helpful comments on this work, Jacqueline Samaridis for excellent technical assistance and Damina Balmer for editorial reading of the manuscript.

### Conflicts of interest

The authors disclose no potential conflicts of interest.

### Financial support

This study was partially supported by the Swiss National Science Foundation (grant 320000-122429/1 to MP).

## REFERENCES

1. Siegel R, Ma J, Zou Z and Jemal A. Cancer statistics, 2014. CA Cancer J Clin. 2014; 64:9-29.
2. Lughezzani G, Briganti A, Karakiewicz PI, Kattan MW, Montorsi F, Shariat SF and Vickers AJ. Predictive and prognostic models in radical prostatectomy candidates: a critical analysis of the literature. Eur Urol. 2010; 58:687-700.
3. Tricoli JV, Schoenfeldt M and Conley BA. Detection of prostate cancer and predicting progression: current and future diagnostic markers. Clin Cancer Res. 2004; 10:3943-3953.
4. Eeles R, Goh C, Castro E, Bancroft E, Guy M, Al Olama AA, Easton D and Kote-Jarai Z. The genetic epidemiology of prostate cancer and its clinical implications. Nat Rev Urol. 2014; 11:18-31.
5. De Marzo AM, Platz EA, Sutcliffe S, Xu J, Gronberg H, Drake CG, Nakai Y, Isaacs WB and Nelson WG. Inflammation in prostate carcinogenesis. Nat Rev Cancer. 2007; 7:256-269.
6. Abend JR, Jiang M and Imperiale MJ. BK virus and human cancer: innocent until proven guilty. Semin Cancer Biol.

2009; 19:252-260.

7. Hirsch HH and Steiger J. Polyomavirus BK. Lancet Infect Dis. 2003; 3:611-623.
8. Egli A, Infanti L, Dumoulin A, Buser A, Samaridis J, Stebler C, Gosert R and Hirsch HH. Prevalence of polyomavirus BK and JC infection and replication in 400 healthy blood donors. J Infect Dis. 2009; 199:837-846.
9. Tognon M, Corallini A, Martini F, Negrini M and Barbanti-Brodano G. Oncogenic transformation by BK virus and association with human tumors. Oncogene. 2003; 22:5192-5200.
10. Das D, Wojno K and Imperiale MJ. BK virus as a cofactor in the etiology of prostate cancer in its early stages. J Virol. 2008; 82:2705-2714.
11. Sais G, Wyler S, Hudolin T, Banzola I, Mengus C, Bubendorf L, Wild PJ, Hirsch HH, Sulser T, Spagnoli GC and Provenzano M. Differential patterns of large tumor antigen-specific immune responsiveness in patients with BK polyomavirus-positive prostate cancer or benign prostatic hyperplasia. J Virol. 2012; 86:8461-8471.
12. Delbue S, Matei DV, Carloni C, Pecchenini V, Carluccio S, Villani S, Tringali V, Brescia A and Ferrante P. Evidence supporting the association of polyomavirus BK genome with prostate cancer. Med Microbiol Immunol. 2013; 202:425-430.
13. Touze A, Le Bidre E, Laude H, Fleury MJ, Cazal R, Arnold F, Carlotti A, Maubec E, Aubin F, Avril MF, Rozenberg F, Tognon M, Maruani A, et al. High levels of antibodies against merkel cell polyomavirus identify a subset of patients with merkel cell carcinoma with better clinical outcome. J Clin Oncol. 2011; 29:1612-1619.
14. Newton R, Ribeiro T, Casabonne D, Alvarez E, Touze A, Key T and Coursaget P. Antibody levels against BK virus and prostate, kidney and bladder cancers in the EPIC-Oxford cohort. Br J Cancer. 2005; 93:1305-1306.
15. Castellsague X, Pawlita M, Roura E, Margall N, Waterboer T, Bosch FX, de Sanjose S, Gonzalez CA, Dillner J, Gram IT, Tjonneland A, Munk C, Pala V, et al. Prospective seroepidemiologic study on the role of Human Papillomavirus and other infections in cervical carcinogenesis: evidence from the EPIC cohort. Int J Cancer. 2014; 135:440-452.
16. Delbue S, Ferrante P and Provenzano M. Polyomavirus BK and prostate cancer: an unworthy scientific effort? Oncoscience. 2014; 1:296-303.
17. De Marzo AM, Marchi VL, Epstein JI and Nelson WG. Proliferative inflammatory atrophy of the prostate: implications for prostatic carcinogenesis. Am J Pathol. 1999; 155:1985-1992.
18. Das D, Shah RB and Imperiale MJ. Detection and expression of human BK virus sequences in neoplastic prostate tissues. Oncogene. 2004; 23:7031-7046.
19. Provenzano M, Bracci L, Wyler S, Hudolin T, Sais G, Gosert R, Zajac P, Palu G, Heberer M, Hirsch HH and Spagnoli GC. Characterization of highly frequent epitope-specific CD45RA+/CCR7+/- T lymphocyte responses against p53-binding domains of the human polyomavirus BK large tumor antigen in HLA-A*0201+ BKV-seropositive donors. J Transl Med. 2006; 4:47.
20. Li J, Melenhorst J, Hensel N, Rezvani K, Sconocchia G, Kilical Y, Hou J, Curfman B, Major E and Barrett AJ. T-cell responses to peptide fragments of the BK virus T antigen: implications for cross-reactivity of immune response to JC virus. J Gen Virol. 2006; 87:2951-2960.
21. Ramaswami B, Popescu I, Macedo C, Luo C, Shapiro R, Metes D, Chalasani G and Randhawa PS. The polyomavirus BK large T-antigen-derived peptide elicits an HLA-DR promiscuous and polyfunctional CD4+ T-cell response. Clin Vaccine Immunol. 2011; 18:815-824.
22. Roncarolo MG, Gregori S, Battaglia M, Bacchetta R, Fleischhauer K and Levings MK. Interleukin-10-secreting type 1 regulatory T cells in rodents and humans. Immunol Rev. 2006; 212:28-50.
23. Sato T, Terai M, Tamura Y, Alexeev V, Mastrangelo MJ and Selvan SR. Interleukin 10 in the tumor microenvironment: a target for anticancer immunotherapy. Immunol Res. 2011; 51:170-182.
24. Chen ML, Pittet MJ, Gorelik L, Flavell RA, Weissleder R, von Boehmer H and Khazaie K. Regulatory T cells suppress tumor-specific CD8 T cell cytotoxicity through TGF-beta signals *in vivo*. Proc Natl Acad Sci U S A. 2005; 102:419-424.
25. Mumm JB, Emmerich J, Zhang X, Chan I, Wu L, Mauze S, Blaisdell S, Basham B, Dai J, Grein J, Sheppard C, Hong K, Cutler C, et al. IL-10 elicits IFNgamma-dependent tumor immune surveillance. Cancer Cell. 2011; 20:781-796.
26. Knowles WA, Pipkin P, Andrews N, Vyse A, Minor P, Brown DW and Miller E. Population-based study of antibody to the human polyomaviruses BKV and JCV and the simian polyomavirus SV40. J Med Virol. 2003; 71:115-123.
27. Kean JM, Rao S, Wang M and Garcea RL. Seroepidemiology of human polyomaviruses. PLoS Pathog. 2009; 5:e1000363.
28. Whiteside TL. Immune responses to malignancies. J Allergy Clin Immunol. 2010; 125:S272-283.
29. Zhong S, Randhawa PS, Ikegaya H, Chen Q, Zheng HY, Suzuki M, Takeuchi T, Shibuya A, Kitamura T and Yogo Y. Distribution patterns of BK polyomavirus (BKV) subtypes and subgroups in American, European and Asian populations suggest co-migration of BKV and the human race. J Gen Virol. 2009; 90:144-152.
30. Jelcic I, Aly L, Binder TM, Jelcic I, Bofill-Mas S, Planas R, Demina V, Eiermann TH, Weber T, Girones R, Sospedra M and Martin R. T cell epitope mapping of JC polyoma virus-encoded proteome reveals reduced T cell responses in HLA-DRB1*04:01+ donors. J Virol. 2013; 87:3393-3408.
31. Pastrana DV, Ray U, Magaldi TG, Schowalter RM, Cuburu

N and Buck CB. BK polyomavirus genotypes represent distinct serotypes with distinct entry tropism. J Virol. 2013; 87:10105-10113.

32. Siebrasse EA, Reyes A, Lim ES, Zhao G, Mkakosya RS, Manary MJ, Gordon JI and Wang D. Identification of MW polyomavirus, a novel polyomavirus in human stool. J Virol. 2012; 86:10321-10326.
33. Hrbacek J, Urban M, Hamsikova E, Tachezy R and Heracek J. Thirty years of research on infection and prostate cancer: no conclusive evidence for a link. A systematic review. Urol Oncol. 2013; 31:951-965.
34. Bodaghi S, Comoli P, Bosch R, Azzi A, Gosert R, Leuenberger D, Ginevri F and Hirsch HH. Antibody responses to recombinant polyomavirus BK large T and VP1 proteins in young kidney transplant patients. J Clin Microbiol. 2009; 47:2577-2585.
35. Simon RM, Paik S and Hayes DF. Use of archived specimens in evaluation of prognostic and predictive biomarkers. J Natl Cancer Inst. 2009; 101:1446-1452.
36. Epstein JI, Allsbrook WC, Jr., Amin MB, Egevad LL and ISUP Grading Committee. The 2005 International Society of Urological Pathology (ISUP) Consensus Conference on Gleason Grading of Prostatic Carcinoma. Am J Surg Pathol. 2005; 29:1228-1242.
37. Sobin LH and Wittekind C. TNM: classification of malignant tumours. 6th ed. New York: Wiley-Liss; 2002.
38. Sobin LH, Gospodarowicz MK and Wittekind C. TNM classification of malignant tumours. 7th ed. Chichester: Wiley-Blackwell; 2009.
39. McShane LM, Altman DG, Sauerbrei W, Taube SE, Gion M and Clark GM. Reporting recommendations for tumor marker prognostic studies (REMARK). J Natl Cancer Inst. 2005; 97:1180-1184.
40. Ginevri F, Azzi A, Hirsch HH, Basso S, Fontana I, Cioni M, Bodaghi S, Salotti V, Rinieri A, Botti G, Perfumo F, Locatelli F and Comoli P. Prospective monitoring of polyomavirus BK replication and impact of pre-emptive intervention in pediatric kidney recipients. American journal of transplantation: official journal of the American Society of Transplantation and the American Society of Transplant Surgeons. 2007; 7:2727-2735.
41. Kardas P, Sadeghi M, Weissbach FH, Chen T, Hedman L, Auvinen E, Hedman K and Hirsch HH. Inter- and Intralaboratory Comparison of JC Polyomavirus Antibody Testing Using Two Different Virus-Like Particle-Based Assays. Clin Vaccine Immunol. 2014; 21:1581-1588.
42. Provenzano M, Panelli MC, Mocellin S, Bracci L, Sais G, Stroncek DF, Spagnoli GC and Marincola FM. MHC-peptide specificity and T-cell epitope mapping: where immunotherapy starts. Trends Mol Med. 2006; 12:465-472.
43. Livak KJ and Schmittgen TD. Analysis of relative gene expression data using real-time quantitative PCR and the 2(-Delta Delta C(T)) Method. Methods. 2001; 25:402-408.
44. Blanche P, Dartigues JF and Jacqmin-Gadda H. Estimating and comparing time-dependent areas under receiver operating characteristic curves for censored event times with competing risks. Stat Med. 2013; 32:5381-5397.

Testing of patients undergoing radical prostatectomy from primary prostate cancer for antibodies against BKPyV LTag and VP1 revealed no association between BKPyV VP1 antibody level and the risk of prostate cancer recurrence. That was in contrast to anti-LTag response correlating with the clinical course of prostate cancer patients after radical prostatectomy. Due to oncogenic activity of LTag the increased antibody activity against LTag would be expected in cases with high risk of biochemical recurrence. This study underlines how important is the choice of appropriate antigen in order to give a correct answer to assigned study question.

# 6 Discussion

Although JCPyV and BKPyV infections are usually asymptomatic, both viruses can lead to serious diseases in patients with immune response impairment. JCPyV can cause progressive multifocal leukoencephalopathy (PML) in patients with HIV-AIDS, malignancies or autoimmune diseases under immunosuppressive treatment. Whereas increased BKPyV replication can induce polyomavirus-associated nephropathy (PyVAN) in kidney transplant recipients or hemorrhagic cystitis (PyVHC) after allogeneic hematopoietic stem cell transplantation. Due to more frequent application of immunosuppression, the risk of developing these diseases has increased drastically in the last few decades. Therefore, investigation of JCPyV and BKPyV infection has been receiving significantly more attention.

This thesis addresses the following aspects:

1. Use of virus like particles as a tool to study the fate and innate immune response to primary JCPyV and BKPyV viremia.
2. Optimization of VLP-based ELISA for JCPyV and BKPyV IgG detection.
3. Development of preadsorption inhibition assay in order to precisely define JCPyV and BKPyV IgG serostatus for samples with ambiguous ELISA result.
4. Application of optimized JCPyV/BKPyV VLP-based ELISA in clinical case studies.
5. Investigation of prognostic value of ELISA utilizing either BKPyV VP1 VLPs or BKPyV LTag as antigen.

Clinical models of JCPyV and BKPyV infection are currently lacking. Their initial infection route and organ distribution are also not understood. Following respiratory or gastrointestinal transmission, JCPyV and BKPyV colonize the renourinary tract - the major site of persistence. To reach the renourinary tract, a viremic phase has been postulated, but the fate of JCPyV and BKPyV primary viremia is currently unknown. Like most of HPyV*s*, JCPyV and BKPyV replication is highly specific to the human host, which precludes studies of virus replication in animal models. However, the α2,6-linked and α2,3-linked sialic acid receptors used by JCPyV and BKPyV, respectively, are widespread in vertebrates, including mice. Therefore we decided to study the fate of BKPyV and JCPyV VLPs in blood and their cellular site of uptake in a mouse model (Simon-Santamaria et al., p. 54). Four different VLPs were used: (1) JCPyV wild-type-VP1 VLPs; (2) BKPyV wild-type-VP1 VLPs; (3) JCPyV L55F-VP1 VLPs and (4) JCPyV S269F-VP1 VLPs. The latter two VLPs carry mutations in major capsid protein 1 (VP1) which have been found exclusively in patients with PML (97). These

substitutions affect amino acids located at or close to binding sites for sialic acid structures, which enables viral interactions with cellular receptors and hence viral infectivity (98). Moreover, both mutants, in contrast to wild-type VLPs, lack the ability to trigger hemagglutination. This might suggest that L55F and S269F mutations may influence the cell tropism of JCPyV in human by abrogating the ability to bind to sialylated molecules on a variety of peripheral cell types, but retain the ability to bind CNS glial cells (99). By using above-mentioned VLPs, which are a good model system for virions, we observed that the effective clearance of both JCPyV and BKPyV takes place in liver sinusoidal endothelial cells (LSECs) (2, 355). Some differences between the JCPyV VLPs and BKPyV VLPs clearance patterns were observed. While JCPyV VLPs were almost completely removed from the circulation within 10 minutes, it took significantly longer time for BKPyV VLPs, suggesting either higher stability of BKPyV VLPs in comparison to 3 variants of JCPyV VLPs, a rapid saturation of BKPyV binding receptors or interaction of BKPyV VLPs with blood factors, delaying the blood clearance. Moreover, in natural host cells BKPyV is reported to be internalized via caveolin-mediated endocytosis whereas JCPyV via clathrin-mediated endocytosis (356). This could also be an explanation of our results, because LSECs rely on clathrin-mediated endocytosis to maintain their signature scavenging activity. Despite this efficient clearance mechanism, VLPs still reached the kidney and were efficiently taken up in some microvessels of renal medulla and the spleen marginal zone reticuloendothelium, suggesting a role in viremic organ tropism. It suggests that LSECs may play a key role in the mostly asymptomatic course of primary JCPyV and BKPyV infection, leaving only little virus to escape and reach the renal medulla and possibly the spleen, an important site of viruses persistence. For two PML mutants, L55F and S269F, blood half-life and tissue distribution of VLPs were similar to the wild-type VLPs, which indicate the involvement of non-sialic acid receptors in cellular uptake.

Further studies would be require to establish whether JCPyV or BKPyV uptake in LSECs would lead to destruction of all internalized virus particles, or allow for endosomal escape and intracellular replication of a fraction of the internalized virions. Additionally, a better understanding of LSEC-mediated polyomavirus clearance may shed light into the role of these cells in the development of polyomavirus-associated diseases. This may also allow developing the strategies to harness this process for immunocompromised subjects at risk of high-level polyomavirus replication.

In the next part of the thesis we focused on validation and optimization of virus-like particle (VLPs)-based testing for JCPyV- and BKPyV-specific IgG (Kardas et. al., p. 72).

The diagnosis of JCPyV or BKPyV infection can employ detection of either viral DNA or specific antiviral antibodies. However, it has been shown previously that in some cases DNA detection is not enough sensitive indicator of viral infection, including examples of PML patients with no detectable JCPyV DNA in urine and blood samples or individuals with undetectable urinary JCPyV shedding, albeit with JCPyV-specific antibodies (2, 310, 357, 358). Therefore JCPyV and BKPyV serology has become the critical first choice analysis to classify patients exposed to both viruses. It is also receiving increasing attention as potential predictors of the risk of polyomavirus-associated diseases. Despite the obvious advantages of neutralization, ELISA has become the most common serological testing for detection of JCPyV- and BKPyV-specific antibodies. It usually uses viral capsid protein 1 (VP1) as the antigen for detection of specific anti-JCPyV and anti-BKPyV antibodies. VP1 can be used in the form of monomers, pentamers or VLPs (2). However, it has been confirmed that utilizing VLPs in ELISA makes the assay more sensitive and specific in comparison to ELISA using VP1 either in monomer or pentamer form (2, 325, 359).

The positive JCPyV or BKPyV serostatus indicates not only past exposure, but also viral persistence and the associated risk of high-level replication in case of immune function impairment, resulting eventually in PyV disease (71, 90, 317, 360). Unfortunately correct identification of IgG positive and negative results could be problematic due to lack of universal standardized ELISA procedure, differences in antigen preparation and serum dilutions, empirically derived cutoffs, and lack of WHO-approved international reference serum.

During validation and optimization of virus-like particle (VLPs)-based testing for JCPyV- and BKPyV-specific IgG we demonstrated that although no statistically significant differences in intraassay and interassay variability were revealed for JCPyV serology of 400-fold diluted sera from 400 healthy donors, qualitative differences were seen in the identification of the individual JCPyV serostatus (Kardas et. al., p. 72). By interlaboratory comparison of our ELISA result with results obtained in independent VLP-based assay in Helsinki, discordant JCPyV IgG results have been observed for 10% samples. The discordance resulted from sera with a low IgG activity close to the cutoffs of both assays. Performance of normalization to a reference serum was shown to improve the overall assay performance by reducing the rate of discordance. Since the discordances in this low OD range could still be caused by false-positive (e.g. cross-reactive) or false-negative (e.g. low IgG) results, we developed preadsorption assay to better verify the serostatus of discordant samples. By reduction in JCPyV IgG activity after preincubation with JCPyV VLPs and cutoff of 35%, we were able to

solve the serostatus for previously discordant samples. Importantly, we also excluded BKPyV antibody cross-reactivity by testing JCPyV IgG positive sera in preadsorption with BKPyV VLPs and observing IgG inhibition at low 8% level. In conclusion, our findings demonstrate that serological assays for JCPyV IgG need to take under consideration whether epidemiological questions or individual risk assessments are to be addressed. We confirmed that VLP-based ELISA with normalization step can serve as a reliable tool for JCPyV IgG serology. Additionally, the preadsorption assay can help with unequivocal determination of JCPyV serostatus for samples with low IgG levels.

Further, we reinvestigated the performance of our normalized VLP-based assay and adapted it to BKPyV IgG detection (Kardas et al., p. 82). To find the best testing conditions, each serum from 400 healthy blood donors was tested at 100-, 200- and 400-fold dilutions. We observed that 1:200 dilution provided the best trade-off between sensitivity and specificity with respective values being 98.3% and 97.5% for JCPyV IgG, and 100% and 98% for BKPyV IgG. Thus, the 1:200 dilution in the normalized ELISA format might be the most appropriate for seroepidemiological studies when large sample size is considered. The 1:100 dilution provided the highest sensitivity for JCPyV and BKPyV IgG detection and no false-negative results. If combined with preadsorption reduction for confirmation, this approach might be the most suitable for individual patient counseling. The 1:400 dilution can provide first approximation of higher and lower JCPyV- and BKPyV-specific IgG levels. As relative antibody levels and their change over time should be explored in clinical settings, this dilution seems to be appropriate for specific clinical setting including intrathecal antibodies or pretransplant serology (105, 361, 362). With this study we showed that for seroepidemiology studies, normalized JCPyV and BKPyV IgG ELISA at 1:200 serum dilution provides optimal sensitivity and specificity with the lowest false-positive and false-negative rate. However, for individual risk assessment, 100-, 200-, and 400-fold dilutions combined with preadsorption for low-reactive sera might be the most appropriate.

Next, our normalized VLP-based ELISA was applied to investigate JCPyV and BKPyV seroprevalence in clinical case studies: (1) positive JCPyV IgG serostatus for PML patient was in line with other PML symptoms including high level of JCPyV DNA detected in cerebrospinal fluid (CSF), NCCR mutations characteristic for PML and brain lesions shown by magnetic resonance imaging (MRI) (Kurmann et al., p. 90); (2) positive JCPyV IgG and IgM and negative BKPyV IgG and IgM serostatus for a boy after kidney transplantation confirmed the diagnosis of JCPyV-associated nephropathy (Lautenschlager et al., p. 99); (3) testing of 122 immunocompetent and 63 immunocompromised patients demonstrated age

dependency of BKPyV IgG level, with the highest values between 20 and 30 years (Schmidt et al., p. 106); (4) positive BKPyV IgG serostatus for serum samples from pediatric allogeneic hematopoietic stem cell transplant patient was in accordance with a significant BKPyV viruria and viremia and start of PyVHC (Koskenvuo et al., p. 119).

As a conclusion of this part of the thesis, our findings demonstrate that serological assays for JCPyV and BKPyV need to take into account whether epidemiological questions or individual risk assessments need to be addressed. Testing of serum sample in 100-, 200-, and 400-fold dilution series in a normalized VLP ELISA provides a convenient determination of JCPyV and BKPyV-specific antibody status and levels. Additionally, preadsorption assay could be applied to low-level antibody sera in order to rule out false-positives, and therefore avoid unnecessary withholding of an effective treatment option, and false-negatives, for better estimation of the risk of PyV-associated diseases.

For future investigation of unknown sera samples the following conditions are suggested to be fulfilled: (1) sample should be tested in at least duplicates to avoid technical errors; (2) every ELISA should include reference serum for results normalization; (3) samples with low IgG activities should be additionally tested in preadsorption assay. Quality assessment programs with appropriate training for laboratory technicians would be recommended in order to globally standardize the ELISA performance and antigen preparation. Moreover, reference sera approved by WHO might significantly enhance testing reproducibility and permit clarification of potential role of PyV serology in clinical practice.

T cell immunity to polyomaviruses has been studied mostly for large T antigen (LTag) and capsid protein VP1 (285-297). Both proteins are good ELISA antigen candidates due to their immunogenicity and capability to stimulate B cell responses (298). Therefore we decided to use both proteins as antigens in ELISA for screening of BKPyV IgG response among 226 patients undergoing radical prostatectomy from primary prostate cancer (Keller et al., p. 125). We evaluated whether the preoperative antibody responses to BKPyV LTag and VP1 were associated with the risk of biochemical recurrence of prostate cancer. No evidence for an association between BKPyV VP1 serostatus and the risk of prostate cancer recurrence was observed. However, an antibody response to LTag was associated with the clinical course of prostate cancer patients after radical prostatectomy. Due to the fact that LTag may lead to the oncogenic transformation of BKPyV infected glandular prostate cells, an increased antibody activity against this oncogenic protein would be expected in cases with high risk of biochemical recurrence. In this study we revealed that the preoperative LTag serology may be a valuable biomarker for a prediction of favorable prostate cancer

prognosis after radical prostatectomy. Finally, this study underlines how important is to choose an antigen which will be adequate to assigned study question.

# 7 References


1. Johne R, Buck CB, Allander T, Atwood WJ, Garcea RL, Imperiale MJ, Major EO, Ramqvist T, and Norkin LC. Taxonomical developments in the family Polyomaviridae. *Archives of virology.* 2011;156(9):1627-34.
2. Hirsch HH, Kardas P, Kranz D, and Leboeuf C. The human JC polyomavirus (JCPyV): virological background and clinical implications. *APMIS : acta pathologica, microbiologica, et immunologica Scandinavica.* 2013;121(685–727.
3. Zurhein G, and Chou SM. Particles Resembling Papova Viruses in Human Cerebral Demyelinating Disease. *Science.* 1965;148(1477-9.
4. Gardner SD, Field AM, Coleman DV, and Hulme B. New human papovavirus (B.K.) isolated from urine after renal transplantation. *Lancet.* 1971;1(7712):1253-57.
5. Garcea RL, and Imperiale MJ. Simian virus 40 infection of humans. *J Virol.* 2003;77(9):5039-45.
6. Coursaget P, Mahtab S, Nicol JTJ, Gardair C, and Touzé A. Human Merkel cell polyomavirus: virological background and clinical implications. *APMIS : acta pathologica, microbiologica, et immunologica Scandinavica.* 2013;121(755–69.
7. van der Meijden E, Janssens RW, Lauber C, Bouwes Bavinck JN, Gorbalenya AE, and Feltkamp MC. Discovery of a new human polyomavirus associated with trichodysplasia spinulosa in an immunocompromized patient. *PLoS Pathog.* 2010;6(7):e1001024.
8. Schowalter RM, Pastrana DV, Pumphrey KA, Moyer AL, and Buck CB. Merkel cell polyomavirus and two previously unknown polyomaviruses are chronically shed from human skin. *Cell Host Microbe.* 2010;7(6):509-15.
9. Scuda N, Hofmann J, Calvignac-Spencer S, Ruprecht K, Liman P, Kuhn J, Hengel H, and Ehlers B. A novel human polyomavirus closely related to the african green monkey-derived lymphotropic polyomavirus. *J Virol.* 2011;85(9):4586-90.
10. Buck CB, Phan GQ, Raiji MT, Murphy PM, McDermott DH, and McBride AA. Complete genome sequence of a tenth human polyomavirus. *J Virol.* 2012;86(19):10887.
11. Korup S, Rietscher J, Calvignac-Spencer S, Trusch F, Hofmann J, Moens U, Sauer I, Voigt S, Schmuck R, and Ehlers B. Identification of a novel human polyomavirus in organs of the gastrointestinal tract. *PloS one.* 2013;8(3):e58021.

12. Mishra N, Pereira M, Rhodes RH, An P, Pipas JM, Jain K, Kapoor A, Briese T, Faust PL, and Lipkin WI. Identification of a novel polyomavirus in a pancreatic transplant recipient with retinal blindness and vasculitic myopathy. *The Journal of infectious diseases.* 2014;210(10):1595-9.
13. Babakir-Mina M, Ciccozzi M, Perno CF, and Ciotti M. The human polyomaviruses KI and WU: Virological background and clinical implications. *APMIS : acta pathologica, microbiologica, et immunologica Scandinavica.* 2013;121(746–54.
14. Knowles WA, Pipkin P, Andrews N, Vyse A, Minor P, Brown DW, and Miller E. Population-based study of antibody to the human polyomaviruses BKV and JCV and the simian polyomavirus SV40. *J Med Virol.* 2003;71(1):115-23.
15. Egli A, Infanti L, Dumoulin A, Buser A, Samaridis J, Stebler C, Gosert R, and Hirsch HH. Prevalence of Polyomavirus BK and JC Infection and Replication in 400 Healthy Blood Donors. *The Journal of infectious diseases.* 2009;199(837-46.
16. Kean JM, Rao S, Wang M, and Garcea RL. Seroepidemiology of human polyomaviruses. *PLoS Pathog.* 2009;5(3):e1000363.
17. Nicol JT, Robinot R, Carpentier A, Carandina G, Mazzoni E, Tognon M, Touze A, and Coursaget P. Age-specific seroprevalences of merkel cell polyomavirus, human polyomaviruses 6, 7, and 9, and trichodysplasia spinulosa-associated polyomavirus. *Clinical and vaccine immunology : CVI.* 2013;20(3):363-8.
18. Rinaldo CH, and Hirsch HH. The human polyomaviruses: from orphans and mutants to patchwork family. *APMIS : acta pathologica, microbiologica, et immunologica Scandinavica.* 2013;121(681–4.
19. Imperiale MJ, Major, E.O. In: Knipe DM, Howley, P.M. ed. *Fields Virology*. Philadelphia, PA, USA: Lippincott Williams & Wilkins, Wolters Kluwer; 2007:2263-98.
20. Shishido-Hara Y, Ichinose S, Higuchi K, Hara Y, and Yasui K. Major and minor capsid proteins of human polyomavirus JC cooperatively accumulate to nuclear domain 10 for assembly into virions. *J Virol.* 2004;78(18):9890-903.
21. Gasparovic ML, Gee GV, and Atwood WJ. JC virus minor capsid proteins Vp2 and Vp3 are essential for virus propagation. *J Virol.* 2006;80(21):10858-61.
22. Frisque RJ, Bream GL, and Cannella MT. Human polyomavirus JC virus genome. *J Virol.* 1984;51(2):458-69.
23. Moens U, and Rekvig OP. In: Kamel Khalili GLS ed. *Human Polyomaviruses: Molecular and Clinical Perspectives*. Wiley; 2001.

24. Gerits N, and Moens U. Agnoprotein of mammalian polyomaviruses. *Virology.* 2012;432(2):316-26.
25. Unterstab G, Gosert R, Leuenberger D, Lorentz P, Rinaldo CH, and Hirsch HH. The polyomavirus BK agnoprotein co-localizes with lipid droplets. *Virology.* 2010;399(2):322-31.
26. Agostini HT, Deckhut A, Jobes DV, Girones R, Schlunck G, Prost MG, Frias C, Perez-Trallero E, Ryschkewitsch CF, and Stoner GL. Genotypes of JC virus in East, Central and Southwest Europe. *J Gen Virol.* 2001;82(Pt 5):1221-331.
27. Yogo Y, Sugimoto C, Zheng HY, Ikegaya H, Takasaka T, and Kitamura T. JC virus genotyping offers a new paradigm in the study of human populations. *Rev Med Virol.* 2004;14(3):179-91.
28. Ikegaya H, Iwase H, Zheng HY, Nakajima M, Sakurada K, Takatori T, Fukayama M, Kitamura T, and Yogo Y. JC virus genotyping using formalin-fixed, paraffin-embedded renal tissues. *J Virol Methods.* 2005;126(1-2):37-43.
29. Rinaldo CH, Tylden GD, and Sharma BN. The human polyomavirus BK (BKPyV): virological background and clinical implications. *APMIS : acta pathologica, microbiologica, et immunologica Scandinavica.* 2013;121(728–45.
30. Pastrana DV, Ray U, Magaldi TG, Schowalter RM, Cuburu N, and Buck CB. BK polyomavirus genotypes represent distinct serotypes with distinct entry tropism. *J Virol.* 2013;87(18):10105-13.
31. Pastrana DV, Brennan DC, Cuburu N, Storch GA, Viscidi RP, Randhawa PS, and Buck CB. Neutralization serotyping of BK polyomavirus infection in kidney transplant recipients. *PLoS Pathog.* 2012;8(4):e1002650.
32. Baksh FK, Finkelstein SD, Swalsky PA, Stoner GL, Ryschkewitsch CF, and Randhawa P. Molecular genotyping of BK and JC viruses in human polyomavirus-associated interstitial nephritis after renal transplantation. *Am J Kidney Dis.* 2001;38(2):354-65.
33. Randhawa PS, Vats A, Zygmunt D, Swalsky P, Scantlebury V, Shapiro R, and Finkelstein S. Quantitation of viral DNA in renal allograft tissue from patients with BK virus nephropathy. *Transplantation.* 2002;74(4):485-8.
34. Luo C, Bueno M, Kant J, Martinson J, and Randhawa P. Genotyping Schemes for Polyomavirus BK using Gene Specific Phylogenetic Trees and SNP Analysis. *J Virol.* 2008;24(24.

35. Zheng HY, Nishimoto Y, Chen Q, Hasegawa M, Zhong S, Ikegaya H, Ohno N, Sugimoto C, Takasaka T, Kitamura T, et al. Relationships between BK virus lineages and human populations. *Microbes Infect.* 2007;9(2):204-13.

36. Nishimoto Y, Takasaka T, Hasegawa M, Zheng HY, Chen Q, Sugimoto C, Kitamura T, and Yogo Y. Evolution of BK virus based on complete genome data. *J Mol Evol.* 2006;63(3):341-52.

37. Elphick GF, Querbes W, Jordan JA, Gee GV, Eash S, Manley K, Dugan A, Stanifer M, Bhatnagar A, Kroeze WK, et al. The human polyomavirus, JCV, uses serotonin receptors to infect cells. *Science.* 2004;306(5700):1380-3.

38. Ravichandran V, and Major EO. Viral proteomics: a promising approach for understanding JC virus tropism. *Proteomics.* 2006;6(20):5628-36.

39. Grinnell BW, Padgett BL, and Walker DL. Distribution of nonintegrated DNA from JC papovavirus in organs of patients with progressive multifocal leukoencephalopathy. *The Journal of infectious diseases.* 1983;147(4):669-75.

40. Eash S, Tavares R, Stopa EG, Robbins SH, Brossay L, and Atwood WJ. Differential distribution of the JC virus receptor-type sialic acid in normal human tissues. *Am J Pathol.* 2004;164(2):419-28.

41. Bayliss J, Karasoulos T, and McLean CA. Frequency and large T (LT) sequence of JC polyomavirus DNA in oligodendrocytes, astrocytes and granular cells in non-PML brain. *Brain Pathol.* 2012;22(3):329-36.

42. Dugan AS, Gasparovic ML, and Atwood WJ. Direct correlation between sialic acid binding and infection of cells by two human polyomaviruses (JC virus and BK virus). *J Virol.* 2008;82(5):2560-4.

43. Komagome R, Sawa H, Suzuki T, Suzuki Y, Tanaka S, Atwood WJ, and Nagashima K. Oligosaccharides as receptors for JC virus. *J Virol.* 2002;76(24):12992-3000.

44. Querbes W, O'Hara BA, Williams G, and Atwood WJ. Invasion of host cells by JC virus identifies a novel role for caveolae in endosomal sorting of noncaveolar ligands. *J Virol.* 2006;80(19):9402-13.

45. Low JA, Magnuson B, Tsai B, and Imperiale MJ. Identification of gangliosides GD1b and GT1b as receptors for BK virus. *J Virol.* 2006;80(3):1361-6.

46. Dugan AS, Eash S, and Atwood WJ. An N-linked glycoprotein with alpha(2,3)-linked sialic acid is a receptor for BK virus. *J Virol.* 2005;79(22):14442-5.

47. Tsai B, and Inoue T. A virus takes an "L" turn to find its receptor. *Cell Host Microbe.* 2010;8(4):301-2.

48. Dugan AS, Eash S, and Atwood WJ. Update on BK virus entry and intracellular trafficking. *Transpl Infect Dis.* 2006;8(2):62-7.

49. Jiang M, Abend JR, Tsai B, and Imperiale MJ. Early events during BK virus entry and disassembly. *J Virol.* 2009;83(3):1350-8.

50. Eash S, Querbes W, and Atwood WJ. Infection of vero cells by BK virus is dependent on caveolae. *J Virol.* 2004;78(21):11583-90.

51. Bastiani M, and Parton RG. Caveolae at a glance. *Journal of cell science.* 2010;123(Pt 22):3831-6.

52. Martin S, and Parton RG. Caveolin, cholesterol, and lipid bodies. *Semin Cell Dev Biol.* 2005;16(2):163-74.

53. Nelson CD, Derdowski A, Maginnis MS, O'Hara BA, and Atwood WJ. The VP1 subunit of JC polyomavirus recapitulates early events in viral trafficking and is a novel tool to study polyomavirus entry. *Virology.* 2012;428(1):30-40.

54. Lilley BN, and Ploegh HL. A membrane protein required for dislocation of misfolded proteins from the ER. *Nature.* 2004;429(6994):834-40.

55. Lilley BN, Gilbert JM, Ploegh HL, and Benjamin TL. Murine polyomavirus requires the endoplasmic reticulum protein Derlin-2 to initiate infection. *J Virol.* 2006;80(17):8739-44.

56. Schelhaas M, Malmstrom J, Pelkmans L, Haugstetter J, Ellgaard L, Grunewald K, and Helenius A. Simian Virus 40 depends on ER protein folding and quality control factors for entry into host cells. *Cell.* 2007;131(3):516-29.

57. Pante N, and Kann M. Nuclear pore complex is able to transport macromolecules with diameters of about 39 nm. *Molecular biology of the cell.* 2002;13(2):425-34.

58. Ishaq M, and Stoner GL. Differential expression of mRNAs for JC virus large and small tumor antigens in brain tissues from progressive multifocal leukoencephalopathy patients with and without AIDS. *Proc Natl Acad Sci U S A.* 1994;91(17):8283-7.

59. Bollag B, Hofstetter CA, Reviriego-Mendoza MM, and Frisque RJ. JC virus small T antigen binds phosphatase PP2A and Rb family proteins and is required for efficient viral DNA replication activity. *PloS one.* 2010;5(5):e10606.

60. Orba Y, Suzuki T, Makino Y, Kubota K, Tanaka S, Kimura T, and Sawa H. Large T antigen promotes JC virus replication in G2-arrested cells by inducing ATM- and ATR-mediated G2 checkpoint signaling. *The Journal of biological chemistry.* 2010;285(2):1544-54.

61. Simmons DT. SV40 large T antigen functions in DNA replication and transformation. *Adv Virus Res.* 2000;55(75-134.

62. Harris KF, Christensen JB, and Imperiale MJ. BK virus large T antigen: interactions with the retinoblastoma family of tumor suppressor proteins and effects on cellular growth control. *J Virol.* 1996;70(4):2378-86.

63. Khalili K, Gordon J, and White MK. The polyomavirus, JCV and its involvement in human disease. *Adv Exp Med Biol.* 2006;577(274-87.

64. Bullock PA, Seo YS, and Hurwitz J. Initiation of simian virus 40 DNA synthesis in vitro. *Mol Cell Biol.* 1991;11(5):2350-61.

65. Fairman M, Prelich G, Tsurimoto T, and Stillman B. Identification of cellular components required for SV40 DNA replication in vitro. *Biochim Biophys Acta.* 1988;951(2-3):382-7.

66. Fanning E, and Zhao K. SV40 DNA replication: from the A gene to a nanomachine. *Virology.* 2009;384(2):352-9.

67. Stolt A, Sasnauskas K, Koskela P, Lehtinen M, and Dillner J. Seroepidemiology of the human polyomaviruses. *J Gen Virol.* 2003;84(Pt 6):1499-504.

68. Carruthers RL, and Berger J. Progressive multifocal leukoencephalopathy and JC Virus-related disease in modern neurology practice. *Mult Scler Relat Disord.* 2014;3(4):419-30.

69. Gorelik L, Lerner M, Bixler S, Crossman M, Schlain B, Simon K, Pace A, Cheung A, Chen LL, Berman M, et al. Anti-JC virus antibodies: implications for PML risk stratification. *Ann Neurol.* 2010;68(3):295-303.

70. Lautenschlager I, Jahnukainen T, Kardas P, Lohi J, Auvinen E, Mannonen L, Dumoulin A, Hirsch HH, and Jalanko H. A Case of Primary JC Polyomavirus Infection-Associated Nephropathy. *American journal of transplantation : official journal of the American Society of Transplantation and the American Society of Transplant Surgeons.* 2014;14(12):2887-92.

71. Viscidi RP, Khanna N, Tan CS, Li X, Jacobson L, Clifford DB, Nath A, Margolick JB, Shah KV, Hirsch HH, et al. JC virus antibody and viremia as predictors of progressive multifocal leukoencephalopathy in human immunodeficiency virus-1-infected individuals. *Clinical infectious diseases : an official publication of the Infectious Diseases Society of America.* 2011;53(7):711-5.

72. Wuthrich C, Kesari S, Kim WK, Williams K, Gelman R, Elmeric D, De Girolami U, Joseph JT, Hedley-Whyte T, and Koralnik IJ. Characterization of lymphocytic

infiltrates in progressive multifocal leukoencephalopathy: co-localization of CD8(+) T cells with JCV-infected glial cells. *J Neurovirol.* 2006;12(2):116-28.

73. Gheuens S, Wuthrich C, and Koralnik IJ. Progressive multifocal leukoencephalopathy: why gray and white matter. *Annu Rev Pathol.* 2013;8(189-215.

74. Wuthrich C, Popescu BF, Gheuens S, Marvi M, Ziman R, Denq SP, Tham M, Norton E, Parisi JE, Dang X, et al. Natalizumab-associated progressive multifocal leukoencephalopathy in a patient with multiple sclerosis: a postmortem study. *J Neuropathol Exp Neurol.* 2013;72(11):1043-51.

75. Berger JR. Progressive multifocal leukoencephalopathy. *Handbook of clinical neurology.* 2014;123(357-76.

76. Mateen FJ, Muralidharan R, Carone M, van de Beek D, Harrison DM, Aksamit AJ, Gould MS, Clifford DB, and Nath A. Progressive multifocal leukoencephalopathy in transplant recipients. *Ann Neurol.* 2011;70(2):305-22.

77. Hatchwell E. Is there a (host) genetic predisposition to progressive multifocal leukoencephalopathy? *Front Immunol.* 2015;6(216.

78. Bellaguarda E, Keyashian K, Pekow J, Rubin DT, Cohen RD, and Sakuraba A. Prevalence of Antibodies Against JC Virus in Serum of Patients With Refractory Crohn's Disease and Effects of Natalizumab Therapy. *Clin Gastroenterol Hepatol.* 2015.

79. Alroughani R, Aref H, Bohlega S, Sherooqi IA, Dahdaleh M, Feki I, Jumah MA, Al-Kawi M, Koussa S, and Yamout B. Natalizumab treatment for multiple sclerosis: Middle East and North Africa regional recommendations for patient selection and monitoring. *Mult Scler Relat Disord.* 2014;3(6):753-4.

80. Wittmann T, Horowitz N, Benyamini N, Henig I, Zuckerman T, Rowe JM, Kra-Oz Z, Szwarcwort Cohen M, Oren I, and Avivi I. JC polyomavirus reactivation is common following allogeneic stem cell transplantation and its preemptive detection may prevent lethal complications. *Bone marrow transplantation.* 2015.

81. Verheyen J, Maizus K, Feist E, Tolman Z, Knops E, Saech J, Spengler L, Waterboer T, Burmester GR, Pawlita M, et al. Increased frequency of JC-polyomavirus detection in rheumatoid arthritis patients treated with multiple biologics. *Med Microbiol Immunol.* 2015.

82. Molloy ES, and Calabrese LH. Progressive multifocal leukoencephalopathy: a national estimate of frequency in systemic lupus erythematosus and other rheumatic diseases. *Arthritis and rheumatism.* 2009;60(12):3761-5.

83. Arkema EV, van Vollenhoven RF, and Askling J. Incidence of progressive multifocal leukoencephalopathy in patients with rheumatoid arthritis: a national population-based study. *Annals of the rheumatic diseases.* 2012;71(11):1865-7.

84. Bharat A, Xie F, Baddley JW, Beukelman T, Chen L, Calabrese L, Delzell E, Grijalva CG, Patkar NM, Saag K, et al. Incidence and risk factors for progressive multifocal leukoencephalopathy among patients with selected rheumatic diseases. *Arthritis care & research.* 2012;64(4):612-5.

85. Khanna N, Elzi, L., Mueller, N.J., Garzoni, C., Cavassini, M., Fux, C.A., Vernazza, P., Bernasconi, E., Battegay, M., Hirsch, H.H., for the Swiss HIV Cohort Study. Incidence and Outcome of Progressive Multifocal Leukoencephalopathy in 20 years of the Swiss HIV Cohort Study. *Clinical Infectious Diseases.* 2009;48(1459-66.

86. Engsig FN, Hansen AB, Omland LH, Kronborg G, Gerstoft J, Laursen AL, Pedersen C, Mogensen CB, Nielsen L, and Obel N. Incidence, clinical presentation, and outcome of progressive multifocal leukoencephalopathy in HIV-infected patients during the highly active antiretroviral therapy era: a nationwide cohort study. *The Journal of infectious diseases.* 2009;199(1):77-83.

87. Clifford DB, Ances B, Costello C, Rosen-Schmidt S, Andersson M, Parks D, Perry A, Yerra R, Schmidt R, Alvarez E, et al. Rituximab-associated progressive multifocal leukoencephalopathy in rheumatoid arthritis. *Archives of neurology.* 2011;68(9):1156-64.

88. Bloomgren G, Richman S, Hotermans C, Subramanyam M, Goelz S, Natarajan A, Lee S, Plavina T, Scanlon JV, Sandrock A, et al. Risk of natalizumab-associated progressive multifocal leukoencephalopathy. *The New England journal of medicine.* 2012;366(20):1870-80.

89. Sindic CJ, Trebst C, Van Antwerpen MP, Frye S, Enzensberger W, Hunsmann G, Luke W, and Weber T. Detection of CSF-specific oligoclonal antibodies to recombinant JC virus VP1 in patients with progressive multifocal leukoencephalopathy. *J Neuroimmunol.* 1997;76(1-2):100-4.

90. Khanna N, Wolbers M, Mueller NJ, Garzoni C, Du Pasquier RA, Fux CA, Vernazza P, Bernasconi E, Viscidi R, Battegay M, et al. JC virus-specific immune responses in human immunodeficiency virus type 1 patients with progressive multifocal leukoencephalopathy. *J Virol.* 2009;83(9):4404-11.

91. Ferenczy MW, Marshall LJ, Nelson CD, Atwood WJ, Nath A, Khalili K, and Major EO. Molecular Biology, Epidemiology, and Pathogenesis of Progressive Multifocal

Leukoencephalopathy, the JC Virus-Induced Demyelinating Disease of the Human Brain. *Clinical microbiology reviews.* 2012;25(3):471-506.

92. Gosert R, Kardas P, Major EO, and Hirsch HH. Rearranged JC virus noncoding control regions found in progressive multifocal leukoencephalopathy patient samples increase virus early gene expression and replication rate. *J Virol.* 2010;84(20):10448-56.

93. Jensen PN, and Major EO. A classification scheme for human polyomavirus JCV variants based on the nucleotide sequence of the noncoding regulatory region. *J Neurovirol.* 2001;7(4):280-7.

94. Agostini HT, Ryschkewitsch CF, Singer EJ, and Stoner GL. JC virus regulatory region rearrangements and genotypes in progressive multifocal leukoencephalopathy: two independent aspects of virus variation. *J Gen Virol.* 1997;78 ( Pt 3)(659-64.

95. Ault GS, and Stoner GL. Human polyomavirus JC promoter/enhancer rearrangement patterns from progressive multifocal leukoencephalopathy brain are unique derivatives of a single archetypal structure. *J Gen Virol.* 1993;74 ( Pt 8)(1499-507.

96. Nakamichi K, Kishida S, Tanaka K, Suganuma A, Sano Y, Sano H, Kanda T, Maeda N, Kira J, Itoh A, et al. Sequential changes in the non-coding control region sequences of JC polyomaviruses from the cerebrospinal fluid of patients with progressive multifocal leukoencephalopathy. *Archives of virology.* 2013;158(3):639-50.

97. Maginnis MS, Stroh LJ, Gee GV, O'Hara BA, Derdowski A, Stehle T, and Atwood WJ. Progressive multifocal leukoencephalopathy-associated mutations in the JC polyomavirus capsid disrupt lactoseries tetrasaccharide c binding. *mBio.* 2013;4(3):e00247-13.

98. Sunyaev SR, Lugovskoy A, Simon K, and Gorelik L. Adaptive mutations in the JC virus protein capsid are associated with progressive multifocal leukoencephalopathy (PML). *PLoS Genet.* 2009;5(2):e1000368.

99. Gorelik L, Reid C, Testa M, Brickelmaier M, Bossolasco S, Pazzi A, Bestetti A, Carmillo P, Wilson E, McAuliffe M, et al. Progressive multifocal leukoencephalopathy (PML) development is associated with mutations in JC virus capsid protein VP1 that change its receptor specificity. *The Journal of infectious diseases.* 2011;204(1):103-14.

100. Reid CE, Li H, Sur G, Carmillo P, Bushnell S, Tizard R, McAuliffe M, Tonkin C, Simon K, Goelz S, et al. Sequencing and analysis of JC virus DNA from natalizumab-treated PML patients. *The Journal of infectious diseases.* 2011;204(2):237-44.

101. Hirsch HH, Meylan PR, Zimmerli W, Iten A, Battegay M, and Erb P. HIV-1-infected patients with focal neurologic signs: diagnostic role of PCR for Toxoplasma gondii, Epstein-Barr virus, and JC virus. *Clin Microbiol Infect.* 1998;4(10):577-84.

102. Cinque P, Koralnik IJ, and Clifford DB. The evolving face of human immunodeficiency virus-related progressive multifocal leukoencephalopathy: defining a consensus terminology. *J Neurovirol.* 2003;9 Suppl 1(88-92.

103. Del Valle L, Enam S, Lara C, Ortiz-Hidalgo C, Katsetos CD, and Khalili K. Detection of JC polyomavirus DNA sequences and cellular localization of T-antigen and agnoprotein in oligodendrogliomas. *Clin Cancer Res.* 2002;8(11):3332-40.

104. Crowder CD, Gyure KA, Drachenberg CB, Werner J, Morales RE, Hirsch HH, and Ramos E. Successful outcome of progressive multifocal leukoencephalopathy in a renal transplant patient. *American journal of transplantation : official journal of the American Society of Transplantation and the American Society of Transplant Surgeons.* 2005;5(5):1151-8.

105. Kuhle J, Gosert R, Buhler R, Derfuss T, Sutter R, Yaldizli O, Radue EW, Ryschkewitsch C, Major EO, Kappos L, et al. Management and outcome of CSF-JC virus PCR-negative PML in a natalizumab-treated patient with MS. *Neurology.* 2011;77(23):2010-6.

106. Balduzzi A, Lucchini G, Hirsch HH, Basso S, Cioni M, Rovelli A, Zincone A, Grimaldi M, Corti P, Bonanomi S, et al. Polyomavirus JC-targeted T-cell therapy for progressive multiple leukoencephalopathy in a hematopoietic cell transplantation recipient. *Bone marrow transplantation.* 2011;46(7):987-92.

107. Hall CD, Dafni U, Simpson D, Clifford D, Wetherill PE, Cohen B, McArthur J, Hollander H, Yainnoutsos C, Major E, et al. Failure of cytarabine in progressive multifocal leukoencephalopathy associated with human immunodeficiency virus infection. AIDS Clinical Trials Group 243 Team. *The New England journal of medicine.* 1998;338(19):1345-51.

108. De Luca A, Pezzotti, P., Gasnault, J., Cinque, P., Berenguer, J., Di Giambenedetto, S., Cingolani, A., Taofik, Y., Pedale, R., Miralles, P., Larussa, D., Sinha, S., Cauda, R., Marra, C. M., Ammassari, A., and Antinori, A. Survival and neurological outcome with or without cidofovir (CDV) in AIDS-related progressive multifocal leukoencephalopathy (PML) on HAART: A multicohort analysis. *J Neurovirol.* 2005;11 ((S2)):S16-S124.

109. De Luca A, Ammassari A, Pezzotti P, Cinque P, Gasnault J, Berenguer J, Di Giambenedetto S, Cingolani A, Taoufik Y, Miralles P, et al. Cidofovir in addition to

antiretroviral treatment is not effective for AIDS-associated progressive multifocal leukoencephalopathy: a multicohort analysis. *Aids.* 2008;22(14):1759-67.

110. Pohlmann C, Hochauf K, Rollig C, Schetelig J, Wunderlich O, Bandt D, Ehninger G, Jacobs E, and Rohayem J. Chlorpromazine combined with cidofovir for treatment of a patient suffering from progressive multifocal leukoencephalopathy. *Intervirology.* 2007;50(6):412-7.

111. Lanzafame M, Ferrari S, Lattuada E, Corsini F, Deganello R, Vento S, and Concia E. Mirtazapine in an HIV-1 infected patient with progressive multifocal leukoencephalopathy. *Le infezioni in medicina : rivista periodica di eziologia, epidemiologia, diagnostica, clinica e terapia delle patologie infettive.* 2009;17(1):35-7.

112. Park JH, Ryoo S, Noh HJ, Seo JM, Kang HH, Shin JS, Seo SW, and Na DL. Dual therapy with cidofovir and mirtazapine for progressive multifocal leukoencephalopathy in a sarcoidosis patient. *Case reports in neurology.* 2011;3(3):258-62.

113. Gosert R, Rinaldo CH, Wernli M, Major EO, and Hirsch HH. CMX001 (1-O-hexadecyloxypropyl-cidofovir) inhibits polyomavirus JC replication in human brain progenitor-derived astrocytes. *Antimicrobial agents and chemotherapy.* 2011;55(5):2129-36.

114. Koralnik IJ, Wuthrich C, Dang X, Rottnek M, Gurtman A, Simpson D, and Morgello S. JC virus granule cell neuronopathy: A novel clinical syndrome distinct from progressive multifocal leukoencephalopathy. *Ann Neurol.* 2005;57(4):576-80.

115. Du Pasquier RA, Corey S, Margolin DH, Williams K, Pfister LA, De Girolami U, Mac Key JJ, Wuthrich C, Joseph JT, and Koralnik IJ. Productive infection of cerebellar granule cell neurons by JC virus in an HIV+ individual. *Neurology.* 2003;61(6):775-82.

116. Dang X, Vidal JE, Oliveira AC, Simpson DM, Morgello S, Hecht JH, Ngo LH, and Koralnik IJ. JC virus granule cell neuronopathy is associated with VP1 C terminus mutants. *J Gen Virol.* 2012;93(Pt 1):175-83.

117. Dang X, and Koralnik IJ. A granule cell neuron-associated JC virus variant has a unique deletion in the VP1 gene. *J Gen Virol.* 2006;87(Pt 9):2533-7.

118. Wuthrich C, Dang X, Westmoreland S, McKay J, Maheshwari A, Anderson MP, Ropper AH, Viscidi RP, and Koralnik IJ. Fulminant JC virus encephalopathy with productive infection of cortical pyramidal neurons. *Ann Neurol.* 2009;65(6):742-8.

119. Behzad-Behbahani A, Klapper PE, Vallely PJ, Cleator GM, and Bonington A. BKV-DNA and JCV-DNA in CSF of patients with suspected meningitis or encephalitis. *Infection.* 2003;31(6):374-8.

120. Blake K, Pillay D, Knowles W, Brown DW, Griffiths PD, and Taylor B. JC virus associated meningoencephalitis in an immunocompetent girl. *Archives of disease in childhood.* 1992;67(7):956-7.

121. Tan CS, and Koralnik IJ. Progressive multifocal leukoencephalopathy and other disorders caused by JC virus: clinical features and pathogenesis. *Lancet neurology.* 2010;9(4):425-37.

122. Drachenberg CB, Hirsch HH, Papadimitriou JC, Gosert R, Wali RK, Munivenkatappa R, Nogueira J, Cangro CB, Haririan A, Mendley S, et al. Polyomavirus BK versus JC replication and nephropathy in renal transplant recipients: a prospective evaluation. *Transplantation.* 2007;84(3):323-30.

123. Kazory A, Ducloux D, Chalopin JM, Angonin R, Fontaniere B, and Moret H. The first case of JC virus allograft nephropathy. *Transplantation.* 2003;76(11):1653-5.

124. Mengelle C, Kamar N, Mansuy JM, Sandres-Saune K, Legrand-Abravanel F, Miedouge M, Rostaing L, and Izopet J. JC virus DNA in the peripheral blood of renal transplant patients: a 1-year prospective follow-up in France. *J Med Virol.* 2011;83(1):132-6.

125. Randhawa P, Baksh F, Aoki N, Tschirhart D, and Finkelstein S. JC virus infection in allograft kidneys: analysis by polymerase chain reaction and immunohistochemistry. *Transplantation.* 2001;71(9):1300-3.

126. Del Valle L, Gordon J, Assimakopoulou M, Enam S, Geddes JF, Varakis JN, Katsetos CD, Croul S, and Khalili K. Detection of JC virus DNA sequences and expression of the viral regulatory protein T-antigen in tumors of the central nervous system. *Cancer Res.* 2001;61(10):4287-93.

127. Rencic A, Gordon J, Otte J, Curtis M, Kovatich A, Zoltick P, Khalili K, and Andrews D. Detection of JC virus DNA sequence and expression of the viral oncoprotein, tumor antigen, in brain of immunocompetent patient with oligoastrocytoma. *Proc Natl Acad Sci U S A.* 1996;93(14):7352-7.

128. Caldarelli-Stefano R, Boldorini R, Monga G, Meraviglia E, Zorini EO, and Ferrante P. JC virus in human glial-derived tumors. *Human pathology.* 2000;31(3):394-5.

129. Krynska B, Del Valle L, Croul S, Gordon J, Katsetos CD, Carbone M, Giordano A, and Khalili K. Detection of human neurotropic JC virus DNA sequence and expression of

the viral oncogenic protein in pediatric medulloblastomas. *Proc Natl Acad Sci U S A.* 1999;96(20):11519-24.

130. Hirsch HH, and Steiger J. Polyomavirus BK. *Lancet Infect Dis.* 2003;3(10):611-23.

131. Chesters PM, Heritage J, and McCance DJ. Persistence of DNA sequences of BK virus and JC virus in normal human tissues and in diseased tissues. *The Journal of infectious diseases.* 1983;147(4):676-84.

132. Sundsfjord A, Osei A, Rosenqvist H, Van Ghelue M, Silsand Y, Haga HJ, Rekvig OP, and Moens U. BK and JC viruses in patients with systemic lupus erythematosus: prevalent and persistent BK viruria, sequence stability of the viral regulatory regions, and nondetectable viremia. *The Journal of infectious diseases.* 1999;180(1):1-9.

133. Ling PD, Lednicky JA, Keitel WA, Poston DG, White ZS, Peng R, Liu Z, Mehta SK, Pierson DL, Rooney CM, et al. The dynamics of herpesvirus and polyomavirus reactivation and shedding in healthy adults: a 14-month longitudinal study. *The Journal of infectious diseases.* 2003;187(10):1571-80.

134. Ramos E, Drachenberg CB, Papadimitriou JC, Hamze O, Fink JC, Klassen DK, Drachenberg RC, Wiland A, Wali R, Cangro CB, et al. Clinical course of polyoma virus nephropathy in 67 renal transplant patients. *J Am Soc Nephrol.* 2002;13(8):2145-51.

135. Hirsch HH, Knowles W, Dickenmann M, Passweg J, Klimkait T, Mihatsch MJ, and Steiger J. Prospective study of polyomavirus type BK replication and nephropathy in renal-transplant recipients. *The New England journal of medicine.* 2002;347(7):488-96.

136. Nickeleit V, Klimkait T, Binet IF, Dalquen P, Del Zenero V, Thiel G, Mihatsch MJ, and Hirsch HH. Testing for polyomavirus type BK DNA in plasma to identify renal-allograft recipients with viral nephropathy. *The New England journal of medicine.* 2000;342(18):1309-15.

137. Viscount HB, Eid AJ, Espy MJ, Griffin MD, Thomsen KM, Harmsen WS, Razonable RR, and Smith TF. Polyomavirus polymerase chain reaction as a surrogate marker of polyomavirus-associated nephropathy. *Transplantation.* 2007;84(3):340-5.

138. Wadei HM, Rule AD, Lewin M, Mahale AS, Khamash HA, Schwab TR, Gloor JM, Textor SC, Fidler ME, Lager DJ, et al. Kidney transplant function and histological clearance of virus following diagnosis of polyomavirus-associated nephropathy (PVAN). *American journal of transplantation : official journal of the American Society of Transplantation and the American Society of Transplant Surgeons.* 2006;6(5 Pt 1):1025-32.

139. Barouch DH, Faquin WC, Chen Y, Koralnik IJ, Robbins GK, and Davis BT. BK virus-associated hemorrhagic cystitis in a Human Immunodeficiency Virus-infected patient. *Clinical infectious diseases : an official publication of the Infectious Diseases Society of America.* 2002;35(3):326-9.

140. Bogdanovic G, Priftakis P, Giraud G, Kuzniar M, Ferraldeschi R, Kokhaei P, Mellstedt H, Remberger M, Ljungman P, Winiarski J, et al. Association between a high BK virus load in urine samples of patients with graft-versus-host disease and development of hemorrhagic cystitis after hematopoietic stem cell transplantation. *J Clin Microbiol.* 2004;42(11):5394-6.

141. Elidemir O, Chang IF, Schecter MG, and Mallory GB. BK virus-associated hemorrhagic cystitis in a pediatric lung transplant recipient. *Pediatr Transplant.* 2007;11(7):807-10.

142. Fioriti D, Degener AM, Mischitelli M, Videtta M, Arancio A, Sica S, Sora F, and Pietropaolo V. BKV infection and hemorrhagic cystitis after allogeneic bone marrow transplant. *Int J Immunopathol Pharmacol.* 2005;18(2):309-16.

143. Petrogiannis-Haliotis T, Sakoulas G, Kirby J, Koralnik IJ, Dvorak AM, Monahan-Earley R, PC DEG, U DEG, Upton M, Major EO, et al. BK-related polyomavirus vasculopathy in a renal-transplant recipient. *The New England journal of medicine.* 2001;345(17):1250-5.

144. Vallbracht A, Lohler J, Gossmann J, Gluck T, Petersen D, Gerth HJ, Gencic M, and Dorries K. Disseminated BK type polyomavirus infection in an AIDS patient associated with central nervous system disease. *Am J Pathol.* 1993;143(1):29-39.

145. Binet I, Nickeleit V, Hirsch HH, Prince O, Dalquen P, Gudat F, Mihatsch MJ, and Thiel G. Polyomavirus disease under new immunosuppressive drugs: a cause of renal graft dysfunction and graft loss. *Transplantation.* 1999;67(6):918-22.

146. Randhawa PS, Finkelstein S, Scantlebury V, Shapiro R, Vivas C, Jordan M, Picken MM, and Demetris AJ. Human polyoma virus-associated interstitial nephritis in the allograft kidney. *Transplantation.* 1999;67(1):103-9.

147. Ramos E, Drachenberg CB, Portocarrero M, Wali R, Klassen DK, Fink JC, Farney A, Hirsch H, Papadimitriou JC, Cangro CB, et al. BK virus nephropathy diagnosis and treatment: experience at the University of Maryland Renal Transplant Program. *Clin Transpl.* 2002:143-53.

148. Sharma SG, Nickeleit V, Herlitz LC, de Gonzalez AK, Stokes MB, Singh HK, Markowitz GS, and D'Agati VD. BK polyoma virus nephropathy in the native kidney. *Nephrology,*

*dialysis, transplantation : official publication of the European Dialysis and Transplant Association - European Renal Association.* 2012;28(3):620-31.

149. Hirsch HH, Brennan DC, Drachenberg CB, Ginevri F, Gordon J, Limaye AP, Mihatsch MJ, Nickeleit V, Ramos E, Randhawa P, et al. Polyomavirus-associated nephropathy in renal transplantation: interdisciplinary analyses and recommendations. *Transplantation.* 2005;79(10):1277-86.

150. Nickeleit V, Hirsch HH, Binet IF, Gudat F, Prince O, Dalquen P, Thiel G, and Mihatsch MJ. Polyomavirus infection of renal allograft recipients: from latent infection to manifest disease. *J Am Soc Nephrol.* 1999;10(5):1080-9.

151. Nickeleit V, Hirsch HH, Zeiler M, Gudat F, Prince O, Thiel G, and Mihatsch MJ. BK-virus nephropathy in renal transplants-tubular necrosis, MHC-class II expression and rejection in a puzzling game. *Nephrology, dialysis, transplantation : official publication of the European Dialysis and Transplant Association - European Renal Association.* 2000;15(3):324-32.

152. Hirsch HH, and Randhawa P. BK virus in solid organ transplant recipients. *American journal of transplantation : official journal of the American Society of Transplantation and the American Society of Transplant Surgeons.* 2009;9 Suppl 4(S136-46.

153. Hirsch HH. In: Bowden P, Ljungman, P., Snydman, D.R. ed. *Transplant Infections*. Philadelphia, Baltimore, New York, London, Buenos Aires, Hong Kong, Sydney, Tokyo.: Lippincott Williams & Wilkins; 2010:465-82.

154. Funk GA, Gosert, R., Comoli, P., Ginevri, F., Hirsch, H.H. Polyomavirus BK replication dynamics in vivo and in silico to predict cytopathology and viral clearance in kidney transplants. *American journal of transplantation : official journal of the American Society of Transplantation and the American Society of Transplant Surgeons.* 2008;8(2368-77.

155. Drachenberg RC, Drachenberg CB, Papadimitriou JC, Ramos E, Fink JC, Wali R, Weir MR, Cangro CB, Klassen DK, Khaled A, et al. Morphological spectrum of polyoma virus disease in renal allografts: diagnostic accuracy of urine cytology. *American journal of transplantation : official journal of the American Society of Transplantation and the American Society of Transplant Surgeons.* 2001;1(4):373-81.

156. Mylonakis E, Goes N, Rubin RH, Cosimi AB, Colvin RB, and Fishman JA. BK virus in solid organ transplant recipients: an emerging syndrome. *Transplantation.* 2001;72(10):1587-92.

157. Howell DN, Smith SR, Butterly DW, Klassen PS, Krigman HR, Burchette JL, Jr., and Miller SE. Diagnosis and management of BK polyomavirus interstitial nephritis in renal transplant recipients. *Transplantation.* 1999;68(9):1279-88.

158. Hirsch HH, and Randhawa P. BK Polyomavirus in Solid Organ Transplantation. *American journal of transplantation : official journal of the American Society of Transplantation and the American Society of Transplant Surgeons.* 2013;13 Suppl 4(179-88.

159. Randhawa P, Ho A, Shapiro R, Vats A, Swalsky P, Finkelstein S, Uhrmacher J, and Weck K. Correlates of quantitative measurement of BK polyomavirus (BKV) DNA with clinical course of BKV infection in renal transplant patients. *J Clin Microbiol.* 2004;42(3):1176-80.

160. Singh HK, Donna Thompson B, and Nickeleit V. Viral Haufen are urinary biomarkers of polyomavirus nephropathy: New diagnostic strategies utilizing negative staining electron microscopy. *Ultrastruct Pathol.* 2009;33(5):222-35.

161. Purighalla R, Shapiro R, McCauley J, and Randhawa P. BK virus infection in a kidney allograft diagnosed by needle biopsy. *Am J Kidney Dis.* 1995;26(4):671-3.

162. Hardinger KL, Koch MJ, Bohl DJ, Storch GA, and Brennan DC. BK-Virus and the Impact of Pre-Emptive Immunosuppression Reduction: 5-Year Results. *American journal of transplantation : official journal of the American Society of Transplantation and the American Society of Transplant Surgeons.* 2010;2010(5.

163. Schaub S, Hirsch HH, Dickenmann M, Steiger J, Mihatsch MJ, Hopfer H, and Mayr M. Reducing immunosuppression preserves allograft function in presumptive and definitive polyomavirus-associated nephropathy. *American journal of transplantation : official journal of the American Society of Transplantation and the American Society of Transplant Surgeons.* 2010;10(12):2615-23.

164. Ginevri F, Azzi A, Hirsch HH, Basso S, Fontana I, Cioni M, Bodaghi S, Salotti V, Rinieri A, Botti G, et al. Prospective monitoring of polyomavirus BK replication and impact of pre-emptive intervention in pediatric kidney recipients. *American journal of transplantation : official journal of the American Society of Transplantation and the American Society of Transplant Surgeons.* 2007;7(12):2727-35.

165. Wu SW, Chang HR, Hsieh MC, Chiou HL, Lin CC, and Lian JD. Early diagnosis of polyomavirus type BK infection in tailoring immunosuppression for kidney transplant patients: screening with urine qualitative polymerase chain reaction assay. *Transplant Proc.* 2008;40(7):2389-91.

166. Johnston O, Jaswal D, Gill JS, Doucette S, Fergusson DA, and Knoll GA. Treatment of polyomavirus infection in kidney transplant recipients: a systematic review. *Transplantation.* 2010;89(9):1057-70.

167. Bjorang O, Tveitan H, Midtvedt K, Broch LU, Scott H, and Andresen PA. Treatment of polyomavirus infection with cidofovir in a renal-transplant recipient. *Nephrology, dialysis, transplantation : official publication of the European Dialysis and Transplant Association - European Renal Association.* 2002;17(11):2023-5.

168. Williams JW, Javaid B, Kadambi PV, Gillen D, Harland R, Thistlewaite JR, Garfinkel M, Foster P, Atwood W, Millis JM, et al. Leflunomide for polyomavirus type BK nephropathy. *The New England journal of medicine.* 2005;352(11):1157-8.

169. Ali SH, Chandraker A, and DeCaprio JA. Inhibition of Simian virus 40 large T antigen helicase activity by fluoroquinolones. *Antivir Ther.* 2007;12(1):1-6.

170. Sener A, House AA, Jevnikar AM, Boudville N, McAlister VC, Muirhead N, Rehman F, and Luke PP. Intravenous immunoglobulin as a treatment for BK virus associated nephropathy: one-year follow-up of renal allograft recipients. *Transplantation.* 2006;81(1):117-20.

171. Bedi A, Miller CB, Hanson JL, Goodman S, Ambinder RF, Charache P, Arthur RR, and Jones RJ. Association of BK virus with failure of prophylaxis against hemorrhagic cystitis following bone marrow transplantation. *J Clin Oncol.* 1995;13(5):1103-9.

172. Peinemann F, de Villiers EM, Dorries K, Adams O, Vogeli TA, and Burdach S. Clinical course and treatment of haemorrhagic cystitis associated with BK type of human polyomavirus in nine paediatric recipients of allogeneic bone marrow transplants. *Eur J Pediatr.* 2000;159(3):182-8.

173. Seber A, Shu XO, Defor T, Sencer S, and Ramsay N. Risk factors for severe hemorrhagic cystitis following BMT. *Bone marrow transplantation.* 1999;23(1):35-40.

174. Arthur RR, Shah KV, Baust SJ, Santos GW, and Saral R. Association of BK viruria with hemorrhagic cystitis in recipients of bone marrow transplants. *The New England journal of medicine.* 1986;315(4):230-4.

175. Azzi A, Cesaro S, Laszlo D, Zakrzewska K, Ciappi S, De Santis R, Fanci R, Pesavento G, Calore E, and Bosi A. Human polyomavirus BK (BKV) load and haemorrhagic cystitis in bone marrow transplantation patients. *J Clin Virol.* 1999;14(2):79-86.

176. Bogdanovic G, Ljungman P, Wang F, and Dalianis T. Presence of human polyomavirus DNA in the peripheral circulation of bone marrow transplant patients with and without hemorrhagic cystitis. *Bone marrow transplantation.* 1996;17(4):573-6.

177. Koskenvuo M, Dumoulin A, Lautenschlager I, Auvinen E, Mannonen L, Anttila VJ, Jahnukainen K, Saarinen-Pihkala UM, and Hirsch HH. BK polyomavirus-associated hemorrhagic cystitis among pediatric allogeneic bone marrow transplant recipients: treatment response and evidence for nosocomial transmission. *J Clin Virol.* 2013;56(1):77-81.

178. Erard V, Kim HW, Corey L, Limaye A, Huang ML, Myerson D, Davis C, and Boeckh M. BK DNA viral load in plasma: evidence for an association with hemorrhagic cystitis in allogeneic hematopoietic cell transplant recipients. *Blood.* 2005;106(3):1130-2.

179. Priftakis P, Bogdanovic G, Kalantari M, and Dalianis T. Overrepresentation of point mutations in the Sp1 site of the non-coding control region of BK virus in bone marrow transplanted patients with haemorrhagic cystitis. *J Clin Virol.* 2001;21(1):1-7.

180. Kawakami M, Ueda S, Maeda T, Karasuno T, Teshima H, Hiraoka A, Nakamura H, Tanaka K, and Masaoka T. Vidarabine therapy for virus-associated cystitis after allogeneic bone marrow transplantation. *Bone marrow transplantation.* 1997;20(6):485-90.

181. Held TK, Biel SS, Nitsche A, Kurth A, Chen S, Gelderblom HR, and Siegert W. Treatment of BK virus-associated hemorrhagic cystitis and simultaneous CMV reactivation with cidofovir. *Bone marrow transplantation.* 2000;26(3):347-50.

182. Focosi D, Maggi F, Pistolesi D, Benedetti E, Papineschi F, Galimberti S, Ceccherini-Nelli L, and Petrini M. Hyperbaric oxygen therapy in BKV-associated hemorrhagic cystitis refractory to intravenous and intravesical cidofovir: case report and review of literature. *Leukemia research.* 2009;33(4):556-60.

183. Coleman DV, Mackenzie EF, Gardner SD, Poulding JM, Amer B, and Russell WJ. Human polyomavirus (BK) infection and ureteric stenosis in renal allograft recipients. *J Clin Pathol.* 1978;31(4):338-47.

184. Rajpoot DK, Gomez A, Tsang W, and Shanberg A. Ureteric and urethral stenosis: a complication of BK virus infection in a pediatric renal transplant patient. *Pediatr Transplant.* 2007;11(4):433-5.

185. Hwang YY, Sim J, Leung AY, Lie AK, and Kwong YL. BK virus-associated bilateral ureteric stenosis after haematopoietic SCT: viral kinetics and successful treatment. *Bone marrow transplantation.* 2013;48(5):745-6.

186. Lopes da Silva R, Ferreira I, Teixeira G, Cordeiro D, Mafra M, Costa I, Bravo Marques JM, and Abecasis M. BK virus encephalitis with thrombotic microangiopathy in an allogeneic hematopoietic stem cell transplant recipient. *Transpl Infect Dis.* 2011;13(2):161-7.

187. Behre G, Becker M, and Christopeit M. BK virus encephalitis in an allogeneic hematopoietic stem cell recipient. *Bone marrow transplantation.* 2008;42(7):499.

188. Dalianis T, and Hirsch HH. In: Robertson ES, Medicine PSo, University of Pennsylvania P, PA, USA, and erle@upenn.edu eds. *Cancer Associated Viruses*. Springer: Springer Sciences & Business Media; 2012:419-32.

189. Abend JR, Jiang M, and Imperiale MJ. BK virus and human cancer: innocent until proven guilty. *Semin Cancer Biol.* 2009;19(4):252-60.

190. Dalianis T, and Hirsch HH. Human polyomaviruses in disease and cancer. *Virology.* 2013;437(2):63-72.

191. Medzhitov R. Recognition of microorganisms and activation of the immune response. *Nature.* 2007;449(7164):819-26.

192. Medzhitov R, and Janeway CA, Jr. How does the immune system distinguish self from nonself? *Semin Immunol.* 2000;12(3):185-8; discussion 257-344.

193. Medzhitov R, and Janeway CA, Jr. Decoding the patterns of self and nonself by the innate immune system. *Science.* 2002;296(5566):298-300.

194. Janeway CA, Jr. The immune system evolved to discriminate infectious nonself from noninfectious self. *Immunol Today.* 1992;13(1):11-6.

195. Janeway CA, Jr. How the immune system protects the host from infection. *Microbes Infect.* 2001;3(13):1167-71.

196. Janeway CA, Jr., and Medzhitov R. Innate immune recognition. *Annu Rev Immunol.* 2002;20(197-216.

197. Schnittler HJ, Mahner F, Drenckhahn D, Klenk HD, and Feldmann H. Replication of Marburg virus in human endothelial cells. A possible mechanism for the development of viral hemorrhagic disease. *J Clin Invest.* 1993;91(4):1301-9.

198. Vuorinen T, Vainionpaa R, Heino J, and Hyypia T. Enterovirus receptors and virus replication in human leukocytes. *J Gen Virol.* 1999;80 ( Pt 4)(921-7.

199. Wahl-Jensen VM, Afanasieva TA, Seebach J, Stroher U, Feldmann H, and Schnittler HJ. Effects of Ebola virus glycoproteins on endothelial cell activation and barrier function. *J Virol.* 2005;79(16):10442-50.

200. Ludlow M, Allen I, and Schneider-Schaulies J. Systemic spread of measles virus: overcoming the epithelial and endothelial barriers. *Thromb Haemost.* 2009;102(6):1050-6.

201. Dalrymple NA, and Mackow ER. Roles for endothelial cells in dengue virus infection. *Adv Virol.* 2012;2012(840654.

202. Breiner KM, Schaller H, and Knolle PA. Endothelial cell-mediated uptake of a hepatitis B virus: a new concept of liver targeting of hepatotropic microorganisms. *Hepatology.* 2001;34(4 Pt 1):803-8.

203. Pfaender S, Heyden J, Friesland M, Ciesek S, Ejaz A, Steinmann J, Steinmann J, Malarski A, Stoiber H, Tsiavaliaris G, et al. Inactivation of hepatitis C virus infectivity by human breast milk. *The Journal of infectious diseases.* 2013;208(12):1943-52.

204. Weiss C, and Clark HF. Rapid inactivation of rotaviruses by exposure to acid buffer or acidic gastric juice. *J Gen Virol.* 1985;66 ( Pt 12)(2725-30.

205. Veloso Alves Pereira I, Buchmann B, Sandmann L, Sprinzl K, Schlaphoff V, Dohner K, Vondran F, Sarrazin C, Manns MP, Pinto Marques Souza de Oliveira C, et al. Primary biliary acids inhibit hepatitis D virus (HDV) entry into human hepatoma cells expressing the sodium-taurocholate cotransporting polypeptide (NTCP). *PloS one.* 2015;10(2):e0117152.

206. Dunkelberger JR, and Song WC. Complement and its role in innate and adaptive immune responses. *Cell Res.* 2010;20(1):34-50.

207. Walport MJ. Complement. First of two parts. *The New England journal of medicine.* 2001;344(14):1058-66.

208. Stetson DB, and Medzhitov R. Type I interferons in host defense. *Immunity.* 2006;25(3):373-81.

209. Kotenko SV, Gallagher G, Baurin VV, Lewis-Antes A, Shen M, Shah NK, Langer JA, Sheikh F, Dickensheets H, and Donnelly RP. IFN-lambdas mediate antiviral protection through a distinct class II cytokine receptor complex. *Nat Immunol.* 2003;4(1):69-77.

210. Pierce AT, DeSalvo J, Foster TP, Kosinski A, Weller SK, and Halford WP. Beta interferon and gamma interferon synergize to block viral DNA and virion synthesis in herpes simplex virus-infected cells. *J Gen Virol.* 2005;86(Pt 9):2421-32.

211. Randall RE, and Goodbourn S. Interferons and viruses: an interplay between induction, signalling, antiviral responses and virus countermeasures. *J Gen Virol.* 2008;89(Pt 1):1-47.

212. Samarajiwa SA, Forster S, Auchettl K, and Hertzog PJ. INTERFEROME: the database of interferon regulated genes. *Nucleic Acids Res.* 2009;37(Database issue):D852-7.

213. Der SD, Zhou A, Williams BR, and Silverman RH. Identification of genes differentially regulated by interferon alpha, beta, or gamma using oligonucleotide arrays. *Proc Natl Acad Sci U S A.* 1998;95(26):15623-8.

214. Samuel CE. Antiviral actions of interferons. *Clinical microbiology reviews.* 2001;14(4):778-809, table of contents.

215. Chawla-Sarkar M, Lindner DJ, Liu YF, Williams BR, Sen GC, Silverman RH, and Borden EC. Apoptosis and interferons: role of interferon-stimulated genes as mediators of apoptosis. *Apoptosis.* 2003;8(3):237-49.

216. Le Bon A, and Tough DF. Links between innate and adaptive immunity via type I interferon. *Curr Opin Immunol.* 2002;14(4):432-6.

217. Sabbah A, Chang TH, Harnack R, Frohlich V, Tominaga K, Dube PH, Xiang Y, and Bose S. Activation of innate immune antiviral responses by Nod2. *Nat Immunol.* 2009;10(10):1073-80.

218. Seth RB, Sun L, and Chen ZJ. Antiviral innate immunity pathways. *Cell Res.* 2006;16(2):141-7.

219. Kawai T, and Akira S. Antiviral signaling through pattern recognition receptors. *J Biochem.* 2007;141(2):137-45.

220. Compton T, Kurt-Jones EA, Boehme KW, Belko J, Latz E, Golenbock DT, and Finberg RW. Human cytomegalovirus activates inflammatory cytokine responses via CD14 and Toll-like receptor 2. *J Virol.* 2003;77(8):4588-96.

221. Kim M, Osborne NR, Zeng W, Donaghy H, McKinnon K, Jackson DC, and Cunningham AL. Herpes simplex virus antigens directly activate NK cells via TLR2, thus facilitating their presentation to CD4 T lymphocytes. *J Immunol.* 2012;188(9):4158-70.

222. Boehme KW, Guerrero M, and Compton T. Human cytomegalovirus envelope glycoproteins B and H are necessary for TLR2 activation in permissive cells. *J Immunol.* 2006;177(10):7094-102.

223. Cai M, Li M, Wang K, Wang S, Lu Q, Yan J, Mossman KL, Lin R, and Zheng C. The herpes simplex virus 1-encoded envelope glycoprotein B activates NF-kappaB

through the Toll-like receptor 2 and MyD88/TRAF6-dependent signaling pathway. *PloS one.* 2013;8(1):e54586.

224. Leoni V, Gianni T, Salvioli S, and Campadelli-Fiume G. Herpes simplex virus glycoproteins gH/gL and gB bind Toll-like receptor 2, and soluble gH/gL is sufficient to activate NF-kappaB. *J Virol.* 2012;86(12):6555-62.

225. Fiola S, Gosselin D, Takada K, and Gosselin J. TLR9 contributes to the recognition of EBV by primary monocytes and plasmacytoid dendritic cells. *J Immunol.* 2010;185(6):3620-31.

226. Krug A, French AR, Barchet W, Fischer JA, Dzionek A, Pingel JT, Orihuela MM, Akira S, Yokoyama WM, and Colonna M. TLR9-dependent recognition of MCMV by IPC and DC generates coordinated cytokine responses that activate antiviral NK cell function. *Immunity.* 2004;21(1):107-19.

227. Honda K, Yanai H, Mizutani T, Negishi H, Shimada N, Suzuki N, Ohba Y, Takaoka A, Yeh WC, and Taniguchi T. Role of a transductional-transcriptional processor complex involving MyD88 and IRF-7 in Toll-like receptor signaling. *Proc Natl Acad Sci U S A.* 2004;101(43):15416-21.

228. Honda K, Yanai H, Negishi H, Asagiri M, Sato M, Mizutani T, Shimada N, Ohba Y, Takaoka A, Yoshida N, et al. IRF-7 is the master regulator of type-I interferon-dependent immune responses. *Nature.* 2005;434(7034):772-7.

229. Verstak B, Nagpal K, Bottomley SP, Golenbock DT, Hertzog PJ, and Mansell A. MyD88 adapter-like (Mal)/TIRAP interaction with TRAF6 is critical for TLR2- and TLR4-mediated NF-kappaB proinflammatory responses. *The Journal of biological chemistry.* 2009;284(36):24192-203.

230. Akira S, and Takeda K. Toll-like receptor signalling. *Nature reviews Immunology.* 2004;4(7):499-511.

231. Lawrence T. The nuclear factor NF-kappaB pathway in inflammation. *Cold Spring Harb Perspect Biol.* 2009;1(6):a001651.

232. Tak PP, and Firestein GS. NF-kappaB: a key role in inflammatory diseases. *J Clin Invest.* 2001;107(1):7-11.

233. Tsujimura H, Tamura T, Kong HJ, Nishiyama A, Ishii KJ, Klinman DM, and Ozato K. Toll-like receptor 9 signaling activates NF-kappaB through IFN regulatory factor-8/IFN consensus sequence binding protein in dendritic cells. *J Immunol.* 2004;172(11):6820-7.

234. Okamoto M, Oshiumi H, Azuma M, Kato N, Matsumoto M, and Seya T. IPS-1 is essential for type III IFN production by hepatocytes and dendritic cells in response to hepatitis C virus infection. *J Immunol.* 2014;192(6):2770-7.

235. Kumar H, Kawai T, Kato H, Sato S, Takahashi K, Coban C, Yamamoto M, Uematsu S, Ishii KJ, Takeuchi O, et al. Essential role of IPS-1 in innate immune responses against RNA viruses. *The Journal of experimental medicine.* 2006;203(7):1795-803.

236. Vivier E, Tomasello E, Baratin M, Walzer T, and Ugolini S. Functions of natural killer cells. *Nat Immunol.* 2008;9(5):503-10.

237. Stern M, Elsasser H, Honger G, Steiger J, Schaub S, and Hess C. The number of activating KIR genes inversely correlates with the rate of CMV infection/reactivation in kidney transplant recipients. *American journal of transplantation : official journal of the American Society of Transplantation and the American Society of Transplant Surgeons.* 2008;8(6):1312-7.

238. Olson JA, Leveson-Gower DB, Gill S, Baker J, Beilhack A, and Negrin RS. NK cells mediate reduction of GVHD by inhibiting activated, alloreactive T cells while retaining GVT effects. *Blood.* 2010;115(21):4293-301.

239. Bryson JS, and Flanagan DL. Role of natural killer cells in the development of graft-versus-host disease. *J Hematother Stem Cell Res.* 2000;9(3):307-16.

240. van Duin D, Avery RK, Hemachandra S, Yen-Lieberman B, Zhang A, Jain A, Butler RS, Barnard J, Schold JD, Fung J, et al. KIR and HLA interactions are associated with control of primary CMV infection in solid organ transplant recipients. *American journal of transplantation : official journal of the American Society of Transplantation and the American Society of Transplant Surgeons.* 2014;14(1):156-62.

241. Gonzalez A, Schmitter K, Hirsch HH, Garzoni C, van Delden C, Boggian K, Mueller NJ, Berger C, Villard J, Manuel O, et al. KIR-associated protection from CMV replication requires pre-existing immunity: a prospective study in solid organ transplant recipients. *Genes Immun.* 2014;15(7):495-9.

242. Trydzenskaya H, Juerchott K, Lachmann N, Kotsch K, Kunert K, Weist B, Schonemann C, Schindler R, Nickel P, Melzig MF, et al. The genetic predisposition of natural killer cell to BK virus-associated nephropathy in renal transplant patients. *Kidney international.* 2013;84(2):359-65.

243. Atkinson JP, and Frank MM. Effect of cortisone therapy on serum complement components. *J Immunol.* 1973;111(4):1061-6.

244. Jenne CN, and Kubes P. Immune surveillance by the liver. *Nat Immunol.* 2013;14(10):996-1006.

245. Racanelli V, and Rehermann B. The liver as an immunological organ. *Hepatology.* 2006;43(2 Suppl 1):S54-62.

246. Braet F, and Wisse E. Structural and functional aspects of liver sinusoidal endothelial cell fenestrae: a review. *Comp Hepatol.* 2002;1(1):1.

247. Wu J, Meng Z, Jiang M, Zhang E, Trippler M, Broering R, Bucchi A, Krux F, Dittmer U, Yang D, et al. Toll-like receptor-induced innate immune responses in non-parenchymal liver cells are cell type-specific. *Immunology.* 2010;129(3):363-74.

248. Knolle PA, and Limmer A. Control of immune responses by savenger liver endothelial cells. *Swiss Med Wkly.* 2003;133(37-38):501-6.

249. Sorensen KK, McCourt P, Berg T, Crossley C, Le Couteur D, Wake K, and Smedsrod B. The scavenger endothelial cell: a new player in homeostasis and immunity. *Am J Physiol Regul Integr Comp Physiol.* 2012;303(12):R1217-30.

250. Nie Y, and Wang YY. Innate immune responses to DNA viruses. *Protein Cell.* 2013;4(1):1-7.

251. Rathinam VA, and Fitzgerald KA. Innate immune sensing of DNA viruses. *Virology.* 2011;411(2):153-62.

252. Upton JW, Kaiser WJ, and Mocarski ES. DAI/ZBP1/DLM-1 complexes with RIP3 to mediate virus-induced programmed necrosis that is targeted by murine cytomegalovirus vIRA. *Cell Host Microbe.* 2012;11(3):290-7.

253. Chiu YH, Macmillan JB, and Chen ZJ. RNA polymerase III detects cytosolic DNA and induces type I interferons through the RIG-I pathway. *Cell.* 2009;138(3):576-91.

254. Ribeiro A, Wornle M, Motamedi N, Anders HJ, Grone EF, Nitschko H, Kurktschiev P, Debiec H, Kretzler M, Cohen CD, et al. Activation of innate immune defense mechanisms contributes to polyomavirus BK-associated nephropathy. *Kidney international.* 2012;81(1):100-11.

255. Zhong B, Yang Y, Li S, Wang YY, Li Y, Diao F, Lei C, He X, Zhang L, Tien P, et al. The adaptor protein MITA links virus-sensing receptors to IRF3 transcription factor activation. *Immunity.* 2008;29(4):538-50.

256. Ishikawa H, Ma Z, and Barber GN. STING regulates intracellular DNA-mediated, type I interferon-dependent innate immunity. *Nature.* 2009;461(7265):788-92.

257. Veeranki S, and Choubey D. Interferon-inducible p200-family protein IFI16, an innate immune sensor for cytosolic and nuclear double-stranded DNA: regulation of subcellular localization. *Mol Immunol.* 2012;49(4):567-71.

258. Unterholzner L, Keating SE, Baran M, Horan KA, Jensen SB, Sharma S, Sirois CM, Jin T, Latz E, Xiao TS, et al. IFI16 is an innate immune sensor for intracellular DNA. *Nat Immunol.* 2010;11(11):997-1004.

259. Gariano GR, Dell'Oste V, Bronzini M, Gatti D, Luganini A, De Andrea M, Gribaudo G, Gariglio M, and Landolfo S. The intracellular DNA sensor IFI16 gene acts as restriction factor for human cytomegalovirus replication. *PLoS Pathog.* 2012;8(1):e1002498.

260. Zhang Z, Yuan B, Bao M, Lu N, Kim T, and Liu YJ. The helicase DDX41 senses intracellular DNA mediated by the adaptor STING in dendritic cells. *Nat Immunol.* 2011;12(10):959-65.

261. Yang P, An H, Liu X, Wen M, Zheng Y, Rui Y, and Cao X. The cytosolic nucleic acid sensor LRRFIP1 mediates the production of type I interferon via a beta-catenin-dependent pathway. *Nat Immunol.* 2010;11(6):487-94.

262. Li Y, Chen R, Zhou Q, Xu Z, Li C, Wang S, Mao A, Zhang X, He W, and Shu HB. LSm14A is a processing body-associated sensor of viral nucleic acids that initiates cellular antiviral response in the early phase of viral infection. *Proc Natl Acad Sci U S A.* 2012;109(29):11770-5.

263. Beckham CJ, and Parker R. P bodies, stress granules, and viral life cycles. *Cell Host Microbe.* 2008;3(4):206-12.

264. Mok BW, Song W, Wang P, Tai H, Chen Y, Zheng M, Wen X, Lau SY, Wu WL, Matsumoto K, et al. The NS1 protein of influenza A virus interacts with cellular processing bodies and stress granules through RNA-associated protein 55 (RAP55) during virus infection. *J Virol.* 2012;86(23):12695-707.

265. Petrilli V, Dostert C, Muruve DA, and Tschopp J. The inflammasome: a danger sensing complex triggering innate immunity. *Curr Opin Immunol.* 2007;19(6):615-22.

266. Fernandes-Alnemri T, Yu JW, Juliana C, Solorzano L, Kang S, Wu J, Datta P, McCormick M, Huang L, McDermott E, et al. The AIM2 inflammasome is critical for innate immunity to Francisella tularensis. *Nat Immunol.* 2010;11(5):385-93.

267. Ganz T. Defensins: antimicrobial peptides of innate immunity. *Nature reviews Immunology.* 2003;3(9):710-20.

268. Chong KT, Thangavel RR, and Tang X. Enhanced expression of murine beta-defensins (MBD-1, -2,- 3, and -4) in upper and lower airway mucosa of influenza virus infected mice. *Virology.* 2008;380(1):136-43.

269. Duits LA, Nibbering PH, van Strijen E, Vos JB, Mannesse-Lazeroms SP, van Sterkenburg MA, and Hiemstra PS. Rhinovirus increases human beta-defensin-2 and -3 mRNA expression in cultured bronchial epithelial cells. *FEMS Immunol Med Microbiol.* 2003;38(1):59-64.

270. Kota S, Sabbah A, Chang TH, Harnack R, Xiang Y, Meng X, and Bose S. Role of human beta-defensin-2 during tumor necrosis factor-alpha/NF-kappaB-mediated innate antiviral response against human respiratory syncytial virus. *The Journal of biological chemistry.* 2008;283(33):22417-29.

271. Zins SR, Nelson CD, Maginnis MS, Banerjee R, O'Hara BA, and Atwood WJ. The human alpha defensin HD5 neutralizes JC polyomavirus infection by reducing endoplasmic reticulum traffic and stabilizing the viral capsid. *J Virol.* 2014;88(2):948-60.

272. Dugan AS, Maginnis MS, Jordan JA, Gasparovic ML, Manley K, Page R, Williams G, Porter E, O'Hara BA, and Atwood WJ. Human alpha-defensins inhibit BK virus infection by aggregating virions and blocking binding to host cells. *The Journal of biological chemistry.* 2008;283(45):31125-32.

273. Galocha B, Hill A, Barnett BC, Dolan A, Raimondi A, Cook RF, Brunner J, McGeoch DJ, and Ploegh HL. The active site of ICP47, a herpes simplex virus-encoded inhibitor of the major histocompatibility complex (MHC)-encoded peptide transporter associated with antigen processing (TAP), maps to the NH2-terminal 35 residues. *The Journal of experimental medicine.* 1997;185(9):1565-72.

274. Brachet V, Raposo G, Amigorena S, and Mellman I. Ii chain controls the transport of major histocompatibility complex class II molecules to and from lysosomes. *J Cell Biol.* 1997;137(1):51-65.

275. Heath WR, and Carbone FR. Cross-presentation in viral immunity and self-tolerance. *Nature reviews Immunology.* 2001;1(2):126-34.

276. Huber M, and Trkola A. Humoral immunity to HIV-1: neutralization and beyond. *J Intern Med.* 2007;262(1):5-25.

277. Gerna G, Sarasini A, Patrone M, Percivalle E, Fiorina L, Campanini G, Gallina A, Baldanti F, and Revello MG. Human cytomegalovirus serum neutralizing antibodies

block virus infection of endothelial/epithelial cells, but not fibroblasts, early during primary infection. *J Gen Virol.* 2008;89(Pt 4):853-65.

278. Terajima M, Cruz J, Co MD, Lee JH, Kaur K, Wrammert J, Wilson PC, and Ennis FA. Complement-dependent lysis of influenza a virus-infected cells by broadly cross-reactive human monoclonal antibodies. *J Virol.* 2011;85(24):13463-7.

279. Logvinoff C, Major ME, Oldach D, Heyward S, Talal A, Balfe P, Feinstone SM, Alter H, Rice CM, and McKeating JA. Neutralizing antibody response during acute and chronic hepatitis C virus infection. *Proc Natl Acad Sci U S A.* 2004;101(27):10149-54.

280. Hangartner L, Zellweger RM, Giobbi M, Weber J, Eschli B, McCoy KD, Harris N, Recher M, Zinkernagel RM, and Hengartner H. Nonneutralizing antibodies binding to the surface glycoprotein of lymphocytic choriomeningitis virus reduce early virus spread. *The Journal of experimental medicine.* 2006;203(8):2033-42.

281. Stoermer KA, and Morrison TE. Complement and viral pathogenesis. *Virology.* 2011;411(2):362-73.

282. McCullough KC, Parkinson D, and Crowther JR. Opsonization-enhanced phagocytosis of foot-and-mouth disease virus. *Immunology.* 1988;65(2):187-91.

283. Seidel UJ, Schlegel P, and Lang P. Natural killer cell mediated antibody-dependent cellular cytotoxicity in tumor immunotherapy with therapeutic antibodies. *Front Immunol.* 2013;4(76.

284. Janeway CA, Jr., and Bottomly K. Signals and signs for lymphocyte responses. *Cell.* 1994;76(2):275-85.

285. Binggeli S, Egli A, Schaub S, Binet I, Mayr M, Steiger J, and Hirsch HH. Polyomavirus BK-Specific Cellular Immune Response to VP1 and Large T-Antigen in Kidney Transplant Recipients. *American journal of transplantation : official journal of the American Society of Transplantation and the American Society of Transplant Surgeons.* 2007;7(5):1131-9.

286. Chen Y, Trofe J, Gordon J, Autissier P, Woodle ES, and Koralnik IJ. BKV and JCV large T antigen-specific CD8(+) T cell response in HLA A*0201(+) kidney transplant recipients with polyomavirus nephropathy and patients with progressive multifocal leukoencephalopathy. *J Clin Virol.* 2008;42(2):198-202.

287. Chen Y, Trofe J, Gordon J, Du Pasquier RA, Roy-Chaudhury P, Kuroda MJ, Woodle ES, Khalili K, and Koralnik IJ. Interplay of cellular and humoral immune responses against BK virus in kidney transplant recipients with polyomavirus nephropathy. *J Virol.* 2006;80(7):3495-505.

288. Hammer MH, Brestrich G, Andree H, Engelmann E, Rosenberger C, Tillmann H, Zwinger S, Babel N, Nickel P, Volk HD, et al. HLA type-independent method to monitor polyoma BK virus-specific CD4 and CD8 T-cell immunity. *American journal of transplantation : official journal of the American Society of Transplantation and the American Society of Transplant Surgeons.* 2006;6(3):625-31.

289. Krymskaya L, Sharma MC, Martinez J, Haq W, Huang EC, Limaye AP, Diamond DJ, and Lacey SF. Cross-reactivity of T lymphocytes recognizing a human cytotoxic T-lymphocyte epitope within BK and JC virus VP1 polypeptides. *J Virol.* 2005;79(17):11170-8.

290. Li J, Melenhorst J, Hensel N, Rezvani K, Sconocchia G, Kilical Y, Hou J, Curfman B, Major E, and Barrett AJ. T-cell responses to peptide fragments of the BK virus T antigen: implications for cross-reactivity of immune response to JC virus. *J Gen Virol.* 2006;87(Pt 10):2951-60.

291. Prosser SE, Orentas RJ, Jurgens L, Cohen EP, and Hariharan S. Recovery of BK virus large T-antigen-specific cellular immune response correlates with resolution of bk virus nephritis. *Transplantation.* 2008;85(2):185-92.

292. Provenzano M, Bracci L, Wyler S, Hudolin T, Sais G, Gosert R, Zajac P, Palu G, Heberer M, Hirsch HH, et al. Characterization of highly frequent epitope-specific CD45RA+/CCR7+/- T lymphocyte responses against p53-binding domains of the human polyomavirus BK large tumor antigen in HLA-A*0201+ BKV-seropositive donors. *J Transl Med.* 2006;4(47.

293. Ramaswami B, Popescu I, Macedo C, Metes D, Bueno M, Zeevi A, Shapiro R, Viscidi R, and Randhawa PS. HLA-A01-, -A03-, and -A024-binding nanomeric epitopes in polyomavirus BK large T antigen. *Hum Immunol.* 2009;70(9):722-8.

294. Ramaswami B, Popescu I, Macedo C, Luo C, Shapiro R, Metes D, Chalasani G, and Randhawa PS. The Polyomavirus BK Large T-Antigen-Derived Peptide Elicits an HLA-DR Promiscuous and Polyfunctional CD4+ T-Cell Response. *Clinical and vaccine immunology : CVI.* 2011;18(5):815-24.

295. Randhawa PS, Popescu I, Macedo C, Zeevi A, Shapiro R, Vats AN, and Metes D. Detection of CD8+ T cells sensitized to BK virus large T antigen in healthy volunteers and kidney transplant recipients. *Hum Immunol.* 2006;67(4-5):298-302.

296. van Aalderen MC, Remmerswaal EB, Heutinck KM, Ten Brinke A, Pircher H, van Lier RA, and Ten Berge IJ. Phenotypic and Functional Characterization of Circulating

Polyomavirus BK VP1-Specific CD8+ T Cells in Healthy Adults. *J Virol.* 2013;87(18):10263-72.

297. Zhou W, Sharma M, Martinez J, Srivastava T, Diamond DJ, Knowles W, and Lacey SF. Functional Characterization of BK Virus-Specific CD4(+) T Cells with Cytotoxic Potential in Seropositive Adults. *Viral Immunol.* 2007;20(3):379-88.

298. Bredholt G, Rekvig OP, Andreassen K, Moens U, and Marion TN. Differences in the reactivity of CD4+ T-cell lines generated against free versus nucleosome-bound SV40 large T antigen. *Scand J Immunol.* 2001;53(4):372-80.

299. Andreassen K, Moens U, Nossent H, Marion TN, and Rekvig OP. Termination of human T cell tolerance to histones by presentation of histones and polyomavirus T antigen provided that T antigen is complexed with nucleosomes. *Arthritis and rheumatism.* 1999;42(11):2449-60.

300. Coleman S, Gibbs A, Butchart E, Mason MD, Jasani B, and Tabi Z. SV40 large T antigen-specific human T cell memory responses. *J Med Virol.* 2008;80(8):1497-504.

301. Pipas JM. Common and unique features of T antigens encoded by the polyomavirus group. *J Virol.* 1992;66(7):3979-85.

302. Andreassen K, Bendiksen S, Kjeldsen E, Van Ghelue M, Moens U, Arnesen E, and Rekvig OP. T cell autoimmunity to histones and nucleosomes is a latent property of the normal immune system. *Arthritis and rheumatism.* 2002;46(5):1270-81.

303. Drummond JE, Shah KV, and Donnenberg AD. Cell-mediated immune responses to BK virus in normal individuals. *J Med Virol.* 1985;17(3):237-47.

304. Comoli P, Azzi A, Maccario R, Basso S, Botti G, Basile G, Fontana I, Labirio M, Cometa A, Poli F, et al. Polyomavirus BK-specific immunity after kidney transplantation. *Transplantation.* 2004;78(8):1229-32.

305. Comoli P, Basso S, Azzi A, Moretta A, De Santis R, Del Galdo F, De Palma R, Valente U, Nocera A, Perfumo F, et al. Dendritic cells pulsed with polyomavirus BK antigen induce ex vivo polyoma BK virus-specific cytotoxic T-cell lines in seropositive healthy individuals and renal transplant recipients. *J Am Soc Nephrol.* 2003;14(12):3197-204.

306. Blyth E, Clancy L, Simms R, Gaundar S, O'Connell P, Micklethwaite K, and Gottlieb DJ. BK Virus-Specific T Cells for Use in Cellular Therapy Show Specificity to Multiple Antigens and Polyfunctional Cytokine Responses. *Transplantation.* 2011;92(10):1077-84.

307. Mueller K, Schachtner T, Sattler A, Meier S, Friedrich P, Trydzenskaya H, Hinrichs C, Trappe R, Thiel A, Reinke P, et al. BK-VP3 as a new target of cellular immunity in BK virus infection. *Transplantation.* 2011;91(1):100-7.

308. Schachtner T, Muller K, Stein M, Diezemann C, Sefrin A, Babel N, and Reinke P. BK virus-specific immunity kinetics: a predictor of recovery from polyomavirus BK-associated nephropathy. *American journal of transplantation : official journal of the American Society of Transplantation and the American Society of Transplant Surgeons.* 2011;11(11):2443-52.

309. Du Pasquier RA, Schmitz JE, Jean-Jacques J, Zheng Y, Gordon J, Khalili K, Letvin NL, and Koralnik IJ. Detection of JC virus-specific cytotoxic T lymphocytes in healthy individuals. *J Virol.* 2004;78(18):10206-10.

310. Jelcic I, Aly L, Binder TM, Jelcic I, Bofill-Mas S, Planas R, Demina V, Eiermann TH, Weber T, Girones R, et al. T Cell Epitope Mapping of JC Polyoma Virus-Encoded Proteome Reveals Reduced T Cell Responses in HLA-DRB1*04:01+ Donors. *J Virol.* 2013;87(6):3393-408.

311. Koralnik IJ, Du Pasquier RA, Kuroda MJ, Schmitz JE, Dang X, Zheng Y, Lifton M, and Letvin NL. Association of prolonged survival in HLA-A2+ progressive multifocal leukoencephalopathy patients with a CTL response specific for a commonly recognized JC virus epitope. *J Immunol.* 2002;168(1):499-504.

312. Du Pasquier RA, Clark KW, Smith PS, Joseph JT, Mazullo JM, De Girolami U, Letvin NL, and Koralnik IJ. JCV-specific cellular immune response correlates with a favorable clinical outcome in HIV-infected individuals with progressive multifocal leukoencephalopathy. *J Neurovirol.* 2001;7(4):318-22.

313. Gheuens S, Bord E, Kesari S, Simpson DM, Gandhi RT, Clifford DB, Berger JR, Ngo L, and Koralnik IJ. Role of CD4+ and CD8+ T-cell responses against JC virus in the outcome of patients with progressive multifocal leukoencephalopathy (PML) and PML with immune reconstitution inflammatory syndrome. *J Virol.* 2011;85(14):7256-63.

314. Du Pasquier RA, Kuroda MJ, Zheng Y, Jean-Jacques J, Letvin NL, and Koralnik IJ. A prospective study demonstrates an association between JC virus-specific cytotoxic T lymphocytes and the early control of progressive multifocal leukoencephalopathy. *Brain.* 2004;127(Pt 9):1970-8.

315. Marzocchetti A, Tompkins T, Clifford DB, Gandhi RT, Kesari S, Berger JR, Simpson DM, Prosperi M, De Luca A, and Koralnik IJ. Determinants of survival in progressive multifocal leukoencephalopathy. *Neurology.* 2009;73(19):1551-8.

316. Jilek S, Jaquiery E, Hirsch HH, Lysandropoulos A, Canales M, Guignard L, Schluep M, Pantaleo G, and Du Pasquier RA. Immune responses to JC virus in patients with multiple sclerosis treated with natalizumab: a cross-sectional and longitudinal study. *Lancet neurology.* 2010;9(3):264-72.

317. Aly L, Yousef S, Schippling S, Jelcic I, Breiden P, Matschke J, Schulz R, Bofill-Mas S, Jones L, Demina V, et al. Central role of JC virus-specific CD4+ lymphocytes in progressive multi-focal leucoencephalopathy-immune reconstitution inflammatory syndrome. *Brain.* 2011;134(Pt 9):2687-702.

318. Bucks CM, Norton JA, Boesteanu AC, Mueller YM, and Katsikis PD. Chronic antigen stimulation alone is sufficient to drive CD8+ T cell exhaustion. *J Immunol.* 2009;182(11):6697-708.

319. Chakera A, Bennett S, Lawrence S, Morteau O, Mason PD, O'Callaghan CA, and Cornall RJ. Antigen-specific T cell responses to BK polyomavirus antigens identify functional anti-viral immunity and may help to guide immunosuppression following renal transplantation. *Clinical and experimental immunology.* 2011;165(3):401-9.

320. Leuenberger D, Andresen PA, Gosert R, Binggeli S, Strom EH, Bodaghi S, Rinaldo CH, and Hirsch HH. Human polyomavirus type 1 (BK virus) agnoprotein is abundantly expressed but immunologically ignored. *Clinical and Vaccine Immunology.* 2007;14(8):959-68.

321. Lagatie O, Van Loy T, Tritsmans L, and Stuyver LJ. Antibodies reacting with JCPyV_VP2 _167-15mer as a novel serological marker for JC polyomavirus infection. *Virology journal.* 2014;11(174.

322. Horsfall FL, Jr. Virus-neutralization tests: implications and interpretations. *Ann N Y Acad Sci.* 1957;69(4):633-43.

323. Keller XE, Kardas P, Acevedo C, Sais G, Poyet C, Banzola I, Mortezavi A, Seifert B, Sulser T, Hirsch HH, et al. Antibody response to BK polyomavirus as a prognostic biomarker and potential therapeutic target in prostate cancer. *Oncotarget.* 2015;6(8):6459-69.

324. Sunden Y, Suzuki T, Orba Y, Umemura T, Asamoto M, Nagashima K, Tanaka S, and Sawa H. Characterization and application of polyclonal antibodies that specifically recognize JC virus large T antigen. *Acta Neuropathol.* 2006;111(4):379-87.

325. Bodaghi S, Comoli, P., Boesch, R., Azzi, A., Gosert, R., Leuenberger, D., Ginevri, F., Hirsch, H.H. Antibody Responses to Recombinant Polyomavirus BK Large T and VP1 Proteins in Pediatric Kidney Transplant Patients. *J Clin Micro.* 2009;47(8):2577-85.

326. Knowles WA, and Sasnauskas K. Comparison of cell culture-grown JC virus (primary human fetal glial cells and the JCI cell line) and recombinant JCV VP1 as antigen for the detection of anti-JCV antibody by haemagglutination inhibition. *J Virol Methods.* 2003;109(1):47-54.

327. Cinque P, Dumoulin, A., Hirsch, H.H. In: Jerome K ed. *Laboratory Diagnosis of Viral Infections*. Informa Healthcare USA; 2009:401-24.

328. Lundstig A, and Dillner J. Serological diagnosis of human polyomavirus infection. *Adv Exp Med Biol.* 2006;577(96-101.

329. Boldorini R, Allegrini S, Miglio U, Paganotti A, Cocca N, Zaffaroni M, Riboni F, Monga G, and Viscidi R. Serological evidence of vertical transmission of JC and BK polyomaviruses in humans. *J Gen Virol.* 2011;92(Pt 5):1044-50.

330. Wallen WC, London WT, Traub RG, Peterson KE, and Witzel NL. Antibody responses to JC virus-associated antigens by tumor-bearing owl monkeys. *Progress in clinical and biological research.* 1983;105(261-70.

331. Hangartner L, Zinkernagel RM, and Hengartner H. Antiviral antibody responses: the two extremes of a wide spectrum. *Nature reviews Immunology.* 2006;6(3):231-43.

332. Paulson KG, Carter JJ, Johnson LG, Cahill KW, Iyer JG, Schrama D, Becker JC, Madeleine MM, Nghiem P, and Galloway DA. Antibodies to merkel cell polyomavirus T antigen oncoproteins reflect tumor burden in merkel cell carcinoma patients. *Cancer Res.* 2010;70(21):8388-97.

333. Sais G, Wyler S, Hudolin T, Banzola I, Mengus C, Bubendorf L, Wild PJ, Hirsch HH, Sulser T, Spagnoli GC, et al. Differential patterns of large tumor antigen-specific immune responsiveness in patients with BK polyomavirus-positive prostate cancer or benign prostatic hyperplasia. *J Virol.* 2012;86(16):8461-71.

334. Major HG, Rees SD, and Frier BM. Driving and diabetes: DVLA response to Lonnen et al. *Diabet Med.* 2009;26(2):191.

335. Hamilton RS, Gravell M, and Major EO. Comparison of antibody titers determined by hemagglutination inhibition and enzyme immunoassay for JC virus and BK virus. *J Clin Microbiol.* 2000;38(1):105-9.

336. Baneyx F, and Mujacic M. Recombinant protein folding and misfolding in Escherichia coli. *Nat Biotechnol.* 2004;22(11):1399-408.

337. Hurault de Ligny B, Godin M, Lobbedez T, El Haggan W, Pujo M, Etienne I, and Ryckelynck JP. [Virological, epidemiological and pathogenic aspects of human polyomaviruses]. *Presse Med.* 2003;32(14):656-8.

338. Gedvilaite A, Dorn DC, Sasnauskas K, Pecher G, Bulavaite A, Lawatscheck R, Staniulis J, Dalianis T, Ramqvist T, Schonrich G, et al. Virus-like particles derived from major capsid protein VP1 of different polyomaviruses differ in their ability to induce maturation in human dendritic cells. *Virology.* 2006;354(2):252-60.

339. Zeltins A. Construction and characterization of virus-like particles: a review. *Mol Biotechnol.* 2013;53(1):92-107.

340. Sominskaya I, Skrastina D, Dislers A, Vasiljev D, Mihailova M, Ose V, Dreilina D, and Pumpens P. Construction and immunological evaluation of multivalent hepatitis B virus (HBV) core virus-like particles carrying HBV and HCV epitopes. *Clinical and vaccine immunology : CVI.* 2010;17(6):1027-33.

341. Frazer IH. Prevention of cervical cancer through papillomavirus vaccination. *Nature reviews Immunology.* 2004;4(1):46-54.

342. Zabel F, Kundig TM, and Bachmann MF. Virus-induced humoral immunity: on how B cell responses are initiated. *Curr Opin Virol.* 2013;3(3):357-62.

343. Zabel F, Mohanan D, Bessa J, Link A, Fettelschoss A, Saudan P, Kundig TM, and Bachmann MF. Viral particles drive rapid differentiation of memory B cells into secondary plasma cells producing increased levels of antibodies. *J Immunol.* 2014;192(12):5499-508.

344. Braun M, Jandus C, Maurer P, Hammann-Haenni A, Schwarz K, Bachmann MF, Speiser DE, and Romero P. Virus-like particles induce robust human T-helper cell responses. *Eur J Immunol.* 2012;42(2):330-40.

345. Soto CM, and Ratna BR. Virus hybrids as nanomaterials for biotechnology. *Curr Opin Biotechnol.* 2010;21(4):426-38.

346. Jegerlehner A, Zabel F, Langer A, Dietmeier K, Jennings GT, Saudan P, and Bachmann MF. Bacterially produced recombinant influenza vaccines based on virus-like particles. *PloS one.* 2013;8(11):e78947.

347. Freivalds J, Dislers A, Ose V, Pumpens P, Tars K, and Kazaks A. Highly efficient production of phosphorylated hepatitis B core particles in yeast Pichia pastoris. *Protein Expr Purif.* 2011;75(2):218-24.

348. Hofmann KJ, Cook JC, Joyce JG, Brown DR, Schultz LD, George HA, Rosolowsky M, Fife KH, and Jansen KU. Sequence determination of human papillomavirus type 6a

and assembly of virus-like particles in Saccharomyces cerevisiae. *Virology.* 1995;209(2):506-18.

349. Biemelt S, Sonnewald U, Galmbacher P, Willmitzer L, and Muller M. Production of human papillomavirus type 16 virus-like particles in transgenic plants. *J Virol.* 2003;77(17):9211-20.

350. Mason HS, Lam DM, and Arntzen CJ. Expression of hepatitis B surface antigen in transgenic plants. *Proc Natl Acad Sci U S A.* 1992;89(24):11745-9.

351. Tsuda S, Yoshioka K, Tanaka T, Iwata A, Yoshikawa A, Watanabe Y, and Okada Y. Application of the human hepatitis B virus core antigen from transgenic tobacco plants for serological diagnosis. *Vox Sang.* 1998;74(3):148-55.

352. Bodaghi S, Comoli P, Bosch R, Azzi A, Gosert R, Leuenberger D, Ginevri F, and Hirsch HH. Antibody responses to recombinant polyomavirus BK large T and VP1 proteins in young kidney transplant patients. *J Clin Microbiol.* 2009;47(8):2577-85.

353. Nguyen NL, Le BM, and Wang D. Serologic evidence of frequent human infection with WU and KI polyomaviruses. *Emerg Infect Dis.* 2009;15(8):1199-205.

354. Warnke C, Pawlita M, Dehmel T, Posevitz-Fejfar A, Hartung HP, Wiendl H, Kieseier BC, and Adams O. An assay to quantify species-specific anti-JC virus antibody levels in MS patients. *Mult Scler.* 2013;19(9):1137-44.

355. Hirsch HH. BK virus: opportunity makes a pathogen. *Clinical infectious diseases : an official publication of the Infectious Diseases Society of America.* 2005;41(3):354-60.

356. Neu U, Stehle T, and Atwood WJ. The Polyomaviridae: Contributions of virus structure to our understanding of virus receptors and infectious entry. *Virology.* 2009;384(2):389-99.

357. Koralnik IJ, Boden D, Mai VX, Lord CI, and Letvin NL. JC virus DNA load in patients with and without progressive multifocal leukoencephalopathy. *Neurology.* 1999;52(2):253-60.

358. Tornatore C, Berger JR, Houff SA, Curfman B, Meyers K, Winfield D, and Major EO. Detection of JC virus DNA in peripheral lymphocytes from patients with and without progressive multifocal leukoencephalopathy. *Ann Neurol.* 1992;31(4):454-62.

359. Chang D, Fung CY, Ou WC, Chao PC, Li SY, Wang M, Huang YL, Tzeng TY, and Tsai RT. Self-assembly of the JC virus major capsid protein, VP1, expressed in insect cells. *J Gen Virol.* 1997;78(1435-9.

360. Schmidt T, Adam C, Hirsch HH, Janssen MW, Wolf M, Dirks J, Kardas P, Ahlenstiel-Grunow T, Pape L, Rohrer T, et al. BK Polyomavirus-Specific Cellular Immune

Responses Are Age-Dependent and Strongly Correlate With Phases of Virus Replication. *American journal of transplantation : official journal of the American Society of Transplantation and the American Society of Transplant Surgeons.* 2014;14(6):1334-45.

361. Weber F, Goldmann C, Kramer M, Kaup FJ, Pickhardt M, Young P, Petry H, Weber T, and Luke W. Cellular and humoral immune response in progressive multifocal leukoencephalopathy. *Ann Neurol.* 2001;49(5):636-42.

362. Alstadhaug K, Croughs T, Henriksen S, Leboeuf C, Sereti I, Hirsch H, and Rinaldo CH. In: Neurology J ed. JAMA Neurology; 2014:E1-E5.

# 8 Acknowledgements

First and foremost, I would like to thank professor Hans H. Hirsch for the opportunity to prepare my thesis in the Department of Biomedicine here in Basel, for his guidance and supervision, which have taught me a lot about scientific life.

I would also like to sincerely thank my Faculty Representative - professor Antonius G. Rolink - and my Co-referee - professor Roberto Speck - for willing to join my Committee on such a short notice.

I am thankful to everyone in the lab – Julia, Céline, Tobi, Christiane, Guni – they were always there for me to answer my questions or help me out with the experiments. And Ksenia, for the Adobe Illustrator crash course! Of course, I am also grateful for all coffee breaks and nice discussions with other members of our research team and a major part of the diagnostic team!

I would like to thank my best friends - Justyna, Magda, Kamila - for a lifelong support! And Alexis, for The Brazilian Trail.

Dziekuje serdecznie Rodzicom, Krystynie i Emilowi, oraz mojej siostrze, Justynie, i bratu, Damianowi. Bez Was nie byloby mnie dzisiaj tutaj. Dziekuje Wam za okazywane mi wsparcie i dodawanie wiary w moje mozliwosci.